

OPTIMIZATION OF BUPRENORPHINE DOSING IN PREGNANT WOMEN

by

Hongfei Zhang

MS, University of Pittsburgh, 2015

Submitted to the Graduate Faculty of
School of Pharmacy in partial fulfillment
of the requirements for the degree of
Doctor of Philosophy

University of Pittsburgh

2019

UNIVERSITY OF PITTSBURGH
SCHOOL OF PHARMACY

This dissertation was presented

By

Hongfei Zhang

It was defended on

April 18th, 2019

and approved by

Steve Caritis, MD, Professor, Obstetrics, Gynecology and Reproductive Sciences, School of
Medicine, Magee Womens Hospital

Samuel Poloyac, Pharm.D, PhD, Professor, Pharmaceutical Sciences, School of Pharmacy

Jan Beumer, Pharm.D, PhD, Associate Professor, Pharmaceutical Sciences, School of Pharmacy

Junmei Wang, PhD, Associate Professor, Pharmaceutical Sciences, School of Pharmacy

Dissertation Advisor: **Raman Venkataramanan**, PhD, Professor, Pharmaceutical Sciences,
School of Pharmacy, Professor, Pathology, School of Medicine

Copyright © by Hongfei Zhang

2019

Optimization of buprenorphine dosing in pregnant women

Hongfei Zhang, PhD

University of Pittsburgh, 2019

The primary objective of this work was to optimize buprenorphine (BUP) dosing based on exposure in treating opioid addiction in pregnant women. A combination of clinical pharmacokinetic study and modeling and simulation was used to accomplish this.

The clinical study evaluated BUP pharmacokinetics (PK) during pregnancy and postpartum. Up to 3 studies were performed in each participant during 1st-, 2nd-half of pregnancy, and postpartum. At each study visit, multiple blood samples and specific pharmacodynamics measurements were collected. Plasma concentrations of BUP were quantified using UPLC-MS/MS. In this study BUP exposure was lower during pregnancy compared to postpartum.

A physiologically-based pharmacokinetic (PBPK) model of intravenous and sublingual BUP was developed and verified using 14 independent BUP PK studies. This PBPK model predicted decreased BUP exposure during pregnancy compared to postpartum, consistent with the observations from the clinical study.

Non-linear mixed effects modeling using a first-order conditional estimation with interaction to analyze changes in BUP PK in pregnant women was conducted. Buprenorphine PK data were well-characterized by a two-compartment model with first-order absorption with enterohepatic recirculation and first-order elimination. The model estimated population apparent clearance (CL/F) of BUP in a typical pregnant woman was 469 L/h. Pregnancy was associated with a 1.64-folds increase in CL/F of BUP compared to postpartum period. A pharmacodynamic (PD) analysis showed that the average area under curves of COWS scores during pregnancy were significantly greater than postpartum period following administration of BUP, which is consistent with the

observed lower buprenorphine exposure during pregnancy. The relationship between pupillary diameters and BUP concentration was described by a sigmoidal E_{max} model with a hypothetical effect compartment. The calculated IC_{50} of BUP concentration for pupillary diameter changes was not significantly different during pregnant and postpartum, suggesting that there may not be any significant change in the sensitivity and /or number of μ -opioid receptors in the brain in pregnant women compared to non-pregnant women.

Overall, the clinical observations and the two different modeling approaches demonstrated that BUP exposure is decreased during pregnancy and this alteration in BUP exposure is associated a decreased response to BUP in pregnancy.

Table of Contents

PREFACE.....	xxiii
1.0 Introduction.....	1
1.1 Pain - Treatment of pain - Opioids	1
1.2 Current treatments of opioid addiction.....	3
1.2.1 Full agonist of mu-opioid receptor	3
1.2.2 Partial agonist of mu-opioid receptor	5
1.2.3 Antagonist of mu-opioid receptor.....	10
1.2.4 Non-opioid Treatment	11
1.3 Physiological changes during pregnancy.....	12
1.3.1 Uterus	14
1.3.2 Placenta and fetus	14
1.3.3 Cardiovascular system.....	19
1.3.4 Liver	20
1.3.5 Renal system	20
1.4 Impacts of pregnancy on the pharmacokinetics of drugs.....	21
1.4.1 Absorption	21
1.4.2 Distribution.....	23
1.5 The prediction of pregnancy induced pharmacokinetic changes of drugs based on Biopharmaceutics Classification System.....	30
1.6 Pharmacotherapy of opioid use disorder in pregnant women	31
1.7 The current dosing issue of buprenorphine in pregnancy	34

1.8 The pharmacokinetic and pharmacodynamic relationship of buprenorphine.....	35
1.9 Difficulty in performing pharmacokinetic studies in pregnant women and alternative approaches to evaluate pharmacokinetics in pregnancy	37
1.10 Hypothesis and Objectives.....	41
2.0 Development and Validation of a Sensitive Ultra-Performance Liquid Chromatography-Tandem Mass Spectrometric Assay for Simultaneous Determination of Buprenorphine and Three Metabolites in Human Plasma: Application in a Clinical Pharmacokinetic Study in Pregnant Women	44
2.1 Abstract	44
2.2 Introduction	46
2.3 Materials and methods.....	50
2.3.1 Chemicals and Reagents.....	50
2.3.2 Chromatographic Conditions	52
2.3.3 Mass Spectrometric Conditions.....	53
2.3.4 Standards and quality control samples preparation	54
2.3.5 Plasma samples preparation	54
2.3.6 Bioanalytical method validation	55
2.4 Results.....	58
2.4.1 Accuracy and precision	62
2.4.2 Recovery and matrix effect	65
2.4.3 Stability	67
2.4.4 Analysis of buprenorphine and three metabolites in pregnant women	69
2.4.5 Alterations of buprenorphine metabolic pathway during pregnancy.....	74

2.5 Discussion	83
2.6 Conclusions	86
3.0 A Physiologically Based Pharmacokinetic Modeling Approach to Predict Buprenorphine Pharmacokinetics following Intravenous & Sublingual Administration	88
3.1 Abstract	89
3.2 Introduction	91
3.3 Methods	93
3.3.1 General workflow for model building and model validation	94
3.3.2 IV Buprenorphine - PBPK model development.....	98
3.3.3 IV BUP Clinical Pharmacokinetic Studies: Model validation	104
3.3.4 SL BUP - PBPK model development.....	106
3.3.5 SL BUP Clinical Pharmacokinetic Studies: Model validation.....	108
3.3.6 Virtual Patient Population	111
3.3.7 SL BUP Steady State Exposure Simulations	111
3.4 Results.....	112
3.4.1 BUP Exposure Prediction following a single IV BUP dose in healthy subjects:	112
3.4.2 Modeling prediction following a SL of BUP in healthy volunteers	115
3.5 Discussion	121
4.0 Gestational Changes in Buprenorphine Exposure: A Physiologically Based Pharmacokinetic Analysis	127
4.1 Abstract	128

4.2 Introduction	129
4.3 Methods	132
4.3.1 A PBPK model for BUP in non-pregnant subjects	133
4.3.2 A PBPK model for BUP in pregnant subjects	134
4.3.3 Comparison during pregnancy and the post-partum (non-pregnant period)	141
4.3.4 Nomenclature of targets and ligands.....	141
4.4 Results.....	142
4.4.1 Steady state BUP systemic exposure prediction.....	142
4.4.2 Evaluation of the predictive performance of the BUP PBPK model in pregnant women	144
4.5 Discussion	151
4.6 Conclusions	162
5.0 Model-based analysis to evaluate alterations in buprenorphine pharmacokinetics during pregnancy	163
5.1 Abstract	164
5.2 Introduction	166
5.3 Method.....	168
5.3.1 Study Design	168
5.3.2 Determination of plasma concentration of buprenorphine.....	170
5.3.3 Population Pharmacokinetic Analysis	171
5.3.4 Software	173
5.4 Results.....	173

5.4.1	Structural model of the population pharmacokinetic model following sublingual administration of buprenorphine	175
5.4.2	Covariate identification	180
5.4.3	Model evaluation	182
5.5	Discussion	186
5.6	Conclusions	191
6.0	Pharmacodynamic analysis of buprenorphine in pregnant women.....	192
6.1	Abstract	193
6.2	Introduction	196
6.3	Method.....	200
6.3.1	Clinical study design	200
6.3.2	Determination of buprenorphine concentration in plasma.....	201
6.3.3	Measurement of pupillary diameter.....	202
6.3.4	Assessment of craving score and COWS score.....	203
6.3.5	Population pharmacokinetic /pharmacodynamic Analysis.....	203
6.3.6	Software	206
6.4	Results.....	207
6.4.1	Clinical data.....	207
6.4.2	COWS scores and BUP exposure during pregnancy and postpartum	207
6.4.3	Buprenorphine induced miotic effect	211
6.4.3.1	Basic exposure and response exploration	211
6.4.3.2	Model analysis.....	214
6.4.4	Model evaluation	215

6.5 Discussion	220
6.6 Conclusions	224
7.0 SUMMARY AND FUTURE DIRECTIONS.....	226
7.1 Summary and Clinical Inference	227
7.2 Limitations	235
7.3 Future Directions.....	237
7.4 Appendix	Error! Bookmark not defined.
7.5 Appendix A.1 Physiochemical and pharmacokinetic parameters used to develop buprenorphine profile in Simcyp®.....	240
7.6 Appendix A.2 Key pharmacokinetic parameters of buprenorphine in non-pregnant subjects (range, or mean±SD)	Error! Bookmark not defined.
7.7 Appendix B. Clinical Opioid Withdrawal Scale	243
7.8 BIBLIOGRAPHY.....	247

List of Tables

Table 1-1 Pharmacokinetic characteristics of different buprenorphine formulations approved by the FDA.....	8
Table 1-2. Physiological changes during pregnancy	13
Table 1-3. Enzymes identified in human placenta ([131, 134-136])	18
Table 1-4. Pregnancy induced changes in drug metabolizing enzyme activities.....	28
Table 1-5. The summary of pregnancy induced physiological changes and potential impacts on pharmacokinetics of drugs.....	29
Table 2-1. Gradient method used to separate buprenorphine and three metabolites.....	52
Table 2-2. The ion pairs for multiple reaction monitoring	53
Table 2-3. Inter-day and Intra-day accuracy of buprenorphine and three metabolites (expressed as a percentage of the nominal concentration).....	63
Table 2-4. Inter-day and Intra-day precision of buprenorphine and three metabolites (expressed as coefficient of variation)	64
Table 2-5. Recovery and matrix effect of buprenorphine and three metabolites in human plasma samples.....	66
Table 2-6. Stability of buprenorphine and three metabolites in human plasma samples (expressed as mean of nominal concentration \pm SD %)	68
Table 2-7. Buprenorphine pharmacokinetic parameters during pregnancy and postpartum period	72

Table 2-8. Comparisons of BUP PK from our in-house clinical PK studies at postpartum period and non-pregnant population from literatures following multiple doses of SL BUP administration (expressed as mean (SD))	73
Table 2-9. The AUC ratios of CYP- and UGT- mediated metabolism of buprenorphine during pregnancy compared to postpartum (expressed as mean (SD)).....	75
Table 3-1. Summary of BUP physiochemical parameters	96
Table 3-2. Distribution parameters for BUP drug profile	99
Table 3-3. Values used in equation 2 to scale rhCYPs data to the entire human body (Adapted from healthy population in SimCyp®).....	102
Table 3-4. Intrinsic clearance and ISEF values associated with enzymes primarily involved in buprenorphine metabolism.....	103
Table 3-5. Intravenous buprenorphine clinical pharmacokinetic studies	105
Table 3-6. Sublingual buprenorphine dosing allocation between depot and non-depot components	107
Table 3-7. First-order absorption model parameter values.....	107
Table 3-8. SL BUP clinical PK single dose studies considered for modeling	109
Table 3-9. SL BUP clinical PK multiple dose studies considered for modeling.....	110
Table 3-10. Goodness of fit for IV BUP model in healthy subjects	114
Table 3-11. Goodness of fit for SL BUP model in healthy subjects.....	117
Table 3-12. Goodness of fit for sublingual buprenorphine models in healthy volunteers at steady state.....	118
Table 3-13. Results from mass balance study following administration of radiolabeled IV BUP.....	123

Table 4-1. Distribution parameters for BUP PBPK model in pregnant women.....	136
Table 4-2. Summary of gestational age associated physiologic parameters incorporated into SimCyp® healthy population.....	137
Table 4-3. Goodness of fit of BUP SL model in pregnancy and postpartum (PK parameters were expressed as mean (SD)).....	146
Table 4-4. Pharmacokinetic parameters of buprenorphine during pregnancy and postpartum following 8 mg BID BUP SL administration (geometric mean ± SD). 147	
Table 4-5. Characteristics of study participants	158
Table 4-6. Summary of gestational age associated physiologic parameters incorporated into SimCyp® healthy population model_2	158
Table 4-7. The goodness of fit of model predictions with the observed clinical data	161
Table 5-1. Characteristics of study participants	174
Table 5-2. Parameter estimates of final population pharmacokinetic model for buprenorphine following sublingual administration in pregnant women.....	181
Table 6-1. The AUCs of Clinical Opioid Withdrawal Scale score and BUP exposure within a dose interval during pregnancy and postpartum (expressed as mean (SD)).....	209
Table 6-2. Parameter estimates of final population pharmacokinetic /pharmacodynamic model for buprenorphine following sublingual administration in pregnant women	217

List of Figures

Figure 1-1. Drug transporters in placenta.....	17
Figure 1-2. Relationship between buprenorphine trough concentration and overall exposure (AUC₀₋₁₂) at steady state in pregnant women [201].....	38
Figure 2-1. Buprenorphine metabolic pathway	48
Figure 2-2. Chemical structure of buprenorphine (A), buprenorphine-D₄ (B), norbuprenorphine (C), norbuprenorphine-D₃ (D), buprenorphine-3-β-D-glucuronide (E), buprenorphine-D₄-3-β-D-glucuronide (F), norbuprenorphine glucuronide (G), norbuprenorphine glucuronide-D₃ (H).....	51
Figure 2-3. Representative chromatogram of pooled blank human plasm without spiked with internal standards. (A) buprenorphine-D₄-3-β-D-glucuronide; (B) buprenorphine-3-β-D-glucuronide; (C) Norbuprenorphine glucuronide-D₃; (D) Norbuprenorphine glucuronide (E) buprenorphine-D₄; (F) buprenorphine; (G) Norbuprenorphine-D₃; (H) Norbuprenorphine	59
Figure 2-4. Representative chromatogram of pooled blank human plasm spiked with internal standards. (A) buprenorphine-D₄-3-β-D-glucuronide; (B) buprenorphine-3-β-D-glucuronide; (C) Norbuprenorphine glucuronide-D₃; (D) Norbuprenorphine glucuronide (E) buprenorphine-D₄; (F) buprenorphine; (G) Norbuprenorphine-D₃; (H) Norbuprenorphine	60
Figure 2-5. Representative chromatogram spiked with buprenorphine (0.05 ng/mL, 4A), norbuprenorphine (0.2 ng/mL, 4B), buprenorphine glucuronide (0.2 ng/mL, 4C), and	

norbuprenorphine glucuronide (0.2 ng/mL, 4D) with their respective deuterated internal standards.	61
Figure 2-6. Plasma concentration vs time profiles of buprenorphine, norbuprenorphine, buprenorphine glucuronide and norbuprenorphine glucuronide following sublingual administration of buprenorphine in one pregnant women.	70
Figure 2-7. Dose normalized buprenorphine mean concentration time profile (expressed as mean± SD).....	71
Figure 2-8. Dose normalized norbuprenorphine mean concentration time profile (expressed as mean± SD).....	76
Figure 2-9. Dose normalized buprenorphine glucuronide mean concentration time profile (expressed as mean± SD).....	77
Figure 2-10. Dose normalized norbuprenorphine glucuronide mean concentration time profile (expressed as mean± SD).....	78
Figure 2-11. The ratios of AUC of norbuprenorphine and AUC of norbuprenorphine glucuronide to the AUC of buprenorphine at 1 st -and 2 nd -trimester vs postpartum.	79
Figure 2-12. The ratios of AUC of norbuprenorphine and AUC of norbuprenorphine glucuronide to the AUC of buprenorphine at 3 rd -trimester vs postpartum	80
Figure 2-13. The ratios of AUC of buprenorphine glucuronide to the AUC of buprenorphine at 1 st -and 2 nd trimester vs postpartum	81
Figure 2-14. The ratios of AUC of buprenorphine glucuronide to the AUC of buprenorphine at 3 rd -trimester vs postpartum.....	82
Figure 3-1. Compartmental structure of the full BUP IV and SL PBPK models. The schematic shows how SL and IV administration was modeled.	97

Figure 3-2. Predicted and observed concentration-time profiles following a single IV push doses of BUP.	113
Figure 3-3. Predicted and observed concentration-time profiles following a single SL doses of BUP in 100 virtual healthy subjects.	116
Figure 3-4. Steady state predicted and observed concentration-time profiles following daily SL doses of BUP in healthy subjects.	119
Figure 3-5. Predicted plasma and brain concentration-time profiles following a 16 mg SL doses of BUP in healthy subjects.	120
Figure 4-1. Quantitative mass balance diagram describing buprenorphine (BUP) absorption, distribution, metabolism and excretion after sublingual and intravenous (IV) administration. BUPG, Buprenorphine glucuronide; NBUP, Nor-buprenorphine; NBUPG, Nor-buprenorphine glucuronide	139
Figure 4-2. Sensitivity analysis to simulate the impact of the abundance of CYPs, UGTs and renal function on buprenorphine total clearance	140
Figure 4-3. Predicted mean concentration–time profiles at steady-state following administration of 8 mg sublingual twice daily buprenorphine during 1st trimester, 2nd trimester, 3rd trimester, and postpartum in 100 virtual female subjects spread across 10 trials	143
Figure 4-4. Predicted and observed dose normalized concentration–time profiles at steady-state following administration sublingual twice daily buprenorphine	148
Figure 4-5. Predicted and observed concentration–time profiles at steady-state following administration of 8 mg sublingual twice daily buprenorphine	149

Figure 4-6. Percent of 100 virtual subjects with buprenorphine plasma concentration above 1 ng/ml in one dosing interval at steady-state following administration of 8 mg sublingual twice daily during postpartum, 1st, 2nd, 3rd trimester.....	150
Figure 4-7. Buprenorphine mean concentration-time profiles in 100 virtual pregnant women at 1st, 2nd, 3rd trimesters following 8 mg sublingual twice daily dosing.	159
Figure 5-1. Schematic diagram of buprenorphine structure model following sublingual administration	178
Figure 5-2. Sensitivity analysis of the interindividual variability of the percentage of enterohepatic recirculation (EHCP). (A) The impact of fixed values of variance of EHCP vs. OFV (B) The impact of fixed values of variance of EHCP vs. relative standard error of model parameters.....	179
Figure 5-3. Goodness of fit diagnostic plots for buprenorphine concentrations fitted of final model.....	183
Figure 5-4. Predictive performance of the final model using visual predictive check plots.	185
Figure 6-1. Mean COWS score time profiles following administration of a SL BUP dose.	208
Figure 6-2. BUP plasma concentration vs Clinical Opioid Withdrawal Scale score.	210
Figure 6-3. The changes of AUCs of COWS score from baseline vs BUP AUC.	210
Figure 6-4. BUP plasma concentration vs pupillary diameter	211
Figure 6-5. BUP exposure (AUC) vs the AUC of pupillary diameter	212
Figure 6-6. Time course of pupillary diameter following SL administration of BUP by study occasion	213

Figure 6-7. Schematic diagram of the final population pharmacokinetic /pharmacodynamic model 216

Figure 6-8. Goodness of fit diagnostic plots for buprenorphine population PK /PD final model fit. 218

Figure 6-9. Predictive performance of the final model using prediction-corrected visual predictive check plots. 219

ABBREVIATIONS

AAG	Alpha1-acid glycoprotein
ABC	ATP-binding cassette
AIC	Akaike information criterion
AUC	Area under curve
BCRP	Breast cancer resistance protein
BOV	Between occasions variability
BSV	Between subject variability
BUP	Buprenorphine
BUPG	Buprenorphine glucuronide
C_{max}	Maximum concentration
CL/F	Apparent clearance
CV	Coefficient of variance
CYP	Cytochrome P450
E	Extraction ratio
EC_{50}	Concentrations at 50% of maximum effect
E_{max}	Maximal effect
EHC	Enterohepatic recirculation
ESI	Electron spray ionization
COWS	Clinical Opioid Withdrawal Scale
F	Bioavailability
F_a	Absorption fraction
F_g	Fraction escaping metabolism in gut wall
F_h	Fraction escaping metabolism in liver
FDA	Food and Drug Administration

FOCE-I	First-order conditional estimation with interaction
GFR	Glomerular filtration rate
HPLC	High performance liquid chromatography
IRB	Institutional Review Board
IS	Internal standards
K_i	Inhibitory constant
K_p	Partition of a drug between plasma and tissues
LAAM	Levo-alpha-acetyl-methadol
LC	Liquid chromatography
LogP	Logarithm of the octanol to water partition coefficient
MDRP	Multidrug resistance protein
MRM	Multiple reaction monitoring
NAS	Neonatal abstinence syndrome
NorBUP	Norbuprenorphine
NorBUPG	Norbuprenorphine glucuronide
OCT	Organic cation transporters
OAT	Organic anion transporters
OATP	Organic anion transporting polypeptides
OFV	Objective function value
PBPK	Physiologically based pharmacokinetic
PD	Pharmacodynamic
PET	Positron emission tomography
P-gp	P-glycoprotein
PK	Pharmacokinetic
QC	Quality control
RSE	Relative standard error
SD	Standard deviation
SL	Sublingual

SLC	Solute carrier
T_{\max}	Time to C_{\max}
UGT	Uridine diphosphate glucuronosyltransferases
UPLC	Ultra-performance liquid chromatography
UPLC-MS/MS	Ultra-performance liquid chromatography coupled with mass spectrometry
V	Volume distribution
VPC	Visual predictive check

PREFACE

First and foremost, I would like to express my sincere gratitude to my advisor, Dr. Raman Venkataramanan for his great guidance and support. I appreciate his passion for teaching and science. The knowledge that I have gained from him is a great asset throughout my life. I am forever grateful to have been his student.

I am very fortunate to have Dr. Steve Caritis, Dr. Samuel Poloyac, Dr. Jan Beumer and Dr. Junmei Wang on my dissertation committee. I have been always inspired by Dr. Steve Caritis for his enthusiasm for research in pregnant women. Also, I am very thankful for the opportunity to work with him on buprenorphine use in pregnancy. Dr. Samuel Poloyac has always been instrumental in my progress in the program and gave constructive advice for ways to improve my work and writing. Dr. Jan Beumer gave me great advice on my modeling work. He also enlightened me on the clinical implications of the models. I have benefitted greatly from him. I sincerely thank Dr. Junmei Wang for his great support and encouragement. I sincerely appreciate him for the time that he has spent with me to discuss my research and career.

I would like to thank Hari Kalluri for his help with the development of physiologically-based pharmacokinetic models. I am also grateful for the help provided by Sarah Cook for the development of the population pharmacokinetic model of BUP in pregnancy. I sincerely thank Wenchen Zhao for his help with the analytical work. I would not have been able to complete my work without their help. I also want to express my thanks to our lab members for their friendship and kind advice. Special thanks to Dr. Maggie Folan and Lori M. Schmotzer for being there throughout the six years of my graduate school and to all faculty and staff in the School of Pharmacy.

I thank my mother, father, sister, husband, and sons (Nash Wei and Spence Wei) for their love and endorsement. Words cannot express my love and gratitude to them. They helped me to pursue my dreams and become a better version of myself.

1.0 Introduction

1.1 Pain - Treatment of pain - Opioids

Pain is one of the most prevalent public health problems. Pain can originate from diseases, or surgical, diagnostic and therapeutic procedures. A national Health Survey of 8,781 adults showed that 55.7% of the participants reported pain in the previous 3 months [1]. In addition, it is estimated that up to 71% of the patients experienced pain during their stay in the intensive care unit [2]. Pain contributes significantly to morbidity, mortality and disability of humans. Inadequate pain control can compromise recovery, and negatively impact patient outcomes both physically and psychologically. Pain is one of the sources of stress and agitation in patients. Accordingly, the use of analgesics for treating pain in patients is common.

The pathophysiology of pain is complex. The process of pain includes transduction, transmission, modulation, and perception. The nociceptive pain starts from the activation of peripheral pain receptors, A-delta and C fiber. These afferent nerves translate noxious stimulation into nociceptive impulses, and these impulses are sent along the sensory tracks to the spinal cord and then to the brain. The modulation occurring at the gate of the dorsal horn is the process of lessening or amplifying the pain-related neural signal by the body. The final perception of pain is regulated by the transduction, transmission, modulation, and psychological aspect of the individual [3, 4]. Pain has sensory and emotional components. As a result, every patient experiences pain in a unique manner.

Due to the complicated pathophysiology as well as subjective and emotional nature of pain, the management of pain is a challenge in clinic practice. Prescription opioids are commonly used

in the treatment of pain. Opioids are substances that bind to opioid receptors and the binding can be antagonized by naloxone [5]. Opioids can be either endogenous opiate alkaloids or exogenous chemicals [6]. The term of opioids generally refers to a group of drugs that are naturally derived such as morphine and codeine, semi-synthetics such as hydrocodone and oxycodone, or synthetic chemicals like fentanyl. Because of their effectiveness in relieving pain, opioid medications are the first-line of therapy for treating moderate to severe pain [7, 8].

Opioids can simulate the effect of endorphins, endogenous opioids, to lessen the effects of painful stimuli by interacting with opioid receptors distributed throughout the central nervous system [9-12]. After binding to opioid receptors, opioids can also cause euphoric effects through their involvement in the dopaminergic brain regions involved in the reward system. Moreover, the euphoric effects may be intensified when the medication is taken in ways other than those prescribed – crushing, snorting, injecting, or combining with alcohol or other drugs [13-15]. Opioids are safe when taken as prescribed for a short time period. However, prolonged use may lead to dependence and addiction, as well as tolerance. The impact of opioids on the brain are complex [16, 17]. After entering the brain, exogenous opiates bind to mu-opioid receptors and activate the mesolimbic reward system. The activation of mesolimbic reward system results in the release of dopamine, which causes euphoria. Repeated exposure to opioids makes the brain cells less responsive and higher doses are needed to generate the same amount of dopamine, which is the process of tolerance. Another effect of opioid binding to μ -opioid receptor is the suppression of the release of noradrenaline. With repeated doses of opioids, the activities of neurons are upregulated to maintain normal levels of noradrenaline [16, 17]. When opioids are suddenly stopped, the effect on the inhibition of noradrenaline release is removed. The excessive release of noradrenaline results in irritability, anxiety, and jitter, as well as other withdrawal symptoms. The

long-term use of opioids can result in damage to the brain and lead to compulsive drug-seeking, which is addiction. Addiction leads to drug overdose. Death due to drug overdose has become a nationwide public health crisis in the United States [18-20]. In 2016 and 2017, death involving an opioid contributed to almost 70% of the total drug overdose related deaths [21].

1.2 Current treatments of opioid addiction

Psychosocial intervention alone or pharmacological intervention alone are associated with poor outcomes for patients with opioid addiction [22]. Currently, the most effective treatment for opioid addiction is medication-assisted treatment, which combines counseling, behavioral therapies with the use of medications. Several medications have been approved by the Food and Drug Administration (FDA) for treating opioid addiction including full agonist, partial agonist, and antagonist of mu-opioid receptor.

1.2.1 Full agonist of mu-opioid receptor

Methadone

The use of methadone as a maintenance therapy to treat opioid addiction can be traced back to 1960's [23]. Many clinical studies have demonstrated the effectiveness of methadone maintenance interventions in reducing illicit opioid use, suppressing drug withdrawal, and minimizing craving [24-28]. Methadone is currently recognized as the standard of care for treating opioid addiction. Methadone, a racemic mixture of the R- and S- enantiomers is a synthetic agonist of mu-opioid receptor. Methadone binds to mu-, delta-, and kappa- opioid receptors with similar

pharmacological properties like morphine [29, 30]. Methadone blocks the binding of opioids with the receptors. As with other long-acting opioids, methadone has a better safety profile, for example, less severe abstinence syndrome, than short-acting opioids, such as heroin and morphine [31-33].

Following oral administration, the absolute bioavailability of methadone is approximately 80% with marked interindividual variability (range from 41 – 100%) [34-36]. It is estimated that the first-pass metabolism of methadone in the intestinal tract is around 20%, with cytochrome P450 (CYP) 3A4 being the primary enzyme for methadone metabolism [37, 38]. The mean time for peak plasma concentration ranges from 2.5 to 4 hours [39-41]. At steady-state, the volume of distribution of methadone is 5.9 and 3.3 L/kg for the R- and S- methadone, respectively [42]. As a basic drug, methadone is highly bound to alpha-1-acid glycoprotein in plasma (88%) [43, 44]. Methadone is mainly metabolized via N-demethylation to inactive metabolites by CYP3A4, CYP2B6 and CYP2C19 in the liver [45-47]. In addition, there is a limited amount of methadone that is eliminated as the parent drug through renal excretion. The renal elimination of methadone is urine pH dependent, and the renal clearance can contribute to the total body clearance from 1 to 35% as urine pH varies from 7.8 to 5.2 [48, 49]. The total body clearance of methadone is approximately 8 L/h and the terminal half-life of methadone is 32 hours following intravenous administration in healthy subjects [45].

Levo-alpha-acetyl-methodol (LAAM)

Levo-alpha-acetylmethodol, also known as levomethadyl acetate is a synthetic opioid with a structure similar to methadone. Compared to other mu opioid receptor agonists, LAAM has an extraordinary long duration of action due to its long half-life and active metabolites [50-52]. Many studies have shown that LAAM has similar or better efficacy compared to methadone in preventing

withdrawal symptoms induced by cessation of morphine or heroin [53-57]. LAAM was approved by the FDA as a pharmacotherapy for opioid dependence in the year 1993. However, due to its potential risks for serious and possibly life-threatening proarrhythmic side effect, LAAM has been removed from the market in the United states in the year 2003 [58].

1.2.2 Partial agonist of mu-opioid receptor

Buprenorphine

Buprenorphine is a semi-synthetic derivative of the alkaloid thebaine. Initially, buprenorphine was used as an opioid analgesic for treating moderate to severe pain. In 2002, buprenorphine was approved for the treatment of opioid addiction by the FDA.

In comparison with morphine and methadone, buprenorphine has a very unique pharmacological profile. Buprenorphine has high binding affinity to mu opioid receptor but low intrinsic activity. In mouse mu receptor, transfected Chinese hamster ovary (mMOR-CHO) cells, the inhibitory constant (K_i), a parameter that reflects binding affinity of buprenorphine and morphine are 0.38 and 286 nM, respectively [59]. However, using [D-Ala², N-Me⁴, Gly⁵-ol]-enkephalin (DMGO) as a reference to measure the intrinsic activity of mu opioid receptor agonist binding effect, an in vitro study found that the maximal stimulation of G-protein activation by buprenorphine and morphine are 43 and 106%, respectively [60]. In addition to in vitro studies, the bell-shaped dose response curve of anti-nociception effect in animal studies, the ceiling effects of subjective measurements of agonist effect and minimal respiratory depression of buprenorphine at high doses in clinical studies all support buprenorphine as a partial mu-opioid receptor agonist [61, 62]. Besides binding to mu-opioid receptor, buprenorphine also binds to other opioid receptors. The K_i values are 0.08, 0.8 and 4.5 nM for the binding affinity to mu-, delta-, and kappa-

opioid receptors, respectively [63]. Buprenorphine has no intrinsic activity (antagonist) on the delta-opioid receptor and very low activity on the kappa-opioid receptor [60, 63, 64].

Buprenorphine has a very low oral bioavailability due to its extensive first-pass metabolism, therefore buprenorphine is administered through parenteral, sublingual, transmucosal, subcutaneous or transdermal routes and not orally [65]. The pharmacokinetic characteristics of the formulations of BUP are summarized in Table 1. High interindividual variability in buprenorphine pharmacokinetics following sublingual administration has been reported in multiple clinical studies. In a dose-escalation trial of sublingual buprenorphine conducted by Ciraulo et al., the coefficients of variation in the maximum plasma concentration (C_{max}) and area under curve (AUC) ranged from 40 – 64% [66]. The plasma peak concentrations ranged from 1.93 to 7.2 ng/mL, and the AUC_{0-96} varied from 9.24 to 35.57 ng·h/mL following single 4 mg sublingual administration of buprenorphine in 6 participants in the clinical study reported by Kuhlman et al [67]. Although the absorption after sublingual administration is rapid, the observed time to reach plasma peak concentration (T_{max}) varied from less than 1 to 6 hrs [68, 69]. The relatively long time for plasma peak concentration after sublingual administration may be due to slow release of buprenorphine from the buccal tissue depot [69]. Several factors might impact the absorption and bioavailability of buprenorphine from the sublingual formulation. First of all, only unionized form of buprenorphine that can cross mucous membrane beneath the tongue, diffuses into the capillaries and enters into the venous circulation. Buprenorphine is a basic drug ($pK_{a1} = 9.62$, $pK_{a2} = 8.31$) [70]. Currently, no study has evaluated the associations between the bioavailability of BUP and the pH in the oral cavity with sublingual BUP. However, an in vivo clinical study has demonstrated that the bioavailability of methadone was improved from 34 to 75% when the pH of oral cavity was changed from 6.5 to 8.5 [71]. The normal pH range for oral cavity is around 7.4, but eating or

drinking acidic food can decrease the pH of saliva and mouth, and therefore can decrease the absorption of sublingual buprenorphine. Also, a high percent of BUP in the saliva that is swallowed during the sublingual administration is subjected to extensive first-pass metabolism leading to low oral bioavailability of BUP. Buprenorphine is a lipophilic drug with a logarithm of the octanol to water partition coefficient (LogP) of 4.98 [70]. Due to its high lipophilicity, buprenorphine readily penetrates into tissues. In plasma, buprenorphine is highly bound (96%) to alpha and beta globulin [72]. The apparent volume of distribution at steady state of buprenorphine following intravenous administration is 335 L [67]. Buprenorphine has a variable plasma elimination half-life as shown in Table 1-1 with different formulations. The long half-life reported after subcutaneous injection is due to the slow and continuous release and absorption of buprenorphine from the depot tissue into the body. Following sublingual or transmucosal administration, the half-life is commonly reported in the range of 24-42 hours.

Table 1-1 Pharmacokinetic characteristics of different buprenorphine formulations approved by the FDA

Formulation	Indication	Dosage Strength	Absolute Bioavailability (%)	T _{max} (hrs)	Mean plasma elimination half-life	Reference
Buccal film	Severe pain	75, 150, 300, 450, 600, 750, 900 µg	46-65	0.5-4	27.6 hrs	Belbuca Label [73]
Injection (Intravenous/intramuscular)	Moderate to severe pain	0.3 mg/ 1 mL	100	0.25 [74]	1.2 – 7.2 hrs	Buprenex Label [75]
Transdermal system	Moderate to severe chronic pain	5, 10, 15, 20 µg /hrs	15	72	26 hrs (upon removal of path)	Butrans Label [76]
Buccal film (buprenorphine/naloxone)		2.1 mg/0.3 mg 4.2 mg/0.7 mg 6.3 mg/1 mg	Not reported (Bunavail has a higher bioavailability than Suboxone)	0.5 – 4.02 [74]	14.6 – 27.5 hrs	Bunavail Label [77]
Sublingual tablet	Maintenance treatment of	2, 8 mg	30-55 [67, 78]	1.28 - 1.84	31-35 hrs	Subtex Label [79]
Sublingual tablet (buprenorphine/naloxone)	opioid dependence	1.4 mg/ 0.36 mg 5.7 mg /1.4 mg	40% higher than Suboxone [80, 81]	1.75	24 - 42 hrs	Zubsolv Label [82]
Sublingual film (buprenorphine/naloxone)		2 mg/ 0.5 mg, 8 mg /2 mg, 16 mg /4 mg	46 – 51 [74]	1.25 – 1.72	35 - 37 hrs	Suboxone Label [72], Cassipa Label [83]
Implanted subdermal administration	Low-to-moderate opioid use disorder	74.2 mg/ 24 weeks	Not reported	12	13.7 - 23.8 hrs (upon removal implants) [84]	Probuphine Label [85]
Subcutaneous injection (Extended-release)	Moderate to severe opioid use disorder	100 mg/0.5 mL 300 mg/1.5 mL	Not reported	24	43 – 60 days	Sublocade Label [86]

Plasma clearance of BUP is around 50 L/h after an intravenous injection in healthy volunteers [74, 78, 87, 88]. The blood clearance of buprenorphine is approximate 80 L/hr (the blood to plasma ratio of buprenorphine is 0.6 [89]). Comparing BUP blood clearance with (the hepatic blood flow in healthy subjects (1.5 L/min), the estimated BUP hepatic extraction ratio is approximate 0.9, which indicates BUP to be a high hepatic clearance drug. For a high clearance drug given by oral route, the blood flow, the intrinsic clearance and the unbound fraction of a drug in blood will affect its oral clearance. Buprenorphine is N-dealkylated in the liver to norbuprenorphine, primarily by CYP3A4, which is further conjugated to norbuprenorphine glucuronide [90, 91]. A portion of BUP can also be directly conjugated to buprenorphine glucuronide. Overall, in addition to CYP3A4, and CYP2C8, and Uridine 5'-diphosphoglucuronosyltransferases (UGT1A1, UGT1A3, and UGT2B7) are also involved in buprenorphine metabolism. In vitro study have shown that the N-dealkylated metabolite, norbuprenorphine has high affinity to the mu-opioid receptor that is comparable to that of the parent compound ($K_i = 0.07$ nM) [92]. The high potency of norbuprenorphine to mu-opioid receptor might be a concern for respiratory depression, a common side effect caused by opioid agonists. However, both in vitro and in vivo studies have shown that norbuprenorphine is a substrate of P-glycoprotein 1 (P-gp) efflux transporter and the exposure of norbuprenorphine in the brain is minimal [93, 94]. In contrast, P-gp mediated transport of buprenorphine is very limited [93]. Although buprenorphine glucuronide and norbuprenorphine glucuronide have been shown in vitro to be biologically active, they are expected to have minimal clinical impact due to their high hydrophilicity and poor penetration into the brain [95].

With regards to the excretion of buprenorphine, a mass balance study has shown that following intravenous dosing of buprenorphine, a total of 69% and 30% of the radioactivity was

recovered in the feces and urine, respectively. The unconjugated buprenorphine and norbuprenorphine in feces probably comes from the hydrolysis of the conjugates of buprenorphine and norbuprenorphine that are secreted through the bile into the intestine [96].

1.2.3 Antagonist of mu-opioid receptor

Naltrexone

Naltrexone shows a much higher affinity to mu-opioid receptor than other opioids, including heroin, morphine, methadone and buprenorphine ($K_i = 0.3 \text{ nM}$) [97]. Naltrexone competes with other opioid agonists and occupies opioid receptors due to its higher affinity [98]. As a consequence, naltrexone blocks the euphoric effect of opioid agonists. Naltrexone can precipitate withdrawal symptom in patients who are physically dependent on opioids [99, 100]. Naltrexone has both oral and injectable long-acting sustained release formulations. Despite its effective blockage of opioids, clinical utility of naltrexone is hampered by poor patient retention, especially for its oral formulations [101]. The oral bioavailability of naltrexone ranges from 5 to 40% due to first pass metabolism. Naltrexone has a low extent binding to plasma protein (approximate 20%) and relative large apparent volume of distribution (1350 liters) [102]. The half-life of naltrexone is approximately 6 hours. After administration, naltrexone is extensively metabolized by dihydrodiol dehydrogenase, a cytosolic enzyme [103]. The major metabolite of naltrexone is 6- β -naltrexone, which also shows antagonistic effect at the mu-opioid receptor [104, 105]. The active metabolite, 6-beta-naltrexone has a much longer half-life (24.96 hrs) compared to its parent naltrexone (6 hrs) [106, 107].

Naloxone

Naloxone is a very potent ($K_i = 2.3 \text{ nM}$) mu-opioid receptor antagonist [108]. Naloxone is able to reverse the effects of opioid agonists, such as respiratory depression, by competitively occupying opioid receptors [109, 110]. After injection, the onset of action of naloxone occurs generally within 2 minutes. Naloxone has no effect following oral administration. Naloxone is directly conjugated to form its major metabolite, naloxone-3-glucuronide. A portion of administered dose also undergoes to N-dealkylation [111]. The mean plasma elimination half-life of naloxone is around 2 hours [112]. Due to its short half-life, naloxone is not used as a maintenance treatment of opioid addiction. Many studies have demonstrated that naloxone has no impact on the pharmacokinetics of buprenorphine [69, 88, 113]. Therefore, another clinical utility of naloxone is to prevent intravenous misuse of buprenorphine. Naloxone is added to buprenorphine sublingual formulation, as in Suboxone. Naloxone has minimal absorption following sublingual administration; however, it antagonizes the effects of opioid agonists when patients crush and inject the combination formulation.

1.2.4 Non-opioid Treatment

In 2018, the FDA approved lofexidine to facilitate abrupt opioid discontinuation by mitigating opioid withdrawal symptoms in adults. As an alpha-2 adrenergic agonist, lofexidine decreases norepinephrine release, thereby, lessens the withdrawal syndrome when patients stop taking opioid agonists [114, 115]. Lofexidine is not a treatment for opioid use disorder, but can be used as a treatment for management of opioid withdrawal symptoms during detoxification. The standard treatment duration of lofexidine is up to 14 days. After oral administration, the peak plasma concentration of lofexidine is observed around 3 to 5 hours [116]. The terminal elimination

half-life of lofexidine at steady state is 17-22 hours [116]. Lofexidine is extensively metabolized by CYP2D6 to form its major metabolite, 2,6-dichlorophenol [117]. Both lofexidine and its metabolites are mainly excreted via the kidney [117].

In conclusion, the current treatment for opioid addiction can be grouped into 3 categories, abstinence-based treatment (antagonist of μ -opioid receptor), maintenance-based treatment (agonist of μ -opioid receptor), and adjuvant treatment to facilitate abstinence of opioid (non-opioids). Although abstinence from opioid is the ultimate goal for treating opioid addiction, high rate of relapse in abstinence-based treatment has been reported [118]. The most effective approach for treating opioid addiction would be to gradually decrease methadone or buprenorphine-based maintenance treatment to abstinence. However, there is no clear consensus on how long a patient should receive the maintenance-based treatment before detoxification, as this approach is also associated with high rate of relapse [118].

1.3 Physiological changes during pregnancy

Pregnancy is a very unique status that induces many anatomical and physiological changes in the body to accommodate the development and growth of the fetus. These maternal changes and adaptations in pregnant women occur gradually, bound by certain limits without maternal damage and revert to nonpregnant baseline several weeks after delivery. The causal mechanism of all of these changes has not been totally understood, but many studies have found associations between regulation of hormones and physiological changes during pregnancy [119-121]. The summary of physiological changes during pregnancy are shown in Table 1-2.

Table 1-2. Physiological changes during pregnancy

System	Parameter	Non-pregnant	Pregnant (near term)
Placenta	Blood flow (mL/min) [122]	0	600-700
Uterine	Uterine artery blood flow (mL/min) [123]	50-100	500-1000
Cardiovascular	Cardiac output (L/min) [124]	4.8	7.2
	Stroke volume (mL) [124]	65	82
	Heart rate (beats/min) [124]	75	88
	Plasma Volume (L) [125]	2.6	3.5
Liver	Hepatic artery blood flow (L/min) [126]	0.57	1.06
	Portal vein (L/min) [126]	1.25	1.92
Renal	Glomerular filtration rate [mL/min] [127]	99	151
	Serum creatinine (mg/dL) [125]	0.7	0.5

1.3.1 Uterus

Uterus is the place where the fetus undergoes development and growth during the entire gestation. During pregnancy, uterus contains fetus, placenta and the amniotic sac. In order to provide nutrition, space and protection to the fetus, there is marked increase in uterine size and weight throughout the gestation. For example, uterine artery blood flow gradually increases from 50-100 ml/min in non-pregnant state to 500 – 1000 ml/min at 16th gestational week [123].

1.3.2 Placenta and fetus

Placenta is a temporary organ that develops in the uterus during pregnancy and is expelled from the body upon the birth of the baby. Placenta serves as an interface, which connects the fetus via the umbilical cord to the uterine wall on the maternal side. Placenta plays a critical role in the development and growth of the fetus. Placenta together with the umbilical cord are critical for the exchange of substances between the maternal and the fetal sides, e.g. diffusion of oxygen and carbon dioxide, supplying nutrients to fetus, and removal of waste products from the fetus. Placenta provides immunity to the fetus by transferring maternal immunoglobulins to the fetus. Placenta also serves as an endocrine organ by secretion of hormones that are essential for the development and growth of the fetus [128].

Although placenta is covered by a thick layer of syncytiotrophoblast and is considered to be a barrier separating maternal blood and fetal capillary endothelium, many substances can cross the placental barrier through passive diffusion, carrier-mediated transport or transcytosis [129]. Of the three mechanisms, passive diffusion is the predominate method of passage of chemicals

transplacentally for most lipophilic substances with molecular weight less than 600 Da, such as midazolam and paracetamol [128]. Both ATP-binding cassette (ABC) and solute carrier (SLC) family transporters are expressed in the placenta. For example, P-gp, also known as multidrug resistance protein 1 (MDR1), breast cancer resistance protein (BCRP) and multidrug resistance-associated protein 2 (MRP2) are identified in apical membrane of the trophoblast to efflux substrates from the syncytiotrophoblast to the maternal side. Whereas, MRP1 is found in the basolateral membrane of the trophoblast to transport substances to the fetal side. SLC transporter family members such as organic cation transporters (OCTs), organic anion transporters (OATs), and organic anion transporting polypeptides (OATPs) have also been identified in placenta recently (Figure 1-1) [130].

Besides transporters, several drug metabolizing enzymes have also been identified in the placenta. CYP1A, UGT1A and UGT2B are expressed in human placenta in the 1st trimester. The activities of UGT1A, UGT2B and CYP1A are significantly increased in the placenta of mothers who are smokers [131]. Other studies have also found that the types and abundance of CYPs are variable at different gestational ages and are impacted by maternal disease and social behavior [132, 133]. In full term placenta, CYP1A1, 2E1, 3A4, 3A5, 3A7, and 4B1 have been detected at the protein level. Unlike phase I enzymes, enzymes involved in phase II metabolism is less well studied in the placenta. The presence of UGT1 and UGT2 have been identified in both 1st trimester and full-term placenta. In vitro study has found that enzymes that are responsible for sulfation might also exist in placenta [134]. A summary of the enzymes in human placenta are shown in Table 1-3.

Many studies have reported the presence of CYP1A1, CYP1B1, CYP2C8, CYP2D6, CYP2E1, CYP3A4, CYP3A5, and CYP3A7 in the fetus [135]. Although these enzymes are present

in the placenta and the fetus, the metabolic contribution of these enzymes to the clearance of drug administered to the mother is expected to be minimal due to the small size of the fetus and the low abundance of enzymes in the placenta [135].

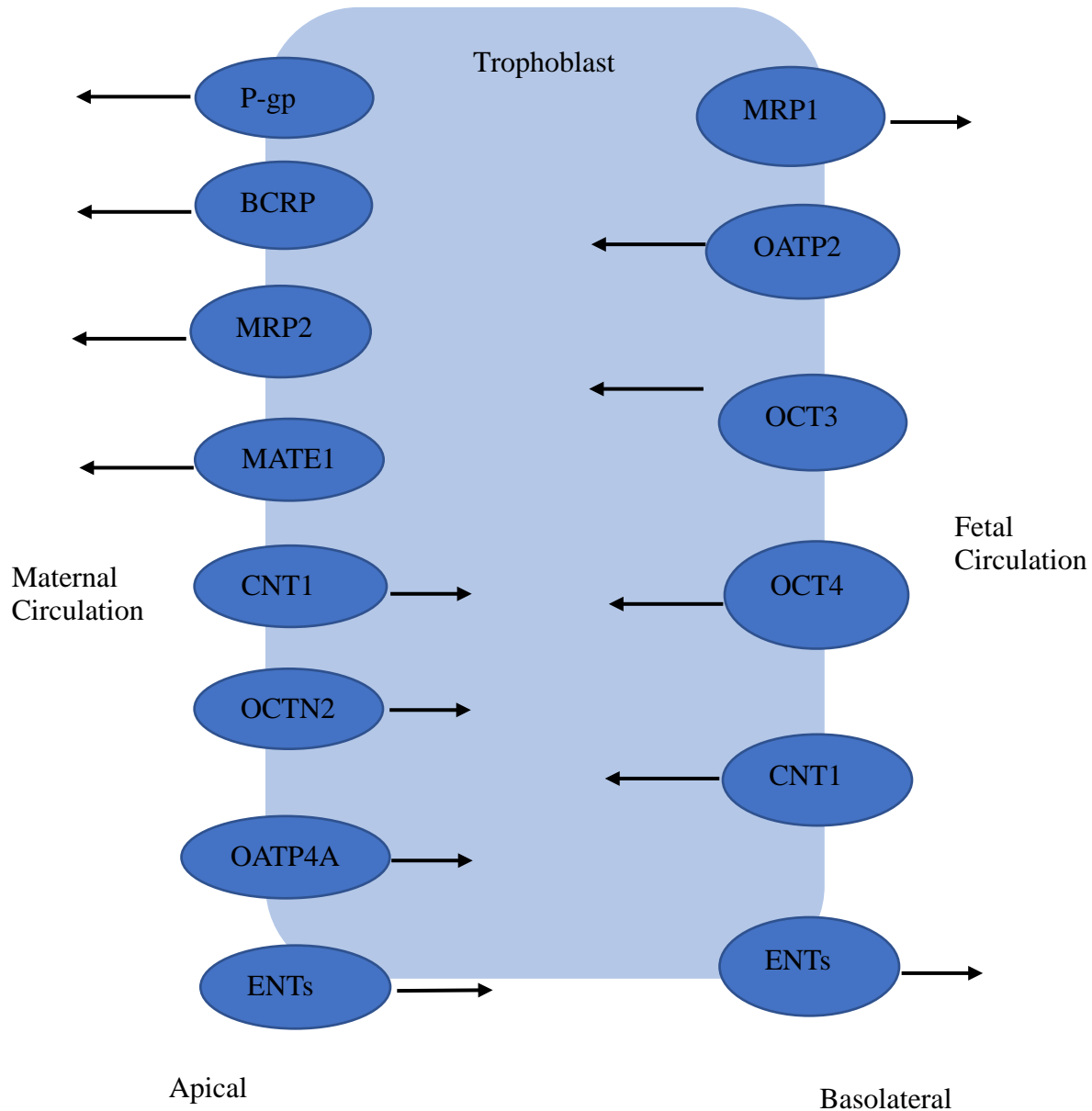


Figure 1-1. Drug transporters in placenta

Modified from reference [130]

BCRP, breast cancer resistance protein; MRP, multidrug resistance-associated protein, CRP, breast cancer resistance protein; BSA, – bisphenol A; CNT1, concentrative nucleoside transporter 1; ENTs, equilibrative nucleoside transporters; MATE1, multidrug and toxin extrusion protein 1; MRP1, multidrug resistance-associated protein 1; OATP2B1, organic anion-transporting polypeptide 2B1; OATP4A1, organic anion-transporting polypeptide 4A1; OCT3, organic cation transporter 3.

Table 1-3. Enzymes identified in human placenta ([131, 134-136])

Enzyme	1 st trimester	Full-term
CYP1A1	+	+
CYP2B6	?	+
CYP2C8	?	+
CYP2E1	-	+
CYP3A4/5	+	+
CYP3A7	+	+
CYP4B1	+	+
UGT1A	+	+
UGT2B4	+	+
UGT2B7	+	+

1.3.3 Cardiovascular system

In pregnant women, profound changes have been seen in the cardiovascular system including changes in blood volume, blood component, and systemic hemodynamics. During pregnancy, the total blood volume and the plasma volume increases by 40-50% [137]. Whereas, the increase of erythrocyte volume is less than the increase in the total blood volume and plasma volume (20 -30%) depending on iron supplementation [137]. The increases are linear within the first 6 weeks of gestational age and then gradually reach a plateau during 28 – 32 weeks of gestation. Normally, these parameters return to baseline by 6 weeks postpartum [137]. The increase in blood volume in the body is to adapt to the demands of blood and oxygen from the fetoplacental unit, as well as to prepare for potential blood loss at delivery. As there is a difference between the increases in plasma volume and erythrocyte volume, physiologic anemia is observed in pregnancy. Hematocrit decreases by 15 to 20 % compared to the value in nonpregnant women. Usually, the decline in erythrocyte volume occurs at 4 weeks after conception, and gradually reaches a maximum around 28 to 32 gestational weeks, and thereafter the hematocrit increases slightly before delivery [138]. Plasma protein levels also decrease during pregnancy. The concentration of plasma albumin decreases from 4.1 – 5.3 (non-pregnant adult), to 3.1 – 5.1, 2.6 – 4.5, and 2.3 – 4.2 g/dL at the 1st, 2nd, and 3rd trimester, respectively [139]. The concentration of plasma α 1-acid glycoprotein decreases from 0.74 (non-pregnant adult), to 0.73, 0.58, and 0.60 g/L at the 1st, 2nd, and 3rd trimester, respectively [140].

Cardiac output is the product of stroke volume and heart rate. In pregnancy, both stroke volume and heart rate are increased, which leads to an increase of cardiac output by 50% [124]. The cardiac output increases dramatically during 1st trimester and reaches a maximum at the end

of 2nd trimester [124]. The increase in cardiac output leads to an increase in blood flow to various tissues and organs, such as uterus, liver and kidney.

1.3.4 Liver

Liver is the largest solid organ in the body and plays critical roles in synthesis, metabolism and secretion. During pregnancy, portal vein blood flow is increased from 1.25 to 1.92 L/min and hepatic arterial blood flow is increased from 0.57 to 1.06 L/min [126]. Pregnancy has no or minimal impact on the size or structure of liver [141]. However, changes have been observed in the hepatic excretory, synthetic, and metabolic functions [141, 142]. Bacq et al. evaluated the changes of liver functions during pregnancy by comparing liver function tests in 103 healthy pregnant women and 103 age matched non-pregnant controls [143]. In the study, they observed that at fasting state, the serum concentrations of albumin, total and free bilirubin were significantly decreased, whereas, the serum concentration of aspartate transaminase (AST) and alanine transaminase (ALT) and serum concentration of total bile acid were not significantly changed during pregnancy [143]. Pregnancy induced changes in the activities of drug metabolizing enzymes are summarized in the section 1.4.3.

1.3.5 Renal system

During pregnancy, the renal system undergoes significant changes both in structure and function to adapt to the changes in cardiovascular system. The length of both kidneys increases by 1-1.5 cm with an increase in blood volume [144]. The renal blood flow increases by 35-60% [145]. The glomerular filtration rate (GFR) is dramatically increased in the 1st trimester and its reaches a

maximum of 180 ml/min around 16 weeks. Then GFR is maintained at the peak level until the 36th weeks of gestation [146].

1.4 Impacts of pregnancy on the pharmacokinetics of drugs

Pregnancy induces many physiological changes including the development of placental-fetal compartment, increase in renal glomerular filtration rate, body volume and hepatic portal blood flow, as well as alterations in drug metabolizing enzyme and transporter mediated drug disposition [125, 145, 147]. These pregnancy-induced physiological changes can impact drug absorption, distribution, metabolism, and elimination [148].

1.4.1 Absorption

Absorption is the movement of a drug from the site of administration to the bloodstream. For an orally administered drug, absorption is the process of the movement of a drug from the gut lumen into the enterocyte in the gut wall. In other words, the fraction of the administered dose that is not lost in the feces nor decomposed in the gut lumen is the fraction that is absorbed (F_a). The primary mechanisms involved in movement of a drug molecule across the cell membrane include passive diffusion, protein-mediated transport, and endocytosis/exocytosis [149]. Passive diffusion is an important and the most common means by which many drugs cross cell membranes. The process of passive diffusion is driven by the concentration gradient of a drug on either side of cell membranes. Protein-mediated transport can be either passive (facilitated diffusion) or active. In the process of facilitated diffusion, the carrier proteins transport drugs in the direction of

concentration gradient with no energy requirement. For the means of active transport, the translocation of drugs is against a concentration gradient and the process is associated with energy expenditure [150]. Endocytosis/exocytosis also needs energy and is an important transport mechanism for large macromolecules such as protein drugs. Active transport plays an important role in drug transport by regulating movement of drug molecule across cell membrane. Multiple drug transporters are present in the intestinal epithelia such as efflux transporters like MDR1, BCRP, and MRP2, and uptake transporters like organic anion transporting polypeptide (OATP), Peptide (PEPT) 1, and monocarboxylate (MCT) 1 [151-153]. Several studies have shown that polymorphism in MDR1 is associated with altered absorption of digoxin and fexofenadine [154, 155]. Changes in absorption due to transporters result in alterations in systemic exposure of drugs and may lead to toxicity or underdosing. The impact of pregnancy on the regulation of drug uptake or efflux transporters has not been well studied.

Additionally, the gastric motility and emptying, food, as well as diseases that affect gastrointestinal physiology could also impact drug absorption. During pregnancy, the decrease in gastric emptying and intestinal motility may result in a decrease in drug absorption rate.

After a drug is absorbed into the intestinal wall, it is transported through the portal vein into the liver. From the liver, the drug is carried to the inferior vena cava, then to the heart, lung and systemic circulation [156]. Due to the presence of enzymes in the gut and liver, a drug may undergo extensive first-pass (presystem) metabolism before reaching the systemic circulation after oral administration. The overall systemic availability (bioavailability, F) of a drug after oral administration is the product of the fraction being absorbed (F_a), the fraction escaping metabolism in the gut wall (F_g), and the fraction escaping metabolism in the liver (F_h). The bioavailability of a drug used during pregnancy may be decreased or increased depending on how the activity of

metabolic enzymes involved in the biotransformation of a drug are altered during pregnancy in the gut and liver. For examples, if a drug is a substrate of CYP3A, the bioavailability of the drug for oral administration may be decreased due to the increase in the activity of CYP3A4 during pregnancy, such as the case with midazolam [157]. Bioavailability can also be altered by changes in uptake and efflux transporters in the gut wall. $F = F_a \times F_g \times F_h$.

1.4.2 Distribution

After a drug enters the body, it distributes to various tissues. The extent of a drug distribution in the body is determined by its lipid solubility (LogP), pKa, and partition between plasma and tissues (K_p). The partitioning of a drug between plasma and tissue is affected by fraction of the drug that is bound to plasma because only the unbound drug can cross cell membranes. The volume distribution (V) is a useful indicator to characterize the extent of drug distribution throughout the body. Volume of distribution is an apparent parameter that relates amount of drug available in the body to its concentrations in blood or plasma. A drug with a volume of distribution of 3 – 5 L implies that most of the administered dose stays within the vascular system and may be highly bound to plasma proteins. For drugs that have large volume of distribution, most of the administered dose stays outside of the vascular system and the drug may be highly bound to the tissues.

Pregnancy increases body fat, total body water, plasma volume, and blood volume. Pregnancy decreases plasma protein concentrations. In pregnancy, the plasma concentration of albumin decreases up to 13% compared to nonpregnant women [125]. The level of alpha1-acid glycoprotein (AAG), which binds basic drugs, is also decreased during pregnancy. As a result of

the decrease in plasma protein concentrations, unbound fraction of a drug will be increased. The apparent volume of distribution of a drug can be calculated as follows

$$V = V_p + \frac{f_{u,P}}{f_{u,T}} \times V_T$$

Where V is the apparent volume of distribution of drug, V_p is the plasma volume, V_T is the total body water minus the plasma volume, $f_{u,P}$ is the ratio of unbound and total drug concentrations in plasma, $f_{u,T}$ is the ratio of unbound and total drug concentrations in tissues.

Therefore, the increase in plasma volume, total body water and a decrease in plasma protein concentration during pregnancy can lead to an increased volume of distribution of certain drugs.

1.4.3 Metabolism

After entering the systemic circulation, a drug is eliminated from the body by metabolism and/or excretion of the parent drug. Drug metabolizing enzymes are widely expressed in various tissues and organs such as the intestinal tract, placenta and kidney, but the liver is the organ that is primarily responsible for the metabolism of most drugs. The hepatic clearance of a drug is influenced by hepatic intrinsic clearance, hepatic blood flow and unbound fraction of drug in the blood. The intrinsic clearance of a drug is determined by the affinity of the drug molecule and the drug metabolizing enzymes, and the abundance of the enzymes. The hepatic extraction ratio (E), characterizes the fraction of the drug that is extracted during single passage, and can be calculated as $((C_a - C_v)/C_a)$, where, C_a is the drug concentration in the arterial blood flow before entering the liver; C_v is the drug concentration in the venous blood leaving the liver. For low clearance drugs ($CL \leq 300$ mL/min) or drugs with low extraction ratio ($E \leq 0.2$), hepatic clearance after intravenous administration is determined by intrinsic clearance and unbound fraction of drug in plasma. For

high clearance drugs ($CL \geq 1050$ mL/min) or drugs with high extraction ratio ($E \geq 0.7$), hepatic clearance after intravenous administration is determined by hepatic blood flow. For intermediate clearance drugs, hepatic blood flow, intrinsic clearance and the unbound fraction of drug in plasma will determine the hepatic clearance.

The effect of pregnancy on hepatic metabolism is drug specific. For a high clearance drug administered by intravenous route, the hepatic clearance is increased due to a significant increase in hepatic blood flow in pregnancy. For a low clearance drug administered by intravenous route, the hepatic clearance is impacted by the changes in specific enzyme activities (intrinsic clearance) and unbound fraction of the drugs in plasma. During pregnancy, the metabolism of drugs mediated by cytochrome P-450 (CYP) 2C9, CYP2D6, CYP3A4, UGT1A4, and UGT2B7 are increased, whereas the metabolism of substrates of CYP1A2 and CYP2C19 are decreased [158]. The mechanism of the changes in the enzyme activities during pregnancy is not completely understood, but many studies have reported association between the activity of drug metabolizing enzymes and hormones levels [158, 159]. The potential mechanism may involve changes in the expression and/or activities of drug metabolizing enzymes that are regulated by different transcriptional factors which are modulated by the altered levels of circulating hormones in the blood during pregnancy [158]. Table 1-4 summarized pregnancy induced changes in drug metabolizing enzyme activities.

1.4.2 Excretion

Kidney is one of the primary organs that eliminate parent drugs and metabolites from the body. The mechanisms of renal excretion include glomerular filtration, tubular secretion and reabsorption. Numerous endogenous and exogenous substances undergo glomerular filtration with

or without secretion and reabsorption. The filtration and reabsorption are passive processes, whereas, secretion is mediated by drug transporters. Normally, only unbound drugs can be filtered by the nephrons. For a drug with filtration as the only mechanism of renal clearance, the renal clearance is a product of the glomerular filtration rate (GFR) and the unbound fraction (f_u). The GFR is increased from 97 ml/min in non-pregnant women to 180 ml/min in pregnancy women [146]. Also, as mentioned before, the unbound fraction of a drug is increased due to the decrease of plasma protein concentration. The renal clearance of a drug such as cefazolin and lithium are known to be increased in pregnancy. (Table 1-5).

In addition to the increase in renal filtration, clinical evidence of increase in active secretion has also been reported in pregnant women. Using digoxin as a probe, Hebert et al. reported an increase in the renal secretion of digoxin mediated by P-gp (1.97-fold at 3rd trimester in comparison to postpartum period) [157]. The renal secretion of metformin increased to 1.53- and 1.34-fold at 2nd and 3rd trimesters. The observed increase in metformin secretion may due to the enhanced activity of renal OCT2 [160]. However, metformin is not a specific substrate for OCT2. It is also a substrate of renal OCT1, and the multidrug and excursion pump (MATE). The observed results might be confounded by the other factors as well.

In summary, pregnancy induces many anatomical and physiological changes. These changes may have extensive impacts on absorption, distribution, metabolism and elimination of drugs used in pregnancy. The alteration of drug pharmacokinetics may result in changes in efficacy and toxicity of drugs used in pregnant women. Many clinical studies have reported significant changes in systemic exposure of certain drugs used during pregnancy [161-163]. Table 1-5 shows

the summary of pregnancy induced physiological changes and potential impacts on pharmacokinetics of drugs.

Table 1-4. Pregnancy induced changes in drug metabolizing enzyme activities

Isoform of Enzyme	Clinical Probe	Gestation vs Postpartum			Example of clinical evidence	Reference
		1 st Trimester	2 nd Trimester	3 rd Trimester		
CYP1A2	Caffeine	↓	↓	↓	The increase in metabolic/parent of renal excretion	[164]
	Caffeine	↓	↓	↓	The decrease of oral clearance of caffeine	[165]
CYP2C19	Proguanil			↓	Plasma concentration of cycloguanil (CYP2C19 mediated biotransformation of proguanil) decreased by 42% of its value at postpartum.	[166]
CYP2D6	dextromethorphan	↑	↑	↑	The increase in dextromethorphan O-demethylation	[165]
	Metoprolol			↑	CL _{iv} increased 2.12-fold	[167]
CYP3A	Midazolam			↑	Unbound CL/F increased 2.1-fold	[157]
	dextromethorphan	↑	↑	↑	The increase in dextromethorphan N-demethylation	[165]
UGT1A4	lamotrigine			↑	The decrease in plasma concentration of lamotrigine	[168]

Table 1-5. The summary of pregnancy induced physiological changes and potential impacts on pharmacokinetics of drugs

Pharmacokinetic characteristics	Pregnancy induced physiological change	Potential impacts to drug pharmacokinetics	Example
Absorption	<p>↓ gastric emptying and gastrointestinal motility, ↑ in gastric pH ↑ in gastrointestinal blood flow Alterations of transporters Alterations of enzymes</p>	<p>↓ or ↑ rate of absorption ↓ or ↑ bioavailability</p>	<p>Midazolam C_{max} decreased by 28% at 3rd trimester compared with postpartum period [137]. The urinary recovery of metoprolol and its metabolites were higher during pregnancy than postpartum [167].</p>
Distribution	<p>↑ in total body water and fat ↓ in plasma protein concentration</p>	<p>↑ in volume of distribution</p>	<p>The volume of distribution of metoprolol following intravenous administration were increased to 1.78-fold during pregnancy [167].</p>
Metabolism	<p>↑ in cardiac output ↑ in portal vein and hepatic blood flow Alterations of enzymes Alterations of transporters</p>	<p>↑ or ↓ in metabolism</p>	<p>The decreased clearance of caffeine mediated by CYP1A2 in pregnancy [164]. The increase in the clearance of metoprolol mediated by CYP2D6 at 3rd trimester [167].</p>
Excretion	<p>↑ in renal blood flow ↓ in plasma protein concentration Alterations of enzymes Alterations of transporters</p>	<p>↑ in renal filtration ↑ or ↓ in renal active secretion</p>	<p>The systemic exposure of cefazolin after intravenous administration of same dose was 70% of that value of postpartum [169]. In pregnancy, the clearance of lithium was approximately 2 times of that value at postpartum [170]. The unbound renal secretion of digoxin was increased from 58 (postpartum) to 109 mL/min (28 – 32 weeks gestation) [171] due to the induction of P-gp activity during pregnancy. The renal secretion of amoxicillin was increased from 0.167 (postpartum) to 280 L/min (2nd trimester) due to the induction of OAT1 activity during pregnancy.</p>

1.5 The prediction of pregnancy induced pharmacokinetic changes of drugs based on Biopharmaceutics Classification System

The Biopharmaceutics Classification System (BCS) was first introduced by Amidon et al. [172]. Based on aqueous solubility and permeability of drugs, the BCS classified drugs into four categories as follows.

Class 1: High solubility and high permeability

Class 2: Low solubility and high permeability

Class 3: High solubility and low permeability

Class 4: Low solubility and low permeability

According to the FDA guidance, a drug is considered highly soluble when the highest strength of a drug product is soluble in 250 mL or less of aqueous media within the pH range of 1 - 6.8 at $37 \pm 1^\circ\text{C}$; and highly permeable when the extent of absorption of a drug product in humans is at least 85 % of the administered dose based on a mass balance determination or in comparison to an intravenous reference dose [173]. Alternatively, drugs with the lowest solubility in aqueous solution being $> 200 \mu\text{g/mL}$ over a pH range of 1–7.5 at 37°C would be considered as to be highly soluble [174]. Benet suggested that the cutoff values for low and high permeability to be < 2.0 or $\geq 3.5 \times 10^{-6} \text{ cm/s}$, respectively, when artificial membrane permeability assay is used to measure the permeability of a drug [174]. The BCS system is widely used to establish in vitro - in vivo correlations and to predict absorption of a drug product. In 2004, Wu and Benet extended the BCS to a Biopharmaceutics Drug Disposition Classification System (BDDCS) to predict the overall in vivo drug disposition based on solubility and permeability of drugs [175]. The BDDCS classified

drugs into four categories as same as BCS. In BDDCS, drugs with high permeability categorized to class 1 and 2 of BCS undergoes extensive metabolism by enzymes, whereas, drugs with low permeability categorized to class 3 and 4 of BCS, are eliminated primarily by renal and /or biliary excretion as unchanged drugs [175]. With regard to the involvement of transporters in the disposition of drugs, for drugs in the class 1 of BCS (high solubility and high permeability), the effects of transporters are minimal in both gut and liver, but the impacts of transporters might be seen in class 2, 3 and 4 of BCS [174].

Based on the physiological changes induced by pregnancy as described in previous sections, we predicted that the metabolism of drugs in BCS class 1 and 2 may be increased due to the increase in hepatic elimination capacity, whereas the clearance of drugs in BCS class 3 and 4 may be increased due to the increase in renal clearance. No study has reported the aqueous solubility of BUP, however, the solubility of BUP in water should be minimal due to its high lipophilicity ($\text{LogP} = 4.98$) [70]. The permeability of BUP in a Caco-2 cell membrane system is 44.7×10^{-6} cm/s [176]. Buprenorphine can be classified as a BCS class 2 drug with low solubility and high permeability. As a BCS class 2 drug, BUP undergoes extensive hepatic metabolism with minimal renal elimination of the parent drug. The increase in hepatic elimination capacity in pregnancy will increase BUP clearance during pregnancy.

1.6 Pharmacotherapy of opioid use disorder in pregnant women

The 2010 National Survey on Drug Use and Health by the National Institutes of Health (NIH) on drug abuse reported a 47% increase in illicit drug use during pregnancy since 2002 (4.4% in 2010 versus 3% in 2002 between the ages of 15 and 44 of pregnant women) [177]. The term

"illicit" refers to the use of illegal drugs, including marijuana, and the misuse of prescription medications, such as cocaine, benzodiazepines, and opiates. During the last decade, Marijuana use has increased 62% in reproductive-aged women [178]. The use of opioids during pregnancy can result in a drug withdrawal syndrome in the newborns called neonatal abstinence syndrome (NAS). Since 2000, there has been a five-fold increase in the number of babies born with NAS [179].

Maternal opioid use is associated with increased obstetrical complications, such as maternal death, cardiac arrest, intrauterine growth restriction and placental abruption [180]. Moreover, antepartum use of opioids results in neonatal abstinence syndrome (NAS), birth defect, stillbirth, and preterm labor [181, 182]. It would be ideal to abstain from opioids throughout the course of pregnancy. However, there are risks associated with stopping opioids in pregnant women as the mother may undergoes intense withdrawal during detoxification. Also, the stress derived from the abstinence in the mother may result in intrauterine stress, which may lead to preterm labor, as well as impact the development and growth of the fetus [183]. Successful detoxification have been reported in several studies [183-185]. However, analysis has found that there were high rates of relapse in these patients [186]. Therefore, detoxification is not a common treatment option in pregnant women with opioid use disorder. Any decision regarding detoxification should be made after full evaluation of the history and severity of substance use disorder in patients and for the best outcomes for both the mother and the fetus.

Currently, the most common treatments for opioid use disorder in pregnant women are medication-assisted maintenance therapy using long-acting μ -opioid receptor agonists such as methadone or buprenorphine [187]. Methadone has been used for decades and many studies have shown the effectiveness of methadone for treating opioid use disorder in pregnant women. Altered metabolism of methadone in pregnant women has been reported by several investigations [188-

190]. For example, Pond et al. studies the PK of methadone at 20 – 34 (phase I), 35 – 40 weeks of gestation (phase II), 1 – 4 weeks (phase III), 8 – 9 weeks (Phase IV) at postpartum in 9 pregnant women who were receiving methadone maintenance therapy. The apparent clearance of methadone was significantly higher during pregnancy than postpartum (311 (phase I) and 256 (phase II) ml/min vs 161 (phase III) and 155 (phase IV) ml/min) [189]. Wolff et al. have also reported alteration in the metabolism of methadone in pregnancy. In the study, they found that the weight adjusted clearance of methadone were 0.17, 0.19, 0.21, and 0.11 L/hr/kg at 1st, 2nd, 3rd trimester and postpartum, respectively[190]. Despite patients taking higher dose of methadone during pregnancy, the trough plasm concentrations and plasma exposures (as measured by AUC) of methadone were lower during pregnancy [190]. The higher maternal methadone dose has been correlated with higher incidence of NAS [191]. Albright et al. studied changes in methadone dose in a single cohort longitudinal study in 139 pregnant women [192]. There was a gradual increase in methadone dose over gestation, and the mean increase in methadone dose was 24 mg [192]. It has been reported that 60 - 80% of newborns undergo NAS after intrauterine exposure to methadone [193]. However, most of the studies were performed in a small cohort, and are nonrandomized or had no control population.

As a pharmacotherapy approved by the FDA for opioid addiction, buprenorphine has comparable efficacy to methadone [194-196]. Recently, studies have found that buprenorphine crosses placenta and buprenorphine exposed neonates may have less severity and lower incidence of NAS [136, 182, 197]. Buprenorphine-exposed neonates require, on an average, 89% less morphine to treat neonatal abstinence syndrome, a 43% shorter hospital stay, and a 58% shorter duration of medical treatment for neonatal abstinence syndrome compared to methadone [198].

These results support the use of buprenorphine as a potential first-line medication for pregnant opioid-dependent women.

1.7 The current dosing issue of buprenorphine in pregnancy

In order to evaluate the safety and efficacy of maternal and prenatal exposure to buprenorphine and methadone, Jones et al conducted a double blinded and double randomized clinical study. In the study they found that 28 of 86 (33%) patients in the buprenorphine group terminated treatment early compared to 16 of 80 patient (18%) in the methadone group. Seventy one percent of the dropout was due to patient dissatisfaction with the buprenorphine treatment. However, in non-pregnant population, there were no significant difference in patient retention between the intermediate and high dose buprenorphine group and methadone groups during opioid maintenance treatment based on a meta-analysis of 31 clinical studies [199]. In addition, analysis in a Pennsylvania state Medicaid program among 2361 pregnant women receiving buprenorphine treatment have found that 40% of these patients had low-to-moderate adherence, early discontinuation, or showed declining adherence. Lower BUP daily dose has been found to be a factor that is associated with early discontinuation [200]. As limited data are available on the alterations of buprenorphine pharmacokinetics and pharmacodynamics during pregnancy, the dosing regimen of buprenorphine in pregnant women are commonly based on the recommendations in non-pregnant women and men.

Clinical observations in Magee Womens Hospital Pittsburgh indicate an increase in buprenorphine dose requirement during pregnancy [201]. Another clinical study that compared the efficacy of buprenorphine and methadone in pregnant women showed 30% of the patients

converted to buprenorphine failed at start, and 71% of them to dropout because of dissatisfaction with buprenorphine [202]. On the published studies, the reported doses of buprenorphine given to pregnant women ranged from 0.4-24 mg/day [203]. We speculate that the lack of clear consensus and the broad dose range may result in dosing bias by individual physician and in turn affect the retention of pregnant women in buprenorphine therapy. As mentioned before, both intrinsic clearance and hepatic blood flow can impact buprenorphine clearance. We predict that pregnancy is associated with increased clearance and decreased exposure of buprenorphine due to enhanced cardiac output, hepatic blood flow, and increased expression and activities of CYP3A4, UGT1A1, and UGT1A3 [165, 204, 205]. Therefore, a better understanding of pregnancy-medicated changes in pharmacokinetics of buprenorphine, as well as the relationship of buprenorphine pharmacokinetics and pharmacodynamics are critical to optimize dosing of buprenorphine in pregnant women. Another challenge in dosing buprenorphine in pregnant women is the need to balance drug exposure in the mother and the fetus. When using buprenorphine as maintenance treatment in pregnant women, the treatment goal is to maximally inhibit drug withdrawal, craving and illicit opioid use with a minimum drug exposure to the fetus.

1.8 The pharmacokinetic and pharmacodynamic relationship of buprenorphine

The Clinical Opioid Withdrawal Scale (COWS) is a common tool used in clinical practice to assess opioid withdrawal. The COWS has both subjective and objective components. For example, the patients are asked about the presence of gastrointestinal upset, bone or joint aches, etc. during evaluation of the severity of drug withdrawal. Therefore, the COWS score is highly impacted by patients' responses to certain questions and can be manipulated by the patients. More

studies are needed to further validate the reliability of COWS for detecting withdrawal. As a maintenance therapy to treat opioid substance dependence, buprenorphine has to cross the brain–blood barrier and bind to mu-opioid receptors in the brain. The ideal marker to assess opioid withdrawal would be buprenorphine concentration in the brain and mu-opioid receptor occupancy. Greenwald et al. have studied the mu-opioid receptor occupancy in the brains of heroin-dependent patients using positron emission tomography (PET) scan and suggested that 50% mu-opioid receptor occupancy is needed to suppress drug withdrawal symptoms in patients [206]. However, it is not feasible to measure buprenorphine brain concentration or the occupancy of mu-opioid receptor in pregnant women. We would like to explore objective physiological measurements, mediated by mu-opioid receptor binding in brain, as a surrogate to mu-opioid receptor occupancy in order to optimize buprenorphine dosing in pregnant women.

Pupillary size is determined by the dilation or constriction of iris through sympathetic and parasympathetic nervous system. Opioids induced pupillary constriction has been observed in human, rabbits and dogs and pupillary dilation are seen in rats, mice, and cats. It has been shown that opioid induced miosis and mydriasis are opioid receptor-mediated as the effects can be blocked by mu-opioid receptor antagonist, naloxone [207]. Currently, the exact site of action is not clear, but it is believed that the site of action should be within the brain as no pupillary effect was observed by intraocular administration of an opioid like morphine. In addition, the effective dose of morphine that causes changes in pupillary size following an intracerebroventricular injection was one hundredth of the intravenous dose [208, 209]. The possible mechanism of the pupillary constriction by opioids may be through the suppression of the inhibitory process of Edinger-Westphal nucleus, a place in midbrain that regulates signal to iris muscle resulting in pupillary constriction [210]. Several studies have reported that pupillary constriction is correlated

with opioid concentration in plasma and higher plasma opioid concentrations result in more pronounced effects on pupillary constriction [211-215]. Use of pupillometry as a marker to optimize dosage of opioids for pain management has been reported [216, 217]. Multiple clinical studies and our preliminary in-house data in pregnant women have demonstrated that buprenorphine can induce pupillary constriction [212, 213]. So, we plan to evaluate the association between the plasma concentration of buprenorphine and pupillary diameter in pregnant women maintained on buprenorphine.

1.9 Difficulty in performing pharmacokinetic studies in pregnant women and alternative approaches to evaluate pharmacokinetics in pregnancy

Given that anatomical and physiological changes during pregnancy, the pharmacokinetics of several drugs are expected to be altered in pregnant women. Modulations in pharmacokinetics of drugs may result in toxicity or lack of efficacy. To study the pharmacokinetics of a drug, a sufficient number of blood samples should be collected to determine the time course of absorption, distribution, metabolism and excretion from each subject. Usually, a pharmacokinetic study requires 9-12 blood samples from each subject over a 3-5 half-lives of a drug. Such intensive blood sampling and the long duration of a PK study adds another practical difficulty in studying PK of drugs in pregnant women. Several approaches may be considered as an alternative to a full PK study in pregnant women.

Limited sampling strategy has been proposed by many investigators. In these studies, drug concentrations at a single time point or abbreviated blood sampling period are used to estimate drug exposures within a dosing interval. For example, Mathew et al. reported a two-point limited

sampling strategy for tacrolimus in stable renal transplant patients. They found that combining the whole blood concentration of tacrolimus at trough and at 1.5 hrs after a dose, or trough and 4 hrs after dose it was possible to estimate AUC_{0-12} of tacrolimus (Regression coefficient was 0.951) [218].

The trough concentration (concentration before the next dose) of a drug at steady state often shows good correlation with drug exposure during a dosing interval, therefore, determination of trough concentration is a common approach used in therapeutic drug monitoring. In our previous study, we found the trough concentrations of BUP to be correlated well with BUP exposure (as measured by AUC) at steady state during the dosing interval of 12 hrs (Figure 1-2) [201].

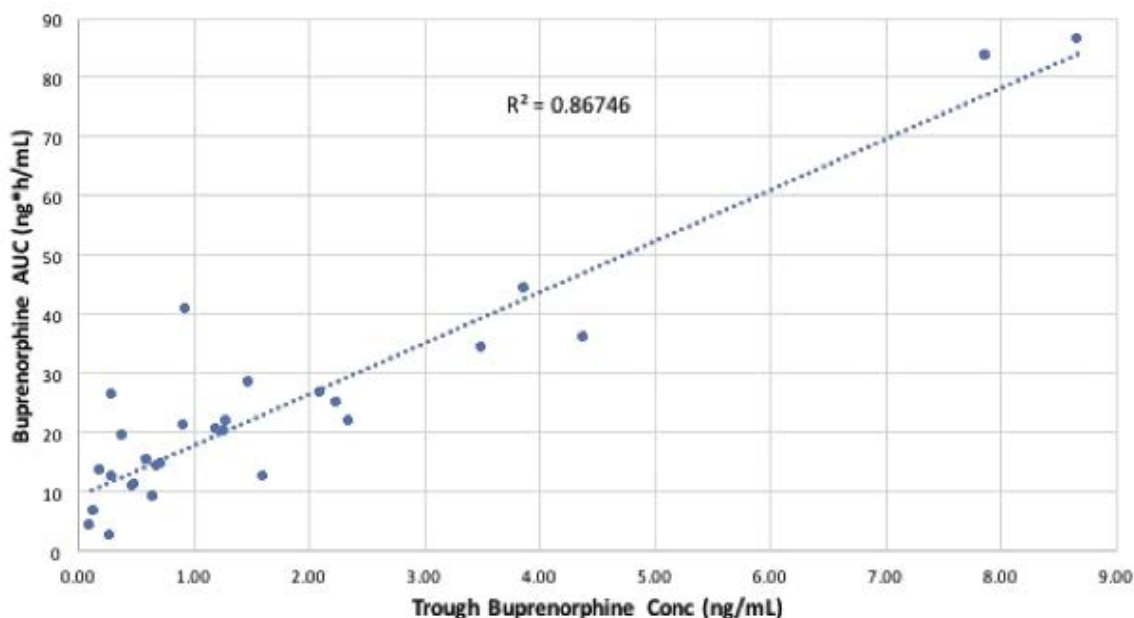


Figure 1-2. Relationship between buprenorphine trough concentration and overall exposure (AUC_{0-12}) at steady state in pregnant women [201]

Physiological-based pharmacokinetic (PBPK) modeling is a sophisticated PK modeling approach that incorporates every major tissue type as a separate physiological compartment. Organ size, organ composition, blood flow, abundance and relative expression of drug metabolizing enzymes and drug transporters, genetic variants of drug disposition proteins, differences between sexes, age dependent ontogeny and other physiological parameters are incorporated when performing PBPK modeling [219]. Physiologically-based pharmacokinetic modeling has been successfully applied to answer some clinical pharmacological questions such as the alteration of PK in pediatric patients and drug-drug interaction. Recently, several PBPK models have been developed to estimate the exposure of opioids such as morphine, methadone and fentanyl in patients [220-223]. Ke et al. have developed a pregnancy PBPK model in which gestational age associated with physiological changes such as cardiac output, GFR and the activities of drug metabolizing enzymes were incorporated into the non-pregnant PBPK model [220]. This PBPK model has successfully predicted an approximate 50 % decrease in the AUC and C_{max} of methadone in the 2nd and 3rd trimester compared to the postpartum period [220]. The PBPK modeling approach provides us an alternative to predict pharmacokinetic alteration of a drug in special patient populations such as pregnant women by incorporating longitudinal physiological changes.

Population PK modeling has the ability to combine and analyze data from limited sampling in each patient. Data from several subjects are pooled together and modeled simultaneously, so there is no need for a full PK sampling in each individual. This feature is one of the advantages of utilizing population PK analysis in pregnant women. Due to two layers of random effects (parameter level and dependent variable level), variance estimation in a population pharmacokinetic modeling analysis is more precise than traditional PK analysis. Additionally,

population PK modeling is a powerful pharmacostatistical methodology to identify and quantify sources of variability in drug disposition in particular patient population. Population derived pharmacokinetic parameters such as clearance and volume of distribution, as well as associations between patient characteristics and differences in pharmacokinetics can be used to guide prescribing for individual patients. Using population PK/PD modeling, we can study the changes in response to a drug with altered drug PK profiles in different circumstances in patients, which is critical for a decision to change the dosing regimen in patients.

1.10 Hypothesis and Objectives

The goal of this study was to optimize buprenorphine dosing in treating opioid addiction in pregnant women through a better understanding of the effect of pregnancy on BUP exposure. Between 2000 and 2009, the rate of opioid use in pregnant women had increased nearly 5-folds. Maternal opioid use is associated with increased obstetrical complications and also results in neonatal abstinence syndrome. During this period, there was a five-fold increase in the number of babies born with NAS. The efficacy of buprenorphine in suppressing withdrawal symptoms appears to be comparable to methadone. Additionally, neonates may have less severe and a lower incidence of NAS after exposure to buprenorphine compared to methadone. Due to abuse potential, patients are required to go to the clinic daily to receive methadone as a maintenance treatment. As a partial mu-opioid receptor agonist, buprenorphine has less abuse potential compared to methadone. Upon the approval of Drug Addiction Treatment Act 2000, buprenorphine has been used as an office-based treatment for opioid addiction since 2002. As an office-based treatment, qualified physicians can prescribe buprenorphine to patients for treatment of opioid addiction bi-weekly or monthly. As a result, receiving buprenorphine as maintenance treatment of opioid dependence is more convenient for patients than methadone, which can potentially improve patient compliance and retention. However, a large cohort of clinical trial that compared the efficacy of buprenorphine and methadone in pregnant women reported that 30% of the patients converted to buprenorphine failed at start, and 71% of them dropout due to dissatisfaction with buprenorphine. This is likely due to the lack of clear consensus on buprenorphine dosing in pregnant women as the current dosage regimen is based on the recommendations in non-pregnant women and men. It is well known that pregnancy is associated with various physiological changes that can potentially alter buprenorphine disposition and brain distribution and impact on the efficacy of buprenorphine

in treating opioid addiction. Use of medications during pregnancy without titration of its dose to account for pregnancy induced altered physiological condition may lead to therapeutic failure or drug related toxicities. As of today, limited information is known about pregnancy mediated changes in the pharmacokinetics and pharmacodynamics of buprenorphine. We hypothesize that model-based analysis can predict alterations in the clearance and exposure of drugs used during pregnancy and can substitute for drug exposure studies which are difficult to perform in pregnant women. Buprenorphine will be used as an example to illustrate the applications of model-based analysis to predict changes in drug clearance across different trimesters in pregnancy.

Through the proposed experiments, we systematically evaluated the impact of pregnancy induced physiological changes on the alterations of pharmacokinetics and pharmacodynamics of buprenorphine. This hypothesis was tested through five specific aims. First, we established and validated a simple and sensitive ultra-performance liquid chromatography - tandem mass spectrometer (UPLC-MS/MS) assay for quantification of buprenorphine and three primary metabolites (norbuprenorphine, buprenorphine glucuronide, and norbuprenorphine glucuronide) in patient plasma samples. Using this assay, we measured the plasma concentrations of buprenorphine and its three metabolites in pregnant women at different trimesters of pregnancy. Additionally, we compared the alterations of buprenorphine pharmacokinetics, as well as the modulations of biotransformation of buprenorphine via N-demethylation and glucuronidation in a small cohort (Chapter 2). Second, we built and validated robust PBPK models using Simcyp® population simulator for intravenous and sublingual buprenorphine in non-pregnant subjects. The proposed PBPK model predicted the time course of buprenorphine systemic exposure with different dosing regimen of buprenorphine in non-pregnant subjects (Chapter 3). Third, we developed a full physiologically-based pharmacokinetic (PBPK) model for buprenorphine in

pregnant women, to predict changes in buprenorphine exposure at different stages of pregnancy, and to demonstrate the utility of PBPK modelling in optimizing buprenorphine pharmacotherapy during pregnancy. In this study, anatomical and gestational changes in physiological parameters were incorporated. Buprenorphine plasma concentrations measured in pregnant women vs time profiles were used to verify the model predicted buprenorphine plasma concentrations (Chapter 4). Fourth, we developed a population PK model to evaluate the changes in buprenorphine PK during pregnancy and to identify potential patient covariates that may influence buprenorphine PK during pregnancy in an attempt to optimize dosing of buprenorphine in pregnant women (Chapter 5). The final aim was to evaluate the relationships between pharmacokinetics and pharmacodynamics of buprenorphine in pregnant women. Clinical Opioid Withdrawal Scale score over a dose interval were compared between pregnancies and postpartum. A population pharmacokinetic/pharmacodynamic model was developed to describe the time course of the changes of pupillary diameter following sublingual administration of buprenorphine in pregnant women (Chapter 6). The pharmacokinetic/pharmacodynamic analysis helped us to understand if the alteration in the pharmacokinetics of BUP is associated with a modulation of the pharmacodynamics of BUP in pregnant women.

2.0 Development and Validation of a Sensitive Ultra-Performance Liquid Chromatography-Tandem Mass Spectrometric Assay for Simultaneous Determination of Buprenorphine and Three Metabolites in Human Plasma: Application in a Clinical Pharmacokinetic Study in Pregnant Women

2.1 Abstract

Introduction: Opioid use disorder has been increased 5-fold in pregnant women. Recently, buprenorphine, a maintenance therapy approved by the FDA, has been increasingly used in pregnant women for treating opioid use disorder. Pregnancy is associated with anatomic and physiological changes, which may lead to altered pharmacokinetics of drugs.

Methods: By developing and validating a sensitive and reliable analytical method to simultaneously determine concentrations of BUP and its three metabolites in human plasma samples to evaluate the alterations in buprenorphine pharmacokinetics in pregnant women.

Results: A rapid, sensitive, and selective method for the determination of buprenorphine and its three metabolites, norbuprenorphine, buprenorphine glucuronide, and norbuprenorphine glucuronide, in human plasma using ultra performance liquid chromatography with tandem mass spectrometry (UPLC–MS/MS) was developed and validated. Plasma samples (200 μ L) were processed by protein precipitation prior to chromatography. Deuterated labelled buprenorphine-D₄, norbuprenorphine-D₃, buprenorphine-D₄-3- β -D-glucuronide, norbuprenorphine glucuronide-D₃ were used as the internal standards (IS). Chromatographic separation was performed using Acquity UPLC Ethylene Bridged Hybrid (BEH) C₁₈ 1.7 μ m column (2.1x100 mm) with a mobile phase consisting of [A] 5% acetonitrile in water containing ammonium acetate (2 mM) and formic

acid (0.1%), and [B] acetonitrile containing ammonium acetate (2 mM) and formic acid (0.1%) delivered at a flow rate of 0.3 mL/min in a gradient elution. The total run-time was 7 min, with buprenorphine, norbuprenorphine, buprenorphine glucuronide and norbuprenorphine glucuronide eluting at 3.3, 1.64, 1.35, and 0.84 min, respectively. The analytes were detected by a XEVO TQS mass spectrometer in positive electron spray ionization (ESI) mode using multiple reaction monitoring (MRM). The assay was linear over the range of 0.05 – 100 ng/mL for buprenorphine, 0.2 – 100 ng/mL for norbuprenorphine, 0.2-200 ng/mL for buprenorphine glucuronide and norbuprenorphine glucuronide. The intra-day and inter-day accuracies expressed as percentage of the nominal concentrations were within 98.2-108.0 %. The intra-day and inter-day precision determined by the coefficient of variations were within 9 %. No significant matrix effects were observed for buprenorphine or the three metabolites in plasma samples. Buprenorphine and the three metabolites were stable under various storage and experimental conditions. This validated method was successfully applied to a clinical pharmacokinetic study after sublingual administration of buprenorphine to pregnant women at different trimesters and postpartum and were able to quantify buprenorphine, norbuprenorphine, buprenorphine glucuronide and norbuprenorphine glucuronide in plasma samples. We observed a lower exposure of buprenorphine and higher AUC ratios of metabolites to parents during pregnancy compared to postpartum.

Conclusions: The AUC ratios of metabolites to parents demonstrated that CYP- and UGT-mediated buprenorphine metabolism were altered during pregnancy compared to postpartum, which may partially explain the lower exposure of buprenorphine during pregnancy.

2.2 Introduction

Currently, the standard of care for treating opioid addiction is methadone. Many clinical studies have demonstrated the effectiveness of methadone maintenance interventions in reducing illicit opioid use, by suppressing drug withdrawal, and craving [24-28]. The use of methadone as a maintenance therapy to treat opioid addiction can be traced back to 1960's [23]. Due to safety concerns, methadone treatment must be practiced in a highly structured clinic. Also, daily visit to the clinic is required for patients in a methadone treatment program.

Buprenorphine is a semisynthetic opioid agent and has been indicated as a medication-assisted treatment for opioid dependence since 2002 by the FDA. Although buprenorphine is a relatively new pharmacotherapy for treating opioid addiction, it has unique pharmacological properties that make buprenorphine an appealing alternative to methadone treatment. Buprenorphine has a high affinity and low intrinsic activity for mu opioid receptors, which makes it less addictive than methadone and other opioids [60]. As a mixed agonist-antagonist at μ -opioid receptor, buprenorphine exhibits a ceiling effect for respiratory depression [61, 62]. These distinct pharmacological attributes render buprenorphine with enhanced safety compared to methadone. Unlike methadone treatment, buprenorphine is offered as an office-based treatment for opioid use disorder. Under the approval of the Drug Addiction Treatment Act of 2000, qualified physicians can prescribe buprenorphine for opioid addiction in office-based settings, which significantly improves accessibility of buprenorphine to patients as a maintenance therapy for treating opioid use disorder [224].

In addition, buprenorphine use in pregnancy may lead to a decreased incidence of NAS compared to methadone. Jone et al. conducted a double-blind, double-dummy clinical study that randomized 175 pregnant opioid dependent women to either buprenorphine or methadone maintenance groups. The results showed that buprenorphine treatment was superior to methadone based on less morphine requirement to treat neonatal abstinence syndrome, shorter hospital stay, and shorter duration of medical treatment for neonatal abstinence syndrome in buprenorphine-exposed neonates [202]. However, in this study there was a significantly higher dropout rate in the buprenorphine arm than in the methadone treatment group. Approximate 71% of the subjects dropout from buprenorphine treatment due to patient dissatisfaction on buprenorphine [202].

As there is limited information available about the impact of pregnancy on the pharmacokinetics and pharmacodynamics of buprenorphine, the current dosing regimen of buprenorphine in pregnant women is based on the recommendations for non-pregnant patients. However, pregnancy is associated with various physiological changes that may impact buprenorphine clearance during pregnancy. Buprenorphine undergoes extensive gut and hepatic metabolism through N-dealkylation to norbuprenorphine primarily mediated by CYP3A4 and CYP2C8 [90, 91]. Norbuprenorphine is further conjugated to norbuprenorphine glucuronide through UGT1A1 and UGT1A3. A portion of buprenorphine is directly conjugated to buprenorphine glucuronide mediated by UGT1A1, UGT1A3, and UG2B7. Figure 2-1 shows the metabolic pathway of buprenorphine in human. After sublingual administration, changes in hepatic blood flow, intrinsic clearance and the unbound fraction of buprenorphine in plasma will affect the clearance of buprenorphine.

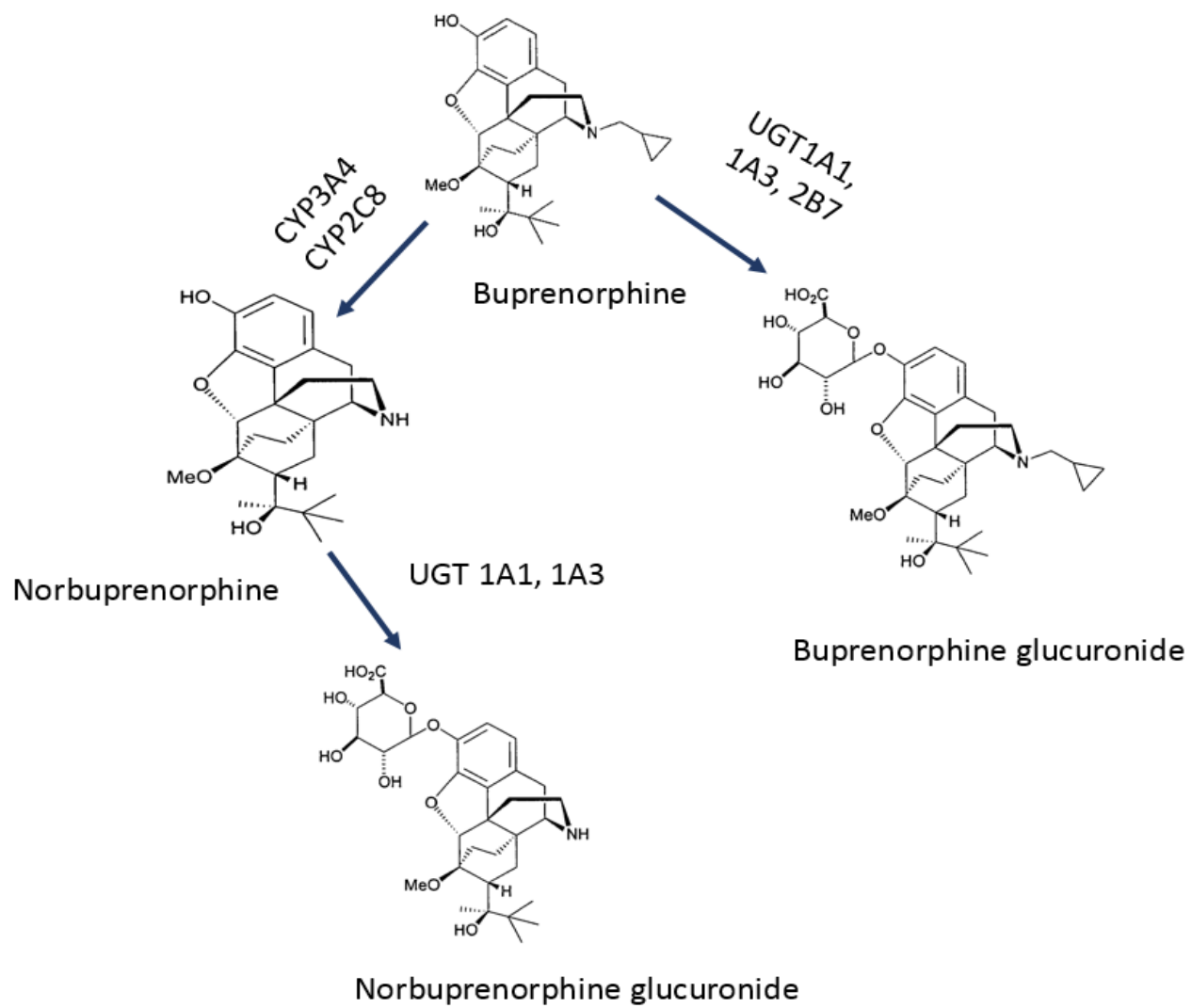


Figure 2-1. Buprenorphine metabolic pathway

Pregnancy is associated with increased cardiac output, hepatic and portal vein blood flow, increased unbound fraction of drugs, as well as increased activities of CYP3A4 and UGT1A4 [137, 167, 168]. Therefore, we predict that buprenorphine systemic exposure will be decreased due to an increase in the total body clearance of buprenorphine in pregnant women. Our pilot study documented lower exposure of BUP during pregnancy [201]. Further research is needed to characterize the pharmacokinetic profile of buprenorphine in a larger number of pregnant women and to study the association between pharmacokinetics and pharmacodynamics of buprenorphine in pregnant women.

In order to evaluate the alterations in buprenorphine pharmacokinetics during pregnancy, it was necessary to develop a sensitive and specific assay method for the determination of buprenorphine and its metabolites in human plasma. Simultaneous quantification of buprenorphine and its three metabolites have been reported in microsome, human umbilical cord, meconium, and urine samples [225-228]. To date, multiple methods have been reported using LC-MS/MS to quantify buprenorphine and norbuprenorphine, but only two methods have been reported simultaneous quantification of buprenorphine and three of its metabolites in plasma samples [229-232]. Both of these methods use solid phase extraction for sample preparation [233, 234]. Solid phase extraction is expensive and time consuming for analyzing large batches of biological samples from clinical pharmacokinetic studies. Low recovery of norbuprenorphine glucuronide was also seen in both of the reported methods. In addition, the method reported by Regina et al. required a large volume of plasma (750 μ L), which may not be practical in a pregnant woman and the neonates for a full clinical pharmacokinetic study with multiple sampling points [234]. This is the first report of a method using simple protein precipitation for plasma sample processing that is specific and sensitive for BUP and three of its metabolites.

The objective of this study was to develop a rapid, highly sensitive and reproducible UPLC-MS/MS analytical method to quantify concentrations of buprenorphine and three of its metabolites in human plasma and to apply this method to process large batches of human plasma samples from clinical pharmacokinetic studies in pregnant women.

2.3 Materials and methods

2.3.1 Chemicals and Reagents

Chemical structures of buprenorphine, norbuprenorphine, buprenorphine glucuronide, norbuprenorphine glucuronide and respective deuterated internal standards, buprenorphine-D₄, norbuprenorphine-D₃, buprenorphine-D₄-3-β-D-glucuronide, norbuprenorphine glucuronide-D₃ are shown in Figure 2-2. They were purchased from Sigma-Aldrich (St. Louis, MO). Ammonium acetate (99.9999 trace metals basis) and Optima™ LC/MS grade acetonitrile, formic acid, methanol and water were obtained from Fisher Scientific (Fair Lawn, NJ, USA). Human plasma was procured from central blood bank of Pittsburgh (Pittsburgh, PA, USA).

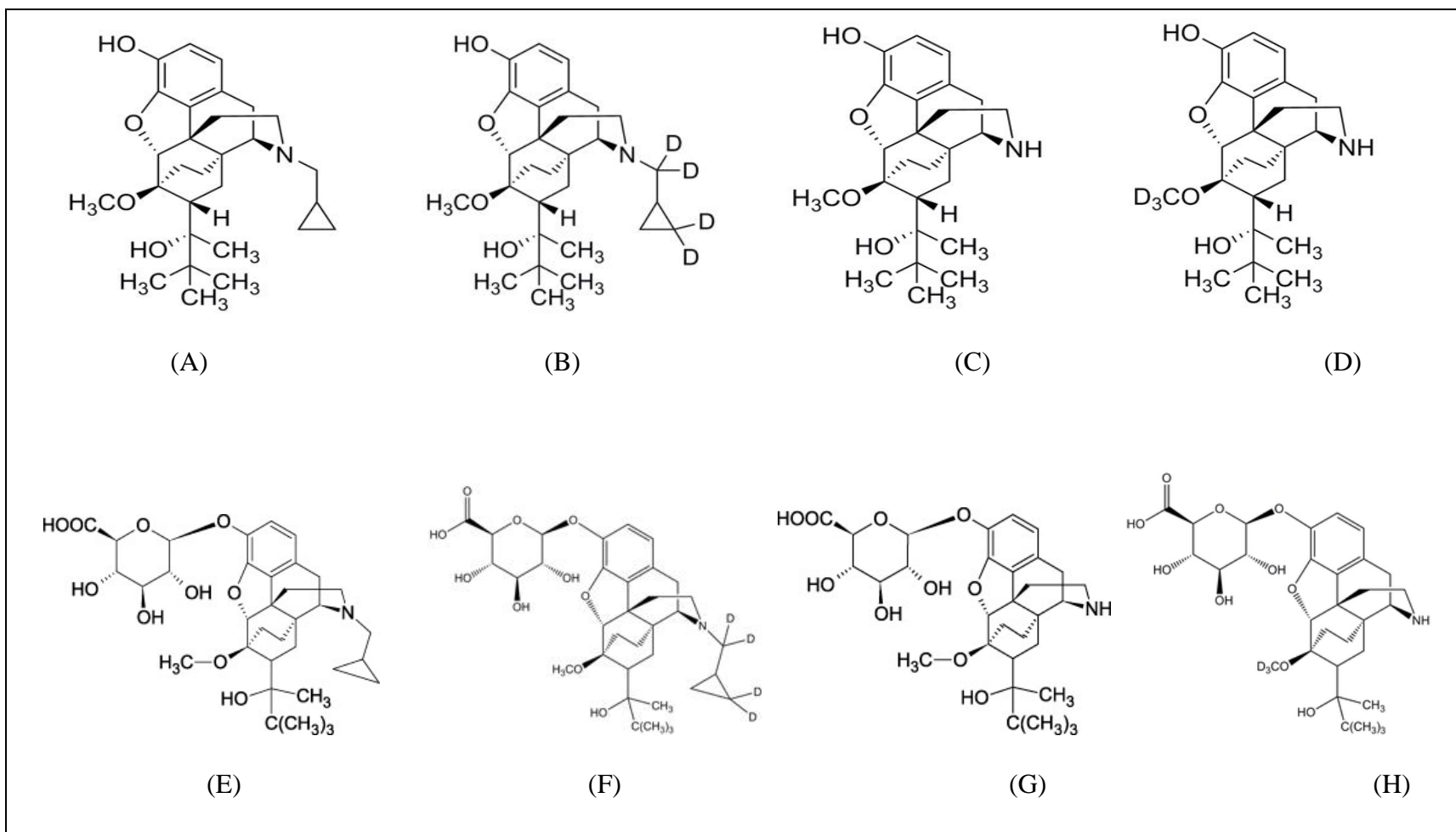


Figure 2-2. Chemical structure of buprenorphine (A), buprenorphine-D4 (B), norbuprenorphine (C), norbuprenorphine-D3 (D), buprenorphine-3-β-D-glucuronide (E), buprenorphine-D4-3-β-D-glucuronide (F), norbuprenorphine glucuronide (G), norbuprenorphine glucuronide-D3 (H)

2.3.2 Chromatographic Conditions

The UPLC system used for the analysis of buprenorphine and three of its metabolites was a Waters Acquity H class model (Waters Corporation, MA, USA). Separation of all components of interest was achieved on Acquity UPLC BEH C₁₈ 1.7 μ m, 2.1 x 100 mm column. The mobile phase A was 5% acetonitrile in water containing ammonium acetate (2 mM) and formic acid (0.1%) and mobile phase B was 95% acetonitrile in water containing ammonium acetate (2 mM) and formic acid (0.1%) at a flow rate of 0.3 mL/min. A sample volume of 2 μ L was injected on column. A gradient method for the mobile phase was used to separate buprenorphine and its three metabolites. The gradient started at 25% of B, maintained for 1.0 min, then increasing to 35% of B from 1.0 min to 1.1 min, maintaining for 2 min, then increased to 100% of B from 3.1 to 4.1 min, maintaining for 2 min, and decreased to 25% of B from 5.1 to 5.2 min, then maintained at 25% of B until 7 min. The gradient method is summarized in Table 2-1. The total run time for each injection was 7 mins.

Table 2-1. Gradient method used to separate buprenorphine and three metabolites

Run Time (min)	Mobile Phase A %	Mobile Phase B %
Up to 1.0	75	25
1.1	65	35
3.1	65	35
4.1	0	100
5.1	0	100
5.2	75	25
7	75	25

2.3.3 Mass Spectrometric Conditions

Mass spectrometric analysis was carried out using a XEVO TQS triple quadrupole mass spectrometer (Waters, Milford, MA, USA) with positive electric spray ionization mode using multiple reaction monitoring (MRM). Multiple reaction monitoring used the precursor to product ion pairs for quantification of compounds used by MRM are summarized in Table 2-2.

The settings of MRM were as follows: capillary voltage, 2.8 kV; source temperature, 150°C; desolvation temperature, 500°C; cone gas flow, 150 L/h; desolvation gas flow, 800 L/h. The LC–MS system was controlled by Masslynx® software version 4.1, and data were collected with the same software.

Table 2-2. The ion pairs for multiple reaction monitoring

Compound	Parent (m/z)	Daughter (m/z)
Buprenorphine	467.99	396.18
Buprenorphine-D ₄	472.22	400.15
Norbuprenorphine	414.02	101.00
Norbuprenorphine-D ₃	417.27	101.07
Buprenorphine-3-β-D-glucuronide	644.10	468.22
Buprenorphine-D ₄ -3-β-D-glucuronide	648.10	472.2
Norbuprenorphine glucuronide	590.10	414.22
Norbuprenorphine glucuronide-D ₃	593.10	417.21

2.3.4 Standards and quality control samples preparation

A stock solution of buprenorphine, norbuprenorphine, buprenorphine glucuronide, norbuprenorphine glucuronide at a concentration of 100 µg/mL was prepared in 100% methanol and was used to spike human blank plasma to obtain 0.05, 0.1, 0.2, 0.5, 1.0, 2.0, 5.0, 10.0, 20.0, 50.0, 100.0 ng/mL of buprenorphine, 0.2, 0.5, 1.0, 2.0, 5.0, 10.0, 20.0, 50.0, 100.0 ng/mL of norbuprenorphine, and 0.2, 0.4, 1.0, 2.0, 4.0, 10.0, 20.0, 40.0, 100.0, 200.0 ng/mL of buprenorphine glucuronide and norbuprenorphine glucuronide as calibration standards. Quality control samples were prepared independently by separately spiking buprenorphine, norbuprenorphine, buprenorphine glucuronide, norbuprenorphine glucuronide stock solutions at a concentration of 100 µg/mL into blank human plasma to obtain QC samples at concentrations of 0.1, 0.2, 4, 40, 80 ng/mL for buprenorphine, 0.2, 4, 40, 80 ng/mL for norbuprenorphine and 0.4, 8, 80 and 160 ng/mL for buprenorphine glucuronide, norbuprenorphine glucuronide. The stock solutions of the deuterated compounds, buprenorphine-D₄, norbuprenorphine-D₃, buprenorphine-D₄-3-β-D-glucuronide, norbuprenorphine glucuronide-D₃ at concentrations of 100 µg/mL were mixed and diluted with 50% methanol in water at concentration of 10 ng/mL, and used as working internal standards solution. These stock solutions, calibration standards, QC samples and internal standards were frozen at -80°C in safe-lock tubes.

2.3.5 Plasma samples preparation

Daily calibration standards, QC samples, and clinical plasma samples were thawed at room temperature. Plasma concentrations of buprenorphine, norbuprenorphine, buprenorphine glucuronide, norbuprenorphine glucuronide were determined by UPLC-MS/MS. Calibration

standards and QC samples were prepared by spiking blank human plasma with stock solution as described in section 2.3.3. Twenty μL of mixed internal standards (buprenorphine-D₄, norbuprenorphine-D₃, buprenorphine-D₄-3- β -D-glucuronide, norbuprenorphine glucuronide-D₃ at 10 ng/mL in 50% methanol) were added to 200 μL of plasma sample in an Eppendorf microcentrifuge tube. To this, 800 μL of 100% acetonitrile (ACN) were added as a protein precipitation solution. The tube was vortexed for 30s, then followed with centrifugation at 15,000 rpm for 15min at room temperature. The supernatant was transferred to a glass tube and was dried under a stream of air. The dried residues were reconstituted in 100 μL of mobile phase (consisting of 2B:1A), vortexed for 30s, and then transferred to an Eppendorf microcentrifuge tube. The tube was centrifuged at 15,000 rpm for 15min at room temperature. The supernatant was transferred to a sample vial for injection. Two μL of the solution was injected on the column.

2.3.6 Bioanalytical method validation

The UPLC-MS/MS method was developed and validated according to the guidance of bioanalytical method validation by the FDA in 2013 [235].

Selectivity

The selectivity was evaluated by analyzing drug-free human plasma from six individuals in order to exclude potential interference in the assay with buprenorphine and its three metabolites from any endogenous substances in plasma.

Calibration curves

The calibration curves were generated by plotting the response ratio of buprenorphine to buprenorphine-D₄, norbuprenorphine to norbuprenorphine-D₃, buprenorphine-3- β -D-glucuronide

to buprenorphine-D₄-3-β-D-glucuronide, norbuprenorphine glucuronide to norbuprenorphine glucuronide-D₃ against nominal concentration of the corresponding four analytes in plasma samples. The calibration curves were fit by linear regression using weighing factor of $1/x^2$. Concentration of analytes in the unknown plasma samples were calculated from their peak area ratios and the calibration curve. The deviations of back calculated concentrations from the nominal concentrations of QC samples were used to check the assay performance over the concentration ranges on each sample run day. The acceptance criteria of accuracy and precision of QC samples are described below.

Accuracy and precision

Accuracy was investigated by intra- and inter-day coefficient of variation (CV). Quality control samples (0.1, 0.2, 4, 40, 80 ng/mL for buprenorphine, 0.2, 4, 40, 80 ng/mL for norbuprenorphine; 0.4, 8, 80, 160 ng/mL for buprenorphine glucuronide and norbuprenorphine glucuronide) were tested. For intra-day accuracy, five samples of each concentration were analyzed on a single day; for inter-day accuracy, a total of five samples of each concentration were measured on three consecutive days. The back-calculated concentrations should be between 85% and 115% of the nominal concentrations.

Precision was evaluated by intra- and inter-day reproducibility. Quality control samples (0.1, 0.2, 4, 40, 80 ng/mL for buprenorphine, 0.2, 4, 40, 80 ng/mL for norbuprenorphine; 0.4, 8, 80, 160 ng/mL for buprenorphine glucuronide and norbuprenorphine glucuronide) were tested. For intra-day precision, five samples of each concentration were assayed on a single day; for inter-day precisions, a total of five samples of each concentration were determined on three consecutive days. The intra-day and inter-day coefficient of variation should be within 15%.

Extraction recovery and matrix effects

The extraction recovery of buprenorphine and three of its metabolites was performed by comparing the responses obtained from extracted QC samples (0.1, 0.2, 4, 40, 80 ng/mL for buprenorphine, 0.2, 4, 40, 80 ng/mL for norbuprenorphine; 0.4, 8, 80, 160 ng/mL for buprenorphine glucuronide and norbuprenorphine glucuronide) with the responses obtained from extracted blank human plasma spiked with buprenorphine, norbuprenorphine, buprenorphine glucuronide and norbuprenorphine glucuronide and internal standards post extraction that represent 100% recovery.

To evaluate the effect of endogenous matrix on the ionization of buprenorphine and three metabolites, responses of buprenorphine and three metabolites at the QC concentrations (0.1, 0.2, 4, 40, 80 ng/mL for buprenorphine, 0.2, 4, 40, 80 ng/mL for norbuprenorphine; 0.4, 8, 80, 160 ng/mL for buprenorphine glucuronide and norbuprenorphine glucuronide) in triplicate were evaluated. The effect of plasma matrix on analytes was defined by comparing the response obtained from extracted blank plasma samples spiked with buprenorphine, norbuprenorphine, buprenorphine glucuronide and norbuprenorphine glucuronide post extraction with the absolute response of reconstitution solvent to which the same amount of analytes were added.

Chemical Stability

The freeze-thaw stability (subjected to three cycles at $-80\text{ }^{\circ}\text{C}$ and room temperature), bench-top stability (subjected to laboratory handling conditions up to 24 hours at room temperature), and storage at $4\text{ }^{\circ}\text{C}$ for 3 days of buprenorphine and three metabolites were studied at QC concentrations (0.1, 0.2, 4, 40, 80 ng/mL for buprenorphine, 0.2, 4, 40, 80 ng/mL for norbuprenorphine; 0.4, 8, 80, 160 ng/mL for buprenorphine glucuronide and norbuprenorphine glucuronide) in plasma.

2.4 Results

Following an injection of the reconstitution solution into UPLC-MS/MS system with positive ion electrospray ionization interface, the retention time of buprenorphine, norbuprenorphine, buprenorphine glucuronide, and norbuprenorphine glucuronide were 3.3, 1.64, 1.35 and 0.84 min, respectively. The assay did not show any significant interference with plasma constituent at the retention times of analytes of each ion pair for MRM. Representative chromatogram of human blank plasma, blank plasma spiked with internal standards are shown in Figure 2-3. Typical chromatogram of plasma samples spiked with buprenorphine at 0.05 ng/mL; norbuprenorphine, buprenorphine glucuronide, and norbuprenorphine glucuronide at 0.2 ng/mL, and their respective internal standards are listed in Figure 2-4. The regression coefficient (r^2) of all calibration curves was higher than 0.99 for buprenorphine, norbuprenorphine, buprenorphine glucuronide, and norbuprenorphine glucuronide.

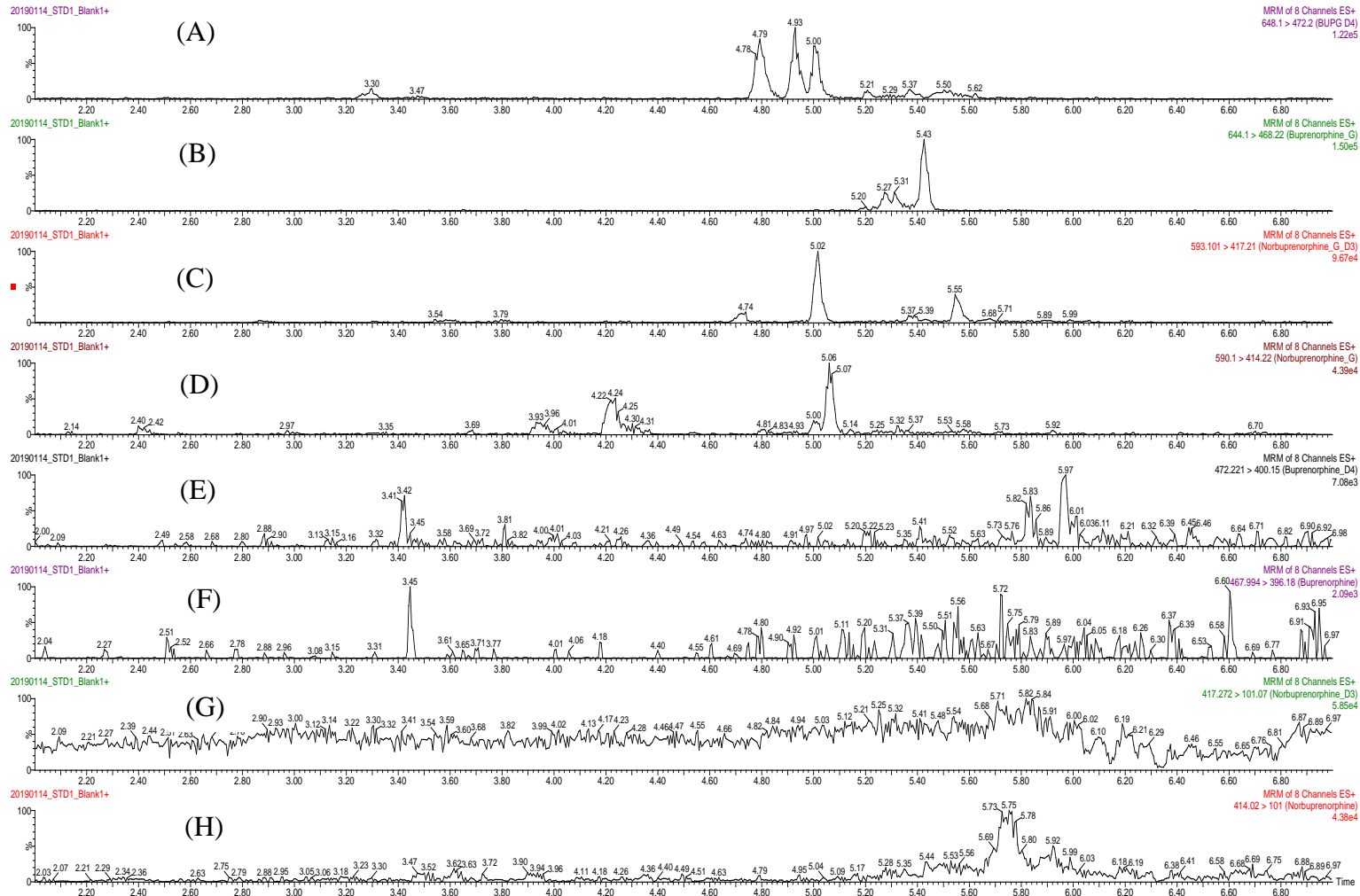


Figure 2-3. Representative chromatogram of pooled blank human plasma without spiked with internal standards. (A) buprenorphine-D₄-3-β-D-glucuronide; (B) buprenorphine-3-β-D-glucuronide; (C) Norbuprenorphine glucuronide-D₃; (D) Norbuprenorphine glucuronide (E) buprenorphine-D₄; (F) buprenorphine; (G) Norbuprenorphine-D₃; (H) Norbuprenorphine

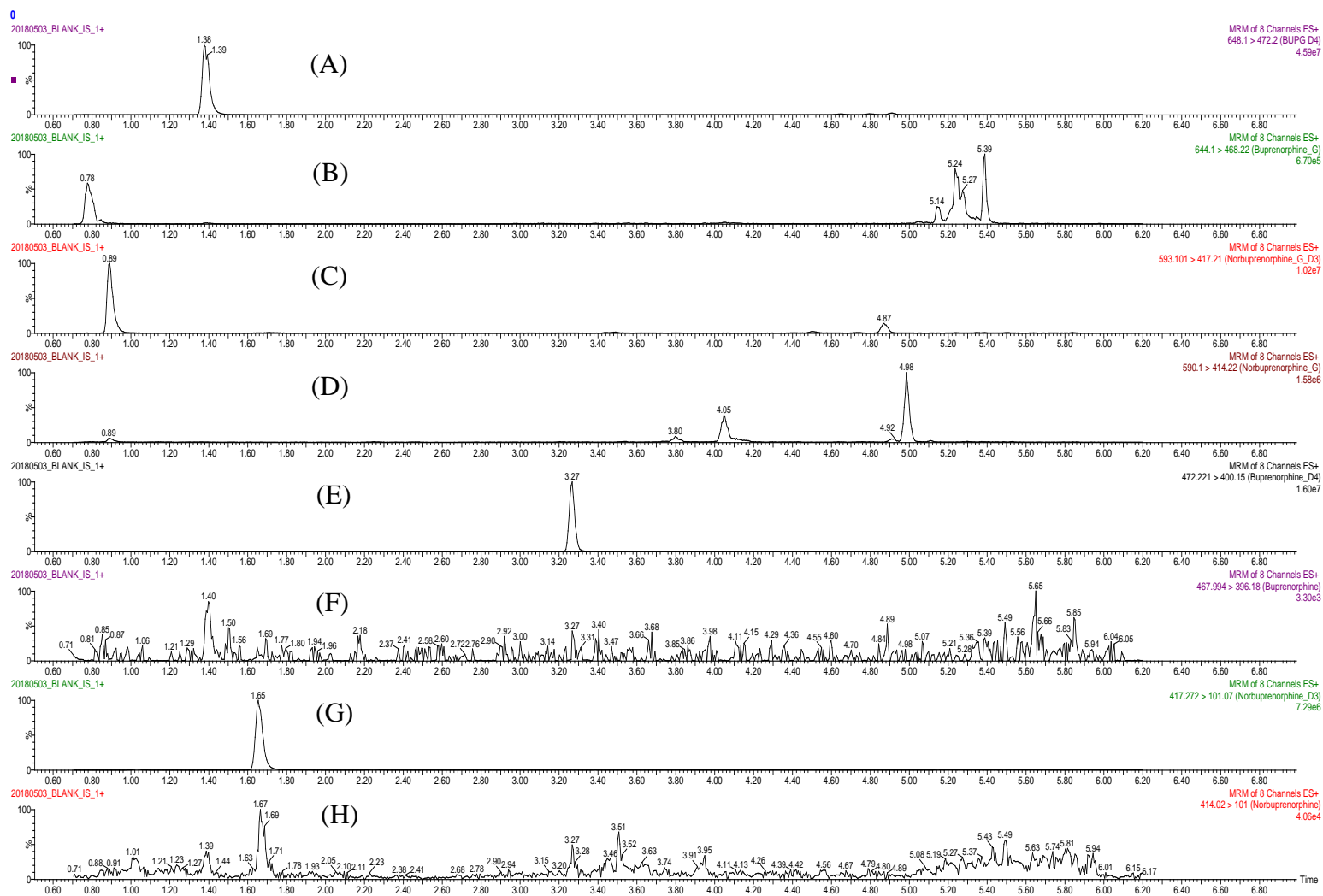


Figure 2-4. Representative chromatogram of pooled blank human plasma spiked with internal standards. (A) buprenorphine-D4-3-β-D-glucuronide; (B) buprenorphine-3-β-D-glucuronide; (C) Norbuprenorphine glucuronide-D₃; (D) Norbuprenorphine glucuronide (E) buprenorphine-D₄; (F) buprenorphine; (G) Norbuprenorphine-D₃; (H) Norbuprenorphine

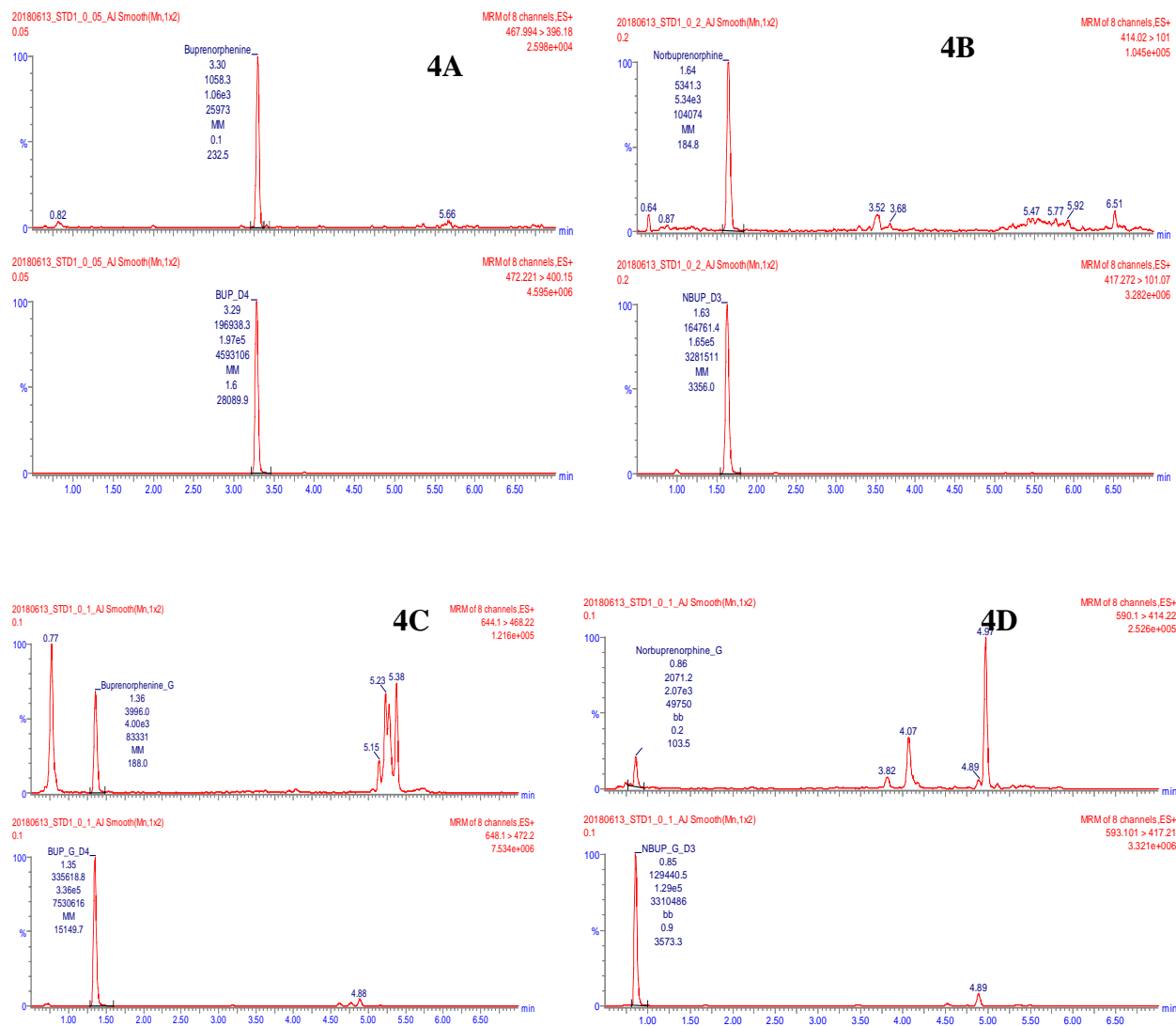


Figure 2-5. Representative chromatogram spiked with buprenorphine (0.05 ng/mL, 4A), norbuprenorphine (0.2 ng/mL, 4B), buprenorphine glucuronide (0.2 ng/mL, 4C), and norbuprenorphine glucuronide (0.2 ng/mL, 4D) with their respective deuterated internal standards.

2.4.1 Accuracy and precision

The QC plasma samples at different concentrations were processed to examine the accuracy and precision of the assay. The intra-day and inter-day accuracies expressed as percentage of the nominal concentrations were within 98.2-108.0 %. The intra-day and inter-day precision determined by the coefficient of variations were within 9 %. Results of the assay precision and accuracy are presented in Table 2-3 and Table 2-4, respectively.

Table 2-3. Inter-day and Intra-day accuracy of buprenorphine and three metabolites (expressed as a percentage of the nominal concentration)

	BUP	NBUP		BUPG	NBUPG
QC Concentration (ng/mL)	Intra-day accuracy (% , n=5)		QC Concentration (ng/mL)	Intra-day accuracy (% , n=5)	
0.1	106.1	NA	0.4	109.5	104.9
0.2	98.7	99.9	8	108.5	108.0
4	102.4	106.5	80	102.6	98.2
40	100.5	103.7	160	108.4	103.0
80	99.8	107.2			
QC Concentration (ng/mL)	Inter-day accuracy (% , n=5)		QC Concentration (ng/mL)	Inter-day accuracy (% , n=5)	
0.1	108.8	NA	0.4	106.5	103.8
0.2	98.7	102.9	8	105.0	107.5
4	105.3	106.0	80	102.7	99.9
40	98.4	102.9	160	105.2	104.0
80	102.2	106.6			

**Table 2-4. Inter-day and Intra-day precision of buprenorphine and three metabolites
(expressed as coefficient of variation)**

	BUP	NBUP		BUPG	NBUPG
QC Concentration (ng/mL)	Intra-day precision (% , n=5)		QC Concentration (ng/mL)	Intra-day precision (% , n=5)	
0.1	2.6	NA	0.4	2.7	3.7
0.2	5.6	6.9	8	2.4	2.4
4	5.9	3.5	80	1.3	3.7
40	1.8	6.0	160	1.1	1.5
80	3.5	2.2			
QC Concentration (ng/mL)	Inter-day precision (% , n=5)		QC Concentration (ng/mL)	Inter-day precision (% , n=5)	
0.1	4.5	NA	0.4	4.1	2.1
0.2	3.8	8.9	8	4.3	3.8
4	1.4	2.4	80	0.8	6.0
40	2.6	5.7	160	3.6	5.1
80	2.5	3.0			

2.4.2 Recovery and matrix effect

The QC plasma samples at different concentrations were processed to examine the recovery of buprenorphine and three metabolites. The recoveries for all analytes were above 85% over the concentration range tested. No significant matrix effects were observed for buprenorphine and its three metabolites from extracted human plasma samples. Results are presented in Table 2-5.

Table 2-5. Recovery and matrix effect of buprenorphine and three metabolites in human plasma samples

	BUP	NBUP		BUPG	NBUPG
QC Concentration (ng/mL)	Recovery (% , n=3)		QC Concentration (ng/mL)	Recovery (% , n=3)	
0.1	95.8	NA	0.4	91.1	90.8
0.2	98.4	102.8	8	99.2	88.6
4	93.2	99	80	94.6	85.6
40	92.3	104.1	160	89.4	86.8
80	86.8	97.9			
QC Concentration (ng/mL)	Matrix effect (% , n=3)		QC Concentration (ng/mL)	Matrix effect (% , n=3)	
0.1	6.7	NA	0.4	-4.3	-13.7
0.2	-2.2	-10.2	8	-1.0	5.3
4	5.2	-12.2	80	1.8	3.5
40	-0.6	-15.3	160	12.6	2.9
80	13.6	-8.2			

2.4.3 Stability

After subjecting the samples to three freeze–thaw cycles, 24 hr bench - top storage at room temperature, and 4 °C storage for 72 hrs, changes in the concentrations for buprenorphine and three metabolites at four concentrations of all the QC samples were within 85-115% of nominal concentrations (Table 2-6). No significant degradation for buprenorphine and its three metabolites was observed in plasma samples under the condition tested.

**Table 2-6. Stability of buprenorphine and three metabolites in human plasma samples
(expressed as mean of nominal concentration \pm SD %)**

	BUP	NBUP		BUPG	NBUPG
QC Concentration (ng/mL)	3 Freeze–thaw cycles (% , n=3)		QC Concentration (ng/mL)	3 Freeze–thaw cycles (% , n=3)	
0.1	105.8 \pm 7.6	NA	0.4	105.4 \pm 7.0	106.0 \pm 1.9
0.2	111.0 \pm 1.3	99.5 \pm 4.0	8	105.5 \pm 1.2	105.4 \pm 4.7
4	112.0 \pm 1.1	107.5 \pm 2.5	80	102.3 \pm 2.5	104.0 \pm 3.8
40	110.9 \pm 0.9	106.9 \pm 4.0	160	101.4 \pm 4.7	106.6 \pm 2.1
80	108.0 \pm 3.4	110.0 \pm 3.1			
QC Concentration (ng/mL)	24 h bench-top (% , n=3)		QC Concentration (ng/mL)	24 h bench-top (% , n=3)	
0.1	110.9 \pm 2.0	NA	0.4	108.3 \pm 7.2	101.7 \pm 7.2
0.2	111.6 \pm 1.0	103.3 \pm 2.9	8	104.2 \pm 1.4	108.3 \pm 3.1
4	110.9 \pm 0.7	110.0 \pm 6.6	80	101.4 \pm 2.5	101.0 \pm 1.4
40	109.0 \pm 0.8	103.8 \pm 1.5	160	100.8 \pm 4.7	109.4 \pm 0.2
80	106.3 \pm 0.9	104.3 \pm 4.2			
QC Concentration (ng/mL)	4 °C storage for 72 hrs (% , n=3)		QC Concentration (ng/mL)	4 °C storage for 72 hrs (% , n=3)	
0.1	112.2 \pm 1.2	NA	0.4	110.0 \pm 4.3	104.9 \pm 4.4
0.2	112.2 \pm 0.8	95.0 \pm 5.0	8	104.2 \pm 0.7	107.5 \pm 2.5
4	112.4 \pm 2.0	105.8 \pm 1.4	80	100.3 \pm 2.5	105.8 \pm 0.7
40	105.3 \pm 0.08	103.8 \pm 2.6	160	104.0 \pm 0.8	100.3 \pm 3.9
80	105.3 \pm 5.3	108.2 \pm 4.0			

2.4.4 Analysis of buprenorphine and three metabolites in pregnant women

This validated UPLC-MS/MS was used to quantify buprenorphine, norbuprenorphine, buprenorphine glucuronide and norbuprenorphine glucuronide in pregnant women following administration of a sublingual dose of buprenorphine at steady state. The study was approved by the Institutional Review Board (IRB) at the University of Pittsburgh. Written informed consent was obtained from all patients prior to initiation of any study-related activities. In this pharmacokinetic study, blood samples were collected at steady state after patients were administered several doses of sublingual buprenorphine. The time courses of buprenorphine, norbuprenorphine, buprenorphine glucuronide and norbuprenorphine glucuronide after a dose in one patient at steady state are shown in Figure 2-6. The mean dose normalized concentration versus time plot of buprenorphine are presented in Figure 2-7. The summary of PK parameters of BUP following SL administration of BUP in the clinical study are listed in Table 2-7. The comparison of the PK parameters of BUP in postpartum period in our clinical study to the PK parameters in non-pregnant population are shown in Table 2-8. Buprenorphine PK parameters at postpartum period is comparable to the PK parameters in non-pregnant population in published reports as shown in Table 2-8.

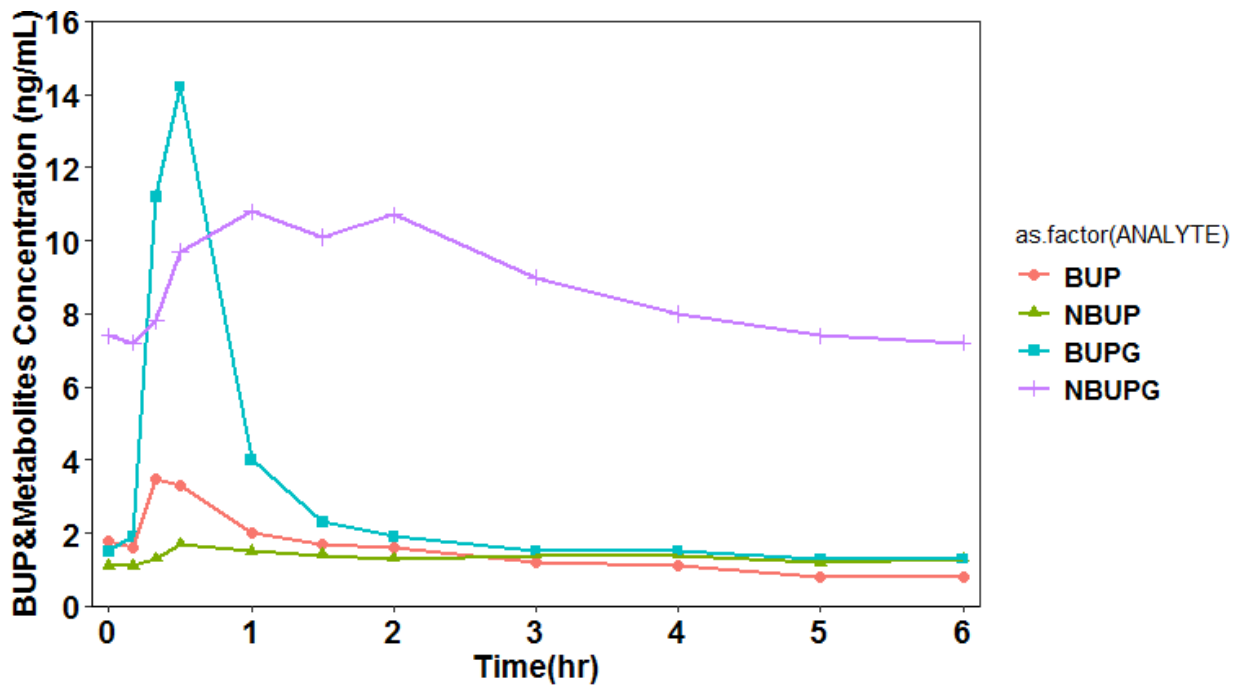


Figure 2-6. Plasma concentration vs time profiles of buprenorphine, norbuprenorphine, buprenorphine glucuronide and norbuprenorphine glucuronide following sublingual administration of buprenorphine in one pregnant women.

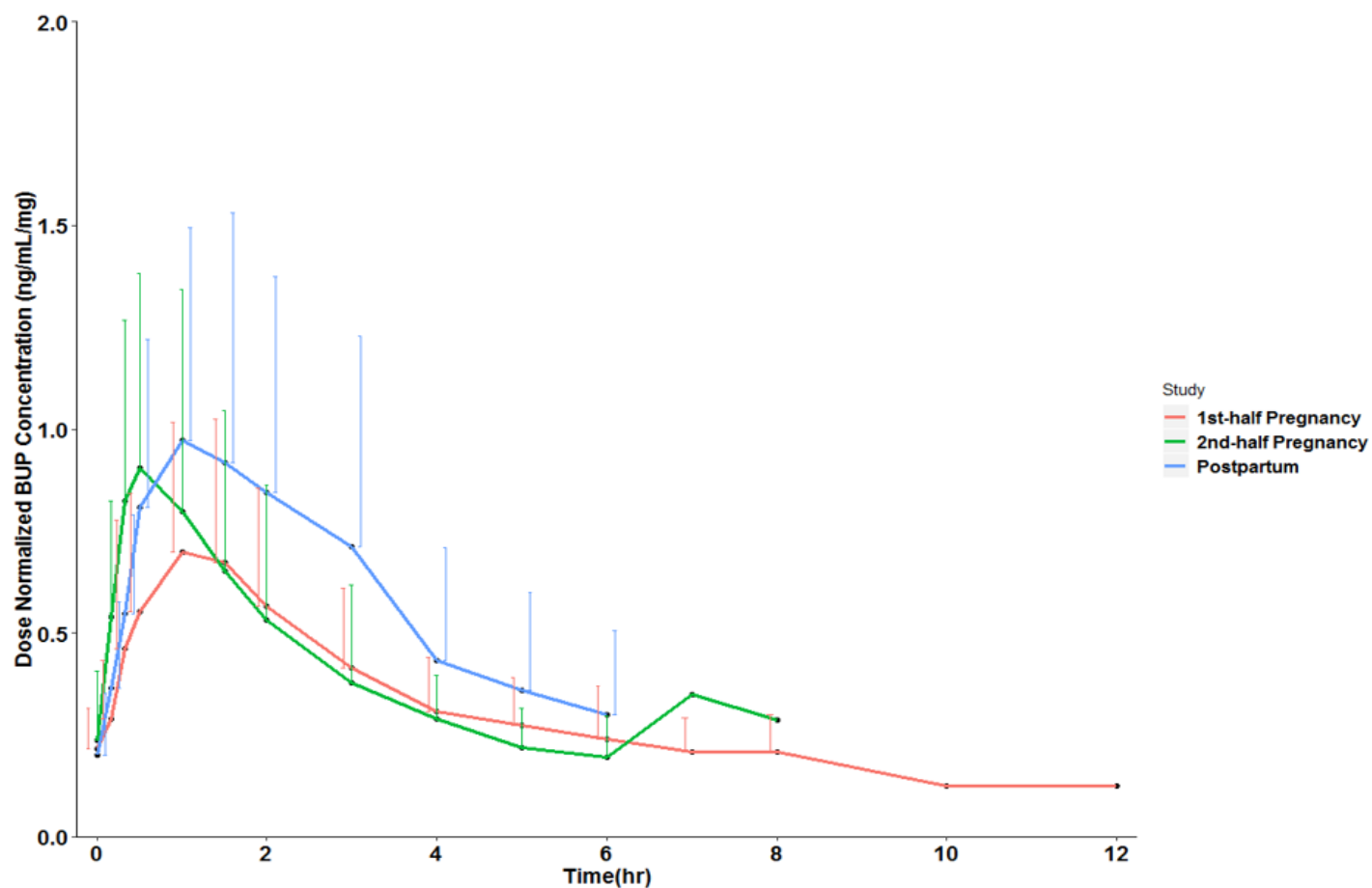


Figure 2-7. Dose normalized buprenorphine mean concentration time profile (expressed as mean \pm SD)

Red, green and blue curve represent study at the 1st-half, 2nd-half of pregnancy and postpartum, respectively. N = 12 (2, 9 and 1 patients completed study in 6, 8 and 12 hrs, respectively), 5 (4 and 1 patients completed study in 6 and 8 hrs, respectively), and 3 (All 3 patients completed study in 6 hrs) at the 1st-half, 2nd-half of pregnancy and postpartum, respectively.

Table 2-7. Buprenorphine pharmacokinetic parameters during pregnancy and postpartum period

Parameter (Mean ± SD)	1 st - half (n=12)	2 nd -half (n=5)	Postpartum (n=3)
Dose (mg)	4.2 ± 1.3	4.8 ± 1.8	4 ± 0
T _{max} (hr)	1.1 ± 0.4	0.6 ± 0.2	1.2 ± 0.3
Dose-normalized (ng/mL/mg)	C _{avg,ss} 0.4 ± 0.2	0.5 ± 0.3	0.6 ± 0.4
Dose-normalized (ng/mL/mg)	AUC _{ss} 2.9 ± 1.1	2.7 ± 1.2	3.7 ± 2.3
Apparent CL _{ss} /F (L/h)	386.5 ± 138.7	420.6 ± 157.4	348.3 ± 190.9

Abbreviation: T_{max}, time to maximum concentration, C_{avg,ss}, average concentration plasma concentration during a dose interval at steady state, AUC_{ss}, area under the plasma concentration-time curve over a dose interval at steady state, CL_{ss}, total body clearance at steady state.

Table 2-8. Comparisons of BUP PK from our in-house clinical PK studies at postpartum period and non-pregnant population from literatures following multiple doses of SL BUP administration (expressed as mean (SD))

Study	Dose Normalized AUC _{0-t,ss}	T _{max}
Compton et al. [236] (16 mg group, n = 16)	3.42 (3.07)	Not reported
Compton et al. [236] (24mg group, n = 15)	3.38 (2.73)	Not reported
Compton et al. [236] (32 mg group, n = 10)	3.67 (3.83)	0.94 (0.5)
Greenwald et al. ^a [237] (2 mg group, n = 5)	3.25	0.9
Greenwald et al. [237] (16 mg group, n = 16)	3.04	1.2
Greenwald et al. [237] (32 mg group, n= 32)	3	1.2
Our in-house data at postpartum (n = 14 ^c)	4.09 (2.34)	0.86 (0.33)

^a Standard deviation were not reported.

^b Values obtained from graph digitized data.

^c Pooled subjects from two BUP clinical studies of postpartum period.

2.4.5 Alterations of buprenorphine metabolic pathway during pregnancy

We analyzed the changes of CYP- and UGT- mediated metabolic pathways of buprenorphine using the concentrations of BUP and three metabolites from the current clinical study, as well as the data from our previous publication [201]. The mean concentration-time profiles of norbuprenorphine, buprenorphine glucuronide and norbuprenorphine glucuronide are shown in Figure 2-8, 2-9, and 2-10. As defined below, the AUC ratios of CYP-mediated metabolites to parent, and the ratios of UGT-mediated metabolite to parent at 1st-and 2nd-trimester vs postpartum and 3rd-trimester vs postpartum were shown in Figure 2-11, 2-12, 2-13 and 2-14, respectively.

$$\frac{AUC_{NorBUP+NorBUPG}}{AUC_{BUP}} = \text{CYP-mediated metabolism of buprenorphine}$$

$$\frac{AUC_{BUPG}}{AUC_{BUP}} = \text{UGT-mediated metabolism of buprenorphine}$$

The area under the curves the plasma molar concentration of BUP, NBUP, BUPG, and NBUPG during a dose interval (AUC_{0-t}) were calculated from time 0 to 12 hours or the end of a dosing interval using trapezoidal rule. Natural logarithmic transformation were applied to the AUC ratios of metabolite/parent to generate approximately normally distributed data for the purpose of statistical analysis. A univariate linear mixed effect model was used to compare the statistical difference in the AUCs ratios of metabolite/parent during pregnancy vs postpartum period. In the linear mixed effect model, time was treated as fixed effect, subject was treated as random effect. The linear mixed effect model was fitted through maximum likelihood estimation in Stata (Version 14.0 SE). The results have shown that the AUC ratios of CYP- and UGT- mediated metabolic pathway were significantly higher during pregnancy compared to postpartum (Table 2-9).

Table 2-9. The AUC ratios of CYP- and UGT- mediated metabolism of buprenorphine during pregnancy compared to postpartum (expressed as mean (SD))

Parameter	1 st - and 2 nd -trimester (n=19)	3 rd -trimester (n=18)	Postpartum (n=14)	p Value
$\frac{AUC_{NorBUP+NorBUPG}}{AUC_{BUP}}$	1.89 (0.56)	1.84 (0.59)	1.33 (0.60)	0.004, 1 st -and 2 nd -trimester vs postpartum 0.013, 3 rd -trimester vs postpartum
$\frac{AUC_{BUPG}}{AUC_{BUP}}$	0.71 (0.70)	2.07 (3.62)	0.30 (0.24)	< 0.001, 1 st -and 2 nd -trimester vs postpartum < 0.001, 3 rd -trimester vs postpartum

The AUC were calculated from molar concentrations of BUP and its three metabolites; A natural logarithmic transformation to ratios were used for the linear mixed effect model analysis.

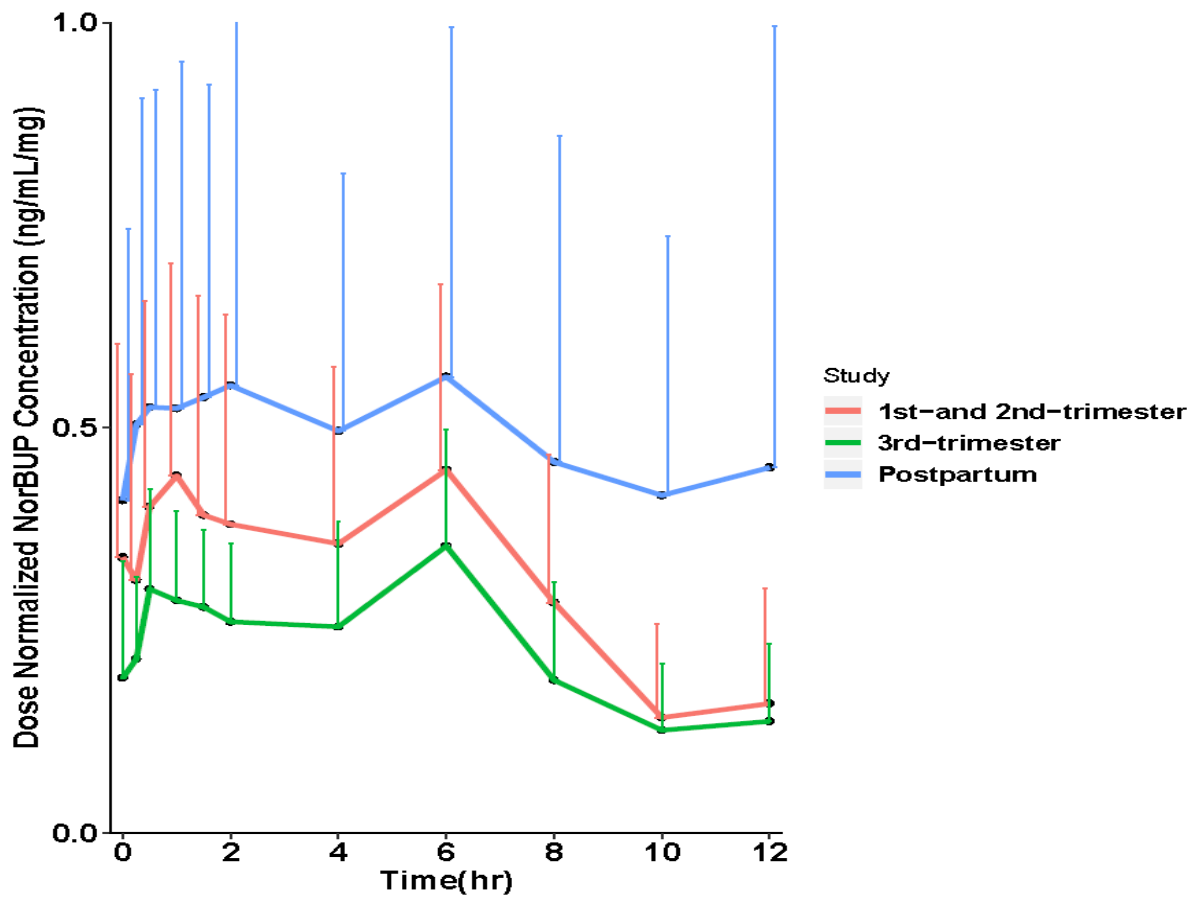
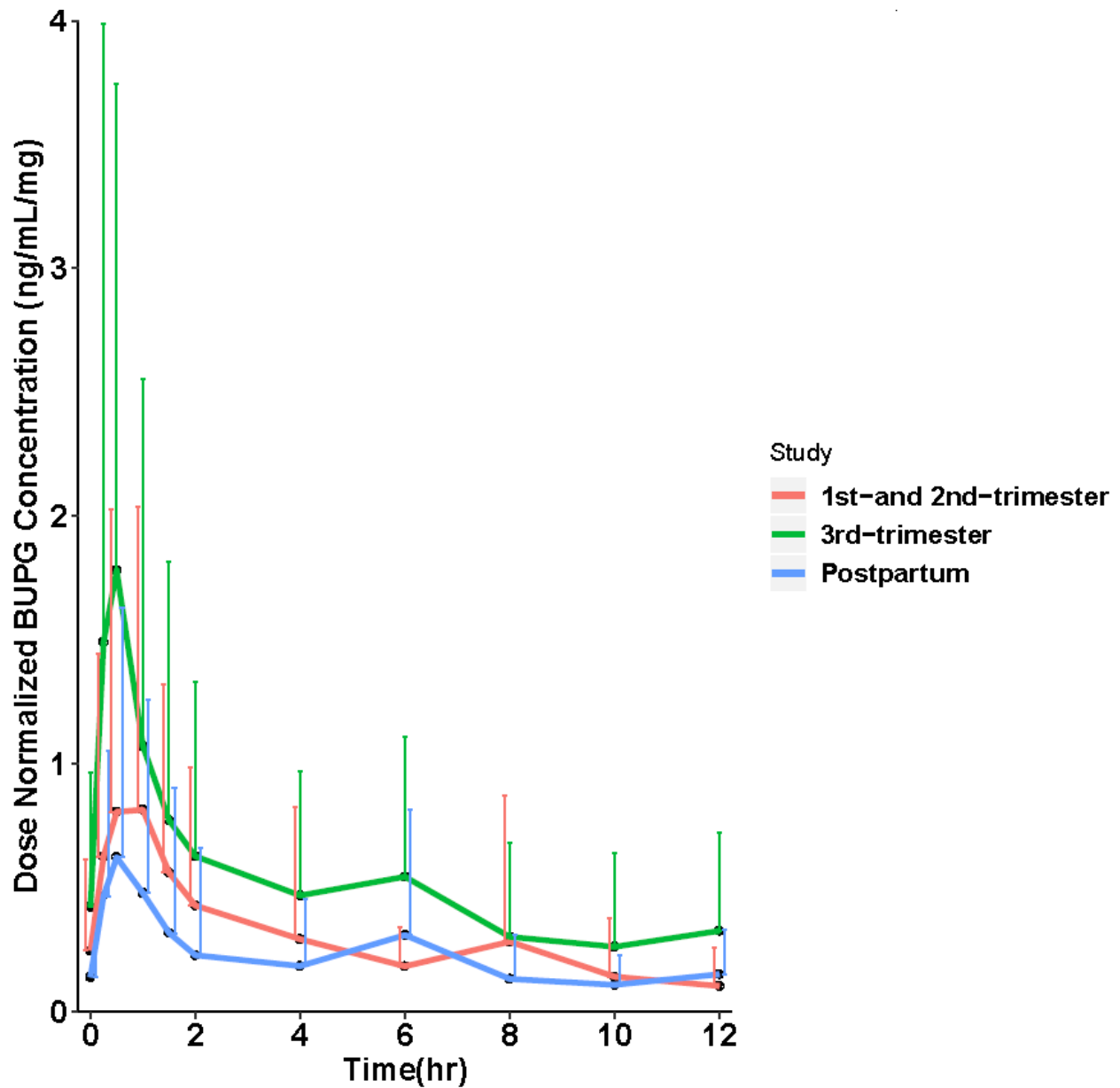


Figure 2-8. Dose normalized norbuprenorphine mean concentration time profile (expressed as mean± SD)

Red, green and blue curve represent study at the 1st- and 2nd-trimester, 3rd-trimester and postpartum, respectively.

N = 19 (2, 9 and 8 patients completed study in 6, 8 and 12 hrs, respectively), 18 (4, 1 and 13 patients completed study in 6, 8 and 12 hrs, respectively), and 14 (3 and 11 patients completed study in 6 and 12 hrs) at the 1st-half, 2nd-half of pregnancy and postpartum, respectively.



**Figure 2-9. Dose normalized buprenorphine glucuronide mean concentration time profile
(expressed as mean± SD)**

N = 19 (2, 9 and 8 patients completed study in 6, 8 and 12 hrs, respectively), 18 (4, 1 and 13 patients completed study in 6, 8 and 12 hrs, respectively), and 14 (3 and 11 patients completed study in 6 and 12 hrs) at the 1st-half, 2nd-half of pregnancy and postpartum, respectively.

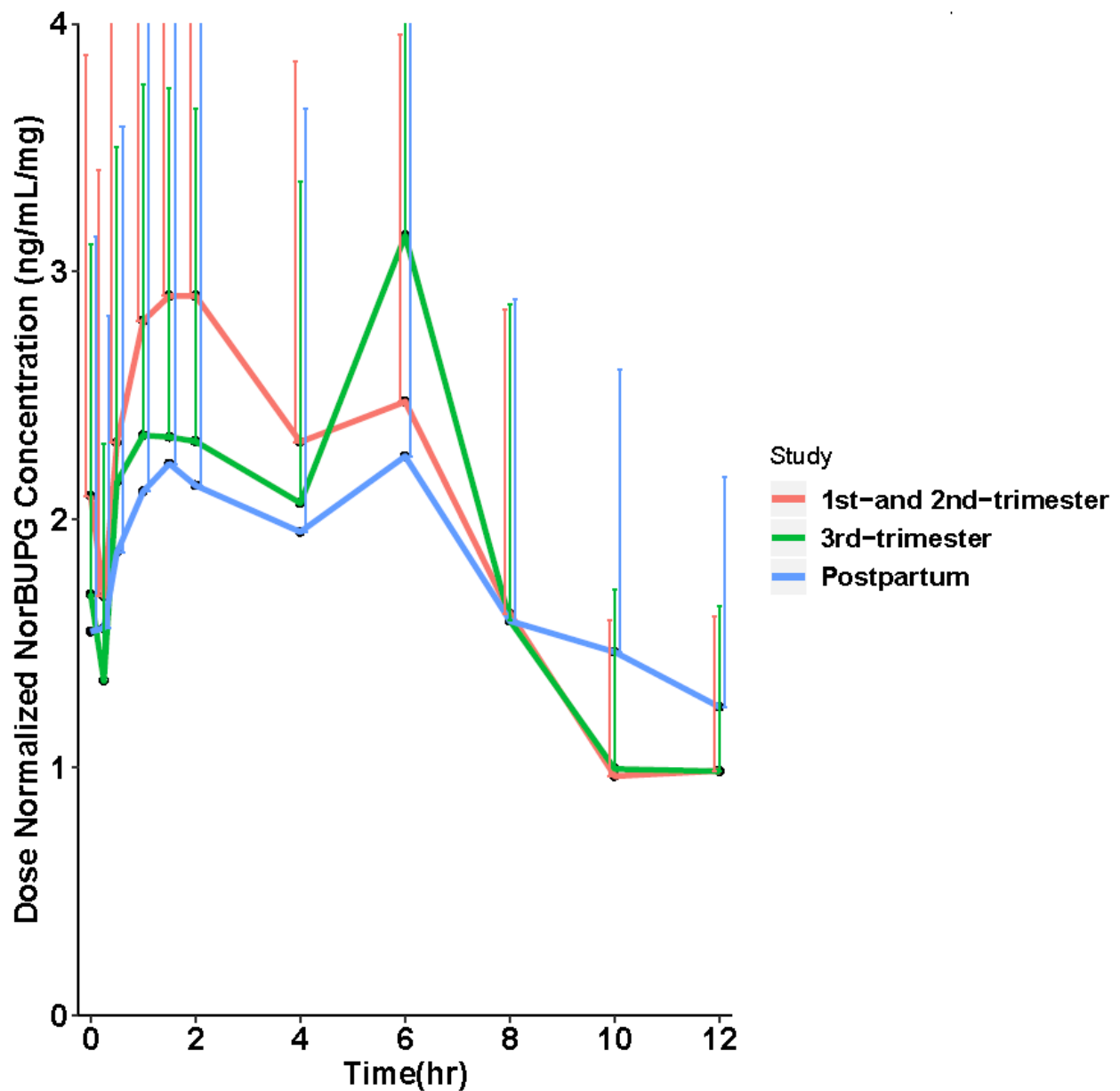


Figure 2-10. Dose normalized norbuprenorphine glucuronide mean concentration time profile (expressed as mean± SD)

N = 19 (2, 9 and 8 patients completed study in 6, 8 and 12 hrs, respectively), 18 (4,1 and 13 patients completed study in 6, 8 and 12 hrs, respectively), and 14 (3 and 11 patients completed study in 6 and 12 hrs) at the 1st-half, 2nd-half of pregnancy and postpartum, respectively.

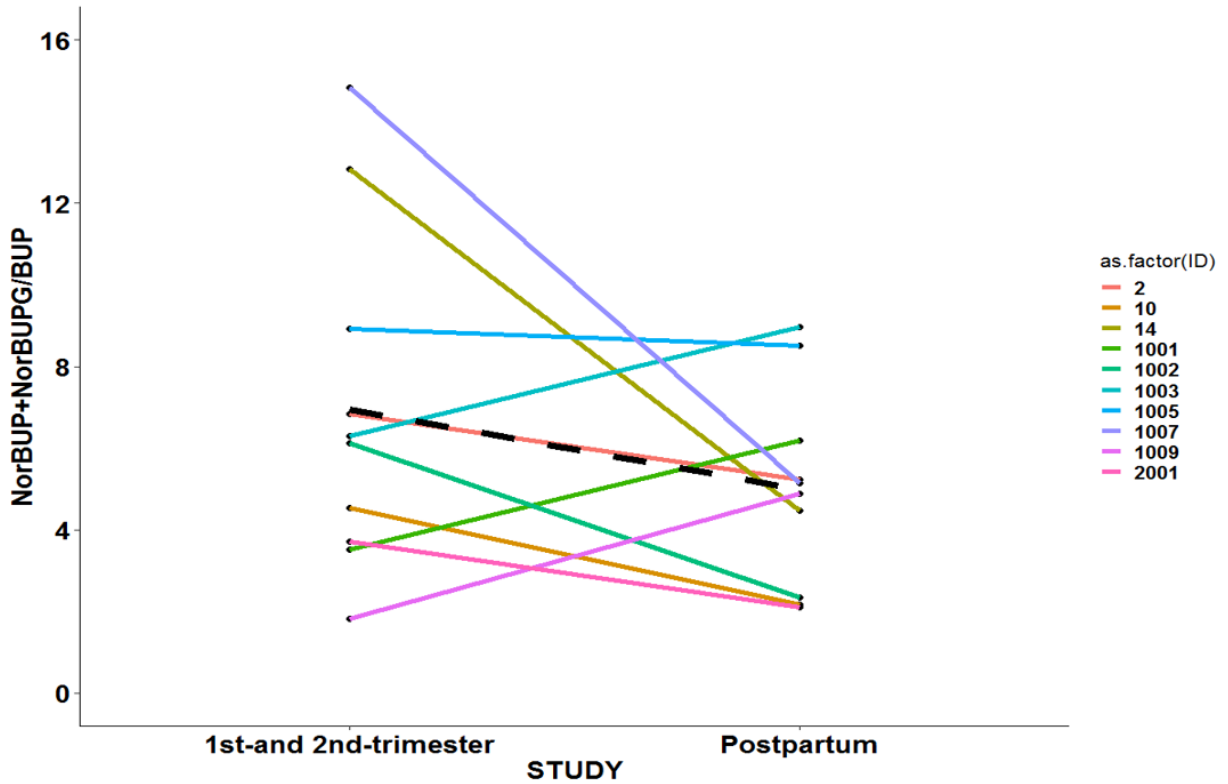


Figure 2-11. The ratios of AUC of norbuprenorphine and AUC of norbuprenorphine glucuronide to the AUC of buprenorphine at 1st-and 2nd-trimester vs postpartum.

Dotted black line is the mean ratios. Each line represents a pair of ratios from one patient. ID is the patient identification number in the studies.

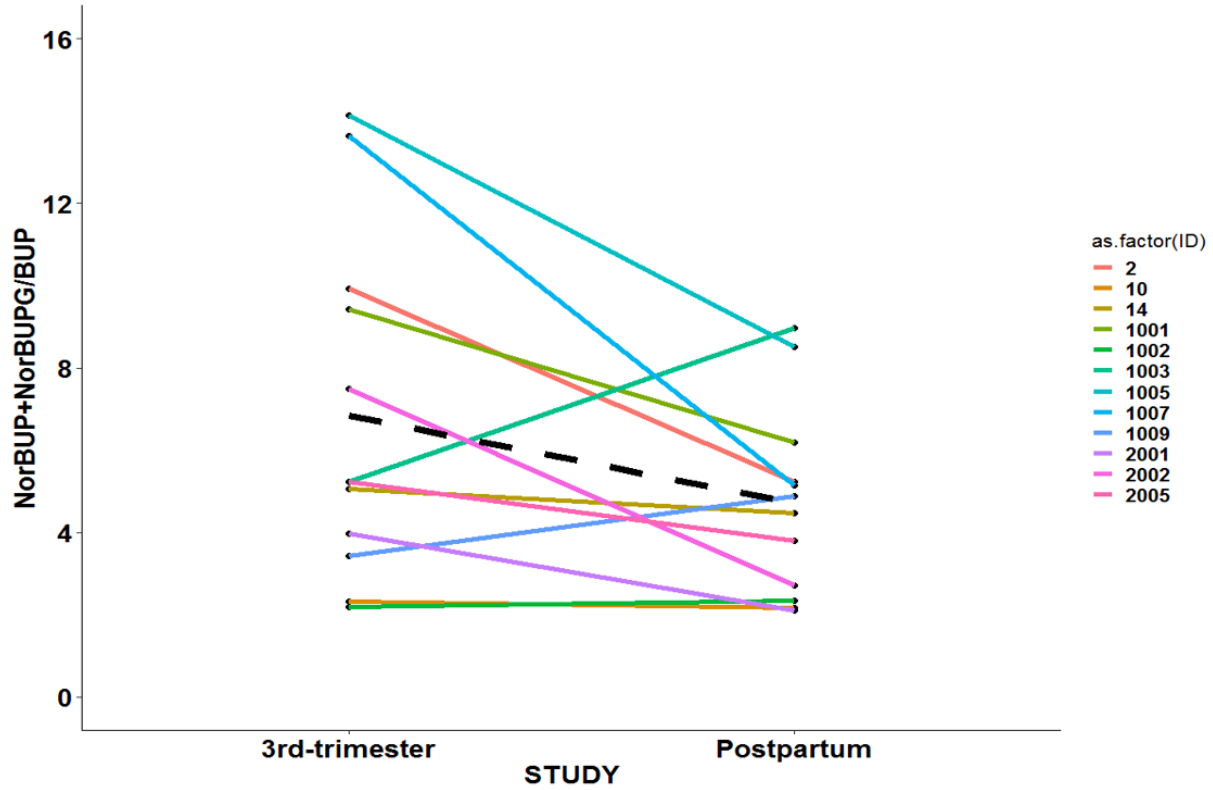


Figure 2-12. The ratios of AUC of norbuprenorphine and AUC of norbuprenorphine glucuronide to the AUC of buprenorphine at 3rd-trimester vs postpartum

Dotted black line is the mean ratios. Each line represents a pair of ratios from one patient. ID is the patient identification number in the studies.

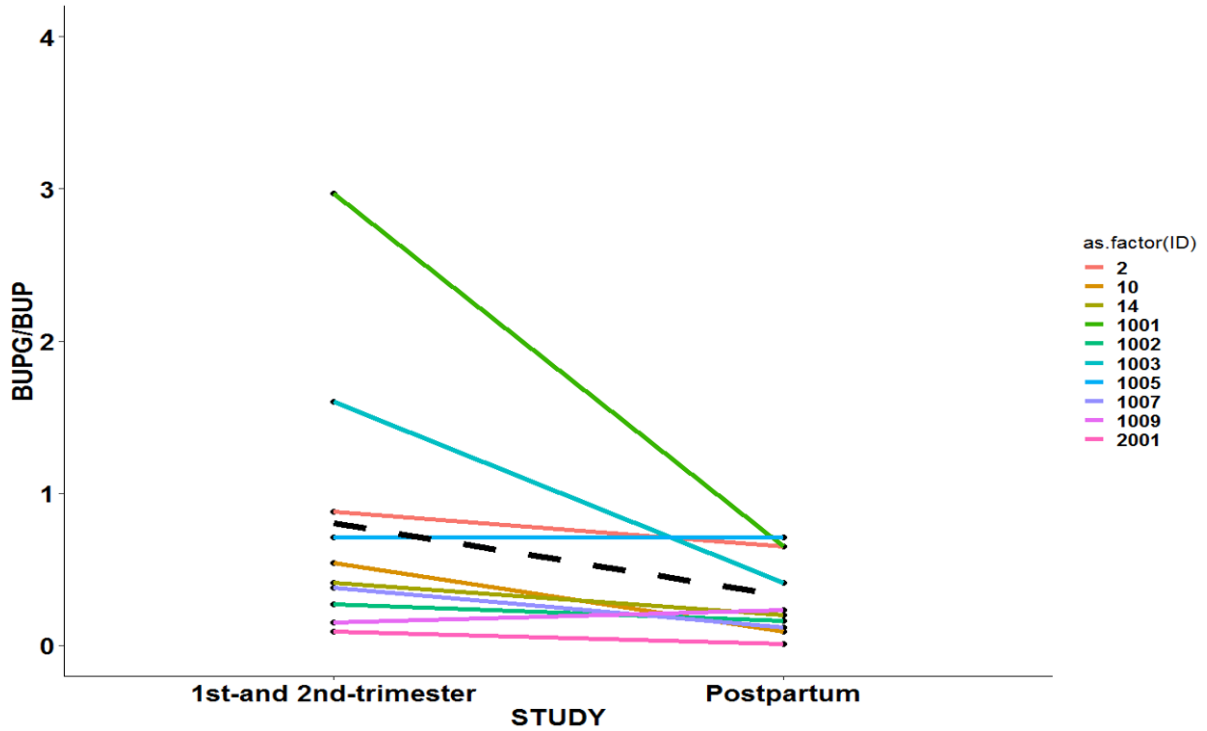


Figure 2-13. The ratios of AUC of buprenorphine glucuronide to the AUC of buprenorphine at 1st-and 2nd trimester vs postpartum

Dotted black line is the mean ratios. Each line represents a pair of ratios from one patient. ID is the patient identification number in the studies.

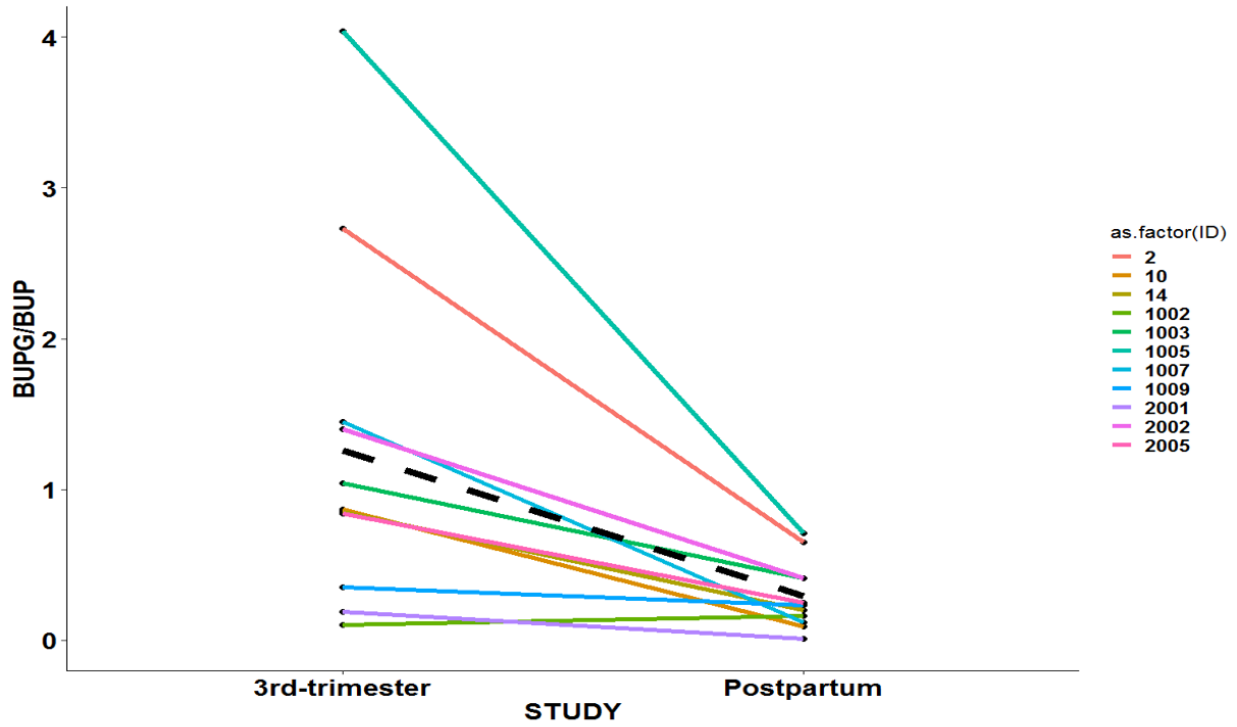


Figure 2-14. The ratios of AUC of buprenorphine glucuronide to the AUC of buprenorphine at 3rd-trimester vs postpartum

Dotted black line is the mean ratios. Each line represents a pair of ratios from one patient. ID is the patient identification number in the studies.

2.5 Discussion

A rapid and sensitive UPLC-MS/MS assay to simultaneously quantify plasma concentrations of buprenorphine, norbuprenorphine, buprenorphine glucuronide and norbuprenorphine glucuronide using a small volume of human plasma was developed and validated. This method displayed linearity over a wide range of concentrations buprenorphine (0.05 - 100 ng/mL), norbuprenorphine (0.2 - 100 ng/mL), and buprenorphine glucuronide and norbuprenorphine glucuronide (0.2 - 200 ng/mL) with acceptable intra- and inter- day precision and accuracy. Following simple protein precipitation, buprenorphine and three metabolites have shown good extraction recovery with no significant matrix effects from human plasma constituents. This assay was successfully applied for the analysis of buprenorphine and its metabolites in a clinical pharmacokinetic study of buprenorphine in pregnant women.

In this method, isotopically labelled molecules of buprenorphine-D₄, norbuprenorphine-D₃, buprenorphine-D₄-3-β-D-glucuronide and norbuprenorphine glucuronide-D₃ were used as internal standards. This is the first time that deuterated labelled buprenorphine glucuronide and deuterated labelled norbuprenorphine glucuronide were used as internal standards to quantify the concentrations of buprenorphine glucuronide and nor buprenorphine glucuronide, respectively. In previously reported analytical method, norbuprenorphine-D₃ was used as an internal standard to quantify the concentrations of norbuprenorphine, buprenorphine glucuronide and nor buprenorphine glucuronide. The deuterated labelled internal standards have similar physiochemical properties compared to the analytical compounds, therefore, normally they have

the same extraction efficiency, chromatographic retention time, matrix effect (if any), and ionization response in mass spectrometry to the analytes to be quantified. The use of deuterated internal standards is very specific for the analytical compounds, which improves the reliability and reproducibility of the assay that we have developed. We did observe signal for norbuprenorphine, buprenorphine glucuronide and norbuprenorphine glucuronide but not buprenorphine when only deuterated internal standards, buprenorphine-D₄, norbuprenorphine-D₃, buprenorphine-D₄-3-β-D-glucuronide and norbuprenorphine glucuronide-D₃ were injected with neat solution or plasma. We made corrections for the responses of norbuprenorphine, buprenorphine glucuronide and norbuprenorphine glucuronide by subtracting the product of the fraction of the signal of non-deuterated compound from corresponding deuterated labelled compound $\left(\frac{\text{Response of non-deuterated compound}}{\text{Response of deuterated compound}}\right)$ in blank plasma spiked with internal standards and the response of corresponding deuterated labelled compound from the absolute response of non-deuterated compound for each run. The equations are shown below.

Corrected response NorBUP = Absolute response NorBUP - $\left(\frac{\text{Response of NorBUP}}{\text{Response of NorBUP-D}_4}\right) \times \text{response NorBUP-D}_4$ in samples

Corrected response BUPG = Absolute response BUPG - $\left(\frac{\text{Response of BUPG}}{\text{Response of BUPG-D}_3}\right) \times \text{response BUPG-D}_3$ in samples

Corrected response NorBUPG = Absolute response NorBUPG - $\left(\frac{\text{Response of NorBUPG}}{\text{Response of NorBUP-D}_4}\right) \times \text{response NorBUPG-D}_4$ in samples

Buprenorphine, three metabolites and their respective internal standards were eluted by 3.3 min, so the total run time for one injection could be shortened to 5 mins. However, a few small

endogenous substances from extracted human plasma appeared after 5 min. Therefore, we set the run time to 7 min to obtain a stable baseline. Only 200 μL plasma was required for this assay, which favors a pharmacokinetic study by decreasing the total blood volume collected from a patient. Furthermore, out of a 100 μL of reconstitution volume, the injection volume was 2 μL , which makes it possible to re-inject samples, multiple times if necessary.

Protein precipitation, liquid-liquid extraction and solid phase extraction are three common methods used to remove proteins or interfering compounds from plasma samples. Protein precipitation using miscible organic solvents, usually methanol or acetonitrile, is the simplest and most rapid approach of sample processing among the three methods. Liquid-liquid extraction method uses immiscible solvents to separate analytes and quantify from the matrix such as plasma. To simultaneously determine buprenorphine, norbuprenorphine and two conjugated glucuronide, liquid-liquid extraction is not suitable due to wide ranging polarity of the four analytes. Compared to protein precipitation and liquid-liquid extraction, solid phase extraction is more time consuming and expensive, but solid phase extraction can produce more purified extracts. Solid phase extraction employs the affinity of analytes to an elution solvent and to the packing material of the stationary phase to separate or purify analytes. The process of a solid phase extraction includes samples pretreatment (usually adding water to dilute plasma samples), cartridge conditioning, sample loading, sample washes, and analytes collection. During the development of the assay, we evaluated protein precipitation and solid phase extraction for the sample preparation. However, the recovery of the analytes were low, especially for buprenorphine glucuronide and norbuprenorphine glucuronide using the solid phase extraction. Buprenorphine has high affinity to mu-opioid receptor, so small concentrations are sufficient for its therapeutic effect in treating

opioid addiction. The low extraction efficiency using solid phase extraction makes it more challenging to accurately determine low concentrations of buprenorphine and all three metabolites.

The plasma concentrations of buprenorphine and three metabolites were comparable to the reported data in other studies. For example, Concheiro et al. reported that the peak concentrations of buprenorphine, norbuprenorphine, buprenorphine glucuronide and norbuprenorphine glucuronide ranged 1.1 - 35.2, 0.8 – 27.5, 1.7 – 31.0, 8.3 – 81.2 ng/mL, respectively, in 3 pregnant women following 14 – 20 mg SL administration of BUP at steady state [238]. In the study conducted by Kuhlman et al., the C_{max} of buprenorphine and norbuprenorphine ranged 0.9 -2.1, 1.26 - 2.25 ng/mL following 8 mg SL administration of BUP at steady state [239].

The AUC ratios of metabolites to parents demonstrated that CYP- and UGT- mediated buprenorphine metabolism were altered during pregnancy compared to postpartum. These results were supported by the observations of increase in the activities of CYP3A4 and UGT1A4 in other studies [165, 168]. The increase in the activities of metabolic enzymes of BUP can partially explain the lower exposure of buprenorphine observed in pregnancy.

2.6 Conclusions

We successfully developed and validated a rapid, sensitive and robust UPLC-MS/MS assay with simple sample preparation to quantify the concentration of buprenorphine, norbuprenorphine, buprenorphine glucuronide and norbuprenorphine glucuronide in human plasma. The advantages of this analytical method include simple sample processing, small plasma volume requirement, high recovery of BUP and three of its metabolites, and short sample run time. We applied the assay to evaluate the pharmacokinetics of buprenorphine and its three metabolites in pregnant women.

This assay enables us to quantify concentration time profiles of buprenorphine, norbuprenorphine, buprenorphine glucuronide and norbuprenorphine glucuronide after low dose of BUP using limited volume of blood samples.

3.0 A Physiologically Based Pharmacokinetic Modeling Approach to Predict Buprenorphine Pharmacokinetics following Intravenous & Sublingual Administration

(This chapter has been published in the British Journal Clinical Pharmacology (2017) 83: 2458–2473)

3.1 Abstract

Introduction: Opioid dependence is associated with high morbidity and mortality. Buprenorphine (BUP) is approved by the FDA to treat opioid dependence. There is a lack of clear consensus on the appropriate dosing of BUP in the presence of inter-patient physiological differences in absorption/disposition, subjective response assessment and other patient comorbidities. The objective of this study is to build and validate robust physiologically-based-pharmacokinetic (PBPK) models for intravenous (IV) and sublingual (SL) BUP in non-pregnant adults as a first step to optimize BUP pharmacotherapy.

Methods: BUP-PBPK modeling and simulations were performed using Simcyp® by incorporating physiochemical properties of BUP, establishing Inter-System Extrapolation Factors (ISEF) based In-Vitro In-Vivo Extrapolation (IVIVE) methods to extrapolate in-vitro enzyme activity data, and using tissue specific K_p estimations. Published data on IV and SL BUP in opioid and non-opioid dependent patients was used to build the models. Fourteen model naïve BUP-PK datasets were used for inter-study and intra-study validations.

Results: IV and SL BUP-PBPK models developed are robust in predicting multi-compartment disposition of BUP over a dosing range of 0.3-32 mg. Predicted plasma concentration-time profiles in virtual patients are consistent with reported data across 5 IV-single dose studies, 5 SL-single dose studies and 4 SL-multiple dose studies. All PK parameter predictions were within 75%-137% of the corresponding observed data. The model developed predicted brain concentration of BUP to be about 4 times higher than that of BUP in plasma.

Conclusion: The validated PBPK models will be used in future studies to predict BUP plasma and brain concentrations based on varying demographic, physiological and pathological characteristics of the patients.

3.2 Introduction

Drug overdose and associated deaths have become a nation-wide crisis in the United States [240]. Data from the Centers for Disease Control and Prevention (CDC) indicate that deaths associated with drug overdose are predominantly driven by an increase in opioid abuse [241-243]. Broadly speaking, the term opioid applies to any endogenous or exogenous substance that interacts with the opioid receptors present in the body [244]. Because of their efficacy in pain management, prescription opioids, such as morphine, hydromorphone, oxycodone, hydrocodone and fentanyl are routinely used in patients [245]. Besides blocking pain-signaling pathway, opiates also activate brain reward system and produce euphoric effects. This makes them highly addictive with prolonged exposure [246, 247].

Opioid dependence is associated with high morbidity and mortality [248, 249]. There is no cure for opioid dependence. Medication-assisted maintenance therapies can reduce complications of opioid dependence, as a consequence of decreased illicit drug use [250, 251]. Currently methadone, buprenorphine (BUP), and naltrexone are the three primary pharmacotherapies approved for treating opioid dependence. The effectiveness of methadone as a maintenance treatment for opioid dependence has been demonstrated in many clinical studies [252, 253]. As a full mu receptor agonist, methadone has abuse potential; consequently methadone maintenance treatment requires daily patient clinic visits. Naltrexone is a mu receptor antagonist; it can reduce illicit drug use by blocking euphoric effects and has no abuse potential, but poor patient retention hampers its routine clinical use [254, 255].

The Food and Drug Administration (FDA) approved BUP for treatment of opioid addiction in 2002. Compared to methadone, BUP is a relatively new drug that has several advantages in clinical practice. BUP exhibits mixed agonist-antagonist opioid effect [256, 257], is highly potent towards kappa (antagonist) and mu (partial agonist) opioid receptors; and it is roughly 50-100 times more potent than morphine [258]. BUP has a ceiling dose-response profile, which limits the risk of major life-threatening adverse effects associated with mu receptor agonists such as respiratory depression [259]. Because of this profile, BUP can provide competitive antagonism to other illicit opioids. In recent times, a sublingual (SL) formulation of BUP (Subutex®) has been shown to be more favorable due to its safety profiles and ease of administration [260]. Suboxone®, a SL BUP formulation in combination with naloxone (full mu receptor antagonist), is another product which was developed and approved to avoid intravenous (IV) abuse.

Despite the proven efficacy of BUP in treating opioid addiction, a meta-analysis showed that patients on BUP had 1.26 times relative risk of discontinuing the treatment compared to patients receiving methadone [261]. In addition, a randomized phase IV study found BUP to be associated with 54% of patient dropout compared to 26% in the methadone group [262]. Several factors such as lack of clear consensus on induction and a maintenance dosing regimen for BUP; subjectivity of the of the Clinical Opioid Withdrawal (COW) scale that is used to determine the dose [263]; confounding effects of factors such as mental health comorbidities, smoking, as well as concomitant medication use that can confound COW scoring and selection of improper BUP dosing would have an impact on the outcomes of BUP therapy and in turn affect compliance. In addition, there is a high inter-patient variability in the bioavailability of BUP due to differences in the extent of absorption with sublingual administration in different patients [264].

A better understanding of the physiological and drug formulation parameters affecting BUP pharmacokinetic and pharmacodynamic profiles is needed to develop a more objective dosing regimen of BUP. Physiologically based pharmacokinetic (PBPK) modeling is a very comprehensive and relatively inexpensive strategy to address the impact of various clinical pharmacotherapeutic factors that impact drug dosing. PBPK modeling approach incorporates a drug's physicochemical properties, human physiological variables and population variability estimates to predict drug exposure [265]. Because PBPK models incorporate anatomical, physiological, and metabolic attributes, any physiological alterations induced by disease, age, gender, genetic polymorphism, and other pathophysiologic conditions can be captured by such models. To the best of our knowledge, the use of PBPK modeling in predicting BUP exposure has not been explored in adult populations. The objective of this study is to predict the time courses of BUP following IV and SL administration of BUP in an attempt to optimize dosing of BUP in patients through the development of BUP PBPK models.

3.3 Methods

BUP PBPK modeling and simulations were conducted using SimCyp® population-based simulator v15.1 (Simcyp limited, Sheffield, UK). WinNonLin software (Phoenix WinNonLin®: version 6.4, Pharsight Corp, Mountainview, CA) was used to simulate steady-state exposure after administration of the SL formulation. Systematic and extensive literature search in MEDLINE through Pubmed was performed to identify published physicochemical properties, plasma protein binding, in-vitro disposition and metabolism profiles of BUP. Similar strategies were used to identify published clinical trials using IV and SL BUP. These data were tabulated and digitized

where necessary for PBPK model building or model validation. The bibliographies of selected articles were also reviewed to identify additional relevant information. GetData Graph Digitizer V.2.26 [266] was used to digitize published BUP clinical pharmacokinetic data.

3.3.1 General workflow for model building and model validation

A full PBPK model was initially developed for IV BUP formulation using physiochemical properties (Table 3-1) [70, 89, 267], in-vitro metabolic profiles [268-270] and published IV BUP clinical PK data in healthy subjects. In the IV model, BUP was modeled to enter the systemic circulation through venous blood (Figure 3-1). Several model naïve IV BUP clinical PK datasets were used to perform inter-study and intra-study validations by comparing mean AUC and C_{\max} values between the observed and predicted data. After establishing a validated IV BUP PBPK model, a SL BUP PBPK model was built by incorporating SL absorption component to the IV model. Sublingual route of administration involves drug being absorbed through reticulated vein underneath oral mucosa, and then entering systemic circulation via facial vein in addition to a portion of the dose being swallowed orally [271]. In order to simulate this, we built a custom administration route that involves inhalation route to mimic the SL absorption, oral absorption to mimic the portion of the drug that is swallowed and a depot release component to mimic the slow release of the drug from the buccal tissue into the systemic circulation (Figure 3-1). Following model building for the SL route, we performed inter-study and intra-study validations similar to the IV model by comparing the mean AUC and C_{\max} values of the predicted model and observed data. Model performance was assessed by intra- and inter-study validations. For the intra-study validations, we used the clinical PK data from different dosing ranges from the same study that is used to build the PBPK profiles. For inter-study validations, we used data from several model

naïve clinical PK studies that were not used in model building. For the validations, we performed visual plots of fitted and the predicted against the observed mean concentration-time profiles. Fifth to 95th percentile intervals (PI) were calculated to show the overall inter-patient variability. The goal was to use IV and SL BUP PBPK models to predict area under the plasma drug concentration-time curve (AUC), which represents the systemic exposure over time following a dose, and compare it to observed data. The criterion for model validation is that the difference of the mean predicted and observed AUC in 100 virtual subjects should fall $\pm 25\%$ for IV model and should fall $\pm 50\%$ for SL model. A wider criterion was chosen for SL model to account for the inherent interpatient variability in dose administered and variable drug absorption by this route.

We were also interested in predicting other BUP PK parameters such as total clearance (CL_{total}) and maximum concentration (C_{max}) as well as their corresponding population variability limits. AUC_{0-t} is the drug exposure between time zero and t hours (the last blood collection time point) and this was estimated using trapezoidal method. $AUC_{0-\infty}$ is the drug exposure between zero hours and infinity and this was estimated by the summation of AUC_{0-t} and extrapolated exposure from C_{last} to infinity ($AUC_{last-\infty} = C_{last}/k$), where k is the terminal disposition rate constant. CL_{total} was calculated per the following equation: $CL = dose/AUC_{0-\infty}$. C_{max} is the observed maximum concentration after administration of a dose.

Table 3-1. Summary of BUP physiochemical parameters

Parameter	Value	Source/Reference
MW (g/mol)	467.64	Pubchem/ DrugBank
Log P _{o:w}	4.98	Avdeef et al. [70]
Compound type	Diprotic Base	
pKa ₁ , pKa ₂	9.62, 8.31	Avdeef et al. [70]
B/P	0.55	Mistry et al. [89]
f _u ^a	0.03*	Walter et al. [267]

Abbreviations: MW: molecular weight; logP: logarithm of the octanol to water partition coefficient, pKa: negative logarithm of the acid dissociation constant, B/P: blood to plasma partition coefficient; f_u: Plasma fraction unbound; ^a f_u was fitted by non-linear mixed effect modeling strategy using parameter estimation module of Simcyp. Nelder-Mead method was used for the minimization. f_u, 0.04, published by Walter et al [267]. was used as the initial estimate.

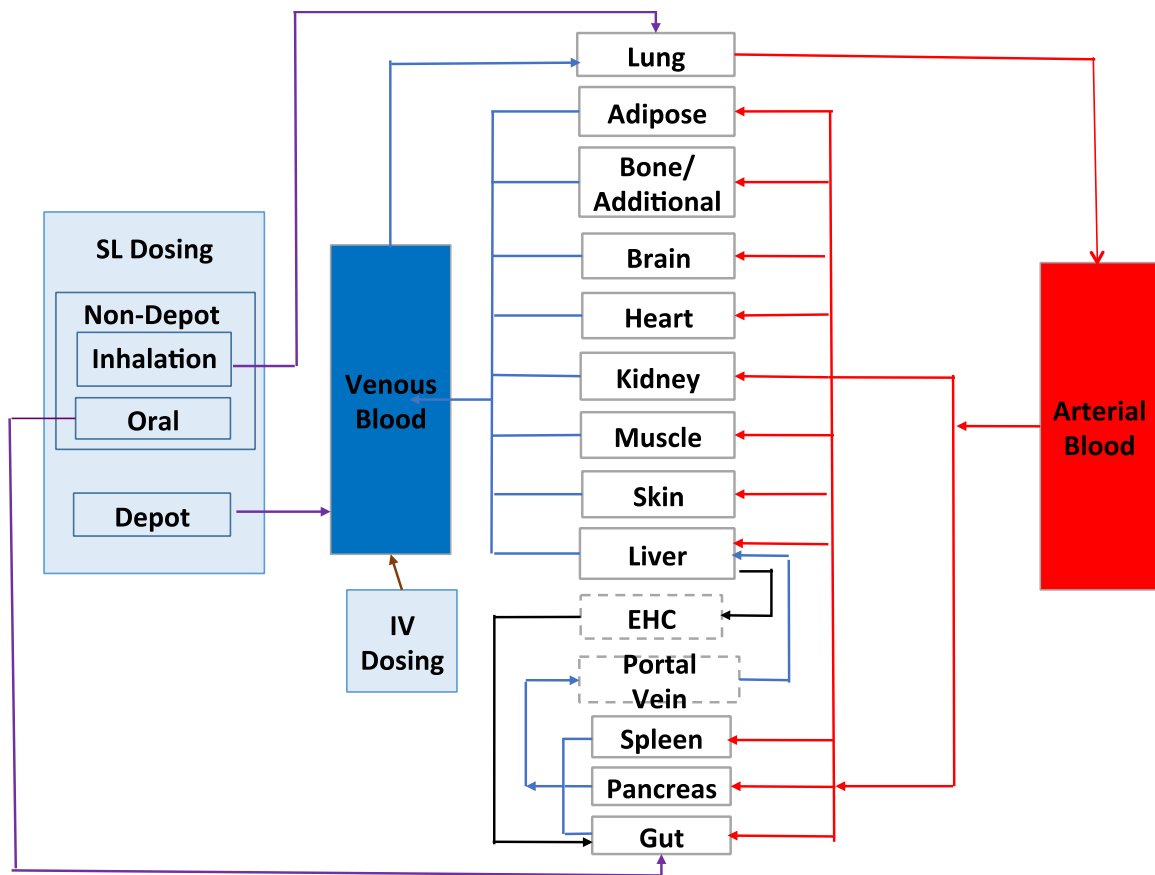


Figure 3-1. Compartmental structure of the full BUP IV and SL PBPK models. The schematic shows how SL and IV administration was modeled.

3.3.2 IV Buprenorphine - PBPK model development

Distribution Profile:

The volume of distribution at steady state (V_{ss}), 2.77 L/kg, reported by Bullingham et al [272] was used as a reference to build the PBPK distribution component. A predicted V_{ss} of 2.48 L/kg was estimated using reported BUP physicochemical properties as well as estimated tissue to plasma partition coefficients (K_p) for all major tissue specific physiological compartments (Table 3-2). V_{ss} (equation 1) is estimated by serial addition of plasma volume (V_p), erythrocyte volume (V_e) and volumes associated with each major tissue (V_t) [273].

$$V_{ss} = V_p + V_e \times (E:P) + \sum V_t \times K_p \quad \dots\dots\dots \text{Equation 1}$$

Where E:P represents erythrocyte to plasma partitioning. The E:P is estimated using the SimCyp® parameter estimation modules based on the information of blood to plasma ratio and hematocrit.

Tissue specific K_p values of BUP for the full-PBPK model were estimated using the corrected Poulin and Theil method [274-276]. Furthermore, sequential sensitivity analysis was performed to further identify and optimize tissue K_p values utilizing non-linear mixed effects modeling methods. In the final model K_p estimates for just the bone/additional compartment had to be optimized and K_p values for all other organ and tissues remained as the predicted values. Table 11 summarizes distribution parameters used in the BUP simulations. A hypothetical additional compartment was incorporated along with the bone and the K_p value for this combined compartment was predicted and optimized using non-linear mixed effects modeling methods using the parameter estimator module of Simcyp®.

Table 3-2. Distribution parameters for BUP drug profile

Parameter	Value
Model	Full PBPK
V_{ss} (L/kg)-predicted ^a	2.48
V_{ss} (L/kg)-observed ^b	2.77
Tissue Partition Coefficients (K_p)	
Adipose	0.0044
Bone/Additional ^c	35
Brain	3.41
Gut	2.69
Heart	0.83
Kidney	1.29
Liver	2.13
Lung	0.29
Pancreas	2.20
Muscle	1.31
Skin	1.60
Spleen	1.31
K_p scalar ^d	0.225

Abbreviation: V_{ss} : Volume of distribution at steady state; ^a Bullingham et al. [272]; ^b V_{ss} predicted and K_p values for all tissue were predicted by corrected Poulin and Theil method [274-276]; ^c Bone/Additional compartment K_p value was optimized using the Simcyp® parameter estimation module, Nelder-Mead method was used for the minimization. The predicted K_p value, 3.73, by Poulin and Theil method was used as the initial value, and (0.001, 100) used as the boundaries; ^d K_p scalar was optimized using the Simcyp® parameter estimation module, Nelder-Mead method was used for the minimization. The default K_p scalar, 1, was used as the initial value, and (0.01, 100) used as the boundaries.

Clearance Profile:

BUP is extensively metabolized to nor-BUP by N-dealkylation, and then both BUP and nor-BUP are further conjugated to BUP glucuronide and nor-BUP glucuronide respectively [277]. The N-dealkylation is primarily mediated by CYP3A4 and CYP2C8, and the glucuronidation is mainly mediated by UGT1A1, 1A3, and 2B7 [268, 277-279]. Together these enzymes are responsible for majority of BUP metabolism with minor contribution from other CYP450 and UGT enzymes. Established in vitro-in vivo extrapolation (IVIVE) methods using enzyme specific microsomal BUP metabolism parameters and inter-system extrapolation factors (ISEF) based estimates were used to extrapolate recombinant in-vitro enzyme activities to in vivo intrinsic clearances (equation 2) [280].

$$CL_{int} = \left[\sum_{j=1}^n \left(\sum_{i=1}^n \frac{ISEF_{ji} \times V_{max_i} (rhCYP_j) \times CYP_j \text{ abundance}}{K_{m_i} (rhCYP_j)} \right) \right] \times MPPGL \times \text{liver weight}$$

.....Equation 2

Where CL_{int} is the sum of V_{max}/K_m of metabolic pathways (i) for each of the involved enzyme (j), V_{max} is the maximum rate of metabolism, K_m is the BUP Michaelis-Menten constant for each individual enzyme, rhCYPs are the recombinantly expressed human cytochrome P450s, MPPGL is the amount of microsomal protein per gram of human liver, CYP_j abundance is the amount of jth enzyme in pmol for every mg microsomal protein of the human liver. The CYP_j abundance, MPPGL, and liver weight are assigned by SimCyp® V.15 for each individual virtual population, which are parts of predicted population variability (Table 3-3).

ISEF is used to scale activity of a unit amount of each enzyme in the recombinant microsomal system to human liver microsomal, and scaling of rhCYPs data to the entire human

body is accomplished through equation 2. ISEF values for each drug metabolizing enzyme can be calculated with either V_{max} and K_m or CL_{int} as given by the following equations:

$$ISEF (V_{max}) = \frac{V_{maxji}(HLM)}{V_{maxi} (rhCYP_j) \times CYP_j \text{ abundance}(HLM)} \dots\dots\dots \text{Equation 3}$$

$$ISEF (CL_{int}) = \frac{CL_{intji}(HLM)}{CL_{inti} (rhCYP_j) \times CYP_j \text{ abundance}(HLM)} \dots\dots\dots \text{Equation 4}$$

CYP_j abundance (HLM) is the estimated abundance of j^{th} CYP enzyme in a human liver.

The intrinsic clearance of BUP and ISEF values associated with enzymes primarily involved in BUP metabolism were listed in Table 3-4.

Table 3-3. Values used in equation 2 to scale rhCYPs data to the entire human body

(Adapted from healthy population in SimCyp®)

Drug Metabolizing Enzyme		Abundance (pmol/mg protein)	CV%
CYP2C8		24	81
CYP3A4		137	41
UGT1A3		23	36
UGT2B7		71	30.4
UGT1A1	EM	48	24
	PM	0.42	50.8
	IM	0.72	39.9
	UM	1.46	30
Mean population liver volume (L)		1.65056	
Mean population liver density (g/L)		1080	
Mean population MPPGL (mg/g)		39.79066	

Abbreviations: EM: Extensive metabolizer; PM: Poor metabolizer; IM: Intermediate metabolizer, UM: Ultra-rapid metabolizer. Except UGT1A1, only EM were included for CYP2C8, CYP3A4, UGT1A3, and UGT2B7 in SimCyp healthy population. CV: Coefficient of variation

Table 3-4. Intrinsic clearance and ISEF values associated with enzymes primarily involved in buprenorphine metabolism

Enzyme	Value	Source/Reference
CYP3A4		
V_{\max} (pmol/min/pmol of isoform)	10.4	Picard et al. [268]
K_m (μM)	13.6	Picard et al. [268]
f_{umic}	0.1	Cubitt et al. [269]
ISEF	2.355	Calculated from equation 3
CYP2C8		
V_{\max} (pmol/min/pmol of isoform)	1.4	Picard et al. [268]
K_m (μM)	12.4	Picard et al. [268]
f_{umic}	0.1	Cubitt et al. [269]
ISEF	8.33	Calculated from equation 3
UGT1A1		
Cl_{int} ($\mu\text{L}/\text{min}/\text{pmol}$ of isoform)	0.0162	Oechsler et al. [281]
f_{umic}	0.1	Cubitt et al. [269]
ISEF	0.636	Calculated from equation 3
UGT1A3		
Cl_{int} ($\mu\text{L}/\text{min}/\text{pmol}$ of isoform)	0.0155	Oechsler et al. [281]
f_{umic}	0.1	Cubitt et al. [269]
ISEF	6.65	Calculated from equation 3
UGT2B7		
Cl_{int} ($\mu\text{L}/\text{min}/\text{pmol}$ of isoform)	0.0116	Oechsler et al. [281]
f_{umic}	0.1	Cubitt et al. [269]
ISEF	5.19	Calculated from equation 3

Abbreviation: f_{umic} : Fraction of unbound drug in the in vitro microsomal incubation

3.3.3 IV BUP Clinical Pharmacokinetic Studies: Model validation

BUP clinical pharmacokinetic studies in healthy opioid dependent and opioid non-dependent subjects listed in Table 3-5 were considered for the study. The 72 hr pharmacokinetic profile from Huestis et al [87] was used for model development (8 mg) and intra-study validation (2,4,12 and 16 mg). One hundred virtual healthy subjects spread over 10 trials were used for each of the PBPK simulation. Data from Bai et al [74], Harris et al [88], and Mendelson et al [78] were used for inter-study validation. As mentioned above mean AUC was primarily compared between observed datasets and predicted simulations. The population variability from the virtual population is presented in the concentration-time plots as 5th and 95th percentile plots. Due to lack of individual concentration-time profiles reported for each observed study and limitations involved in digitizing observed variability data we were not able to compare predicted population variability with observed population variability. The basic demographic information such as age and sex were matched when performing the simulations.

Table 3-5. Intravenous buprenorphine clinical pharmacokinetic studies

No.	N	Subject	Age range	Dosage	C _{max}	AUC _{0-∞}	t _{1/2}	CL _{total}	Reference
	(male /female)		yrs	mg	ng/mL	ng•h/mL	h	L/h	
1	25 (19/6)	Healthy female and male non-opioid dependent	20-53	0.3	2.3	5.2	8.6	58	Bai et al. [74]
2	6 (6/0)	Healthy male non-dependent opioid user	32-39	2	21.6	41.4	21.8	49.8	Huestis et al. [87]
				4	56.3	75.9	27.5	53.2	
				8	110.8	153.3	28	52.4	
				12	164.5	245.1	22.3	54.7	
				16	174.8	269.1	25.6	60	
3	9 (8/1)	Opioid dependent	21-42	4	69.7	70.4 _b	32.1	NA	Harris et al. [88]
4	6 (5/1)	Healthy female and male non-dependent opioid user	21-38	1	14.3	18.4	16.2	62.5	Mendelson et al. [78]

Abbreviations: C_{max}: maximum plasma concentration; AUC_{0-∞}: area under plasma concentration-time curve from time 0 to infinite after a dose; t_{1/2}: half-life; CL_{total}: total clearance; ^a n: Subject numbers; ^b The AUC from Harris et al [88] was reported as 0-24 hrs.

3.3.4 SL BUP - PBPK model development

Absorption Profile:

Modeling and simulation of SL administration is not available in the current version of Simcyp®. A custom depot and non-depot combination approach was used to simulate SL administration. The non-depot component included an inhalation part to mimic SL arterial absorption of BUP and an oral part to represent the portion of the SL formulation that is swallowed and subjected to absorption and metabolism in the GI tract. Despite drug is supposed to diffuse into blood through vessels in the mouth to avoid first-pass metabolism in the gut and liver following SL administration, there is a large portion of the dose is swallowed. This is supported by the results of a clinical study that voriconazole increased the exposure (as measured by AUC) of SL BUP 1.8-fold after pretreatment of voriconazole for 5 days in healthy subjects [282]. The depot route of drug absorption was used to mimic the slow release of BUP from surrounding buccal tissue following SL absorption. BUP is a multi-phasic drug, SL and oral components explained two disposition phases and the depot component explained the disposition during the terminal elimination phase. The percent contribution of each route is listed in Table 3-6. A first-order absorption model was used for prediction of oral absorption profile (Table 3-7).

Table 3-6. Sublingual buprenorphine dosing allocation between depot and non-depot components

Total Dose	SL	Depot	Non-Depot	Non-Breakdown	Depot
	(37.5% of Total Dose)		(62.5% of total dose)	SL	Oral
4 mg	1.5 mg	2.5 mg	10%	90%	
8 mg	3 mg	5 mg	10%	90%	
12 mg	4.5 mg	7.5 mg	10%	90%	
16 mg	6 mg	10 mg	7%	93%	
24 mg	9 mg	15 mg	7%	93%	
32 mg	12 mg	20 mg	7%	93%	

Table 3-7. First-order absorption model parameter values

Parameter	Value	Reference/Source
f_a	0.80	Parameter estimation module
K_a (1/h)	2.34	Parameter estimation module
Q_{gut} (L/h)	8.12	Predicted
f_{uGut}	1	User input

Abbreviations: f_a : Fraction of absorption; K_a : Absorption rate constant; Q_{gut} : nominal flow from gut model; f_{uGut} : unbound fraction within enterocyte

3.3.5 SL BUP Clinical Pharmacokinetic Studies: Model validation

BUP clinical pharmacokinetic studies in healthy non-opioid dependents and opioid dependents listed in Table 3-8 were used for this study. The 72 hr pharmacokinetic data from Ciraulo et al [66] was used for model building (8 mg) and intra-study validation (4, 8, 16 and 24 mg). Data from Harris et al [69] and McAlear et al [283] was used for inter-study validation. Data from Compton et al [284] and Greenwald et al [237] were used for the validation of multiple-dose simulations (Table 3-9). One hundred virtual healthy subjects spread over 10 trials were used for each of the PBPK simulations.

BUP exposure in plasma and the corresponding mu receptor availability was predicted along with predicted BUP brain concentrations using the validated SL BUP PBPK model (16 mg dose) and plasma concentration to mu receptor availability relationship reported by Greenwald et al [60]. BUP brain K_p value (Table 3-2) estimated using the corrected Poulin and Theil method [274-276] was used to simulate BUP exposure profile in brain compartment.

Similar to the IV BUP model validation, mean AUC and C_{max} was primarily compared between observed datasets and predicted simulations. The population variability from the virtual population is presented in the concentration-time plots as 5th and 95th percentile plots. Due to lack of individual concentration-time profiles reported for each observed study and limitations involved in digitizing observed variability data in the literature we were not able to compare predicted population variability with observed population variability. The basic demographic information such as age and sex were matched in the simulations.

Table 3-8. SL BUP clinical PK single dose studies considered for modeling

Ref.	Subject	N	Age range	BUP/NAL	C _{max}	AUC _{0-t} ¹	t _{1/2}	T _{max}
		(male /female)	yrs	mg	ng/mL	ng•h/mL	h	h
Harris et al. [69]	Healthy female and male non-dependent opioid user	8 (7/1)	22-42	4/1	1.8	12.5	NA	1.1
				8/2	3.0	20.2	NA	1.0
				16/4	5.9	34.9	NA	0.8
				16/0	5.5	32.6	NA	1.0
McAleer et al. [283]	Opioid naïve healthy male subjects	27 (27/0)	19-42	2/0	1.6	NA	NA	1.5
				8/0	4.0	31.8	30.0	1.0
				12/0	5.4	41.6	25.6	1.0
				16/0	6.4	52.0	23.9	0.8
				8/2	3.2	24.5	25.5	1.0
				8/2	3.2	24.6	26.8	1.0
Ciraulo et al. [66]	Healthy non-dependent opioid user	23 (16/7)	21-45	4/0	2	9.4	NA	1.1
				8/0	2.6	19.9	NA	1.2
				16/0	4.4	34.9	NA	0.9
				24/0	5.4	48.8	NA	0.9
		15 (14/1)	21-55	4/1	2.3	13.1	NA	1.0
				8/2	3.5	23.2	NA	1.0
				16/4	5.8	39.4	NA	1.1
				24/6	6.4	47.5	NA	1.0

Abbreviations: C_{max}: maximum plasma concentration; AUC_{0-t}: area under plasma concentration-time curve from time 0 to time t after a dose; t_{1/2}: half-life; t_{max}: time to maximum concentration. NAL: Naloxone; ¹AUC_{0-t} is AUC_{0-72h} in Harris et al [69], Ciraulo et al [66] study, and AUC_{0-12h} in McAleer et al [283] study.

Table 3-9. SL BUP clinical PK multiple dose studies considered for modeling

Ref.	Subject	N (male/female)	Age range	BUP/NAL	C _{max}	AUC ₀₋₂₄	t _{1/2}	T _{max}
			yrs	mg	ng/mL	ng•h/mL	h	h
Compton et al. [236]	Healthy female and male dependent opioid user	16 (NP)	18-65	16/0	6.88 ^a	54.7	NA	NA
		15 (NP)		24/0	9.1 ^a	81.1	NA	NA
		10 (NP)		32/0	13.93 ^a	103.0	NA	0.94
Greenwald et al. [237]	Healthy female and male dependent opioid user	5 (3/2)	34-45	2/0	0.85 ^a	6.5	NA	0.9
				16/0	6.3	48.6	NA	1.2
				32/0	13.2	96.0	NA	1.2

Abbreviation: C_{max}: maximum plasma concentration; AUC₀₋₂₄: area under plasma concentration-time curve from time 0 to 24 hours after a dose; t_{1/2}: half-life; CL_{total}: total clearance; NP, not provided. ^a Values calculated from graph digitized data.

3.3.6 Virtual Patient Population

Simcyp® virtual healthy volunteer patient population was used to simulate single dose IV and SL BUP exposure. During model building and validation steps for both models, demographic details of the reported patient populations in considered PK studies (Tables 3-5, 3-8, 3-9) were matched with virtual healthy patient population to avoid altered physiology-based differences. No changes were made to the Simcyp® healthy volunteer patient population file.

Since virtual patient population was used for all PBPK simulations and published clinical PK data was used to build and validate our PBPK models, this work was not submitted for approval to an ethics committee for approval.

3.3.7 SL BUP Steady State Exposure Simulations

Since SimCyp® does not have the ability to perform virtual multiple dosing and drug-drug-interaction simulations for custom defined formulations, we used SimCyp® to predict single dose SL BUP concentration-time profiles for 100 virtual subjects and following this Phoenix® WinNonlin® was used to characterize single dose PK parameters and simulate SL BUP steady state PK. A two compartment, 1st order absorption with a lag time PK model within WNL5 classic modeling module was used to predicted concentration-time profile after a single dose. Gauss-Newton (Levenberg and Hartley) was selected as the minimization method, and the convergence criterion was set as 0.0001. The generated micro rate constants were used as the user supplied initial parameter values for the multiple dose simulation through the same PK model.

3.4 Results

3.4.1 BUP Exposure Prediction following a single IV BUP dose in healthy subjects:

Predicted concentration-time profile of the final BUP PBPK model following 8 mg IV BUP dose was within the range of the observed data published by Huestis et al [87]. The predicted means of concentration-time profiles and 90% PI overlaid with the observed data for the first 24 hrs of the 72 hr data set are shown in Figure 3-2. As shown in the figure 3-2 A the observed data was within the 90% PI of the variability observed around the predicted mean exposure. The predicted and observed mean concentration-time profiles were visually similar. This was true for the inter and intra study validation plots as shown in Figures 3-2 B and 3-2 C, D, E, F respectively. The accuracy of the predicted means of $AUC_{0-\infty}$ and CL_{Total} were within 85-115% of the observed means (Table 3-10). These limits hold true for all doses (2, 4, 12 and 16 mg) tested for intra-study validation.

The model was further validated by two model-naïve clinical PK datasets (Bai et al [74], Harris et al [88], and Mendelson et al [78]) for inter-study validations and the comparisons are listed in Table 19. The accuracy of the predicted means of AUC and CL were within 85-115% of the observed means. These limits held true for all doses (0.3, 1, 4 mg) tested for inter-study validation.

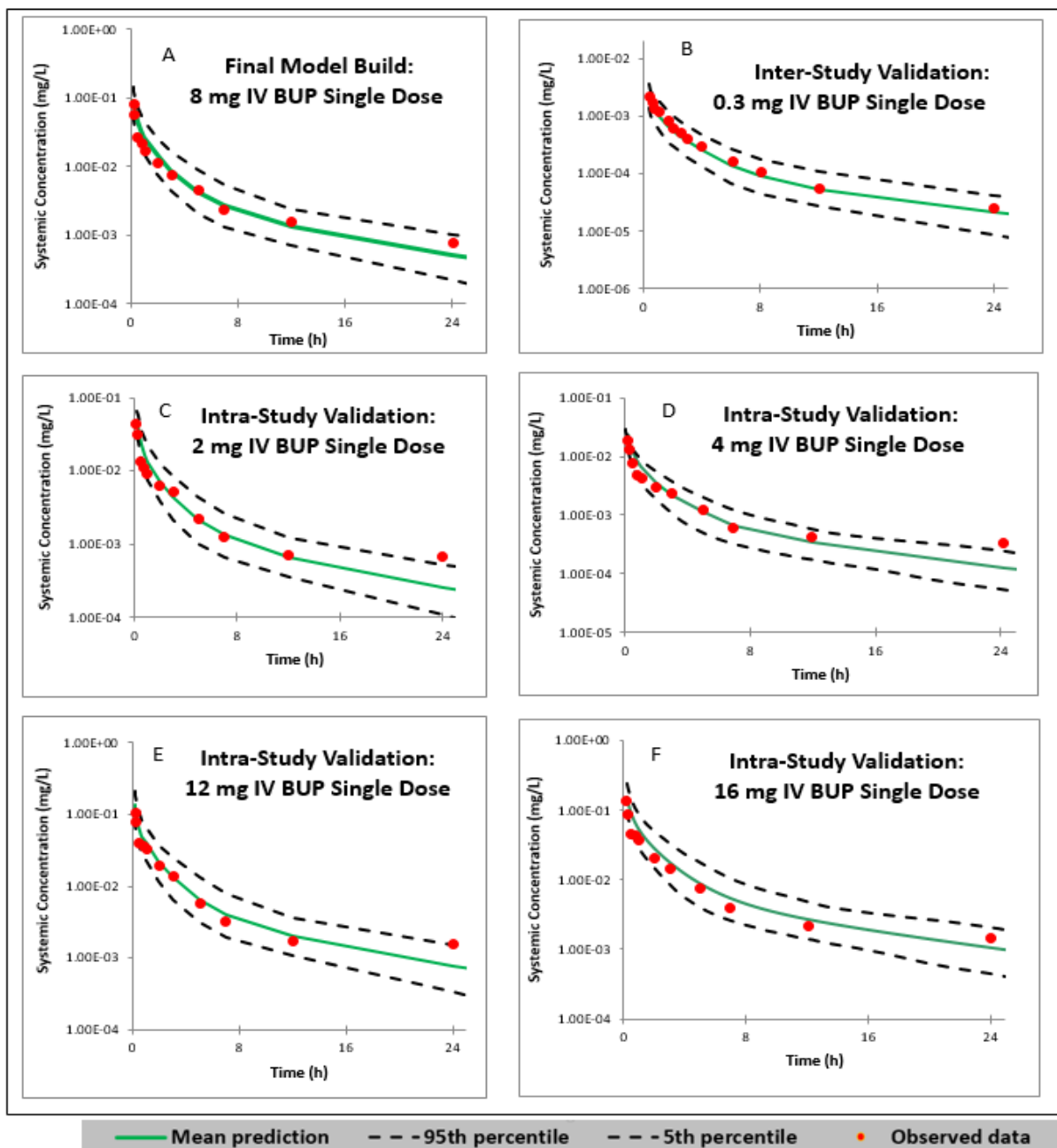


Figure 3-2. Predicted and observed concentration-time profiles following a single IV push doses of BUP.

“A” represents plot of the final model built with and 8 mg IV BUP single dose comparing observed data from Huestis et al. [87]; “B” represents inter-study validation plot with 0.3 mg IV BUP single dose as observed by Bai et al. [74]; C, D, E, and F represents intra-study validation plots with 2, 4, 12 and 16 mg IV BUP single doses respectively as observed by Huestis et al. [87]; 0-24 hrs PK simulations shown here

Table 3-10. Goodness of fit for IV BUP model in healthy subjects

Process	Data source	Dose (mg)	AUC _{0-∞}			CL _{Total}		
			Observed	Predicted (90% PI)	Diff.	Observed	Predicted (90% PI)	Diff.
			mg•h/L	mg•h/L	%	L/h	L/h	%
Final model		8	0.153	0.151 (0.0821 – 0.2688)	1.3	52.4	53.1 (29.8-97.4)	1.3
Intra-study validation		2	0.0414	0.0379 (0.0209 -0.0665)	-8.5	49.8	52.8 (30.1-95.7)	6.0
	Huestis et al [87]	4	0.0759	0.0756 (0.0419 -0.1314)	0.4	53.2	52.9 (30.4-95.5)	0.6
		12	0.245	0.226 (0.123 -0.402)	7.7	54.7	53.1 (29.8-97.6)	2.9
		16	0.2691	0.2886 (0.1561 – 0.5125)	7.2	60.0	55.4 (31.2-102.5)	-7.6
Inter-study validation	Bai et al [74]	0.3	0.0052	0.0049 (0.0025-0.0087)	9.1	57.7 ^a	61.2 (34.5-120)	13
	Harris et al [88]	4	0.0704 ^b	0.0727 (0.0534-0.0958)	3.3	NP	NP	NP
	Mendelson et al [78]	1	0.0184	0.0181 (0.00993-0.0313)	-1.6	62.5	55.2 (31.9-100.7)	-11.7

Abbreviations: AUC_{0-∞}: area under plasma concentration-time curve from time 0 to infinite after a dose; CL_{total}: total body clearance. NP: not provided; PI: percentile interval. ^aBai et al [74] didn't report CL, so the observed CL was calculated by using Dose/ the reported AUC_{0-∞}; ^bHarris et al [88] only reported AUC₀₋₂₄. And CL was not available. Difference (%) = ((predicted– observed mean value)/ observed mean value)*100

3.4.2 Modeling prediction following a SL of BUP in healthy volunteers

The predicted means of concentration-time profiles and 90% PI overlaid with the observed data are shown in Figure 3-3. As shown in the figure 3-3 A the observed data was within the 90% PI of the variability observed around the predicted mean exposure. Moreover, the predicted and observed mean concentration-time profiles were visually similar. This was true for the intra and inter study validation plots as shown in Figures 3-3 B and 3-3 C, D respectively. The accuracy of the predicted means of AUC were within 75-125% of the observed means for all inter and intra-study validations with the exception of a 24 mg single dose study where the accuracy was +137%. The accuracy of the predicted means of C_{\max} were within 80-125% for all the studies (Table 3-11).

The model was further validated by two model-naïve clinical PK datasets published by Harris et al [69] and McAleer et al [283] (Table 3-11) as a measure of inter-study validation. The accuracy of the predicted means of AUC were within 85-115% of the observed means, and the accuracy of the predicted means of C_{\max} were within 80-125% of the observed means. Sixteen, 24, and 32 mg doses of SL BUP at steady state was also validated against studies published by Compton et al [284] (Figure 3-4) and Greenwald et al [237]. Accuracy of AUC and C_{\max} are tabulated in Table 3-12. The accuracy limits for these comparisons were between 85 and 115%.

We were able to predict the brain concentrations of BUP using the model that was developed. BUP brain exposure was predicted to be about 4 times higher than that of plasma (Brain-AUC_{0-72h}: 0.195 mg•h/L; Plasma-AUC_{0-72h}: 0.0536 mg•h/L). We were able to use the mu receptor availability data from Greenwald et al [206] to illustrate the relationship between brain/plasma concentration of BUP and mu receptor occupancy (Figure 3-5).

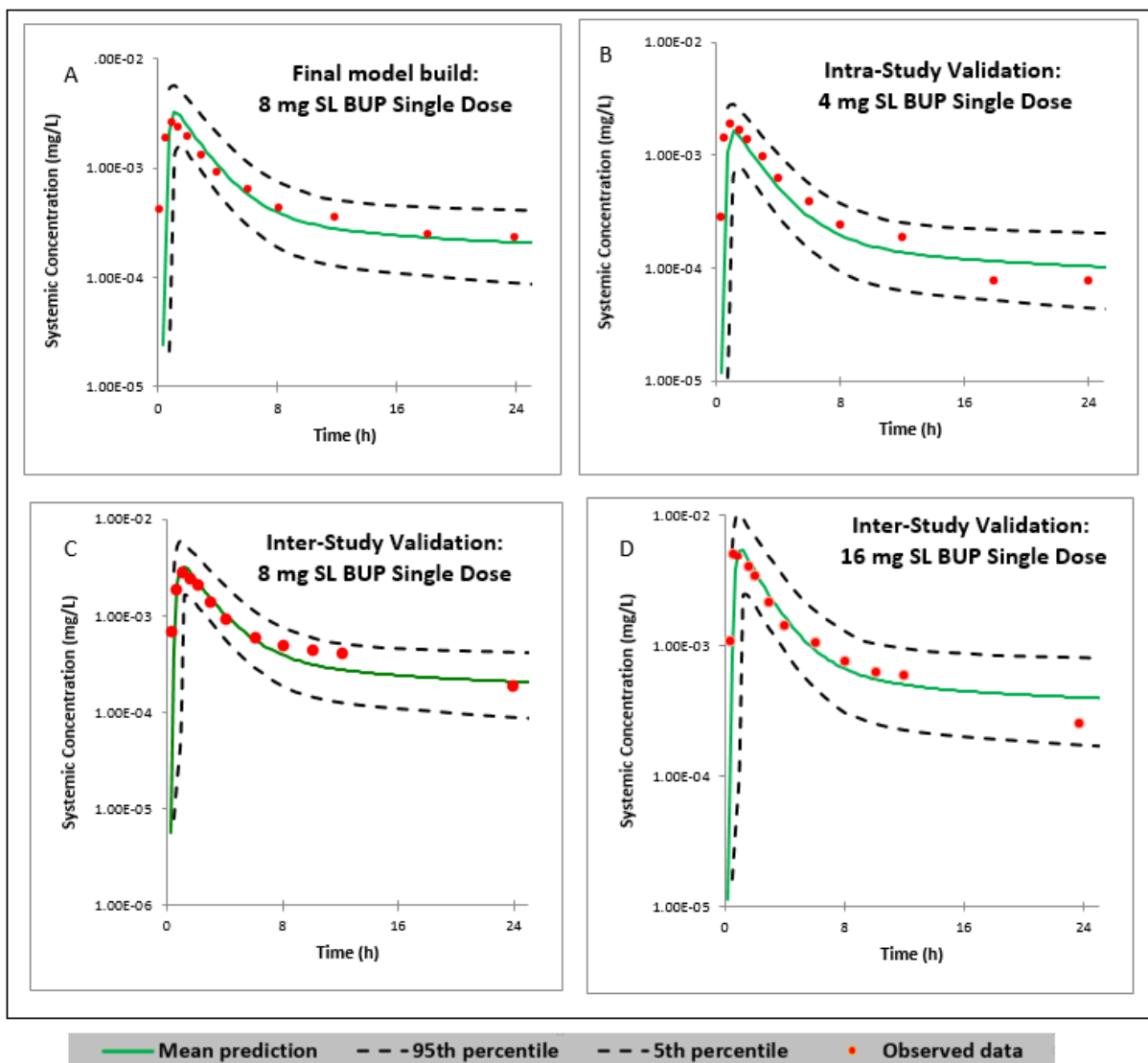


Figure 3-3. Predicted and observed concentration-time profiles following a single SL doses of BUP in 100 virtual healthy subjects.

“A” represents plot of the final model built with an 8 SL BUP single dose comparing observed data from Ciraulo et al. [66]; “B” represents intra-study validation plot with 4 mg SL BUP single dose as observed by Ciraulo et al. [66]; C and D represent inter-study validation plots with 8 and 16 mg SL BUP single dose respectively as observed by Harris et al. [69]; 0-24 hrs of 48 and 72 hrs simulations shown here.

Table 3-11. Goodness of fit for SL BUP model in healthy subjects

Process	Data source	Dose (mg)	AUC _{0-∞}			CL _{Total}		
			Observed	Predicted (90% PI)	Diff.	Observed	Predicted (90% PI)	Diff.
			mg•h/L	mg•h/L	%	L/h	L/h	%
Final model		8	0.0199	0.0221 (0.0100-0.0423)	11.0	0.00265	0.00329 (0.0016-0.0057)	24.2
Intra-study validation	Ciraulo et al [66]	4	0.0094	0.0110 (0.0050-0.0211)	18.1	0.002	0.00164 (0.0008-0.02518)	18
		16	0.0349	0.0395 (0.0175-0.0764)	13.2	0.00442	0.00547 (0.0025-0.0095)	23.8
		24	0.04881	0.0606 (0.0258-0.114)	24.1	0.00541	0.00738 (0.00372-0.0139)	36.4
		4	0.01252	0.00938 (0.00408-0.0174)	-25.1	0.00184	0.00155 (0.0008-0.0029)	-15.8
Inter-study validation	Harris et al [69]	8	0.0202	0.0184 (0.0825-0.0355)	8.9	0.003	0.00326 (0.00162-0.00596)	8.7
		16	0.03489	0.0317 (0.014-0.0631)	9.1	0.00595	0.00547 (0.00246-0.0100)	8.1
	McAlee r et al [283]	8	0.02689	0.0227 (0.00967-0.0423)	-15.6	0.004	0.0031 (0.0016-0.0059)	22.5
		12	0.03652	0.034 (0.0145-0.0635)	-6.9	0.0054	0.00466 (0.00241-0.0806)	-13.7
		16	0.04619	0.0404 (0.0171-0.0760)	-12.5	0.0064	0.0049 (0.0025-0.0092)	-23.4

Abbreviations: AUC_{0-∞}: area under plasma concentration-time curve from time 0 to infinite after a dose; C_{max}: maximum plasma concentration; PI: percentile interval. ^aAUC_{0-t} were 0 to 72 hours for Ciraulo et al [66] and McAlee r et al [283] study, and was 0-48 hours for Harris et al [69] study. Difference (%) = ((predicted– observed mean value)/ observed mean value) *100

Table 3-12. Goodness of fit for sublingual buprenorphine models in healthy volunteers at steady state

Process	Data source	Dose (mg)	AUC _{ss, 0-24}			C _{max,ss}		
			Observed	Predicted (90% PI)	Diff.	Observed	Predicted (90% PI)	Diff.
			mg•h/L	mg•h/L	%	mg/L	mg/L	%
Inter-study validation	Compton et al [236]	16	0.05472	0.05508 (0.00255-0.139)	0.7	0.0068	0.0065 (0.0032-0.0142)	4.4
		24	0.08112	0.08252 (0.0379-0.1767)	1.7	0.0091	0.0099 (0.0487-0.0191)	8.8
		32	0.10301	0.1099 (0.0504-0.2670)	6.7	0.0139	0.0133 (0.0065-0.0288)	4.3
	Greenwald et al [237]	16	0.0486	0.05508 (0.00255-0.139)	13.3	0.0063	0.0065 (0.0032-0.0142)	3.2
		32	0.096	0.1099 (0.0504-0.2670)	14.5	0.0132	0.0133 (0.0065-0.0288)	0.8

Abbreviations: AUC_{ss, 0-24}: area under plasma concentration-time curve from time 0 to infinite after a dose at steady state; C_{max,ss}: maximum plasma concentration at steady state; PI: percentile interval.
 Difference (%) = ((predicted– observed mean value)/ observed mean value)*100

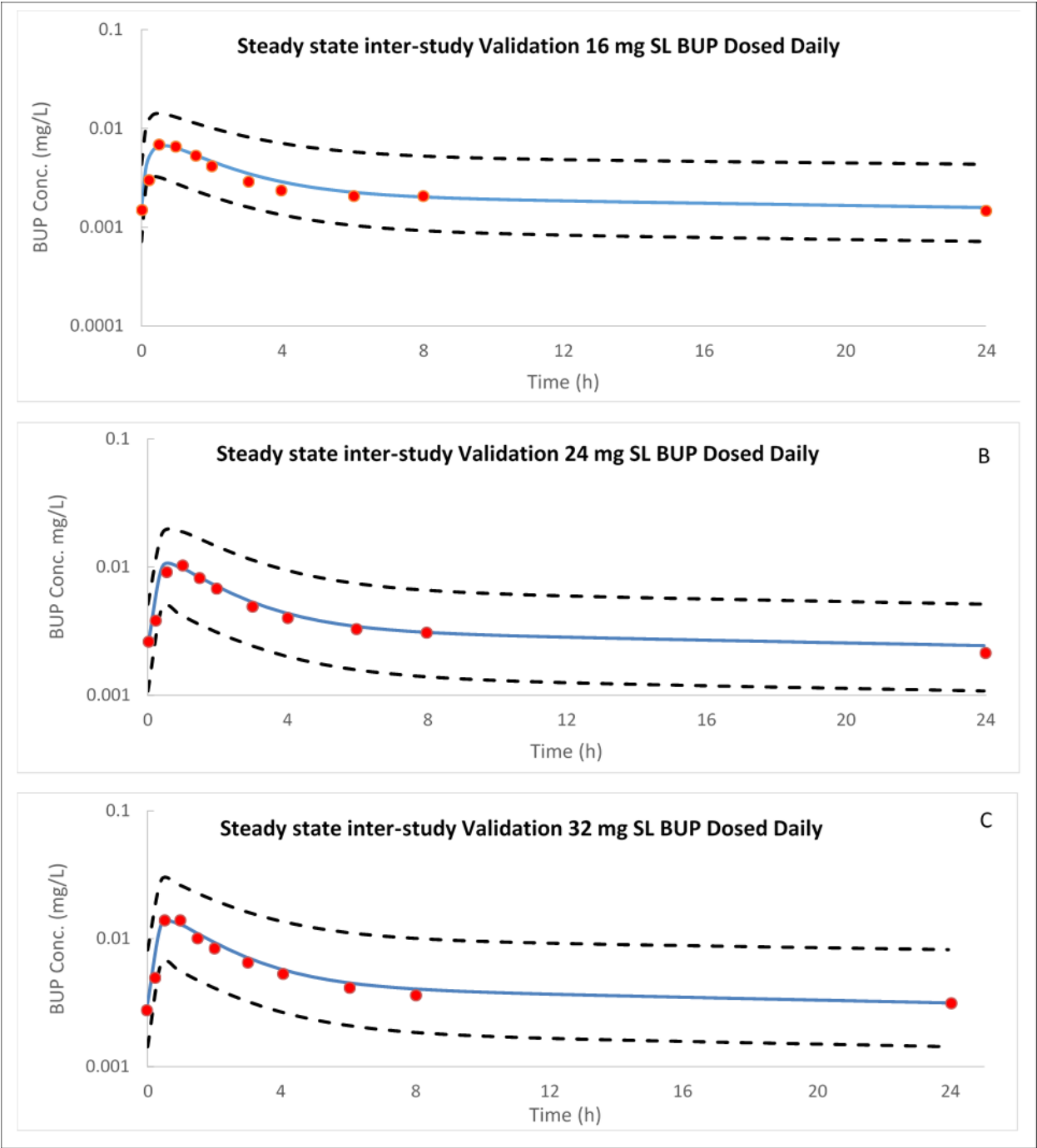


Figure 3-4. Steady state predicted and observed concentration-time profiles following daily SL doses of BUP in healthy subjects.

A, B, and C represent inter-study validation plots with 16 mg, 24 mg, and 32 mg SL BUP respectively as observed by Compton et al. [236].

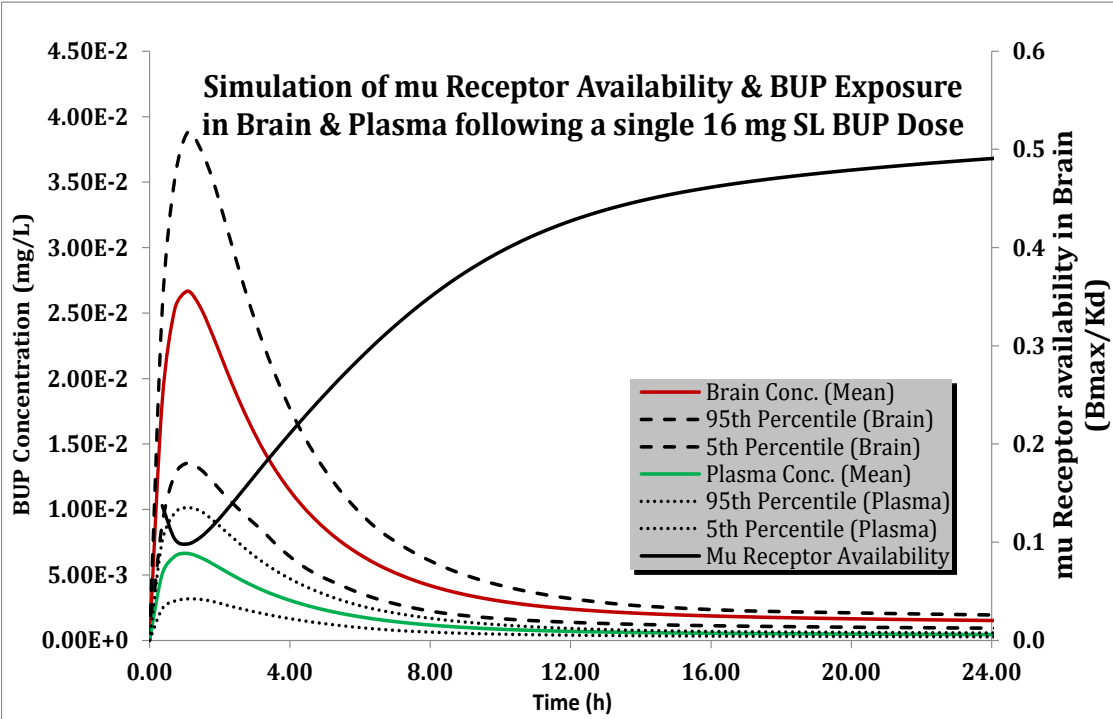


Figure 3-5. Predicted plasma and brain concentration-time profiles following a 16 mg SL doses of BUP in healthy subjects.

mu receptor availability is simulated on the secondary axis.

3.5 Discussion

In this study, we built and validated full-PBPK models of IV and SL BUP in healthy non-opioid dependent and opioid dependent patient populations across a wide range of BUP doses. The full-PBPK models incorporate enzymatic metabolism of BUP, its disposition into 13 major tissues in the body and three modes of absorption following the SL dosage forms. The models are robust in representing the multi-compartment first order disposition of BUP. The predicted concentration-time profiles in the study-matched virtual patient population are consistent with observed data across 14 independent studies (5 intravenous single dose, 5 SL single dose, and 4 SL multiple dose) among healthy non-opioid dependent and opioid dependent patient populations. The predicted IV BUP PK parameters fell within 85%-115% range of the corresponding PK parameters calculated from the IV BUP observed studies. The predicted SL BUP PK parameters fell within 75% to 137% range of corresponding PK parameters calculated from single dose SL BUP observed studies. This range was 100% to 115% when comparing steady state SL BUP PK parameters. Both models were robust in predicting BUP exposure after IV and SL administration in healthy population in the dose ranges of 4 to 32 mg.

BUP is a lipophilic drug with a large volume distribution (200-400 L) [67]. The semi-log concentration-time profile after IV administration shows a rapid drop in systemic concentration followed by a slower terminal phase indicating that BUP is a multi-compartmental drug with three distinct phases of disposition. It undergoes metabolism by various hepatic and gut CYP450 and UGT enzymes making it susceptible to extensive first-pass metabolism [89, 285, 286]. A mass

balance study following radiolabeled IV BUP administration reported 30% of the dose recovered in urine and 69% of the dose recovered in feces. The breakdown of BUP free drug, parent drug and its metabolites with sources of metabolism from this mass balance study is shown in Table 3-13 [287]. The relative contribution of CYP450 enzymes (71.8%) appears to be much higher than UGT enzymes (28.2%) when comparing the known major metabolites of BUP. We would speculate that the relative contribution of CYP450 enzymes following SL administration would be much higher than 71.8% as there is a higher abundance of CYP3A4 and CYP2C8 enzymes in the gut compared to UGT1A1, 1A3, and 2B7 enzymes. In the proposed SL BUP PBPK model, the modeled relative contributions of CYP450 and UGT enzymes are 95.46% and 4.54%. These relative contributions were estimated from recombinant CYP and UGT activities reported in referenced in-vitro study and ISEF based extrapolations [268-270]. Currently we are not able to validate the exact relative contribution of these enzymes as there is no published SL BUP mass balance study and we acknowledge this as a limitation of the PBPK models. Currently SimCyp® does not allow us to perform steady state simulations for the purposes of evaluating the effect of drug-drug interactions with known CYP3A4 inhibitors such as ketoconazole to verify the magnitude of CYP3A4 involvement. A limitation of this study is not having the ability to perform steady-state drug-drug interaction simulations.

Table 3-13. Results from mass balance study following administration of radiolabeled IV BUP

Drug/Metabolite	Enzyme	Urine (%)	Feces (%)
Free BUP	-	1.0	33
BUP-Glu	UGTs	9.4	5
N-BUP	CYP450s	2.7	21
N-BUP-Glu	CYP450s > UGTs	11	2
Other	CYP450s or UGTs	5.9	8
Total		30.0	69.0
Relative contribution of CYP450 and UGT enzymes (%)			
When considering	CYP450s	71.82	
N-BUP, BUP-Glu and N-BUP-Glu	UGTs	28.18	

Abbreviation: BUP-Glu, buprenorphine glucuronide; CYP, cytochrome; N-BUP, norbuprenorphine; N-BUP-Glu, norbuprenorphine glucuronide; UGT, UDP-glucuronosyltransferase

Based on various in-vitro transporter studies, there is no conclusive evidence for the involvement of ABC (ATP binding cassette) and SLC (solute carrier) drug transporters in BUP disposition [176]. Due to its poor oral bioavailability (F=10-15%) [288, 289], SL route of administration is the preferred route and is currently approved by the FDA. The half-life of BUP after SL administration is longer compared to IV administration suggesting a slow release of the drug from a depot to the systemic circulation after SL administration, in addition to the rapid initial absorption [67].

Physiologically, drug absorption following SL administration involves a combination of rapid passive absorption across the SL mucosal membrane, a slow depot release from the buccal tissue depot space, as well as gut absorption from the portion of the formulation that is swallowed. To mimic the three distinct phases, our SL PBPK model incorporates SL, oral and buccal depot release of the drug. Based on the drug absorption and disposition profiles reported in studies considered for building the model, we divided dose into the following routes: 62.5 % non-depot which comprises of 7-10% SL passive absorption into the circulation and 90-93% swallowing in the GI tract; the remaining 37.5% of the dose was attributed to the depot release from the buccal tissue. The percent distribution of the dose among these routes were optimized and validated with model naïve clinical PK datasets of SL BUP. Due to the multi-compartment disposition profile of BUP, the half-life reported for BUP in the literature after SL BUP administration could be different based on how long the PK study is conducted; prospective single dose PK studies that are 12 hrs, 48 hrs and 72 hrs long would yield sequentially increasing calculated half-lives for BUP after SL administration [74, 87, 88].

BUP exposure (C_{\max} and AUC) increases in a linear dose-proportional manner after IV administration. BUP exposure vs dose relationship after SL administration is linear only between the dose ranges of 4 to 12 mg; beyond 16 mg the exposure increase is not dose-proportional. This is consistent with published data [61]. This behavior does not suggest saturation of hepatic metabolism or gut metabolism. We believe this nonlinearity is due to differences in absorption profile and the differences in the percent dose absorbed for orally doses beyond 16 mg (Table 15).

BUP PK profiles after SL administration exhibits a large inter-study variability, especially for the C_{\max} and T_{\max} in single dose administration studies. The large inter-study variability is probably due to the variability in SL administration technique i.e., there could be difference in the proportion of the formulation that is swallowed vs absorbed after SL administration; some patients may not follow directions and may chew the formulation; some patients may retain the SL formulation for varied residence time in the mouth, and some may take whole tablets, while the others may cut or crush and use the product.

In order to treat opioid substance dependence, BUP has to cross the brain-blood barrier and bind to mu opioid receptors. However, currently there are no studies reporting BUP concentrations in the cerebrospinal fluid (CSF). Greenwald et al [206] studied the mu receptor occupancy in the brains of heroin dependent patients and reported a logarithmic relationship between BUP plasma concentrations and mu receptor binding potential or mu receptor availability in brain (B_{\max}/K_d). They also reported that plasma concentration of at least 1 ng/mL is needed for 50% mu-opioid receptor occupancy, in order to depress drug withdrawal syndrome and show efficacy [206].

We were able to illustrate the applicability of the developed model and brain concentration time profiles to the mu receptor occupancy data published by Greenwald et al [206]. Given the

lipophilic properties of BUP, its brain exposure was about 4 times higher than that of plasma (Brain-AUC_{0-72h}: 0.195 mg•h/L; Plasma-AUC_{0-72h}: 0.0536 mg•h/L). The mean plasma BUP concentrations in healthy subjects fall below 1 ng/mL threshold about 9 hours following a 16 mg dose, suggesting loss of efficacy beyond this time range (Figure 9).

Some studies have reported that BUP metabolites such as nor-BUP, BUP-3-glucuronide, and nor-BUP-3-glucuronide may also be biologically active[290, 291]. However, the exposure of BUP-3-glucuronide, and nor-BUP-3-glucuronide in brain should be minimal due to high hydrophilic properties of the glucuronides. The exposure of norbuprenorphine in the brain is also limited based on the reported data from postmortem brain samples. From 6 overdose death cases, the concentrations of norbuprenorphine was 5.8 ng/g (BUP concentration was 151 ng/g) in one postmortem brain sample, and not detectable in the other 5 postmortem brain samples (BUP concentration ranged 7.1 – 76.1 ng/g) [292]. Taken together, the contribution towards anti-nociceptive effect by the metabolites should be very limited. For these reasons, we did not incorporate metabolite profiles of BUP in this study.

Using the PBPK model developed, we will be able to predict plasma and brain concentrations of BUP in patients to optimize BUP dosing in patients. These PBPK models could also be potentially extrapolated to special patient populations such as pregnant women.

4.0 Gestational Changes in Buprenorphine Exposure: A Physiologically Based Pharmacokinetic Analysis

**(This chapter has been published at British Journal Clinical Pharmacology (2018) 84: 2075
–2087)**

4.1 Abstract

Introduction: Buprenorphine (BUP) is approved by the FDA for the treatment of opioid addiction. The current dosing regimen of BUP in pregnant women is based on recommendations designed for non-pregnant adults. However, physiological changes during pregnancy may alter BUP exposure and efficacy. The objectives of this study were to develop a physiologically-based-pharmacokinetic (PBPK) model for BUP in pregnant women, to predict changes in BUP exposure at different stages of pregnancy, and to demonstrate the utility of PBPK modelling in optimising BUP pharmacotherapy during pregnancy.

Methods: A full PBPK model for BUP was initially built and validated in healthy subjects. A fetoplacental compartment was included as a combined compartment in this model to simulate pregnancy induced anatomical and physiological changes. Further, gestational changes in physiological parameters were incorporated in this model. The PBPK model-predictions of BUP exposure in pregnancy, and during the postpartum period were compared to published data from a prospective clinical study.

Results: The predicted BUP plasma concentration-time profiles in the virtual pregnant populations are consistent with the observed data in the 1st, 2nd and 3rd trimesters, and the postpartum period. The differences in the predicted means of dose normalized AUC_{0-t} , and C_{max} were within 2-fold of the corresponding observed means.

Conclusion: PBPK model-based simulation may be a useful tool to optimise BUP pharmacotherapy during pregnancy, obviating the need to perform pharmacokinetic studies in each trimester and the postpartum period that normally require intensive blood sampling.

4.2 Introduction

Drug addiction has become a nationwide health crisis in the United States [293-295]. From 2013 to 2014, the death rate from an overdose of opioids has increased by 14% [296]. Currently, death due to drug overdose has surpassed that of motor vehicle accidents as the leading cause of unintentional deaths in the US [296]. Concurrently, the rate of opiate use in pregnant women has increased nearly 5 fold between 2000 and 2009 [297]. Maternal opioid use is associated with an increase in obstetrical complications, such as maternal death, cardiac arrest, intrauterine growth restriction and placental abruption [180]. Antepartum use of opioids commonly results in neonatal abstinence syndrome (NAS), and is associated with an increased risk of birth defects, stillbirth, and preterm labor [298, 299]. Buprenorphine (BUP) is approved by FDA for treatment of opioid addiction, but it is not approved for use in pregnancy. The efficacy of BUP in suppressing symptoms of withdrawal appears to be comparable to methadone [194, 195, 300]; but treatment with BUP is more convenient to patients and BUP exposed neonates appear to have less severe and less frequent Neonatal Abstinence Syndrome (NAS) [182, 301, 302].

The current dosing of BUP in pregnant women is based on recommendations designed for non-pregnant subjects since limited information is available to optimize BUP dosing in pregnant women. Pregnancy induces many physiological changes including the development of the foetal-placental compartment, an increase in renal filtration, body fluid volume and hepatic portal blood flow, as well as changes in the expression and activity of drug metabolizing enzymes and drug transporters [125, 145, 147]. These pregnancy-induced changes can impact absorption,

distribution, metabolism, and elimination of drugs which may ultimately alter efficacy and safety of medications used in pregnant women.

Response to BUP appears to be related to the plasma concentration of BUP. Greenwald et al. reported that a plasma BUP concentration of 1 ng/mL, is required for prevention of withdrawal symptoms in opioid exposed subjects. This concentration is associated with 50%-60% occupancy of the mu-opioid receptors in the brain [206]. We have demonstrated in a small cohort of pregnant women that plasma concentrations of BUP and the corresponding BUP exposure is significantly reduced during pregnancy compared to the postpartum state [201]. We have suggested that more frequent dosing of buprenorphine will reduce the time that treated women are likely to be sub-therapeutic during pregnancy [201, 303]. Our observations may at least in part explain the report of Jones et al., who in a large clinical trial reported higher study withdrawal rates in subjects assigned to BUP compared with methadone. Apparently, 71% of the dropouts were due to dissatisfaction of the subjects with the dosage of BUP used in that study [202].

A better understanding of BUP exposure in pregnancy is required in order to optimise treatment outcomes in pregnant women with opiate addiction. In our published pilot study, we did not enroll subjects prior to 20 weeks and therefore we were not able to evaluate the changes in BUP pharmacokinetics during the first half of pregnancy [201].

A variety of physiologically based pharmacokinetic (PBPK) modelling approaches have been used in drug development. PBPK modelling is a useful tool for predicting pharmacokinetic changes of a drug during pregnancy. Beside the differences in anatomy and physiology, the PBPK model can incorporate known pregnancy-related alterations in the activities of CYPs, UGTs, and

drug transporters, that can contribute to altered drug metabolism and clearance [304-309]. The objectives of this study were to predict the changes in BUP exposure at different stages of pregnancy through developing a PBPK model of BUP in pregnant women in order to optimizing BUP pharmacotherapy in this understudied population.

4.3 Methods

PBPK modelling and simulations for BUP were conducted using SimCyp® population-based simulator v15.1 (SimCyp limited, Sheffield, UK). WinNonlin software (Phoenix WinNonlin®: version 6.4, Pharsight Corp, Mountainview, CA) was used to simulate steady-state exposure of BUP after administration of the sublingual (SL) formulation. A systematic literature search to identify physiological changes throughout pregnancy, and to identify published clinical trials of BUP was conducted using the Medline database from the National Library Medicine through the PubMed interface. We used the search terms “buprenorphine”, or “subutex”, plus “opioid”, “pharmacokinetic”, “concentration”, and “ng/mL”. The inclusion criteria used were clinical studies that reported PK data on intravenous (IV), and / or SL BUP. We excluded studies that evaluated the PK of BUP in solution or in film formulations or continuous intravenous infusion; were performed in patients with severe disease (compromised liver or renal function); were published prior to BUP availability for sublingual administration (1990 or earlier); utilized a non-specific radioimmunoassay method to quantify BUP concentrations; or used a washout period between the IV and SL study of less than 5 half-lives of BUP. The bibliographies of the selected articles were also reviewed to identify additional relevant information. For PBPK model building and model validation, we used published data reporting the mean plasma concentrations of BUP following IV or SL administration. These mean plasma concentrations of BUP were digitized using GetData Graph Digitizer V.2.26 from the plasma concentration-time profiles of reported BUP clinical studies.

4.3.1 A PBPK model for BUP in non-pregnant subjects

The details of building and validating the IV and SL BUP PBPK models in healthy non-pregnant opioid non-dependent or dependent subjects have been previously published by our group [310]. In that study, we have outlined how a mechanistic BUP PBPK model was established by employing the physiochemical properties of BUP including tissue to plasma partition coefficient (K_p), the first-order absorption (for SL administration), and the kinetic parameters for metabolism and elimination (CYPs and UGTs). The tissue specific K_p values of BUP for the full-PBPK model were estimated using the corrected Poulin and Theil method [274-276]. The inter-system extrapolation factors (ISEF) based in vitro-in vivo extrapolation (IVIVE) methods were used to extrapolate in-vitro enzyme kinetic data. Published data on BUP plasma concentration vs time profile after IV and SL administration in opioid non-dependent and dependent patients were employed to build the models. Sensitivity analysis was performed for parameters (plasma unbound drug fraction (f_u), and all tissue specific K_p values) with no or poor initial estimates. The parameters that were not sensitive were defaulted to the initial prediction estimates; when the parameters were sensitive to the analysis, a systematic optimization on a one-by-one basis using the built-in parameter estimation module was performed. After individual optimization, all the sensitive parameters were re-optimized together in order to get the best fit with the observed data. The SL BUP model was built by adapting the IV PBPK model and adding a BUP absorption component. Similar parameter optimization methods were used to optimize absorption characteristics of BUP after SL administration. Fourteen model naïve BUP-PK datasets were used for inter-study and intra-study validations [310]. Introducing a T_{lag} parameter (lag time between dose administration and the appearance of BUP in the systemic circulation) better explained the SL BUP PBPK model in non-pregnant subjects. The parameter estimation module was used to fit the T_{lag} value and this

fit was verified by visual predictive check. It reduced the prediction error, when comparing the observed and predicted T_{max} , C_{max} and AUC estimates. The physicochemical properties and PK parameters that were used to develop a BUP profile; the key PK parameters of BUP in the non-pregnant subjects are provided in the appendix (Appendix A.1 and Appendix A.2).

4.3.2 A PBPK model for BUP in pregnant subjects

The perfusion limited BUP SL full PBPK model developed in healthy non-pregnant subjects was modified to create the BUP PBPK model in pregnant women [310]. The foetal-placental compartment characteristics in the custom virtual pregnancy population were adapted from the default SimCyp pregnancy population file. As with other compartments, the foetal-placental compartment is also a perfusion-limited compartment and its K_p value was estimated using the corrected Poulin and Theil method [274-276] (Table 4-1). The foetal-placental compartment combines the fetus, placenta, amniotic fluid, uterus and umbilical cord. The foetal-placental compartment is assumed to have the same characteristics as the muscle tissue (SimCyp® assumption). Given the lack of reports on BUP concentrations in the foetus or placenta it was not possible to validate model predictions in the foetal-placental compartment at this point. In this BUP PBPK model in pregnant women, all of the drug components including physiochemical properties of BUP, K_p values, and initial enzyme kinetics that were used were the same as in the BUP PBPK model developed in healthy non-pregnant subjects. The changes applied to the pregnancy BUP PBPK model were selected based on the changes that were expected to impact BUP PK. These include changes in hepatic blood flow, plasma protein level, drug metabolizing

enzyme activities, and the partition between plasma and red blood cells (Table 4-2) [165, 205, 311].

Table 4-1. Distribution parameters for BUP PBPK model in pregnant women

Parameter	Value
Model	Full PBPK
V_{ss} (L/kg)-predicted ^a	2.48
V_{ss} (L/kg)-observed ^b	2.77
Tissue Partition Coefficients (K_p)	
Adipose	0.0044
Bone/Additional ^c	35
Brain	3.41
Gut	2.69
Feto-Placenta	1.31
Heart	0.83
Kidney	1.29
Liver	2.13
Lung	0.29
Pancreas	2.20
Muscle	1.31
Skin	1.60
Spleen	1.31
K_p scalar ^d	0.225

Abbreviation: V_{ss} : Volume of distribution at steady state

^a Bullingham et al. [272];

^b V_{ss} predicted and K_p values for all tissue were predicted by corrected Poulin and Theil method [274-276];

^c Bone/Additional compartment K_p value was optimized using the Simcyp® parameter estimation module, Nelder-Mead method was used for the minimization. The predicted K_p value, 3.73, by Poulin and Theil method was used as the initial value, and (0.001, 100) used as the boundaries;

^d K_p scalar was optimized using the Simcyp® parameter estimation module, Nelder-Mead method was used for the minimization. The default K_p scalar, 1, was used as the initial value, and (0.01, 100) used as the boundaries.

Table 4-2. Summary of gestational age associated physiologic parameters incorporated into SimCyp® healthy population

	Non- Pregnant Female	1 st trimester (≤12 gestation weeks)	2 nd trimester (13-28 gestation weeks)	3 rd trimester (≥ 29 gestation weeks)
Physiological and metabolic change				
Cardiac output [312]	100%	Increased 35%	Increased 40%	Increased 50%
Plasma volume [312]	100%	Increased 12.5%	Increased 32.5%	Increased 50%
Red cell volume [312]	100%	Remain same	Remain same	Increased 30%
Hematocrit [313]	100%	Decreased 3%	Decreased 4%	Decreased 5%
Albumin [313]	100%	Decrease 27%	Decrease 27%	Decrease 27%
Activity of CYP3A4 [165]	100%	Increased 35%	Increased 35%	Increased 38%
Parameter used in model				
Cardiac output scalar	1	1.35	1.4	1.5
Plasma Volume scalar	1	1.125	1.325	1.50
Red blood cell volume scalar	1	1	1	1.3
Hematocrit (%)	38	35	34	33
Albumin (g/L)	49	36	36	36
CYP3A4 (pmol/mg protein)	137	185	185	189

BUP is primarily metabolized by N-dealkylation [277]. This N-dealkylation of BUP is primarily mediated by CYP3A4 in the liver [90, 91]. Although CYP2C8, UGT1A1, UGT1A3, and UGT2B7 are also involved in the metabolism of BUP, their contributions are relatively minor. A quantitative mass-balance diagram describing the absorption, distribution, metabolism and excretion of BUP after sublingual and intravenous (IV) administration as implemented in the PBPK model is shown in Figure 4-1. The mass balance study following IV dosing of BUP showed that a total of 69% and 30% of the radioactivity is recovered in the faeces and urine, respectively [96]. The unconjugated BUP and norbuprenorphine in feces probably comes from the hydrolysis of the conjugates of BUP and norbuprenorphine via biliary excretion [96]. As BUP is primarily eliminated by the liver, the changes in renal function during pregnancy should have minor impact on BUP elimination. This assumption was affirmed by performing a sensitivity analysis (Figure 4-2). Identical BUP concentration-time profiles were observed in all trimesters in the virtual pregnant women with and without an increase (50%) in GFR [311].

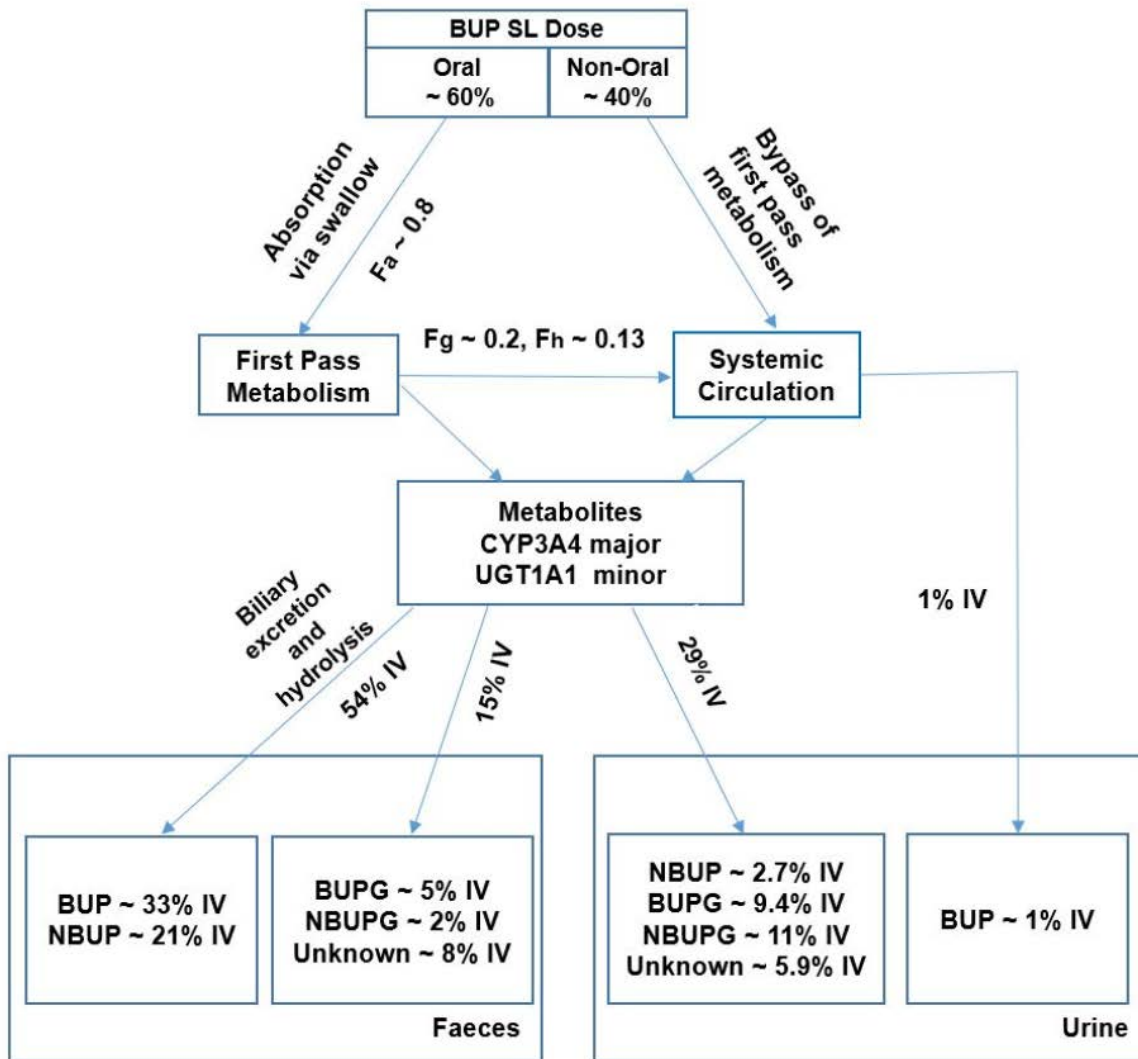


Figure 4-1. Quantitative mass balance diagram describing buprenorphine (BUP) absorption, distribution, metabolism and excretion after sublingual and intravenous (IV) administration. BUPG, Buprenorphine glucuronide; NBUP, Nor-buprenorphine; NBUPG, Nor-buprenorphine glucuronide

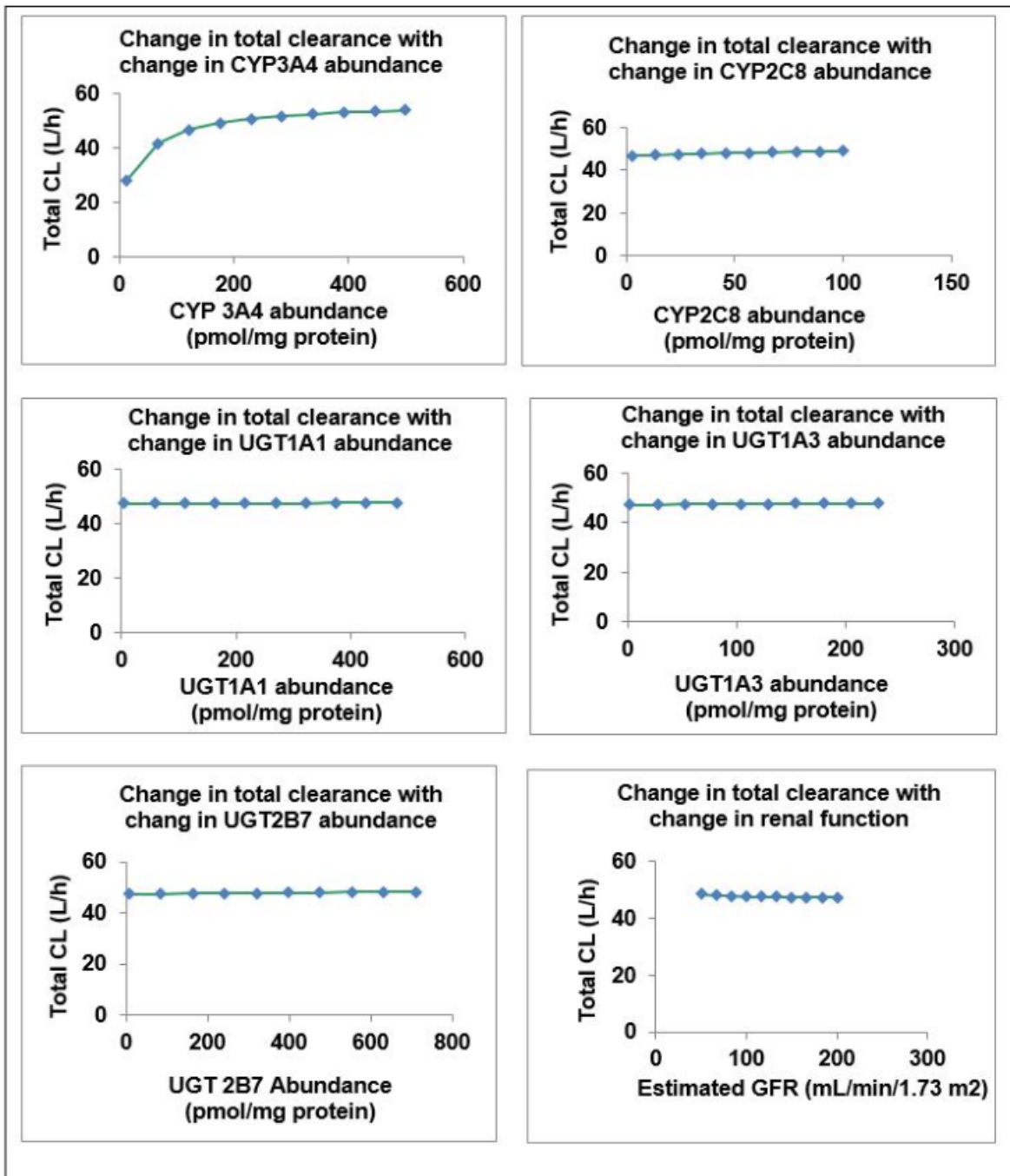


Figure 4-2. Sensitivity analysis to simulate the impact of the abundance of CYPs, UGTs and renal function on buprenorphine total clearance

4.3.3 Comparison during pregnancy and the post-partum (non-pregnant period)

BUP exposure during the postpartum period was simulated in virtual female healthy subjects using SimCyp® population simulator. The simulated BUP exposure during 2nd and 3rd trimesters and the postpartum period were validated using the observed plasma concentrations of BUP from a prospective clinical BUP PK study conducted by our group in pregnant women during pregnancy (2nd and 3rd trimesters) and the postpartum state [201]. In this clinical study, pregnant, women with a singleton gestation who were on a stable twice-daily dose of SL BUP for opioid maintenance therapy for at least 7 days in the second and third trimesters and the postpartum period were evaluated. Participants were recruited through Magee-Womens Hospital of University of Pittsburgh Medical Center (UPMC) and written informed consents were obtained from all participants. Each woman participated at least in two PK studies; once during the postpartum period and once during the second or third trimesters of pregnancy or in both trimesters. At each study visit, a total of 10 blood samples were collected from 0 hours (prior to the morning dose) up to 12 hours after the dose and BUP plasma concentrations in these blood samples were measured using high-performance liquid chromatography with tandem mass spectrometric detection [201]. Our goal was to use the SL BUP pregnancy PBPK model to predict the area under the plasma drug concentration-time curve (AUC) during pregnancy, and to compare it to the observed data. A \pm 50% difference between mean observed AUC in the prospective PK study and mean predicted AUC in 100 virtual pregnant subjects using BUP PBPK model was used as the model validation criteria.

4.3.4 Nomenclature of targets and ligands

Key protein targets and ligands in this article are hyperlinked to corresponding entries in <http://www.guidetopharmacology.org>, the common portal for data from the IUPHAR/BPS Guide to PHARMACOLOGY [314], and are permanently archived in the Concise Guide to PHARMACOLOGY 2017/18 [315, 316].

4.4 Results

4.4.1 Steady state BUP systemic exposure prediction

The disposition profiles of SL BUP following an 8 mg SL BID dose was predicted in 100 virtual pregnant female subjects spread over 10 trials during each trimester, and during the postpartum period. The predicted mean concentration-time profiles are shown in Figure 4-3. After SL BUP administration, plasma concentrations of BUP reached peak levels in approximately 1 hour followed by a rapid decline and a subsequent slow disposition. Lower trough BUP concentrations, peak concentrations, average concentrations, and systemic exposure (AUCs) were observed throughout pregnancy compared to the postpartum period, and the difference was pronounced in the 3rd trimester ($AUC_{0-12,ss}$ was approximately 50% lower in the 3rd trimester vs the postpartum period and 40% lower in 1st and 2nd trimester vs postpartum). Systemic exposure of BUP was similar in the 1st and 2nd trimesters.

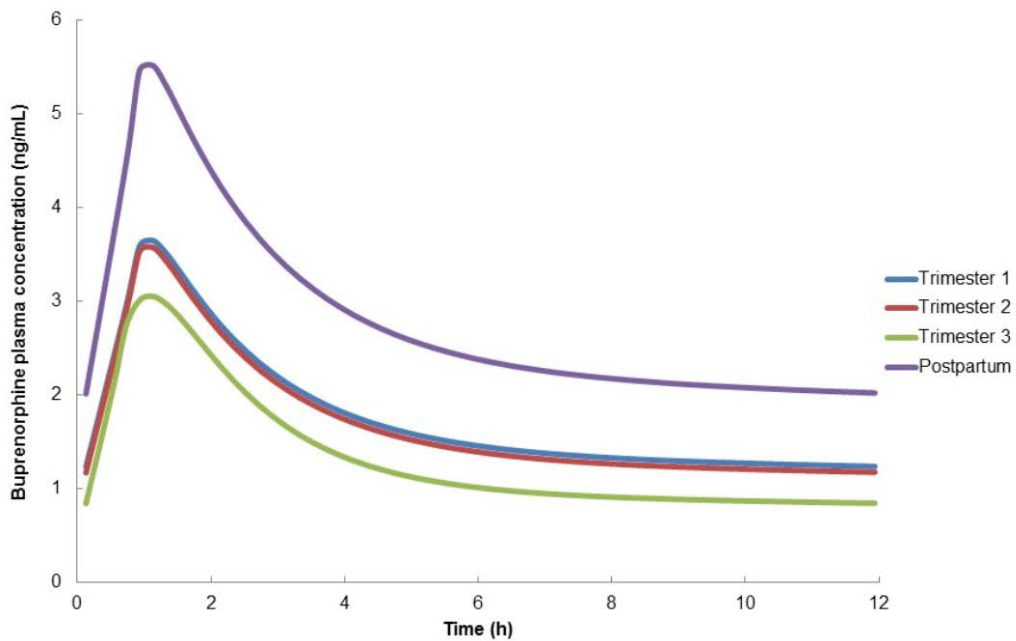


Figure 4-3. Predicted mean concentration–time profiles at steady-state following administration of 8 mg sublingual twice daily buprenorphine during 1st trimester, 2nd trimester, 3rd trimester, and postpartum in 100 virtual female subjects spread across 10 trials

4.4.2 Evaluation of the predictive performance of the BUP PBPK model in pregnant women

Figure 4-4 shows the predicted mean concentration-time profiles (with 5 and 95% confidence intervals) from 100 virtual pregnant women overlaid with the observed clinical data over a 12-hour PK study. As shown in the figure 4-4 A, B and C, the observed dose normalized mean concentration-time profiles were within 90% predicted percentile. The model did not adequately capture the T_{max} . The prediction of T_{max} is not clinically important since withdrawal symptoms are prevented not by the T_{max} of BUP, but rather by the maintenance of BUP plasma concentration above a threshold of 1 ng/mL. The predicted mean dose normalized concentration-time profiles fell within the 5th to 95th percentiles of the observed data. The difference in the predicted means of dose normalized AUC_{0-12} , C_{av} , and C_{max} were within $\pm 25\%$ of the observed means during different trimesters of pregnancy and the postpartum period, with the exception of the dose normalized C_{ave} in the 3rd trimester (-26.3%) (Table 4-3).

Figure 4-5 compares the model predictions against individual observed BUP concentrations in women on a dose of 8 mg bid, the most common dosage used. The observed individual plasma concentrations of BUP were within the 5th -95th percentile of model predicted concentrations. PK parameters for of BUP during pregnancy and postpartum following 8 mg BID SL administration are provided in Table 4-4. The simulations demonstrated that at steady state, with 8 mg BID SL BUP dose, trough plasma concentrations of BUP (at 12 hrs) remained above 1 ng/mL in 88%, 58%, 39%, and 12% of the subjects in the postpartum period, 1st, 2nd, and 3rd trimester. Figure 4-6 depicts the percentage of subjects who are below the BUP concentration required to prevent the appearance

of withdrawal symptoms in pregnant subjects, on an 8 mg BID dose of SL BUP based on the simulations of our PBPK model in pregnant and postpartum women. It demonstrates that in all three trimesters, predicted concentrations are sub-therapeutic in a substantial number of subjects long before the next scheduled dose. Seventy percent of women in the 3rd trimester is subtherapeutic by the 6th hour after a dose.

Table 4-3. Goodness of fit of BUP SL model in pregnancy and postpartum (PK parameters were expressed as mean (SD))

Inter-study validation	Period	Study	AUC ₀₋₁₂ /D	Diff ^d	CL/F	Diff ^d	C _{max} /D	Diff ^d	C _{av} /D	Diff ^d	T _{max}	Diff ^d
			ng•h/mL	%	L/h	%	ng/ml	%	ng/ml	%	h	%
Bastian et al [19]	T2 ^a	Observed (n=7)	2.3 (1.8)		607.8 (270.8)		0.5 (0.2)		0.2 (0.2)		0.4 (0.2)	
		Simulations (n=100)	2.2 (1.2)	-6.4	523.2 (174.3)	-13.9	0.4 (0.2)	-15.4	0.2 (0.10)	-5.3	1.1 (0.2)	155.8
	T3 ^b	Observed (n=13)	2.3 (1.3)		568.1 (282.8)		0.50 (0.2)		0.19 (0.11)		0.9 (1.1)	
		Simulations (n=100)	1.7 (0.8)	-23.4	647.7 (204.4)	14.0	0.39 (0.1)	-22.0	0.14 (0.06)	-26.3	1.1 (0.2)	19.6
	PP ^c	Observed (n=11)	4.2 (2.3)		301.3 (137)		0.8 (0.3)		0.4 (0.2)		0.8 (0.3)	
		Simulations (n=100)	3.8 (1.1)	-7.7	280.2 (77.7)	-7.0	0.7 (0.2)	-10.4	0.3 (0.1)	-8.5	1.1 (0.3)	46.7

Abbreviations: AUC₀₋₁₂/D: Dose normalized area under plasma concentration-time curve from time 0 to 12 hours, CL/F: Oral clearance, C_{max}/D: Dose normalized maximum concentration, C_{av}/D: Dose normalized average concentration, T_{max}: Time to reach maximum concentration.

^aT2: 2nd trimester; ^bT3: 3rd trimester; ^cPP: postpartum

^dDiff (difference)% = (predicted - observed mean value)/observed mean value*100

C_{av}/D=AUC₀₋₁₂/12

Table 4-4. Pharmacokinetic parameters of buprenorphine during pregnancy and postpartum following 8 mg BID BUP SL administration (geometric mean \pm SD)

PK parameters	Our in-house clinical study			Model Prediction		
	2 nd trimester	3 rd trimester	postpartum	2 nd trimester	3 rd trimester	postpartum
No. of subjects	4	4	10	100	100	100
Dose regimen	8 mg bid					
AUC ₀₋₁₂ (ng*h/mL)	15.4 \pm 14.8	12.4 \pm 6.5	27.9 \pm 20.2	16.2 \pm 9.5	13.0 \pm 6.2	29.6 \pm 8.7
CL/F (L/h)	520 \pm 288.8	644.8 \pm 362.3	286.4 \pm 145.7	523.2 \pm 174.3	647.7 \pm 204.4	280.2 \pm 77.7
C _{max} (ng/mL)	3.8 \pm 1.4	2.6 \pm 0.6	5.4 \pm 2.5	3.4 \pm 1.2	3.0 \pm 1.0	5.4 \pm 1.3
T _{max} (h)	1.0 \pm 3.8	0.5 \pm 0.6	0.9 \pm 3.6	1.1 \pm 0.2	1.1 \pm 0.3	1.04 \pm 0.27

Abbreviations: T_{max}: Time to reach maximum concentration, C_{max}: Maximum concentration, AUC₀₋₁₂: Area under plasma concentration-time curve from time 0 to 12 hours; CL/F: Oral clearance

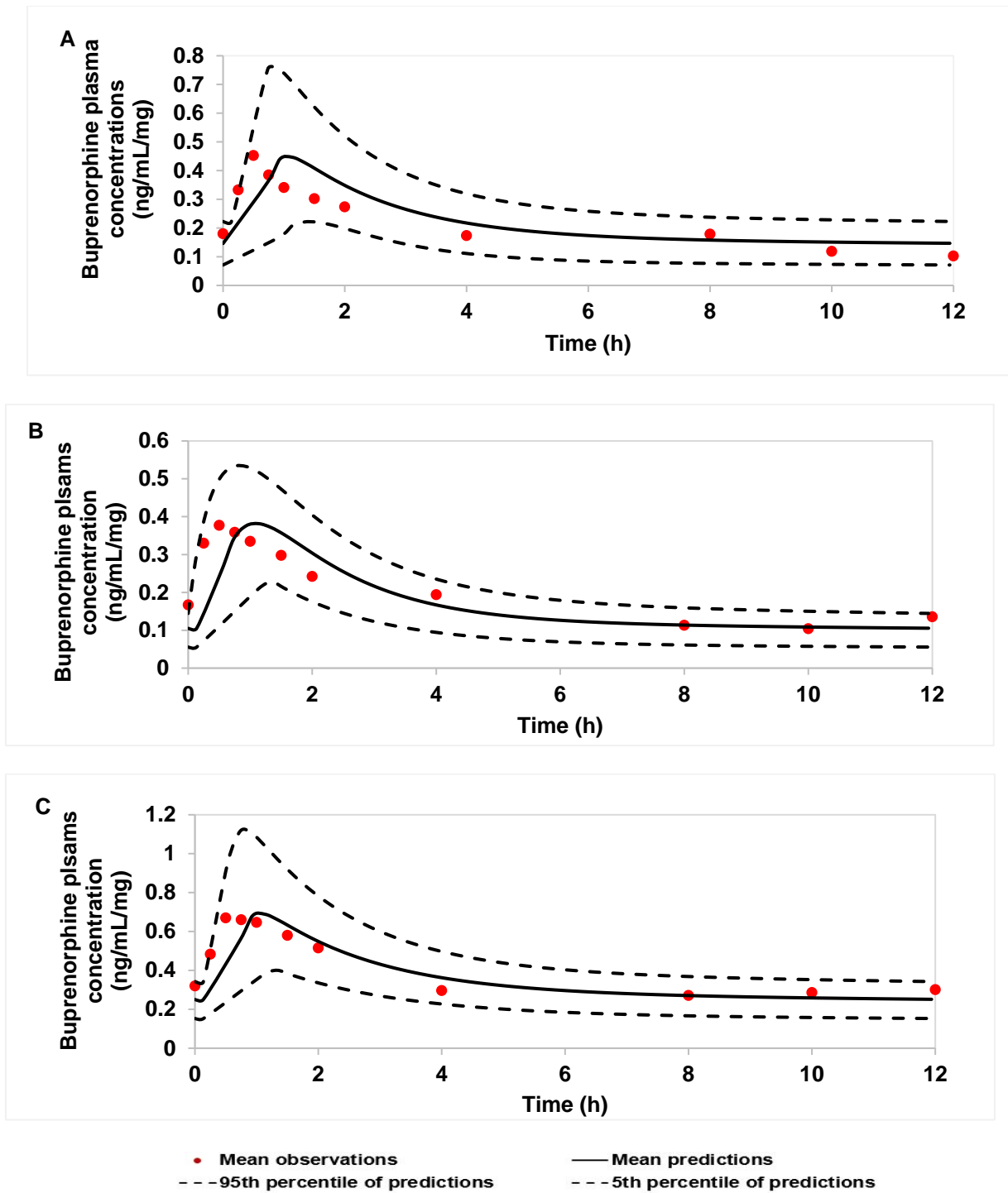


Figure 4-4. Predicted and observed dose normalized concentration–time profiles at steady-state following administration sublingual twice daily buprenorphine
4-4 A, B, and C represent interstudy validation by plotting mean predictions, 5th–95th percentiles of predictions against clinical observed mean concentrations during 2nd trimester, 3rd trimester, and postpartum respectively as observed by Bastian et al.

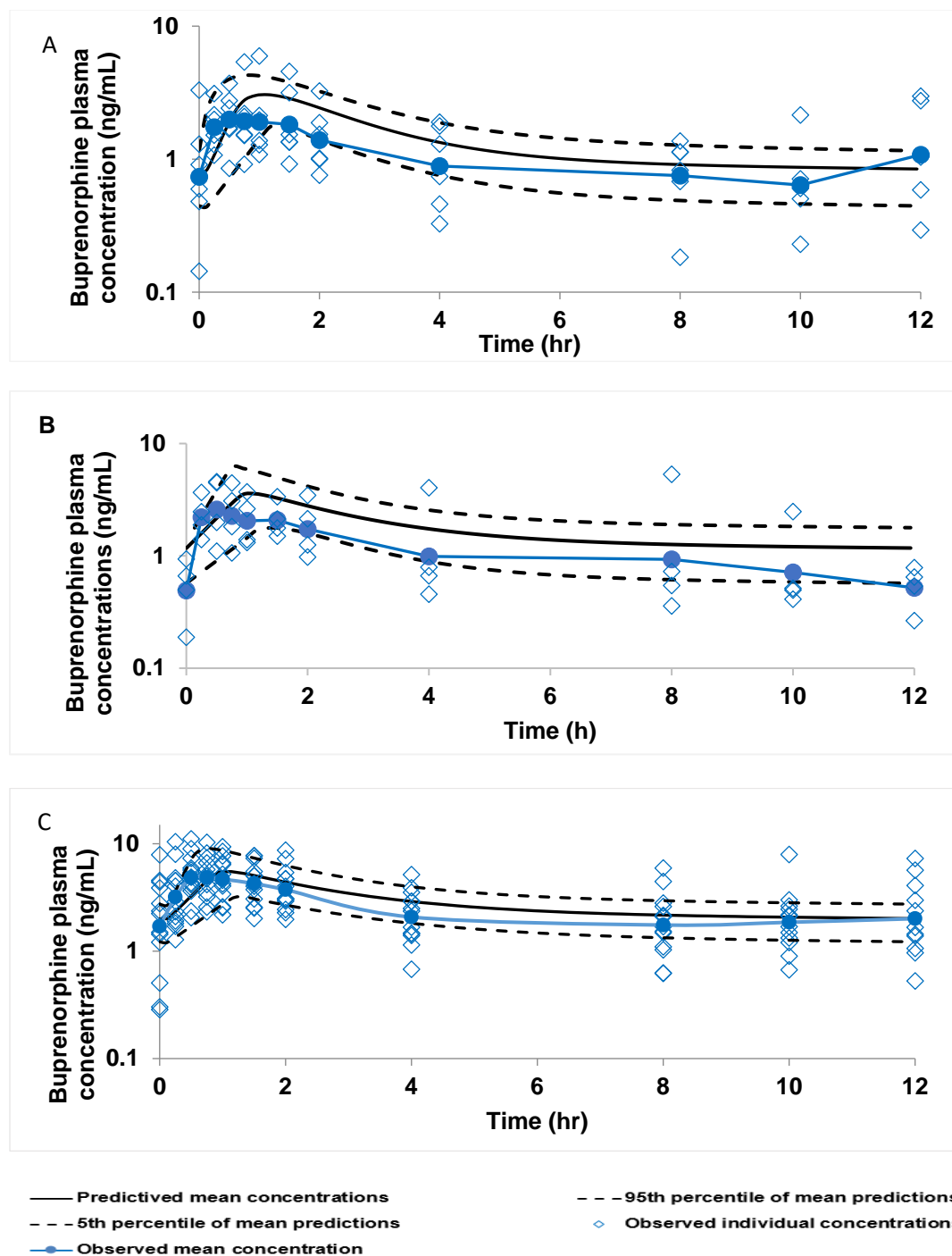


Figure 4-5. Predicted and observed concentration–time profiles at steady-state following administration of 8 mg sublingual twice daily buprenorphine
 4-5 A, B, and C represent interstudy validation by plotting mean predictions, 5th -95th percentiles of predictions against clinical observed mean concentrations, and observed individual concentrations during 2nd trimester (Figure 14A), 3rd trimester (Figure 14B), and postpartum (Figure 14C) as reported by Bastian et al.

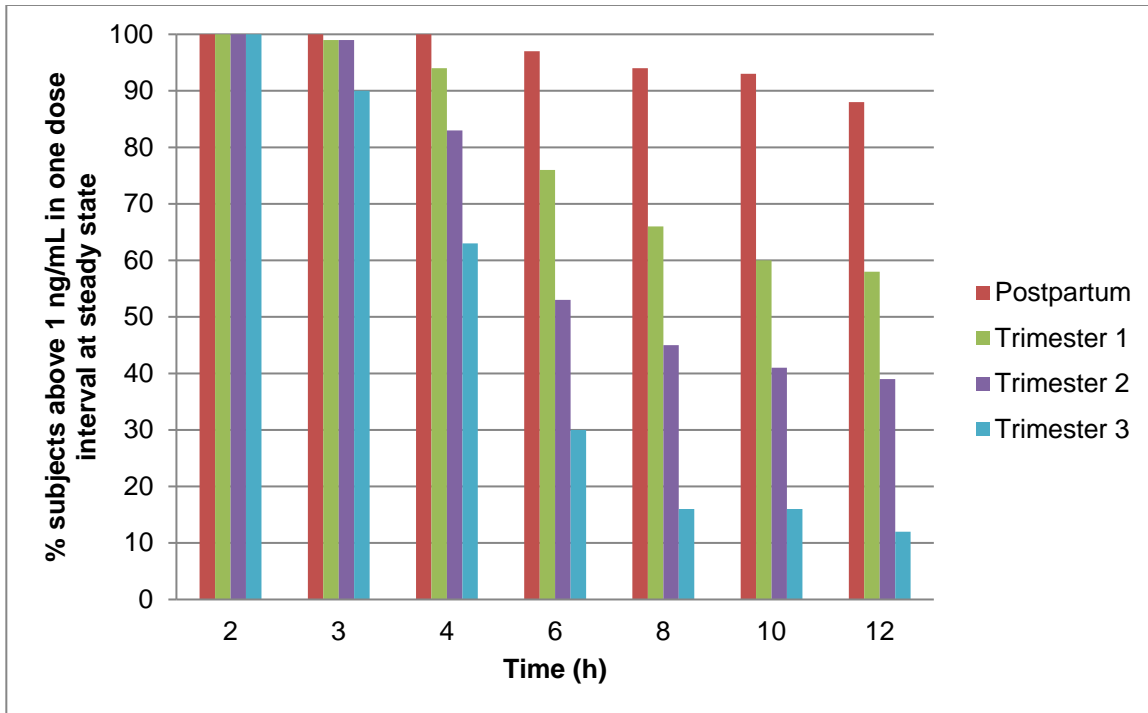


Figure 4-6. Percent of 100 virtual subjects with buprenorphine plasma concentration above 1 ng/ml in one dosing interval at steady-state following administration of 8 mg sublingual twice daily during postpartum, 1st, 2nd, 3rd trimester

4.5 Discussion

In the current study, we developed and validated a SL BUP PBPK model in pregnant women utilizing published data in non-pregnant women and adjusting for recognized anatomical and physiological changes associated with pregnancy that may impact BUP pharmacokinetics during gestation. The performance of our pregnancy model was evaluated by comparing it to the observed plasma concentrations of BUP in pregnant women during the 2nd and 3rd trimester, and after delivery. The predicted plasma concentration-time profiles in the virtual pregnant populations were consistent with the observed data. The model demonstrates that pregnancy is associated with a decrease in BUP systemic exposure, which is more pronounced in the 3rd trimester.

One of the limitations of PBPK modelling in special patient populations is the inability to assess the model predictive performance due to limited availability of drug concentration vs time data. In the current study, the SL BUP PBPK model in pregnant women was systematically developed using a stepwise strategy, where the base model was extensively validated using multitude of studies in non-pregnant populations over a wide range of doses [310]. First, a BUP IV PBPK model was developed for non-pregnant healthy volunteers and then the absorption component was added to the BUP IV PBPK model to describe SL administration of BUP. After validation of the predicted plasma concentrations of BUP for both a single and multiple dose at steady state in a non-pregnant population, we developed the full BUP SL PBPK pregnancy model to predict BUP disposition in pregnant women.

In this study, we built a customized pregnancy PBPK model rather than using the SimCyp® default parameters used for pregnancy, given the differences in certain parameters in the SimCyp® default option and our clinical observations. For example, in SimCyp® the pregnant default parameter describes changes of CYP3A4 activity during the entirety of pregnancy as a bell-shaped variable, increasing gradually at the beginning of pregnancy to a maximum level around 20 weeks of gestation, and then falling to normal level just prior to delivery. However, our in-house data showed that CYP3A4 activity is consistently, and significantly increased throughout pregnancy [165]. The increased CYP3A4 activity in the late stage of pregnancy has also been reported by other groups for as determined by the altered metabolism of midazolam, 4 β -hydroxycholesterol/cholesterol [157, 317]. The physiological changes incorporated into the custom pregnancy population model are provided in Table 24. As there is currently no conclusive data on the involvement of ABC (ATP binding cassette) and SLC (solute carrier) drug transporters in the disposition of BUP [176], we assumed that BUP only passively diffuses across the placenta and is not metabolized by the placenta. Several groups have developed maternal-fetal PBPK models and various compartment structures have been used to model the fetal-placental unit [305, 309]. Still, the primary challenge in building a comprehensive fetal compartment is the limited information on the fetal physiological development and drug exposure in the fetus during pregnancy. In SimCyp®, the fetal-placental unit is considered as a combined compartment in the pregnant women. The fetal-placental unit is simplified as a homogenous organ with the assumption that the components of the unit have similar characteristics of blood perfusion and drug partitioning [140].

In the BUP PBPK model developed, we used the corrected Poulin and Thiel method to estimate BUP distribution between blood and tissue. Both corrected Poulin and Thiel method and

Rodgers and Rowland method utilize drug specific properties such as lipophilicity, pKa and plasma protein binding to estimate drug partitioning among the components of tissue and plasma including water, neutral lipid and phospholipids. The main difference between the two methods is that the approach of Rodgers and Rowland divides tissue water into extracellular and intracellular parts and contains an added acidic phospholipid component for basic drugs. Rodgers and Rowland method also incorporates differences in pH of biological fluids and tissues and helps in modelling of active transporter uptake and efflux activity, whereas this ability is not present in Paulin and Theil method. In general Rodgers and Rowland method has a better predictive performance, but the prediction by this method is not optimal for highly lipophilic and/or highly protein bound drugs with minimal to no transporter involvement [318]. During base model building phase, Rodgers and Rowland method was tested to predict BUP V_{ss} , but due to poor prediction results, corrected Paulin and Theil method was used from that point forward. Buprenorphine is a highly lipophilic drug and is extensively bound to plasma proteins with no transporter mediated disposition characteristics, and the corrected Paulin and Theil method is the preferred method for modelling this particular drug.

In general, the model performed well in predicting BUP exposures within 25% of the observed mean values. Currently there is no guidance on the appropriate variance for goodness of fit or validation criteria for model predictions. We considered a 50% deviation as reasonable, considering the variability in the physiological parameters and disposition of BUP in this population. Although our model predicted the plasma concentration versus time profiles fairly well, the model underestimated the time to maximal concentration (t_{max}); the predicted t_{max} values lagged the actual values by about half an hour. This might be attributable to the fact that patients

in the published clinical study broke the SL tablet into small pieces to reduce the nausea and discomfort of holding the medication under the tongue [201]. Published studies in non-pregnant populations did not control for this variable. Breaking up a tablet decreases the disintegration and dissolution time, and leads to a faster drug absorption, which likely reduced the time to the peak concentrations in the clinical study. The assumption was affirmed by model simulations, as increases of K_a or decrease of lag time shortened the t_{max} without affecting AUC, and C_{max} .

BUP plasma clearance is around 50 L/h after an intravenous injection in healthy volunteers [74, 78, 87, 88]. The blood clearance of buprenorphine is approximate 80 L/hr (the blood to plasma ratio of buprenorphine is 0.6 [89]). Comparing BUP blood clearance with 1.5 L/min (the hepatic blood flow in healthy subjects), the estimated BUP hepatic extraction ratio is approximate 0.9, which indicates BUP is a high hepatic clearance drug. For a drug given by extravascular, the intrinsic clearance, hepatic blood flow and unbound fraction of a drug in blood affect drug clearance. Cardiac output increases from 35% to 50%, and the activity of CYP3A4 increases from 35% to 38% during pregnancy. Therefore, the higher clearance of BUP during after SL administration pregnancy is likely due to higher intrinsic clearance and the increased hepatic blood flow. The increased BUP clearance during gestation leads to a lower systemic exposure in pregnant women.

In clinical practice, most drug dosing regimens are prescribed based on drug specific half-life. In non-pregnant patients, BUP is recommended to be administered as a single daily dose due to its long half-life (31-35 hours) after SL administration [319]. Using positron emission tomography scan, Greenwald et al have reported that the occupancy of mu-opioid receptors in the

brain is correlated with plasma concentrations of BUP [206]. A plasma concentration of BUP of 1 ng/mL is associated to 50% mu-opioid receptor occupancy, a minimum requirement to inhibit drug withdrawal. The recommended plasma concentration of BUP of 1 ng/mL as a threshold for withdrawal suppression is based on a study in non-pregnant subjects [206], and no similar pharmacokinetic-pharmacodynamics studies have been conducted in pregnant women. If we use plasma concentration of 1ng/mL of BUP as a threshold for 50% of mu-opioid receptor occupation [206], among 100 virtual subjects, 40 subjects would be sub-therapeutic in the 1st trimester in about 10 hours after dosing, 47 subjects would be sub-therapeutic in the 2nd trimester in about 6 hours after dosing and 37 subjects would be sub-therapeutic in the 3rd trimester in about 4 hours following administration of 8 mg SL BUP. The model predictions demonstrate the need for an increase in dose or dosing frequency to maintain efficacy of BUP for opioid addiction in pregnancy. The model predictions are in agreement with the current clinical practice in pregnant women. At the Pregnancy Recovery Center at Magee-Womens Hospital, among 62 pregnant women followed up in an opioid agonist treatment program, 68% of the patients chose a three or four times dosing per day to maximally suppress craving/withdrawal symptoms [303].

Recruitment of pregnant women on opioid maintenance therapy during the first trimester of pregnancy is difficult and as such data on BUP PK profiles in the 1st trimester is lacking. The PBPK modelling study provided us additional information during 1st trimester that we were unable to obtain from our clinical study. We have also used the PBPK model to simulate the duration over which the plasma concentration of BUP will be above 1 ng/mL (the threshold to suppress drug withdrawal) with various dosing regimens across three trimesters. Such information enables optimization of BUP dosing during pregnancy.

We verified our SL BUP PBPK pregnancy model by using data from our clinical study data as there are no other published data on BUP PK in pregnancy. We are currently recruiting for a larger prospective BUP clinical study in pregnant women (NCT02863601), and we will be able to further validate this PBPK model upon study completion. In addition, we have collected cord blood samples at delivery in the prior study as well in the on-going BUP study to further optimise and validate the estimates of BUP fetal exposure.

As discussed above, we developed a BUP PBPK model to predict BUP exposure in three trimesters to improve BUP pharmacotherapy in pregnant women. However, previously we were not able to verify the model prediction in 1st trimester of gestation due to lack of observed clinical data.

Recently we performed another BUP PK/PD study in pregnant women to assess the association between BUP plasma concentrations and PD effects. Pregnant, singleton gestation women who were stabilized on sublingual BUP opioid substitution therapy for at least 7 days were recruited in this prospective, open-label, non-randomized longitudinal BUP PK study. Up to 3 studies were performed in each participant including 1st-half pregnancy (gestational week < 20 weeks), 2nd-half pregnancy (gestational week \geq 20 weeks), and postpartum (at least 4 weeks after delivery). The study was approved by the University of Pittsburgh Institutional Review Board. All patients were recruited through Magee-Womens Hospital, and written informed consent was obtained from all participants. At each study visit, a total of 10-13 blood samples were collected from 0 hours up to 12 hours after the dose. Several physiological measurements including craving score, clinical opioid withdrawal (COW) score, pupillary diameter size, galvanic response, respiration rate, blood pressure, as well as body temperature were also collected. Plasma

concentrations of BUP were quantified using a validated HPLC-MS/MS assay (shown in Chapter II). By utilizing the observed BUP plasma concentrations in this study, we further modified the previous BUP PBPK model and verified the predictions of the BUP PBPK model. The summary of the characteristics of study participants and gestational age associated physiological parameters incorporated into the modified model (Model 12) are listed in Table 4-5 and Table 4-6.

Table 4-5. Characteristics of study participants

Characteristic	1 st trimester (<13 gestation weeks, n=4)	2 nd trimester (13 -28 gestation weeks, n=8)	3 rd trimester (≥ 29 gestation weeks, n=5)	Postpartum ¹ (> 4 weeks of delivery, n=3)
Age (year)	28 ± 4	31 ± 5	31 ± 4	31 ± 6
Gestational age (weeks)	11±1	17 ± 2	30 ± 1	NA
Postpartum (weeks)	NA	NA	NA	5 ± 1
Body weight (kg)	76.2 ± 14.7	71.6 ± 12.8	78.0 ± 10.8	68.8 ± 0.6
Albumin (g/dL)	4.1 ± 0.2	3.9 ± 0.3	3.4 ± 0.2	4.1 ± 0.3
Total protein (g/dL)	7.1 ± 0.4	6.9 ± 0.4	6.5 ± 0.6	7 ± 0.3

¹ Albumin and total protein level were missing for one study participant.

Table 4-6. Summary of gestational age associated physiologic parameters incorporated into SimCyp® healthy population model_2

Parameter	1 st trimester (≤12 gestation weeks)	2 nd trimester (13-28 gestation weeks)	3 rd trimester (≥ 29 gestation weeks)
Cardiac output [137]	Increased 13.2%	Increased 26.2%	Increased 36.5%
Plasma volume [137]	Increased 9.5%	Increased 20.6%	Increased 31.4%
Red cell volume [137]	Increased 3.9%	Increased 10.3%	Increased 18.5%
Hematocrit [138]	Decreased 2%	Decreased 8%	Decreased 15%
Albumin [139]	Decrease 13%	Decrease 23%	Decrease 30%
α1-AGP [140]	Decrease 1%	Decrease 22%	Decrease 19%
Activity of CYP3A4 [165]	Increased 35%	Increased 35%	Increased 38%

Using the modified BUP PBPK model in pregnancy, we simulated BUP concentration-time profile following BUP SL 8 mg twice daily dosing in pregnant women at three trimesters as shown in Figure 4-7.

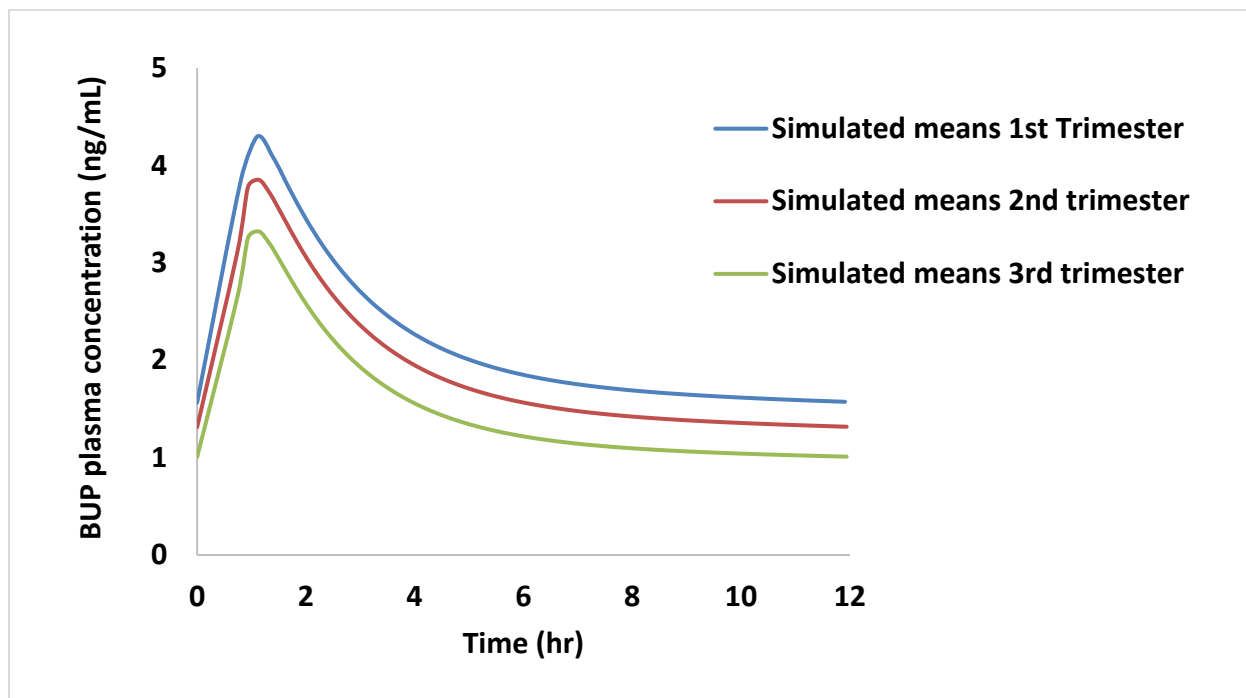


Figure 4-7. Buprenorphine mean concentration-time profiles in 100 virtual pregnant women at 1st, 2nd, 3rd trimesters following 8 mg sublingual twice daily dosing.

The prediction from both of the models were compared with our observed data as shown in Table 4-7. The differences in the predicted means of dose normalized $AUC_{0-t,ss}$ and $C_{max,ss}$ were within 2-fold of the corresponding observed means at 1st, 2nd, 3rd trimesters and postpartum. The predictions from the two models were similar with a higher predicted BUP exposure from model 2 at three trimesters in pregnancy. The observation from the clinical studies showed that BUP exposure were lower at 1st, 2nd, 3rd trimesters compared to postpartum. Also, the decreased BUP exposure were more profound at 2nd, 3rd trimesters.

Table 4-7. The goodness of fit of model predictions with the observed clinical data

Period	Study	Dose (mg)	T _{max} (h)	C _{max,ss} /D (ng/ml)	Ratio (pred/obs)	AUC _{0-t} /D (ng*h/mL)	Ratio (pred/obs)
T1	Observed (n=4)	4 (4)	1.3 (1 - 1.5)	0.83 (0.53 - 1.5)	NA	3.46 (2.11 - 5.57)	
	Model_1 (n=100)	8	1.1	0.45 (0.28 - 0.75)	0.54	2.61 (1.61 - 3.88)	0.75
	Model_2 (n=100)	8	1.1	0.53 (0.30 - 0.89)	0.64	3.29 (1.74 - 5.07)	0.95
T2	Observed (n=15)	5.7 (2 - 12)	0.5 (0 - 2)	0.60 (0.25-1.03)	NA	2.33 (1.22 - 5.47)	NA
	Model_1 (n=100)	8	1.1	0.45 (0.22 - 0.75)	0.75	2.54 (1.26 - 3.93)	1.09
	Model_2 (n=100)	8	1.1	0.48 (0.27 - 0.81)	0.8	2.83 (1.49 - 3.90)	1.21
T3	Observed (n=18)	8.3 (2 -16)	0.8 (0 - 4)	0.62 (0.25 - 1.75)	NA	2.39 (0.83 - 5.40)	NA
	Model_1 (n=100)	8	1.1	0.38 (0.23 - 0.53)	0.61	1.99 (1.09 - 2.87)	0.83
	Model_2 (n=100)	8	1.1	0.42 (0.24 - 0.70)	0.68	2.28 (1.1 5- 3.54)	0.95
PP	Observed (n=14)	7.4 (4 - 8)	1 (0.3 - 1.5)	0.80 (0.51 - 1.62)	NA	4.05 (1.57 - 10.45)	NA
	Simulations (n=100)	8	1.1	0.69 (0.40 - 1.12)	0.86	4.19 (2.54 - 6.0)	1.03

4.6 Conclusions

In conclusion, using the SL BUP PBPK model, we are able to predict maternal plasma concentrations of BUP in pregnant women across various gestational ages. The PBPK model predicted a decrease in BUP exposure during pregnancy and these results are aligned with published clinical study. We have also demonstrated the clinical implication of the SL BUP PBPK model in optimisation of BUP dosing in pregnant women by predicting the duration over which the plasma concentrations will be below the threshold for inhibiting drug withdrawal over a dosing interval. The model predictions demonstrate the need for an increase in dose or dosing frequency to maintain efficacy for opioid addiction during pregnancy.

**5.0 Model-based analysis to evaluate alterations in buprenorphine pharmacokinetics
during pregnancy**

5.1 Abstract

Introduction: Opioid addiction has become a nationwide health crisis in the United States. Buprenorphine (BUP) is an FDA-approved therapy for opioid addiction. The efficacy of BUP in suppressing symptoms of withdrawal appears to be comparable to methadone, but treatment with BUP is more convenient to patients, and BUP exposed neonates appear to have less severe and less frequent Neonatal Abstinence Syndrome (NAS). The current BUP dosing regimen is based on the recommendations designed for non-pregnant subjects. However, pregnancy-induced physiological changes may impact buprenorphine absorption, distribution, metabolism and elimination. Altered pharmacokinetic (PK) profiles have been reported for various therapeutic agents in pregnant women. Our aims were to use a population PK modeling approach to characterize BUP PK during pregnancy and to test potential covariates that may influence BUP PK during pregnancy in an attempt to optimize dosing of BUP in pregnant women.

Methods: Two clinical studies were used for the present modeling analysis. In study 1, pregnant, singleton gestation women who were stabilized on twice-daily sublingual BUP opioid substitution therapy (2- 16 mg) for at least 7 days participated in a prospective, open-label, non-randomized longitudinal BUP PK study. Up to 3 studies (2nd, 3rd trimester, and postpartum) were performed in each participant. The design of the pharmacokinetic study 2 was similar to Study 1, but patient recruitment was classified by the 1st, 2nd – half of pregnancy and postpartum period. The dosing frequency in the participants was not restricted to twice daily dosing regimen. Both of these studies were approved by the University of Pittsburgh Institutional Review Board. Patients were recruited through Magee-Womens Hospital, and written informed consent was obtained from all participants. At each study visit, a total of 10 blood samples were collected from 0 hours up to 12 hours after SL dose of BUP. Plasma concentrations of BUP were quantified using LC-

MS/MS. A total of 527 concentration time points from 51 PK study occasions in 26 patients from study 1 and study 2 were used for this population PK analysis. Non-linear mixed effects modeling using the first-order conditional estimation with interaction (FOCE-I) was conducted in NONMEM. Because BUP was administered sublingually, the structural model evaluation included extensive exploration of different absorption models to optimize model fit during the absorption phase. The effects of demographic and other patient covariates (age, pregnancy, body weight and gestational weeks, albumin, and total protein) were investigated via parameters vs. covariates plots and bootstrap stepwise covariate evaluation.

Results: BUP PK data were well-characterized by a two-compartment model with first-order absorption incorporating enterohepatic recirculation and first-order elimination. Pregnancy was associated with significant differences in BUP PK, with apparent clearance of BUP being increased approximately 1.64 times during pregnancy compared to the postpartum period ($p < 0.001$). A visual predictive check stratified by pregnancy status showed the 5th, 50th, and 95th percentiles of observed BUP plasma concentrations to be within 95% confidence intervals (CI) of 1000 simulated replicate datasets. The model estimated population CL/F for a typical non-pregnant and pregnant woman, were 286 and 469 L/h, respectively.

Conclusions: Pregnancy is the only covariate that is associated with significant changes in the PK of sublingual BUP. The currently recommended dose of BUP may need to be increased or the dosing frequency to be increased in pregnant women in order to achieve comparable systemic exposures in non-pregnant women.

5.2 Introduction

Illicit maternal drug use and subsequent prenatal drug exposure in pregnant women has significantly increased since 2000. The 2010 National Survey on Drug Use and Health conducted by the National Institute on Drug Abuse reports a 47% increase of illicit drug use during pregnancy since 2002 (4.4% in 2010 versus 3% in 2002 between the ages of 15 and 44 of pregnant women)[177]. The term "illicit" refers to the use of illegal drugs, including marijuana, and misuse of prescription medications, such as cocaine, benzodiazepines, and opiates. The use of opioids during pregnancy can result in drug withdrawal syndrome in newborns called neonatal abstinence syndrome (NAS). Since 2000, the incidence of NAS has increased 5 folds [179]. Antepartum use of opioids can also result in intrauterine growth restriction, birth defect, stillbirth, and preterm labor [181, 182]. In addition, maternal opioid use is associated with increased obstetrical complications, such as maternal death, cardiac arrest, and placental abruption [180].

There is no cure for opioid dependence, but medication-assisted maintenance therapies can reduce the overdose death and complications of opioid dependence such as HIV and hepatitis infections, as a consequence of decreased illicit drug use. Currently, methadone, buprenorphine, and naltrexone are the three primary pharmacotherapies for treating opioid dependence. The effectiveness of methadone as a maintenance treatment for opioid dependence has been demonstrated in many clinical studies. As a full agonist of μ -opioid receptor, methadone has abuse potential; therefore, methadone maintenance treatment requires daily patient visits for drug dispensing. Naltrexone is an antagonist of μ -opioid receptor. Naltrexone can root out illicit drug

use by blocking the euphoric effects and has no abuse potential, but poor patient retention hampers its routine clinical use. Many studies have reported that buprenorphine has comparable efficacy to methadone in treating opioid addiction [194-196]. As a partial μ -opioid receptor agonist, buprenorphine has less abuse potential compared to methadone. Therefore, patients usually get one or two weeks supply of buprenorphine during one clinic visit. Recently, several studies have reported that BUP exposed neonates have less severe and lower incidence of NAS [136, 182, 197]. On an average, there were less morphine required, shorter hospital stay, and shorter duration of medical treatment to treat neonatal abstinence syndrome in buprenorphine-exposed neonates [198]. These results support the use of buprenorphine as a potential first-line medication for pregnant opioid-dependent women.

However, there are a few unresolved issues in regards to dosing of buprenorphine in pregnant women. The current dosing regimen of buprenorphine is based on the recommendations in non-pregnant women or men. Clinical observations in Magee-Womens Hospital indicate an increase in buprenorphine dose requirement during pregnancy [201]. Another clinical study that compared the efficacy of buprenorphine and methadone in pregnant women showed that 30% of patients converted to buprenorphine failed at start, and 71% of dropped out because of patient dissatisfaction with buprenorphine [202]. Pregnancy induces a variety of physiological changes including the development of placental-fetal compartment, an increase in renal filtration, body volume and hepatic portal blood flow, as well as changes in the activities of drug metabolizing enzymes and transporters [125, 145, 147]. These pregnancy-induced physiological changes can impact drug absorption, distribution, metabolism, and elimination [148]. Many clinical studies have reported significant changes in the systemic exposure of drugs used during pregnancy.

Specifically, pregnancy results in a decreased rate of absorption due to decreased gastric emptying and decreased intestinal motility. The bioavailability of a drug used during pregnancy may be decreased or increased depending on how the activity of drug metabolic enzymes and transporters are altered in the gut during pregnancy. Pregnancy leads to an increased volume of distribution because of the increased body fat, total body water, plasma volume, and blood volume. Pregnancy effect on drug metabolism is drug specific. For example, the metabolism of drugs mediated by cytochrome P-450 (CYP) 2C9, CYP2D6, CYP3A4, uridine 5'-diphospho-glucuronosyltransferase (UGT) 1A4, and UGT2B7 are enhanced, whereas the metabolism of substrates of CYP1A2 and CYP2C19 are decreased [158]. We hypothesized that buprenorphine clearance will be increased during pregnancy resulting in decreased BUP exposure and this may be responsible for the poor adherence to buprenorphine in pregnancy. The aims of the present study were to characterize BUP PK during pregnancy and to evaluate potential patient demographics that may influence BUP PK during pregnancy through a population PK modeling approach.

5.3 Method

5.3.1 Study Design

Data from two BUP clinical pharmacokinetic studies were included in this population PK analysis.

Study 1 was a prospective, open-label, non-randomized and longitudinal pharmacokinetic study of buprenorphine in pregnant and postpartum subjects. The study was approved by the University of Pittsburgh Institutional Review Board. Patients were recruited through Magee-

Womens Hospital, and written informed consent was obtained from all participants prior to the initiation of any study-related activities. Pregnant, singleton gestation women who were stabilized on twice-daily sublingual BUP opioid substitution therapy (2 - 16 mg) for at least 7 days participated in this study. Up to 3 PK studies were performed in each participant during the 2nd (14 weeks, 0 days through 28 weeks, 0 days), and 3rd trimester (28 weeks, 1 day through term), and postpartum period (after 4 weeks of delivery). At each PK study visit, a total of 10 blood samples were collected in heparinized tubes from each subject at 0 (trough), 0.25, 0.5, 0.75, 1, 1.5, 2, 4, 8 and 12 hours after a dose. After centrifugation of blood, the plasma samples were frozen at -80°C until analyzed.

Study 2 was a prospective, open-label, non-randomized and longitudinal PK/PD study in pregnant women to assess the association between BUP plasma concentrations and PD effects. Pregnant, singleton gestation women who were stabilized on sublingual BUP opioid substitution therapy for at least 7 days were recruited. Up to 3 studies were performed in each participant including 1st-half of pregnancy (gestational week < 20 weeks), 2nd-half of pregnancy (gestational week \geq 20 weeks), and postpartum (at least 4 weeks after delivery). The study was approved by the University of Pittsburgh Institutional Review Board. All patients were recruited through Magee-Womens Hospital, and written informed consent was obtained from all participants. At each study visit, a total of 10-13 blood samples were collected from 0 hours up to 12 hours after the dose or till the end of a dosing interval. Several PD effects and physiological measurements including craving score, clinical opioid withdrawal (COW) score, pupillary diameter size, galvanic response, respiration rate, blood pressure, as well as body temperature were collected.

5.3.2 Determination of plasma concentration of buprenorphine

The concentrations of BUP in plasma samples from study 1 were quantified using a validated ultra-performance liquid chromatography with tandem mass spectrometry (UPLC-MS/MS). Briefly, 500 μ L of plasma samples containing buprenorphine and the deuterated internal standard (buprenorphine-d4) were extracted using pre-conditioned Strata X-C cartridges. The cartridge was washed with 1 mL of 2% formic acid in water twice, followed by 1 mL of 2% formic acid in methanol once. Buprenorphine and the internal standards were eluted from the cartridge and collected in a tube. The eluent was evaporated, reconstituted and an aliquot was injected in an Acquity UPLC Ethylene Bridged Hybrid (BEH) C₁₈ 1.7 μ m column (2.1x100 mm) equipped with Waters ACQUITY UPLC system tandem Thermo TQS Quantum Ultra™ Triple Quadrupole Mass Spectrometer. Calibration curves were linear in the range of 0.05–50 ng/mL. Both the intraday and interday precisions assessed by coefficient of variation values and the accuracy assessed by bias were within 15% of the nominal concentrations.

The concentrations of BUP in plasma samples from study 2 were quantified using a validated assay of ultra-performance liquid with tandem mass spectrometry (UPLC-MS/MS). Two hundred μ L of plasma sample containing deuterated labelled BUP (buprenorphine-D₄) chromatography were processed by protein precipitation prior to chromatography. Chromatographic separation was performed using Acquity UPLC Ethylene Bridged Hybrid (BEH) C₁₈ 1.7 μ m column (2.1x100 mm) with a mobile phase consisting of [A] 5% Acetonitrile in water containing ammonium acetate (2 mM) and formic acid (0.1%), and [B] Acetonitrile containing ammonium acetate (2 mM) and formic acid (0.1%) delivered at a flow rate of 0.3 mL/min in a gradient elution. The analytes were detected by a XEVO TQS mass spectrometer in positive electron spray ionization (ESI) mode using multiple reaction monitoring (MRM). The assay was

linear over the range of 0.05–100 ng/mL for buprenorphine. Both the intraday and interday precisions assessed by coefficient of variation values and the accuracy assessed by bias were within 15% of the nominal concentrations.

5.3.3 Population Pharmacokinetic Analysis

Non-linear mixed effects model (NONMEM) using first-order conditional estimation with interaction (FOCE-I) was applied to develop a population PK model of buprenorphine. In this population PK model, fixed and random effects were estimated to describe the time course of buprenorphine plasma concentration after sublingual administration. The parameter estimation of a model was a process of minimizing the objective function value (OFV, approximately equal to $-2 \times \log$ of the likelihood) using maximum likelihood estimation.

For discrimination between different models, Akaike information criterion (AIC) was used to compare non-nested models. As OFV approximately follows χ^2 distribution, and a likelihood ratio test was employed to compare the difference between two nested models. For adding one additional parameter to a model, a decrease of 3.84, 6.63, or 7.88 in the OFV was used as a cutoff for significant improvement in model fit at respectively 5%, 1% and 0.5% levels of rejecting the null hypothesis (there are no significant difference in the two models) due to type I error. In addition, certain diagnostic plots, such as goodness-of-fit plot, plot of individual observed concentration time profile overlaid with population prediction and individual prediction, plot of conditional weighted residual against time, and plot of individual weighted residual against time were also employed during the model selection.

This population PK model of buprenorphine was developed in two steps. First, the structural model was explored and selected to describe the absorption and disposition of buprenorphine. Because BUP was administered sublingually, structural model evaluation included extensive exploration of different absorption models to optimize modeling fitting in the absorption phase. After optimization of the structure model, the effects of demographic and other patient covariates (age, pregnancy, body weight and gestational weeks, albumin, and total protein) were evaluated through PK parameter vs covariate plots. The covariates that are potentially associated with PK parameters from visual check was further investigated via bootstrap stepwise forward/backward covariate evaluation (SCM, forward addition, $p < 0.05$; backward elimination $p < 0.01$).

The magnitude of the differences between subjects and between occasions within a subject at model parameter level were estimated by the between subject variability (BSV) and between occasions variability (BOV). As a log-normal distribution across the population for each parameter was assumed, exponential models were used to estimate BSV and BOV. The residuals, the difference between observed and predicted concentration of buprenorphine, were assumed to have a normal distribution and centered around zero. Additive only, proportional only, and the combined additive and proportional error models were tested during the selection of the error model.

The performance of the final model fit was evaluated by the goodness-of-fit plot, visual predictive check (VPC), and non-parametric bootstrap. In the VPC procedure, 1000 replicate datasets were simulated with the original dataset design. Variability was introduced into the replicate datasets by random sampling from matrices of random effects in the final model. The VPC plot constructed the 95% prediction intervals of the 5th, 50th and 95th percentiles from the 1000 replicate datasets against the 5th, 50th and 95th percentiles of the observed concentration-time

profiles, which was used to graphically assess whether the simulations from the final model was able to reproduce the central tendency and the variability in the observed dataset. Using sampling with replacement of random subject in the original dataset, 500 of bootstrap datasets were generated containing the same subject numbers as the original dataset. The 90% of the prediction interval of the bootstrap datasets were compared with the parameter estimates from the final model.

5.3.4 Software

The population PK analysis was performed in NONMEM, version 7.3.0. Graphical diagnostics and exploratory analysis were conducted using R (Version 3.4.4) and Xpose version 4. Pirana® was used as an interface to integrate these software.

5.4 Results

A total of 527 concentration time points from 51 PK study occasions in 26 patients from study 1 and study 2 were used for the population PK analysis. The characteristics of study subjects are summarized in Table 5-1.

Table 5-1. Characteristics of study participants

Study 2			
Characteristic	1 st -half pregnancy (<20 gestation weeks, n=12)	2 nd -half pregnancy (≥ 20 gestation weeks, n=5)	Postpartum ¹ (n=3)
Age (year)	30 ± 5	31 ± 4	31 ± 6
Gestational age (weeks)	15 ± 3	30 ± 1	NA
Postpartum (weeks)	NA	NA	5 ± 1
Body weight (kg)	73.1 ± 13.0	78.0 ± 10.8	68.8 ± 0.6
Albumin (g/dL)	3.9 ± 0.3	3.4 ± 0.2	4.1 ± 0.3
Total protein (g/dL)	7.0 ± 0.4	6.5 ± 0.6	7 ± 0.3
Study 1			
Characteristic	2nd trimester (13 -28 gestation weeks, n=7)	3rd trimester (≥ 29 gestation weeks, n=13)	Postpartum (n=11)
Age (year)	26 ± 5	29 ± 5	29 ± 5
Gestational age (weeks)	22 ± 2	34 ± 2	NA
Postpartum (weeks)	NA	NA	6 ± 3
Body weight (kg)	71.4 ± 8.1	74.5 ± 7.7	66.9 ± 8.7
Albumin (g/dL)	3.4 ± 0.2	3.2 ± 0.3	4.1 ± 0.2
Total protein (g/dL)	6.1 ± 0.6	6.0 ± 0.4	6.7 ± 0.6

Note: 1. Albumin and total protein level were missing from one study participant.

5.4.1 Structural model of the population pharmacokinetic model following sublingual administration of buprenorphine

One and two compartment models with first order elimination incorporating several types of absorption profiles were compared. The two-compartment structure model was chosen over the one-compartment model due to a higher AIC value and a U-shaped pattern in the scatterplot of weighted residuals versus population predictions in the one-compartment model. To represent buprenorphine absorption following sublingual administration, 1st-order absorption, zero-order absorption, different combinations of 1st-order and zero-order absorption with or without latency, transit model and enterohepatic circulation (EHC) absorption models were tested. A two-compartment model with 1st-order absorption and enterohepatic circulation, followed by 1st-order elimination were identified as the best structure model to describe buprenorphine absorption and disposition after sublingual administration as illustrated in Figure 5-1. The model assumed that elimination of buprenorphine was only through the central compartment. In order to model the EHC process, a gall bladder compartment was included into the structural model in addition to a central and peripheral compartment. A percentage of the administered buprenorphine dose estimated by the model was transferred to the gall bladder through 1st-order rate constant ($\text{EHCP} = \frac{k_{24}}{k_{20} + k_{24}} \times 100\%$), where k_{24} is the rate constant of the transfer of BUP from central compartment to gall bladder, k_{20} is the rate constant of the elimination of BUP in central compartment.

In addition to the percentage of administered dose of BUP undergoing enterohepatic recirculation (EHCP), the other typical values of the PK parameters estimated by the model

included apparent clearance of buprenorphine (CL/F), the apparent volume of distribution of buprenorphine central compartment (V_2/F), the apparent volume of distribution of buprenorphine peripheral compartment (V_3/F), absorption rate constant k_{12} , the apparent intercompartment clearance of buprenorphine (Q/F). Due to insufficient blood sampling during the EHC process, several assumptions were made to the model according to a reported EHC model [320]. (1) The process of emptying of BUP from gall bladder was assumed to be similar to a bolus injection following 1st-order rate constant, so the duration of the gall bladder emptying and rate constant of buprenorphine from gall bladder to dose compartment was fixed as 0.01hr and 70 hr⁻¹, respectively based on a reported EHC model. Also, the rate constant of slow gall bladder emptying did not significantly impact OFV values and the estimates of other parameters at the range of 10 to 70 hr⁻¹ based on our sensitivity analysis. (2) The emptying of gall bladder occurred at mealtime, 10 hrs after a dose. (3) Any BUP glucuronide excreted into the bile is immediately converted to BUP in the gut. The biotransformation of BUP glucuronide to BUP is not a rate-limiting step.

After entering the gall bladder, BUP was retained and accumulated in the gall bladder compartment until the gall bladder was emptied. During the emptying of the gall bladder, buprenorphine was reintroduced into the dose compartment and was reabsorbed into the central compartment. Two dummy compartments (Compartment 5 and Compartment 6) were used to start and end the emptying of the gall bladder. The differential equations to describe the changes in the mass of buprenorphine in each of the compartment are listed below.

$$\frac{dX_1}{dt} = k_{12} \times X_1 + k_{41} \times X_4 \times \text{FLAG}$$

$$\frac{dX_2}{dt} = k_{12} \times X_1 - k_{20} \times X_2 - k_{23} \times X_2 + k_{32} \times X_3 - k_{24} \times X_2 \times Z$$

$$\frac{dX_3}{dt} = k_{23} \times X_2 - k_{32} \times X_3$$

$$\frac{dX_4}{dt} = k_{24} \times X_2 - k_{41} \times X_4 \times \text{FLAG}$$

$$\frac{dX_5}{dt} = 0$$

$$\frac{dX_6}{dt} = 0$$

X_n represented BUP amount in the n^{th} compartment. The compartment 1, 2, 3, 4, 5, 6 were defined as dose compartment, central compartment, peripheral compartment, gall bladder compartment, dummy compartment to start the emptying of the gall bladder, dummy compartment to end the emptying of the gall bladder. The t represented time, k_{ij} represented the rate constant of the transfer of BUP among the compartments. FLAG is on (FLAG = 1) and off (FLAG = 0) indicator variables to turn on and turn off the emptying of gall bladder. Z was an indicator variable to turn off the buprenorphine entering gall bladder after the emptying of gall bladder before the next dose to prevent buprenorphine reaccumulating in the gall bladder. Due to the high variability of between subjects and insufficient samples collection around the EHC process, the interindividual variance of EHC were fixed at 0.5 based on sensitivity analysis as shown in Figure 5-2.

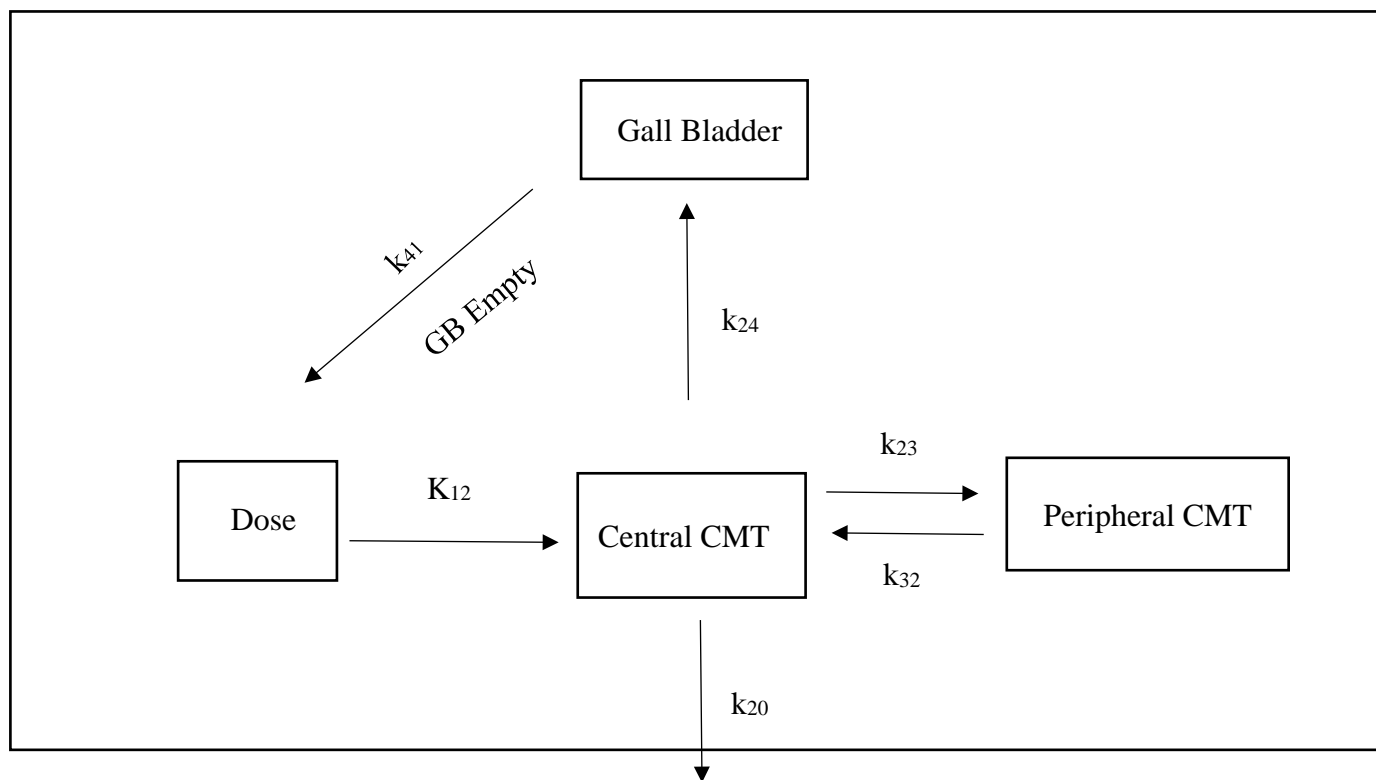


Figure 5-1. Schematic diagram of buprenorphine structure model following sublingual administration

k_{12} , first-order absorption rate constant; k_{23} and k_{32} , rate constants for distribution of buprenorphine between central and peripheral compartment; k_{20} , first-order elimination rate constant of buprenorphine; k_{24} , rate constant for the distribution of buprenorphine from central compartment to gall bladder; k_{41} , rate constant for the distribution of buprenorphine from gall bladder to dose compartment. GB, gall bladder

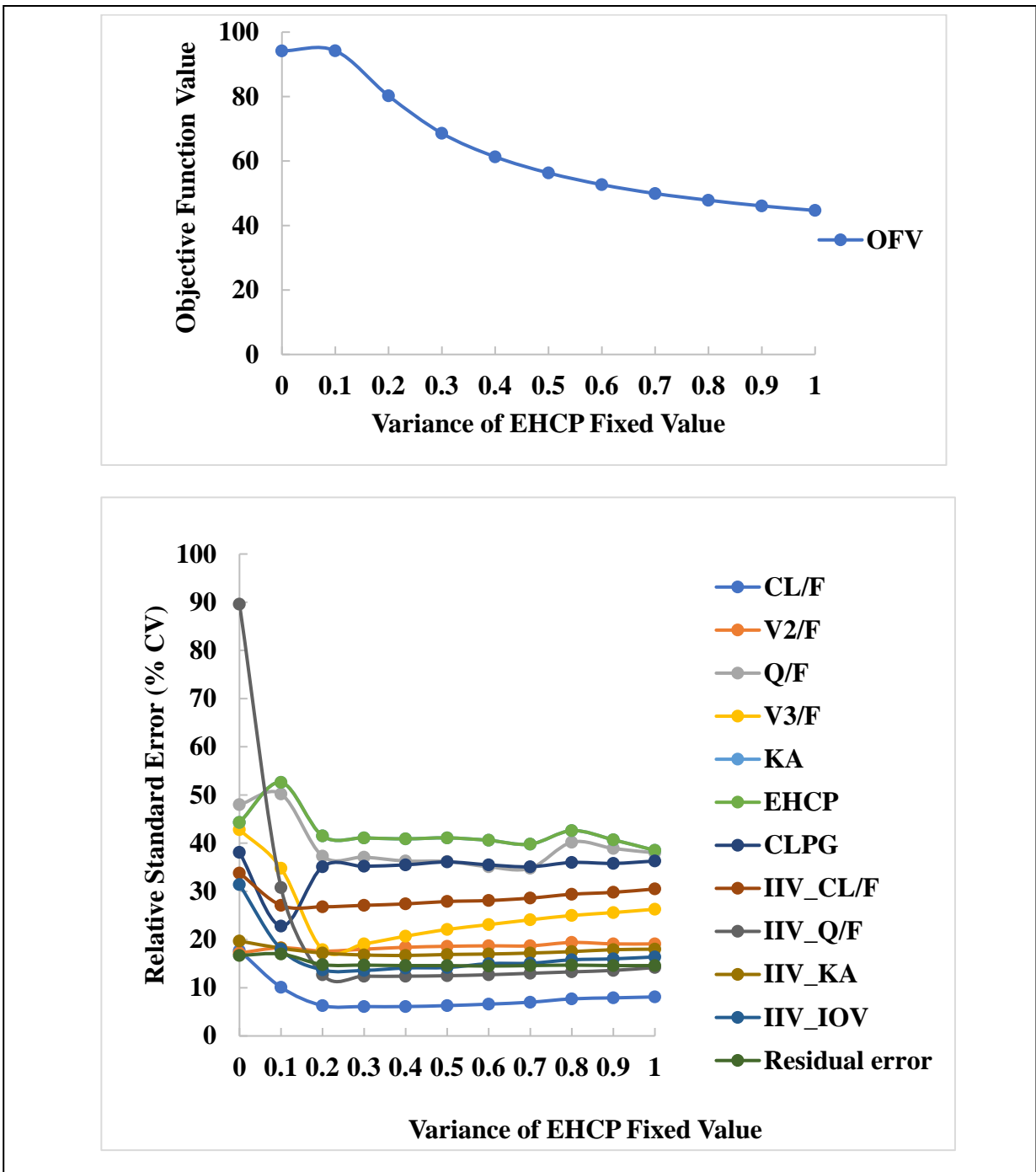


Figure 5-2. Sensitivity analysis of the interindividual variability of the percentage of enterohepatic recirculation (EHCP). (A) The impact of fixed values of variance of EHCP vs. OFV (B) The impact of fixed values of variance of EHCP vs. relative standard error of model parameters

5.4.2 Covariate identification

In 100 simulated bootstrap datasets, the median of the density plot of the distribution of covariate model size was identified as one. Pregnancy was identified as a significant covariate on the apparent clearance of buprenorphine in 60% of the 100 bootstrap datasets. None of the other characteristics including body weight, gestational weeks, serum creatinine, albumin, alanine aminotransferase, and aspartate aminotransferase level in the subjects were identified as important variables to explain BSV of PK parameters in this patient population. There was a statistically significant drop in OFV ($\Delta\text{OFV}=12$) after adding pregnancy in the model ($p<0.005$). As a result, the final model only included pregnancy as a covariate on the apparent clearance of buprenorphine.

The parameter estimates from the final model are shown in Table 5-2. The final model estimated the apparent clearance of buprenorphine to be 469 L/h during pregnancy with 24.4% inter-individual variability. In comparison with pregnancy, the fraction changes on CL/F in the postpartum was -0.391. The median values of the PK parameters from the bootstrap datasets were similar to the parameter estimates from the original dataset.

Table 5-2. Parameter estimates of final population pharmacokinetic model for buprenorphine following sublingual administration in pregnant women

Parameter	Final model estimate (RSE %)	Bootstrap (n=500) Median (95% CI)
Population typical value		
CL/F (L/hr)	469 (6)	465 (392 - 547)
V ₂ /F (L)	751 (19)	761 (481 - 1160)
Q/F (L/hr)	730 (36)	709 (480 - 1100)
V ₃ /F (L)	7790 (22)	8166 (5307 - 13559)
k _a (hr ⁻¹)	1.05 (19)	1.07 (0.72 – 1.55)
EHC %	1.79 (41)	1.75 (0.34 – 3.58)
K ₄₁ (hr ⁻¹)	70 fixed	
ALAG5 (hr)	10 fixed	
ALAG6 (hr)	0.01 fixed	
CLPG	-0.391 (36)	-0.382 (-0.55 - -0.15)
Interindividual variability (expressed as % CV)		
CL/F	24.4 (27.9)	24.8 (0.6 – 37.2)
Q/F	89.6 (12.5)	87.3 (60 – 116.4)
k _a	40.2 (16.9)	39.6 (13.2 – 61.7)
EHC%	70.7 (fixed)	
Interoccasion variability (expressed as % CV)		
CL/F	37.8 (14.2)	36.7 (22.3 – 47.5)
Residual variability (expressed as % CV)		
Proportional error	6.94 (14.6)	6.84 (5 – 8.89)

RSE: relative standard error; CI: confidence interval; CL/F: apparent clearance during pregnancy; V₂/F: apparent volume of distribution of central compartment, Q/F: apparent intercompartment clearance; V₃/F: apparent volume distribution of peripheral compartment; k_a: absorption rate constant; EHC%: The percentage of administered dose of buprenorphine undergoing enterohepatic recirculation; k₄₁: rate constant of buprenorphine transferring from gall bladder to dose compartment; ALAG5: a lag time for starting of emptying of gall bladder; ALAG6: duration of the emptying of gall bladder; CLPG: fraction changes in the clearance of buprenorphine in postpartum.

5.4.3 Model evaluation

In the goodness-of-fit plots, the observed concentration against population predicted concentration or individual predicted concentrations were clustered towards the lines of identity. The conditional weighted residuals data were symmetrically distributed around the line of zero and majority of the residuals were within the range of 2 times of the standard deviations (Figure 5-3).

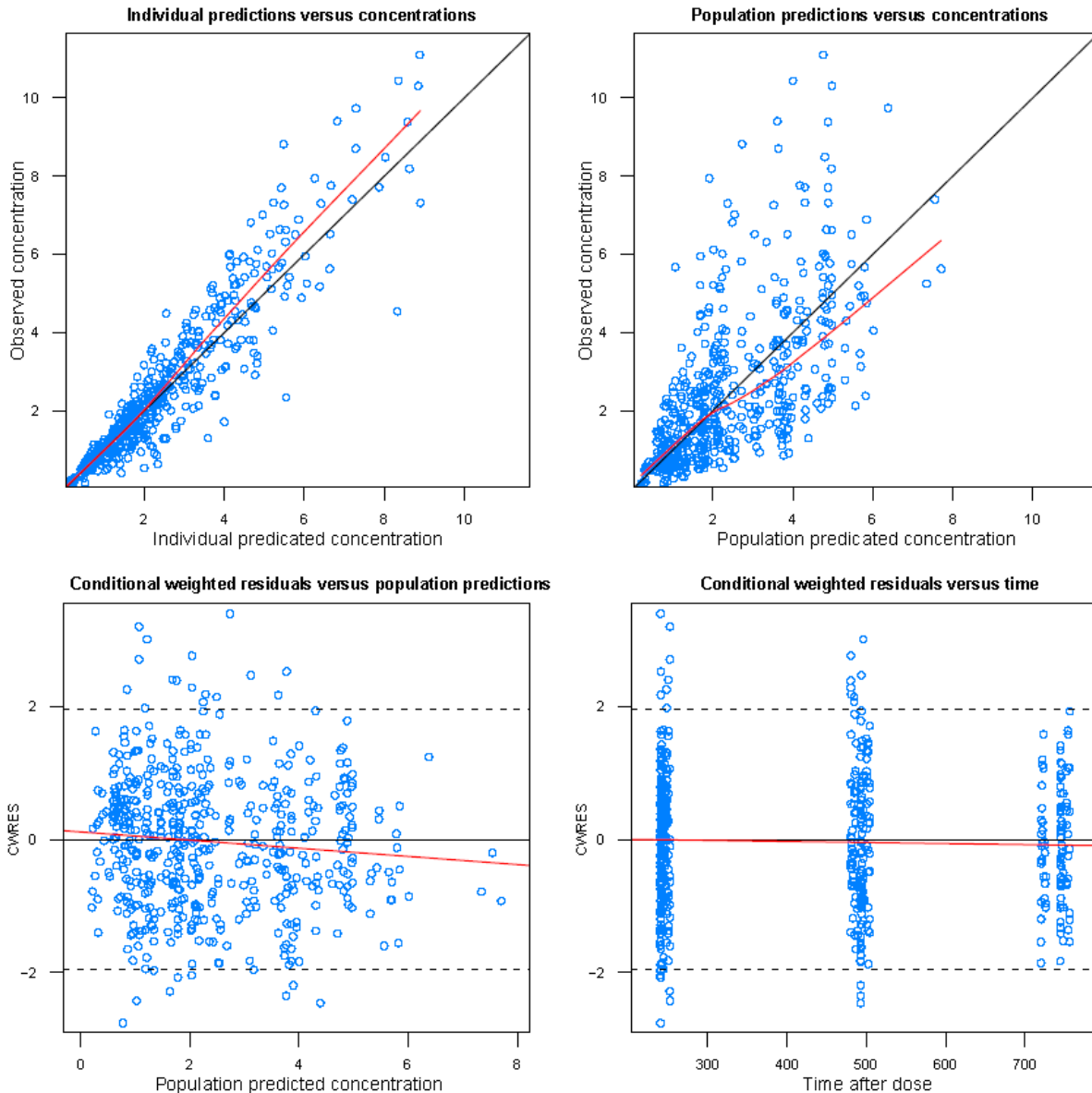


Figure 5-3. Goodness of fit diagnostic plots for buprenorphine concentrations fitted of final model.

(A) Individual predicted buprenorphine concentration vs. observed buprenorphine concentration. (B) Population predicted buprenorphine concentration vs. observed buprenorphine concentration. (C) Conditional weighted residuals vs. population predictions (D) Conditional weighted residuals vs. sample collection time after a dose. The solid black lines in (a) and (b) represent the line of identity and those in (c) and (d) represent the line $y = 0$. The solid red lines in each panel represent loss smooth of the data.

The VPC plot stratified by pregnancy status displayed that the 5th, 50th, and 95th percentiles of the observed BUP plasma concentration were within 95% predicted interval from 1000 simulated replicate datasets. Also, most of the observed concentrations were within the predicted 95% intervals as shown in Figure 5-4.

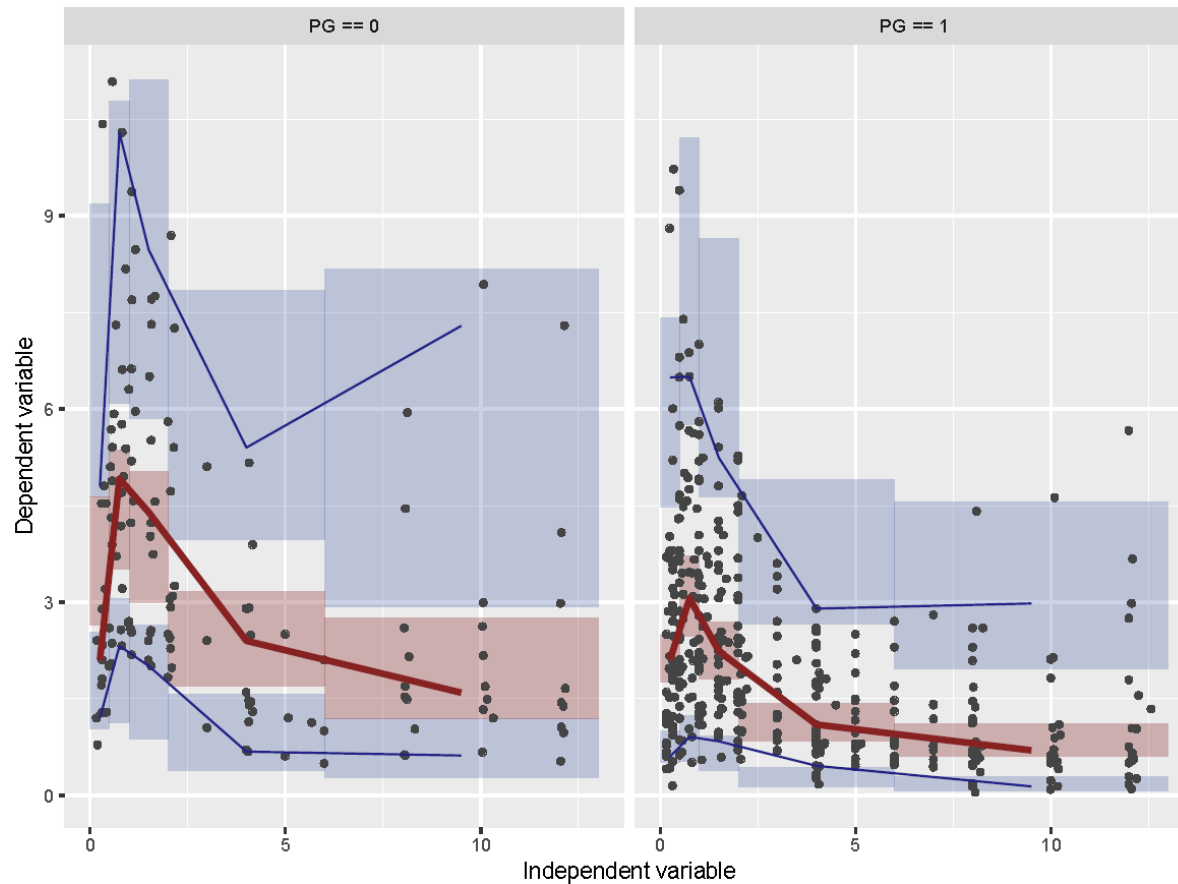


Figure 5-4. Predictive performance of the final model using visual predictive check plots.

The model predicted concentrations of buprenorphine at postpartum (left, PG =0) and at postpartum (right, PG=1) were plotted against observed concentrations at each time point after a dose. Y-axis, Dependent variable represented buprenorphine plasma concentration; x-axis, Independent variable represented time after a dose. Open dots represented observed concentrations, solid blue lines represented the 5th, and 95th percentiles of observed buprenorphine plasma concentrations; the solid red lines represented the 50th percentiles of the observed buprenorphine concentrations; shaded area represented the model predicted 95% confident intervals surrounding the 5th, 50th, and 95th percentiles from 1000 simulated datasets.

5.5 Discussion

In the present study, we developed a population pharmacokinetic model of buprenorphine in women during pregnancy and postpartum period. A two-compartment model with 1st-order absorption with EHC and 1st-order elimination best described the absorption and the disposition of buprenorphine following sublingual administration. Simulation based diagnostic methods, including VPC and non-parametric bootstrap resampling, were applied to evaluate the performance of the final model. Pregnancy was identified as a significant covariate with the apparent clearance of buprenorphine being increased 1.64-fold during pregnancy compared to the postpartum period.

Buprenorphine plasma clearance is around 50 L/h after an intravenous injection in healthy volunteers [74, 78, 87, 88]. The blood clearance of buprenorphine is approximately 80 L/hr (the blood to plasma ratio of buprenorphine is 0.6 [89]). Comparing BUP blood clearance with the hepatic blood flow in healthy subjects (1.5 L/min), the estimated BUP hepatic extraction ratio is approximate 0.9, which indicates BUP is a high hepatic clearance drug. For a drug given by extravascular route, the intrinsic clearance, hepatic blood flow and unbound fraction of a drug in blood can affect clearance of such a drug. After IV administration, BUP is completely metabolized in the liver through N-dealkylation to norbuprenorphine, primarily mediated by CYP3A4. Norbuprenorphine is further converted to norbuprenorphine glucuronide [90, 91]. A portion of buprenorphine directly goes through phase II metabolism mediated by UGT1A1, UGT1A3, and UGT2B7 to buprenorphine glucuronide. Pregnancy is associated with enhanced cardiac output,

hepatic blood flow, and increased expression and activities of CYP3A4, UGT1A1, and UGT1A3 [165, 204, 205]. Also, pregnancy leads to a decrease in plasma protein concentration, which may result in an increase in unbound fraction of buprenorphine in blood [321]. Taken together, the increase in hepatic blood flow and activities of CYP3A4, UGT1A1, 1A3, as well as increase in unbound fraction of buprenorphine in blood may explain the increased apparent clearance of buprenorphine as identified in the model.

In the clinical study, we observed complex absorption profiles in the buprenorphine concentration - time profiles in some subjects. Physiologically, drug absorption following SL administration may involve a rapid passive absorption across the SL mucosal membrane, a slow depot release from the buccal tissue depot space, as well as gut absorption from the portion of the drug dose that is swallowed. During model development, we tested two dose compartments to mimic the complex absorption profiles of sublingual administration of buprenorphine. The process of buprenorphine transferring to the central compartment through the two dose compartments were investigated using 1st-order absorption or zero order absorption kinetic property with or without lag time. However, the fraction of administered dose through each of the dose compartment was unable to be precisely estimated by these models. Also, we tried to fix the fraction of administered dose within each dose compartment, but none of these models fitted the data well. As of now, only two population modeling studies have been conducted with buprenorphine following sublingual administration in humans [322, 323]. The two modeling studies used 1st-order absorption model to describe their data. One of the two studies was conducted in 24 infants. Only one or two plasma samples were collected from each participant at one hour before or after a dose. The time course of buprenorphine after a single SL dose in 5 adult subjects were added in the modeling analysis

[323]. In the second study, the blood samples were collected at 0.5, 1, 2, 4, 6, 8, 12, and 24 after a dose. Both of the clinical studies have sparse blood sampling time points, so the second peak from EHC may have not been observed in the two studies. In our study, we observed a second peak in more than 50% of the plasma concentration-time profiles. We speculate that enterohepatic circulation may be involved in buprenorphine disposition. In an animal study, paired rats, donor and recipient were used to assess EHC of BUP [324]. A cannula was inserted into the bile duct of the donor rat and connected to the duodenum of the recipient rat. Buprenorphine was administered to the donor rats intravenously. In this study, BUP was detected in the plasma of recipient rats. The peak BUP concentration in the recipient rats was observed at 8 hrs after dosing in the donor rats. A second peak of buprenorphine has been also observed in some clinical PK studies. Concheiro et al conducted a PK study of buprenorphine following SL administration at late stage of pregnancy and postpartum in 3 women. The PK profiles at different study occasion in all of the subjects showed a secondary peak after 8 hrs following a SL administration of BUP [238]. McAleer et al. reported the observation of a secondary peak of buprenorphine around 10 hr after administration of 16 mg SL BUP in many participants in a PK study [283]. A total of 105 healthy male subjects with no history of opioid abuse participated in the study. Each participants received two doses of buprenorphine on two study occasions. At each study occasion, a single dose of sublingual BUP was given to the subjects [283]. The observed second peak around 10 hrs after a dose in the clinical study in pregnant women was in agreement with the observations in the studies reported by Concheiro et al. and McAleer et al [225, 283]. The second peaks and elevated concentration of buprenorphine at a later time period after administration of SL buprenorphine may be due to the variability in the absorption introduced by SL administration or the reabsorption of from buprenorphine that is secreted in the bile. However, without administering intravenous

formulation of buprenorphine, the cause of the complex absorption is not identifiable at this point. The presence of a second peak in BUP plasma concentration-time profile might be a result of BUP glucuronide being converted to BUP and being reabsorbed in the gut. However, the model was unable to identify the proportion of metabolism of BUP through N-demethylation and glucuronidation pathways due to relative small patient sample size.

Including EHC in buprenorphine disposition in the current population PK modeling resulted in a decrease of AIC by 33. The model estimated that a typical percentage of EHC of buprenorphine was 1.79% of the administered dose with large intersubject variability. The relative low biliary excretion of buprenorphine was also reported in a rat study [324]. The reason for the large variance in the percentage of BUP undergoing EHC may be the difference in the time of meals and content of the meal which were not strictly controlled in the clinical studies. Due to inadequate blood samples collected around EHC process, it was not possible to precisely estimate the parameter describing the rate and duration of the emptying of the gall bladder, and the interindividual variability of the percentage of BUP undergoing EHC. We have tested the rate constant of emptying of gall bladder from 10 to 70 hr⁻¹. The changes of OFVs were not greater than 3 and there was minimal changes to the estimates of other model parameters, so we fixed the model based on the estimate from the report of other publications on EHC model [320]. Fixing such parameters has also been used in other population PK model with EHC reabsorption [320, 325].

Buprenorphine is a lipophilic drug (LogP = 4.98) with large volume of distribution, and usually two- or three-compartment models are used to describe buprenorphine disposition [70]. In the clinical study, patients were prescribed to take sublingual buprenorphine twice daily. Therefore, the blood samples were collected from time 0 up to 12 hours after a dose. Due to the

clinical study design and patient sample size, two-compartment structural model was selected over three-compartment model to ensure the adequacy of the data for the parameter estimation. Although several characteristics of the patients were tested including age, body weight, BMI, gestational weeks, etc., pregnancy was identified as the only significant covariate to predict buprenorphine apparent clearance in this patient population.

The ability to predict drug exposure during pregnancy is critical to the success of drug therapy in pregnant women. Currently there is an opioid crisis in several countries. Optimizing treatment of opioid addiction is important to address this crisis. While buprenorphine is considered to be a better treatment option compared to methadone in treating substance abuse disorder in pregnant women, there is increased dropout of pregnant patients on buprenorphine therapy. This modeling study provides us a better understanding of the changes in buprenorphine pharmacokinetics during pregnancy. With the modeling result we will be able to tailor BUP dosing during pregnancy, which could potentially improve patient retention in BUP maintenance therapy and improve outcome of NAS in the newborns. A new clinical BUP PK/PD study in pregnant women is ongoing. More patients will be added to the modeling study to enrich the dataset to further improve model development and validation. Genotypes of CYPs and UGTs in study participants will be also included in further analysis. Developing a buprenorphine population PK-PD model to evaluate the exposure and response relationship in pregnant women in order to optimize buprenorphine dosing in pregnant women is our final goal.

5.6 Conclusions

The population pharmacokinetic model-based analysis demonstrated that pregnancy is associated with significant increase in the apparent clearance of BUP following SL administration. The currently recommended doses of BUP may need to be increased or the dosing frequency to be increased from BID to TID in pregnant women in order to achieve exposures comparable to those in non-pregnant women. The pharmacokinetic model-based analysis is a useful tool to evaluate changes in pharmacokinetics of drugs used during pregnancy in an attempt to optimize pharmacotherapy in pregnant women, obviating the need to perform pharmacokinetic studies in each trimester and the postpartum period that normally require intensive blood sampling.

6.0 Pharmacodynamic analysis of buprenorphine in pregnant women

6.1 Abstract

Introduction: Drug addiction has become a nationwide health crisis in the United States. Recently there has been a significant increase in opioid use during pregnancy. Correspondingly, the number of newborns exhibiting opioid withdrawal after birth has increased by 5 times from 2000 to 2012. Several studies have reported that the use of buprenorphine (BUP) results in a lower incidence and less severe neonatal abstinence syndromes (NAS). Our aims were to evaluate the effect of buprenorphine on various psychological and physiological parameters such as Clinical Opioid Withdrawal Scale (COWS) score, and pupillary diameters in order to understand the pharmacodynamics of BUP in pregnancy women.

Methods: Data from two clinical studies were used in the present modeling analysis. Study 1 involved pregnant, singleton gestation women who were stabilized on twice-daily sublingual BUP opioid substitution therapy (2- 16 mg) for at least 7 days prior to the study day. This was a prospective, open-label, non-randomized longitudinal BUP PK study. Up to 3 studies (the 2nd, 3rd trimester, and postpartum) were performed in each participant. The COWS scores and pupillary diameter sizes were collected at trough (before a dose), 4, 8, and 12 hrs after a dose of buprenorphine. For the second study, the design of the pharmacokinetic portion was similar to study 1, but patient recruitment was classified as 1st, 2nd – half of pregnancy and postpartum period. The dosing frequency of BUP in participants was not restricted to twice daily dose regimen only. The COWS scores and pupillary diameters were collected at trough (before a dose), 0.5, 1, 2, 4, 6, 8, 10, 12 hrs or the end of a dose interval based on the dosing frequency in each patient. Both of these studies were approved by the University of Pittsburgh Institutional Review Board. All patients were recruited through Magee-Womens Hospital, and written informed consent was obtained from all participants. At each study visit, a total of 10 blood samples were collected from

0 hours up to 12 hours after a dose or the end of a dosing interval based on the dosing frequency in each patient. Plasma concentrations of BUP were quantified using UPLC-MS/MS. A total of 527 concentration time points, 303 COWS scores, and 303 pupillary diameters from 51 PK study occasions in 26 patients were used for the population PK analysis and PD analysis. Non-linear mixed effects modeling using the first-order conditional estimation with interaction (FOCE-I) method was conducted in NONMEM to analyze the time course of the effect of BUP on pupillary diameter.

Results: Our analysis showed that the average Clinical Opioid Withdrawal Scale (COWS) scores were generally higher during pregnancy than postpartum period following administration of buprenorphine, which is in agreement with the observed lower buprenorphine exposure during pregnancy. A population PK /PD modeling analysis demonstrated that pupillary constriction was induced after administration of buprenorphine. The relationship between pupillary diameter and buprenorphine concentration was described by a sigmoidal E_{max} model with a hypothetical effect compartment. The model revealed that buprenorphine was transferred from central compartment to a biophase compartment with a 1st-order transfer kinetics with a rate constant of 0.723 hr⁻¹ (27.2, CV%). The estimated maximal effect (E_{max}), buprenorphine concentration at effect site exerting a half-maximal effect (IC_{50}) and the shape of the sigmoidal factor were 82.9% (4.2 CV%), 0.63 ng/mL (16.3, CV%), and 82.9 % (4.2, CV%), respectively.

Conclusions: Clinical Opioid withdrawal Scale scores were significantly higher during pregnancy compared to postpartum under the current dose regimen, which suggested a need to increase the dose of BUP in pregnant women to reach similar exposure and therapeutic effect in non-pregnant subject . The IC_{50} of BUP was not significantly different during pregnancy and postpartum in the PK/PD model analysis of buprenorphine concentration and pupillary diameter,

which suggest that there might be no significant changes in the sensitivity or number of μ -opioid receptors during pregnancy compared to non-pregnant women. Clinical studies in a larger number of patients are needed to validate the findings from the present study.

6.2 Introduction

Opioid addiction has become a crisis in the United States. From 1999 to 2017 age-adjusted drug overdose death rate has increased from 6.1 to 21.7 per 100,000 population [326]. In 2017, 68% of the drug overdose deaths involved an opioid [327]. There has been a significant increase in opioid use during pregnancy during this time period. The 2010 national survey on drug use and health conducted by the National Institute on Drug Abuse reported a 47% increase in illicit drug use during pregnancy since 2002 (4.4% in 2010 versus 3% in 2002 between the ages of 15 and 44 of pregnant women) [11]. Another survey conducted between 2005 to 2011 showed that among the 500,000 interviewees, 14% of women received at least one dose of a prescription opioid during gestation [328]. Maternal opioid use leads to increased obstetrical complications, including higher risks of maternal infections, preterm labor, malnutrition, and fetal death [329]. Prenatal opioid exposure can also result in drug withdrawal syndrome in the newborns. The number of newborns with neonatal abstinence syndrome (NAS) has increased from 2.8 per 1,000 births in the year 2004 to 14.4 per 1,000 births in the year 2014 [330]. Despite the barrier function of placenta, many substances are able to cross the placenta and reach the fetus by diffusion, carrier-mediated transport or transcytosis [129]. After birth, infants experience drug withdrawal symptoms due to the sudden cessation of opioids. Infants with NAS may experience sleeping and feeding problems, increased muscle tone, increased crying, irritability, seizures, tremors, diarrhea and fever, etc. [331]. The types and severity of NAS may differ among infants who experience opioid withdrawal. Neonatal abstinence syndrome needs medical interventions. The treatment of NAS requires hospitalization as the dosing and frequency of the pharmacotherapy interventions are tailored based on NAS

scores of newborns throughout the treatment period. Also, since most of the medications used for treating NAS, such as morphine can cause respiratory depression, infants receiving NAS treatment need to be closely monitored. The delay in identifying NAS in newborns may result in infant morbidity and mortality [331]. Due to lengthy hospital stays and intensive medical care, the average cost of healthcare for newborns with NAS is 10 times higher than newborns without NAS [332].

Currently, there is no cure for opioid use disorder. However, medication-assisted treatment that combines the use of medications with behavioral therapies and counselling can effectively improve quality of life, suppress opioid withdrawal symptoms, prevent opioid overdose death, and decrease infections (hepatitis B, C and human immunodeficiency virus) in patients [32, 333]. Methadone has been approved by the FDA for the treatment of opioid use disorder since 1960s'. As a full agonist of μ -opioid receptor, methadone also has abuse potential. Therefore, patients are required to visit the clinic daily in order to get a dose of methadone. Buprenorphine was approved by the FDA as a maintenance therapy for opioid addiction in 2003. Many clinical studies have demonstrated that BUP has comparable efficacy to methadone [16-18]. As a partial agonist of μ -opioid receptor, buprenorphine has less abuse potential. Buprenorphine is regulated as an office-based pharmacotherapy for opioid use disorder. During one clinic visit, patients can be prescribed buprenorphine supply for one or two weeks. In addition, recently a subcutaneous formulation of buprenorphine implanted under skin has been approved by the FDA, which is able to sustain the release of buprenorphine for up to 6 months. Due to better accessibility, buprenorphine may increase patient compliance to medication-assisted treatment compared to methadone.

Neonates with prenatal exposure to methadone or buprenorphine also experience NAS after birth as both of the drugs can pass through the placenta barrier. However, recently several studies

have reported that BUP exposure may result in less severe and lower incidence of NAS in the neonates [15, 19, 20]. On an average, there is a 89% lower morphine requirement, a 43% shorter hospital stay, and a 58% shorter duration of medical treatment in neonates with prenatal exposure to buprenorphine compared to the neonates who have prenatal exposure to methadone [21]. These results support the use of buprenorphine as a potential first-line medication for pregnant opioid-dependent women.

However, there is no clear consensus on how to dose buprenorphine in pregnant women. Due to the lack clinical pharmacokinetic and pharmacodynamic studies of buprenorphine in pregnant women, the current BUP dosing regimen in pregnancy is based on the recommendation for non-pregnant females and males. Pregnancy induces many anatomical and physiological changes that can impact absorption, distribution, metabolism and elimination (ADME) of drugs. The lack of a clear consensus may result in dosing bias by individual physician and in turn may affect retention of a pregnant patient in BUP therapy. Recent observation in a small cohort of pregnant women by our group has shown that BUP exposure is reduced approximately by half during pregnancy compared to the non-pregnant state, but nothing is known about the pharmacodynamics of buprenorphine in pregnant women. One of the challenges in dosing BUP in pregnant women is the need for balance between the exposure of BUP in the mother and in the fetus. In pregnant women, the treatment goal is to maximally inhibit drug withdrawal, craving and illicit opioid use of by the mother with a minimum drug exposure to the fetus. It is desirable to have a better understanding of BUP PK/PD relationship in pregnant women in order to accomplish this.

The Clinical Opioid Withdrawal Scale (COWS) is commonly used in practice to assess opioid withdrawal due to its ease of administration by the clinicians. The dose of medications used

to suppress drug withdrawal is tailored to individuals based on the COWS score. The COWS score has subjective and objective components. The subjective components include restlessness, bone or joint aches, runny nose or tearing, gastrointestinal upset, tremor, yawning, anxiety or irritability. These subjective components can be manipulated by the patients. As a result, COWS score can be impacted by patients' responses to certain questions. The reliability of COWS for detecting withdrawal needs to be validated by additional studies.

There is a need to identify a reliable and readily measurable objective marker to assess opioid withdrawal in pregnant women. As a maintenance therapy to treat opioid substance dependence, BUP crosses brain–blood barrier (BBB) and binds to mu-opioid receptors. The ideal marker to assess opioid withdrawal would be to get an estimate of BUP concentration in the brain and the mu-opioid receptor occupancy. Utilizing positron emission tomography (PET) scan, Greenwald et al. have studied the association of mu-opioid receptor occupancy and opioid withdrawal in heroin-dependent patients. The results of the study showed that 50% of mu-opioid receptor occupancy is a minimal requirement to suppress drug withdrawal symptoms in heroin-dependent patients [24]. However, it is not feasible to routinely measure the mu-opioid receptor occupancy in patients using PET study in the clinic, especially in pregnant women. Therefore, we would like to explore a physiological measurement, mediated by mu-opioid receptor occupancy in the brain, as an objective measurement to facilitate optimal dosing of BUP in pregnant women. Regulation of pupillary diameter is one of the opioid induced effects in the central nervous system. A few clinical studies and our preliminary data in pregnant women have found that BUP can induce pupillary constriction [31, 32]. There might be a potential to use pupillometry as an index to objectively evaluate opioid withdrawal in patients who use BUP to treat opioid addiction.

The objectives of the present study were to evaluate the time courses of the effect of buprenorphine on COWS score and pupillary diameters, and to characterize the pharmacodynamic properties of buprenorphine during pregnancy.

6.3 Method

6.3.1 Clinical study design

Data from two BUP clinical pharmacokinetic and pharmacodynamic studies were included in this pharmacodynamic analysis.

Study 1 was a prospective, open-label, non-randomized and longitudinal pharmacokinetic study of buprenorphine in pregnant and postpartum subjects. This study was approved by the University of Pittsburgh Institutional Review Board. Patients were recruited through Magee-Womens Hospital. Written informed consent was obtained from all participants prior to initiation of any study-related activities. Pregnant, singleton gestation women who were stabilized on twice-daily sublingual BUP opioid substitution therapy (2 - 16 mg) for at least 7 days were participated in this study. Up to 3 PK studies were performed in each participant including 2nd (14 weeks, 0 days through 28 weeks, 0 days), 3rd trimester (28 weeks, 1 day through term), and postpartum period (after 4 weeks of delivery). At each PK study visit, a total of 10 blood samples were collected in heparinized tubes from each subject at 0 (trough), 0.25, 0.5, 0.75, 1, 1.5, 2, 4, 8 and 12 hours after the dose. After centrifugation of blood, plasma samples were frozen at -80°C until analyzed. Several pharmacological effects and physiological measurements including craving score, clinical opioid withdrawal (COW) score, pupillary diameter size, respiration rate, blood

pressure, as well as body temperature were collected at 0 (trough), 4, 8 and 12 hours after buprenorphine dose.

Study 2 was a BUP PK/PD study in pregnant women to assess the association between BUP plasma concentrations and PD effects. Pregnant, singleton gestation women who were stabilized on sublingual BUP opioid substitution therapy for at least 7 days were recruited in this prospective, open-label, non-randomized longitudinal BUP PK study. Up to 3 studies were performed in each participant including 1st-half of pregnancy (gestational week < 20 weeks), 2nd-half of pregnancy (gestational week \geq 20 weeks), and postpartum (at least 4 weeks after delivery). The study was approved by the University of Pittsburgh Institutional Review Board. All patients were recruited through Magee-Womens Hospital, and written informed consent was obtained from all participants. At each study visit, a total of 10-13 blood samples were collected from 0 hours up to 12 hours after the dose or till the end of a dose interval. Several pharmacological effects and physiological measurements including craving score, clinical opioid withdrawal (COW) score, pupillary diameter size, galvanic response, respiration rate, blood pressure, as well as body temperature were collected at 0, 0.5, 1, 1.5, 2, and every two hours afterwards until the end of the dosing interval.

6.3.2 Determination of buprenorphine concentration in plasma

The concentrations of BUP in plasma samples from study 1 were quantified using a validated ultra-performance liquid chromatography with tandem mass spectrometry (UPLC-MS/MS). Briefly, 500 μ L of plasma samples containing buprenorphine and the deuterated internal standard (buprenorphine-d4) were extracted using pre-conditioned Strata X-C cartridges. The cartridge was washed with 1 mL of 2% formic acid in water for two times, followed with 1 mL of

2% formic acid in methanol for one time. Buprenorphine and the internal standard were eluted and collected. The eluent was evaporated, reconstituted and an aliquot was injected in an Acquity UPLC Ethylene Bridged Hybrid (BEH) C₁₈ 1.7 μm column (2.1x100 mm) equipped with Waters ACQUITY UPLC system tandem Thermo TQS Quantum Ultra™ Triple Quadrupole Mass Spectrometer. Calibration curves were linear in the range 0.05–50 ng/mL. Both the intraday and interday precisions assessed by coefficient of variation values and the accuracy assessed by bias were within 15% of the nominal concentrations.

The concentrations of BUP in plasma samples from Study 2 were quantified using a validated ultra-performance liquid with tandem mass spectrometric assay (UPLC-MS/MS). Two hundred of plasma sample containing deuterated compound of buprenorphine-D₄ chromatography were processed with protein precipitation prior to chromatography. Chromatographic separation was performed using Acquity UPLC Ethylene Bridged Hybrid (BEH) C₁₈ 1.7 μm column (2.1x100 mm) with a mobile phase consisting of [A] 5% Acetonitrile in water containing ammonium acetate (2 mM) and formic acid (0.1%), and [B] Acetonitrile containing ammonium acetate (2 mM) and formic acid (0.1%) delivered at a flow rate of 0.3 mL/min in a gradient elution. The analytes were detected by a XEVO TQS mass spectrometer in positive electron spray ionization (ESI) mode using multiple reaction monitoring (MRM). The assay was linear over the range of 0.05–100 ng/mL for buprenorphine. Both the intraday and interday precisions assessed by coefficient of variation values and the accuracy assessed by bias were within 15% of the nominal concentrations.

6.3.3 Measurement of pupillary diameter

Pupillary diameter was measured by trained study nurses using an infrared portable pupillometer (VIP®-300, Neuroptics®, San Clemente, CA). Before the measurement of pupil

diameter, patients were required to sit in a low light room for at least 3 minutes in order to avoid any impact of environmental factors on pupill size. Three repetitive measurements were made (within 30 second) at each time point and the mean value was used in the analysis.

6.3.4 Assessment of craving score and COWS score

The COWS scores were collected by trained study nurses. The area under the curves of COWS scores during a dosing interval (AUC_{0-t}) was calculated from time 0 to 12 hours or the end of a dosing interval using trapezoidal rule. Box-Cox transformation were applied to the AUCs of COWS scores to generate approximately normally distributed data for the purpose of statistical analysis. A univariate linear mixed effect model was used to compare the statistical difference in the AUCs of COWS scores during pregnancy vs postpartum period. In the linear mixed effect model, time was treated as fixed effect, subject was treated as random effect. The linear mixed effect model was fitted through maximum likelihood estimation in Stata (Version 14.0 SE).

6.3.5 Population pharmacokinetic /pharmacodynamic Analysis

Non-linear mixed effects model (NONMEM) using the first-order conditional estimation with interaction (FOCE-I) was applied to develop a buprenorphine population PK/PD model to describe the relationship between plasma concentration of BUP and pupillary diameter.

Stepwise model development approach was applied to develop a PK/PD model. (1). In the PK model, fixed and random effects were estimated to describe the time course of buprenorphine plasma concentration after sublingual administration. (2) The pupillary diameter size was modelled as a function of BUP plasma concentration (C_p) or as a function of predicted BUP

concentration (C_e) in a theoretic effect compartment. In the PD modeling, the PK parameters for each individual estimated by the PK model were incorporated. Fixed and random effects were estimated to describe the time course of pupil diameter driven by C_e or C_p of buprenorphine after a dose.

The buprenorphine population PK model was developed in two steps. First, the structural model was explored and selected to describe the absorption and disposition of buprenorphine. Because BUP was administered sublingually, structural model evaluation included extensive exploration of different absorption models to optimize model fitting in the absorption phase. After optimization of the structural model, the effects of demographic and other patient covariates (age, pregnancy, body weight and gestational weeks, etc.) were evaluated through PK parameter vs covariate plots. The covariates that are potentially associated with PK parameters from visual check was further investigated via bootstrap stepwise forward/ backward covariate evaluation (SCM, forward addition, $p < 0.05$; backward elimination $p < 0.01$).

Based on prior information and plots such as mean pupillary diameter vs time and quartiles of BUP concentration vs pupillary diameter, a sigmoid E_{max} function was assumed for the relationship between pupillary diameter and buprenorphine concentration in plasma (C_p) or in the effect compartment (C_e). The miotic effect of buprenorphine on pupil diameter is evaluated by the following equation,

$$\text{Pupil size} = E_0 - \frac{1}{100} \times E_0 \times \left(\frac{E_{max} \times C_p^\gamma}{EC_{50}^\gamma + C_p^\gamma} \right) \quad (\text{as a function of } C_p)$$

$$\text{Pupil size} = E_0 - \frac{1}{100} \times E_0 \times \left(\frac{E_{max} \times C_e^\gamma}{EC_{50}^\gamma + C_e^\gamma} \right) \quad (\text{as a function of } C_e)$$

Where E_0 is the baseline pupil diameter, E_{max} is the percentage of maximum changes of

buprenorphine induced miotic effect compared to baseline value. EC_{50} is the concentration of buprenorphine at 50% of maximum effect, γ is the shape factor of the sigmoidal E_{max} function.

The parameter estimation of a model was a process of minimization of the objective function value (OFV, approximately equal to $-2 \times \log$ of the likelihood) using maximum likelihood estimation.

For the discrimination between different models, Akaike information criterion (AIC) was used to compare non-nested models. As OFV approximately follows χ^2 distribution and a likelihood ratio test was employed to compare the difference of two nested models. For adding one additional parameter to a model, a decrease of 3.84, 6.63, or 7.88 in OFV was used as a cutoff for significant improvement in model fit at respectively 5%, 1% and 0.5% levels of rejecting the null hypothesis (there are no significant difference in the two models) due to type I error. In addition, certain diagnostic plots, such as goodness-of-fit plot, plot of individual observed concentration time profile overlaid with population prediction and individual prediction, conditional weighted residual against time plot, and individual weighted residual against time plot were also employed during model selection.

The magnitude of the differences between subjects and between occasions within a subject at model parameter level were estimated by the between subject variability (BSV) and between occasions variability (BOV). As a log-normal distribution across the population for each parameter was assumed, the exponential models were used to estimate BSV and BOV. The residuals, (the difference between observed and predicted concentration of buprenorphine), were assumed to have a normal distribution and centered on zero. Additive only, proportional only, and the combined additive and proportional error models were tested during the selection of the error model.

The performance of the final model fitting was evaluated by the goodness-of-fit plot, prediction-corrected visual predictive check (pcVPC), and non-parametric bootstrap. In the VPC procedure, 1000 replicate datasets were simulated with the original dataset design. Variability was introduced into the replicate datasets by random sampling from matrices of random effects in the final model. The VPC plot constructed the 95% prediction interval of the 5th, 50th and 95th percentiles from the 1000 replicate datasets against the 5th, 50th and 95th percentiles of the observed concentration-time profiles, which was used to graphically assess whether the simulations from the final model was able to reproduce the central trend and variability in the observed dataset. Using sampling with replacement of random subject in the original dataset, 200 of bootstrap datasets were generated containing the same subject numbers as the original dataset. The 90% of prediction intervals of the bootstrap datasets were compared with the parameter estimates from the final model.

6.3.6 Software

The population PK /PD analysis was performed in NONMEM, version 7.3.0. Graphical diagnostics and exploratory analysis were conducted using R (Version 3.4.4) and Xpose (Version 4). Pirana® was used as an interface to integrate these software.

6.4 Results

6.4.1 Clinical data

A total of 527 buprenorphine plasma concentrations, 303 COWS scores, and 303 pupillary diameters from 51 PK/PD study occasions in 26 patients from the two clinical studies were used for the PK /PD analysis. The characteristics of study subjects are summarized in Table 28.

6.4.2 COWS scores and BUP exposure during pregnancy and postpartum

The time course of mean COWS score following administration of BUP in the two clinical studies are shown in Figure 6-1. The plots showed that COWS scores were higher during pregnancy than the values during postpartum period. The linear mixed effect model analysis found that the AUCs of COWS scores in a dose interval were significantly higher during pregnancy compared to the values at postpartum period, whereas, the exposure of BUP were significantly lower during pregnancy compared to the values at postpartum period (Table 6-1). We also explored the relationship between BUP exposure and COWS score as shown in Figure 6-2, 6-3.

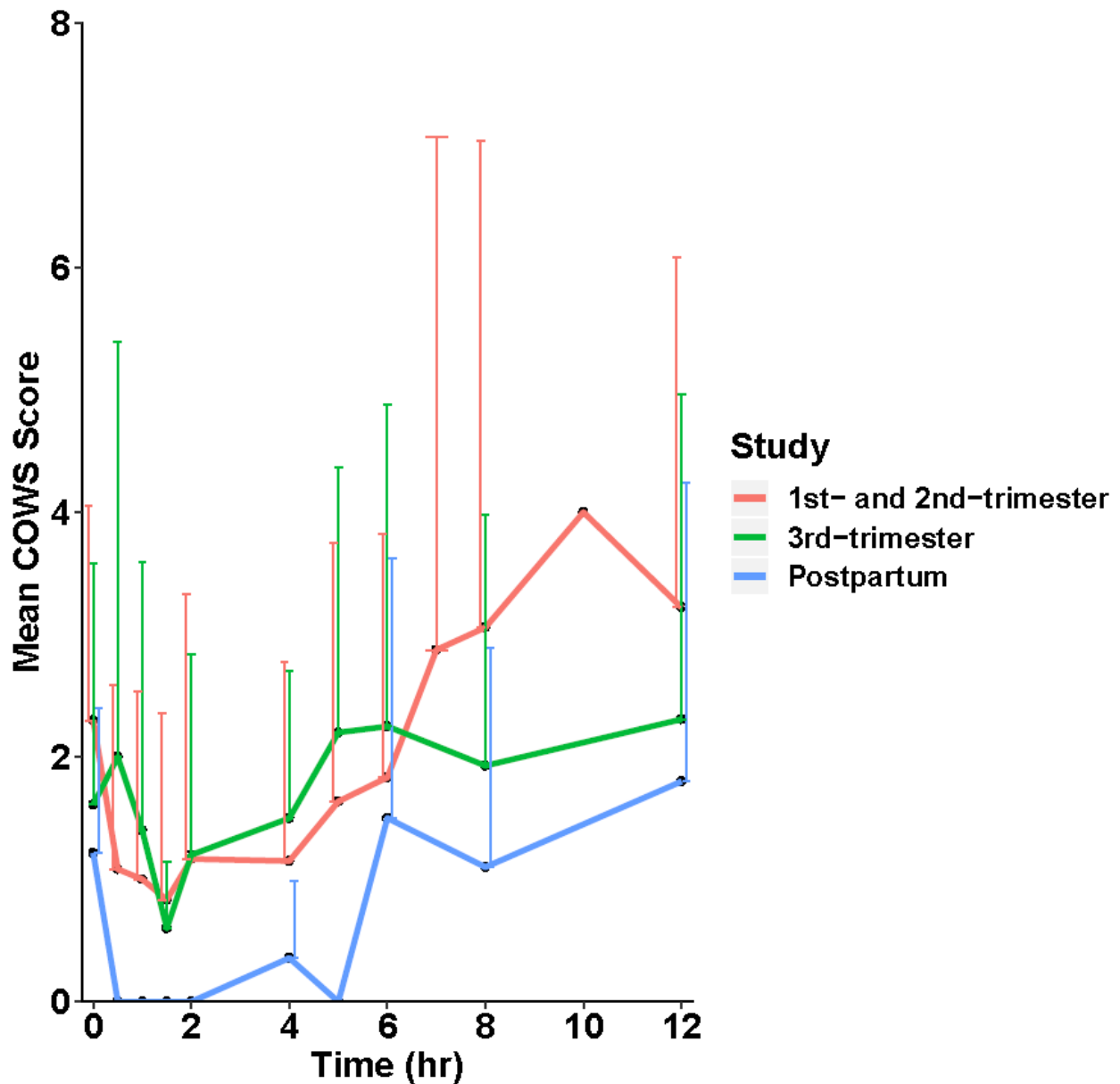


Figure 6-1. Mean COWS score time profiles following administration of a SL BUP dose.

Red, green and blue curves represent study at the 1st- and 2nd-trimester, 3rd-trimester and postpartum, respectively.

N = 19 (2, 9 and 8 patients completed study in 6, 8 and 12 hrs, respectively), 18 (4, 1 and 13 patients completed study in 6, 8 and 12 hrs, respectively), and 14 (3 and 11 patients completed study in 6 and 12 hrs) at the 1st-half, 2nd-half of pregnancy and postpartum, respectively.

Table 6-1. The AUCs of Clinical Opioid Withdrawal Scale score and BUP exposure within a dose interval during pregnancy and postpartum (expressed as mean (SD))

Parameter (Mean (SD))	1 st - and 2 nd -trimester (n = 19)	3 rd -trimester (n = 18)	Postpartum (n = 12)*	P Value
AUC_COWS	16.79 (17.02)	16.50 (12.45)	9.14 (12.61)	0.001, 1 st - and 2 nd -trimester vs postpartum < 0.001, 3 rd - trimester vs postpartum
AUC_BUP	12.36 (5.79)	18.97 (13.09)	28.76 (20.49)	< 0.001, 1 st - and 2 nd -trimester vs postpartum 0.02, 3 rd - trimester vs postpartum

Box-Cox transformation of AUC_COWS; Log transformation of AUC_BUP

*: Two patients terminated study earlier and the AUC of COWS score were not able to calculate.

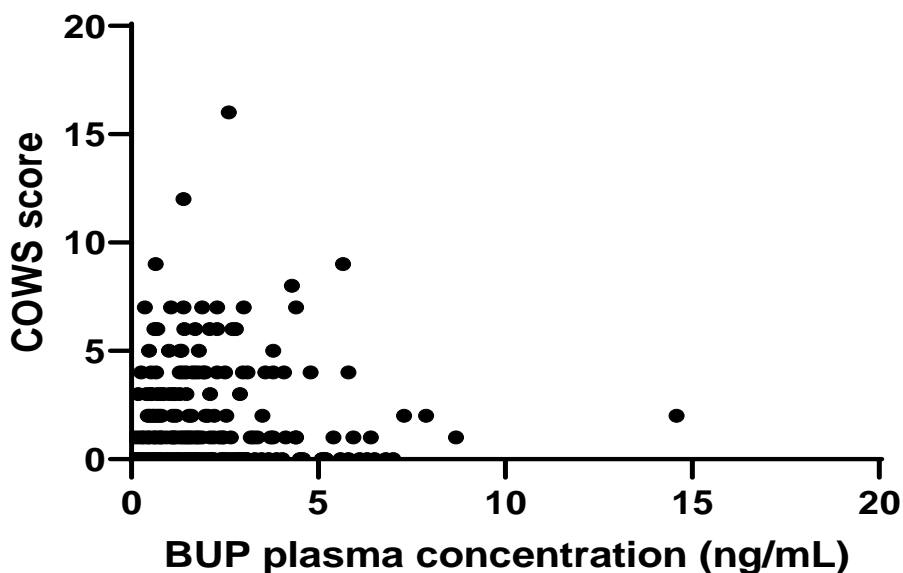


Figure 6-2. BUP plasma concentration vs Clinical Opioid Withdrawal Scale score.

The dot represents COWS score vs BUP plasma concentration that were measured at the same time point. The matrix plot suggests that there is no simple linear correlation between COWS score and buprenorphine plasma concentration.

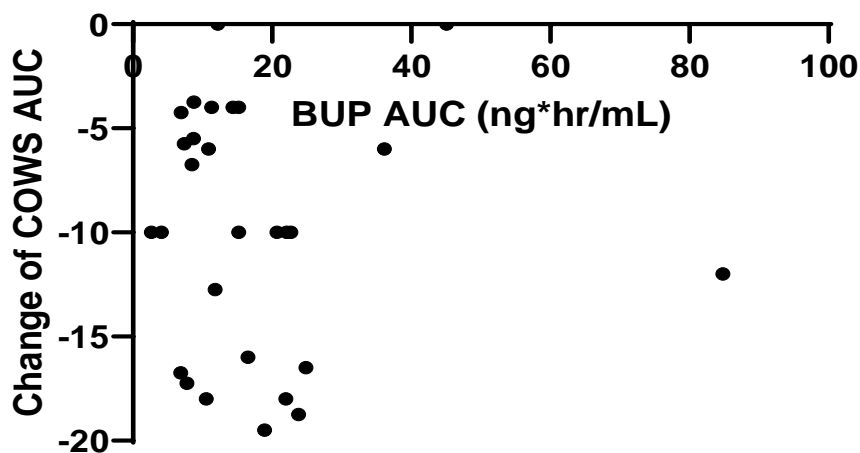


Figure 6-3. The changes of AUCs of COWS score from baseline vs BUP AUC.

The AUC of COWS score at baseline were calculated by applying COWS score at trough to the entire dose interval. The dot represents the change of area under the time course of COWS score vs area under the time course of BUP plasma concentration during one dose interval in one PK study occasion in one patient. The matrix plot suggests that there is no simple linear correlation between the change of the AUC of COWS score and buprenorphine plasma concentration.

6.4.3 Buprenorphine induced miotic effect

6.4.3.1 Basic exposure and response exploration

Before modeling analysis, we did some basic plots to identify the relationship between buprenorphine exposure and pupillary diameter (Figure 6-4, 6-5 and 6-6).

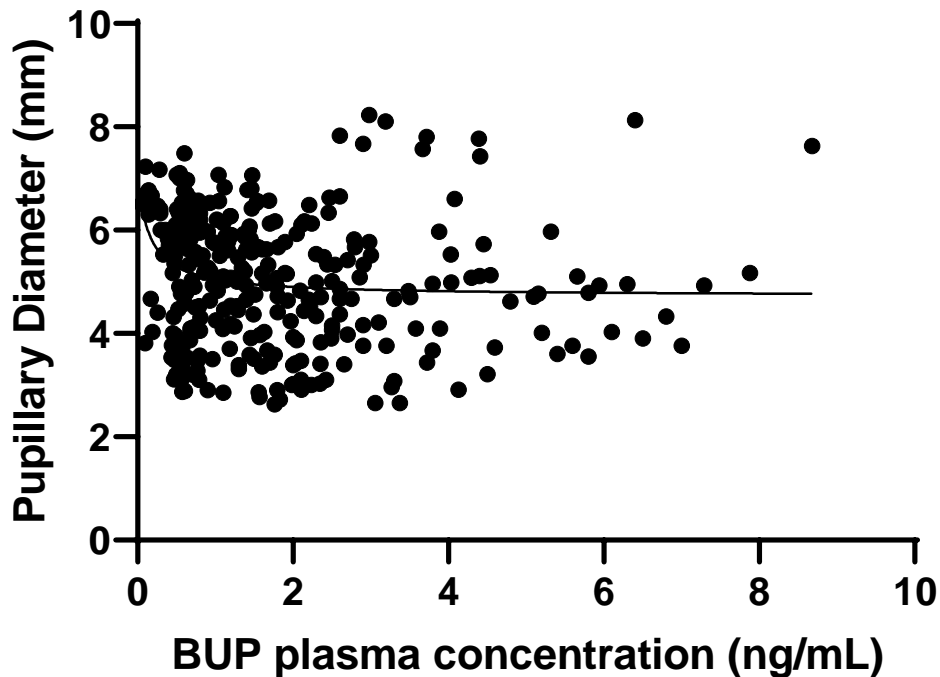


Figure 6-4. BUP plasma concentration vs pupillary diameter

The dot represents pupillary diameter with BUP plasma concentration that were measured at the same time point. The matrix plot between pupillary diameter and buprenorphine plasma concentration suggests that the miotic effect induced by administration of BUP is probably via an E_{max} relationship.

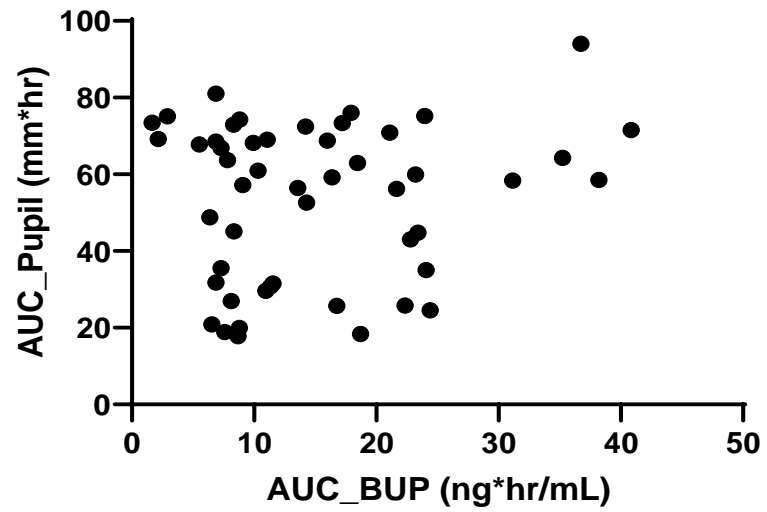


Figure 6-5. BUP exposure (AUC) vs the AUC of pupillary diameter

The dot represents the area under the time course of pupillary diameter vs the area under the time course of BUP plasma concentration during a dose interval in one PK study occasion in one patient. The matrix plot suggests that there is no simple linear correlation between the AUC of pupillary diameter and the AUC of buprenorphine.

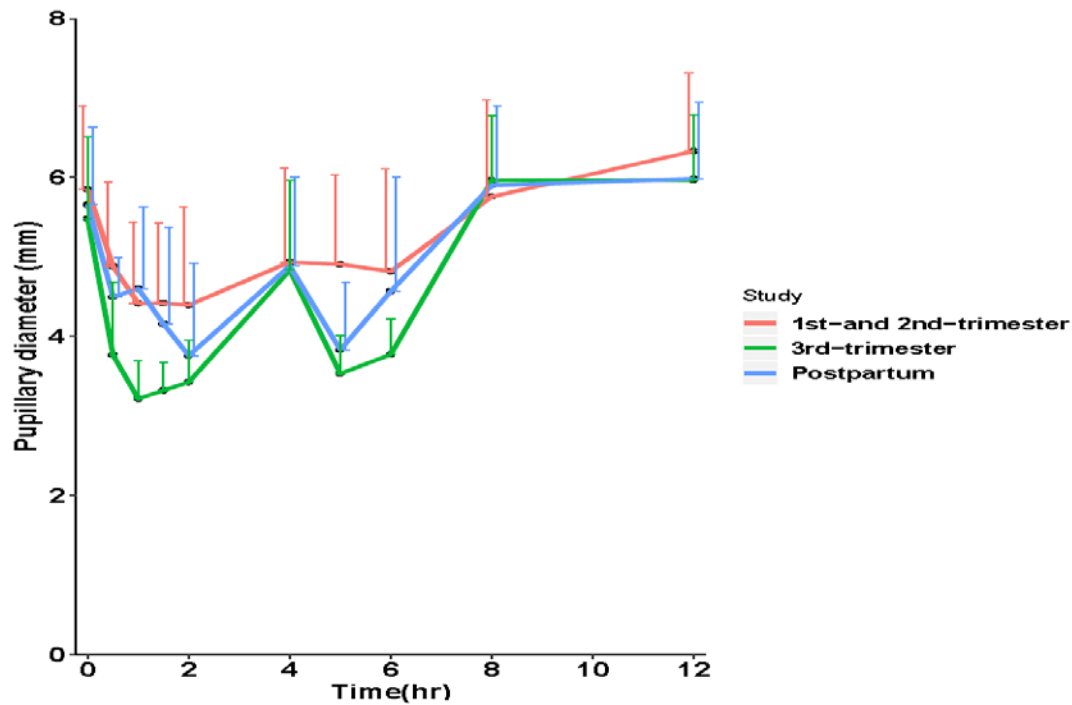


Figure 6-6. Time course of pupillary diameter following SL administration of BUP by study occasion

Red, green and blue curves represent study at the 1st- and 2nd-trimester, 3rd-trimester and postpartum, respectively.

N = 19 (2, 9 and 8 patients completed study in 6, 8 and 12 hrs, respectively), 18 (4, 1 and 13 patients completed study in 6, 8 and 12 hrs, respectively), and 14 (3 and 11 patients completed study in 6 and 12 hrs) at the 1st-half, 2nd-half of pregnancy and postpartum, respectively.

6.4.3.2 Model analysis

The modeling of buprenorphine PK has been reported in Chapter 5. The results of the population PK /PD model showed that a hypothetical effect compartment best described buprenorphine induced miotic effect (Figure 6-7.). Linking pupil diameter sizes to predicted buprenorphine concentrations in a hypothetical effect compartment resulted a drop in AIC of 29.4 compared to a sigmoidal E_{\max} model. As the effect compartment was a hypothetical compartment, there was no mass transfer between central compartment and the hypothetical effect compartment. The differential equation for the hypothetical effect compartment is listed below.

$$\frac{dX_7}{dt} = k_{e0} \times \frac{X_2}{V_2} - k_{e0} \times X_7$$

Where X_2 is the amount of buprenorphine in the central compartment. X_7 is the concentration of buprenorphine in the hypothetical compartment. V_2 was the apparent volume distribution of buprenorphine in the central compartment and t represented time. k_{e0} was the 1st-order rate constant of the transfer of the concentration of BUP from central compartment to the hypothetical effect compartment.

The results of the population PK /PD modelling analysis are shown in Table 6-2. The model estimated that buprenorphine was very potent in inducing miotic effect with a value of EC_{50} at 0.63 ng/mL. The baseline pupillary diameter was estimated as 9.65 mm, which represented the typical pupil diameter size in an opioid addicted patient without buprenorphine exposure. The transfer of BUP from central compartment to the hypothetical effect compartment was modeled by 1st-order kinetics. The estimated rate constant of distribution of BUP from the central compartment to the hypothetical effect compartment was 0.723 hr⁻¹, which indicates that the transfer half-life between plasma and effect site was approximately 57 min ($\ln 2/k_{e0}$). All of the

typical values and variance were estimated precisely, as the relative standard errors were all within 30%.

6.4.4 Model evaluation

In the goodness-of-fit plots, the observed pupillary diameter against population predicted concentration or individual predicted pupillary diameter were clustered towards the lines of identity. The conditional weighted residuals data were symmetrically distributed around the line of zero and majority of the residuals were within the range of 2 times the standard deviations (Figure 6-8).

The VPC plot displayed that the 5th, 50th, and 95th percentiles of the observed pupillary diameter were within 95% predicted interval from 1000 simulated replicate datasets. Also, most of the observed pupillary diameter were within the predicted 95% intervals as shown in Figure 6-9.

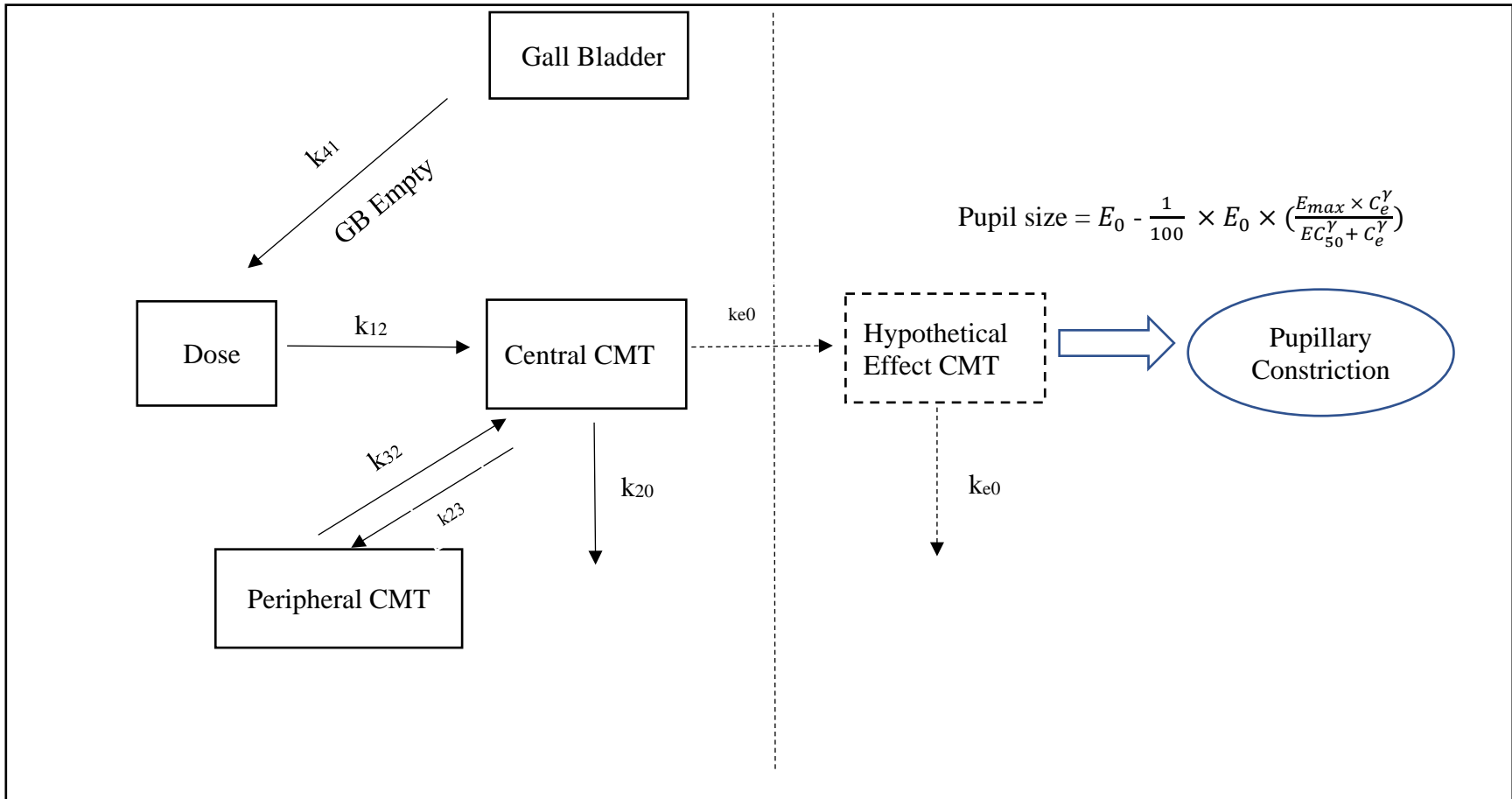


Figure 6-7. Schematic diagram of the final population pharmacokinetic /pharmacodynamic model

k_{12} , first-order absorption rate constant; k_{23} and k_{32} , rate constant for distribution of buprenorphine between central and peripheral compartment; k_{20} , first-order elimination rate constant; k_{41} , rate constant for the distribution of buprenorphine from gall bladder to dose compartment; k_{e0} , rate constant of distribution of BUP from central compartment to the hypothetical effect compartment; GB, gall bladder

Table 6-2. Parameter estimates of final population pharmacokinetic /pharmacodynamic model for buprenorphine following sublingual administration in pregnant women

Parameter	Final model estimate (RSE %)	Bootstrap (n=500) Median (95% CI)
Population typical value		
E _{max} (%)	82.9 (4.2)	69.9 (36.1 – 96.4)
EC ₅₀ (ng/mL)	0.63 (16.3)	0.65 (0.29 – 1.63)
Gamma	0.396 (15.3)	0.518 (0.253 – 1.479)
Baseline (mm)	9.65 (0.3)	9.16 (6.67 – 9.99)
k _{e0} (hr ⁻¹)	0.723 (27.2)	0.722 (0.366 – 1.157)
Interindividual variability (expressed as % CV)		
Baseline	18.8 (18.5)	15.9 (0.1 – 24.5)
Gamma	68.8 (28.2)	80.2 (44.0 – 126.6)
Interoccasion variability (expressed as % CV)		
Baseline	9.7 (20.5)	9.2 (4.3 – 15.5)
Residual variability		
Additive error (mm)	0.24 (9.3)	0.34 (0.19 – 0.28)

CI: confidence interval; E_{max}: percentage of maximum changes of buprenorphine induced miotic effect compared to baseline pupillary diameter; IC₅₀: buprenorphine concentration to product a half-maximal effect; Gamma: the shape of the sigmoidal factor; Baseline: pupil diameter size in opioid addicted patient without buprenorphine exposure in the body of patients; k_{e0}, rate constant of distribution of BUP from central compartment to the hypothetical effect compartment.

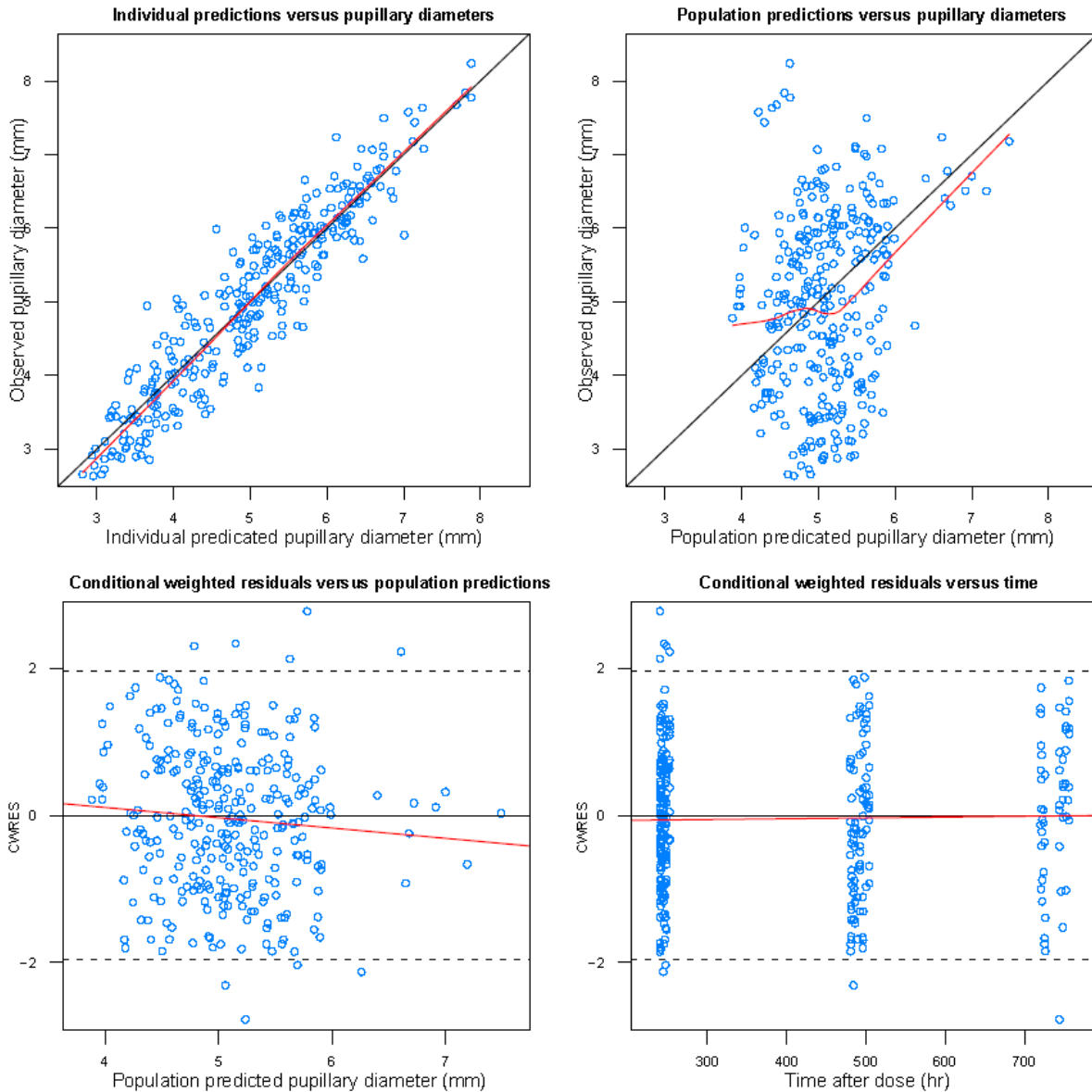


Figure 6-8. Goodness of fit diagnostic plots for buprenorphine population PK /PD final model fit.

(A) Individual predicted pupil diameter vs. observed pupil diameter. (B) Population predicted pupil diameter vs. observed pupil diameter. (C) Conditional weighted residuals vs. population predictions (D) Conditional weighted residuals vs. sample collection time after a dose. The solid black lines in (a) and (b) represent the line of identity and those in (c) and (d) represent the line $y = 0$. The solid red lines in each panel represent loess smooth of the data.

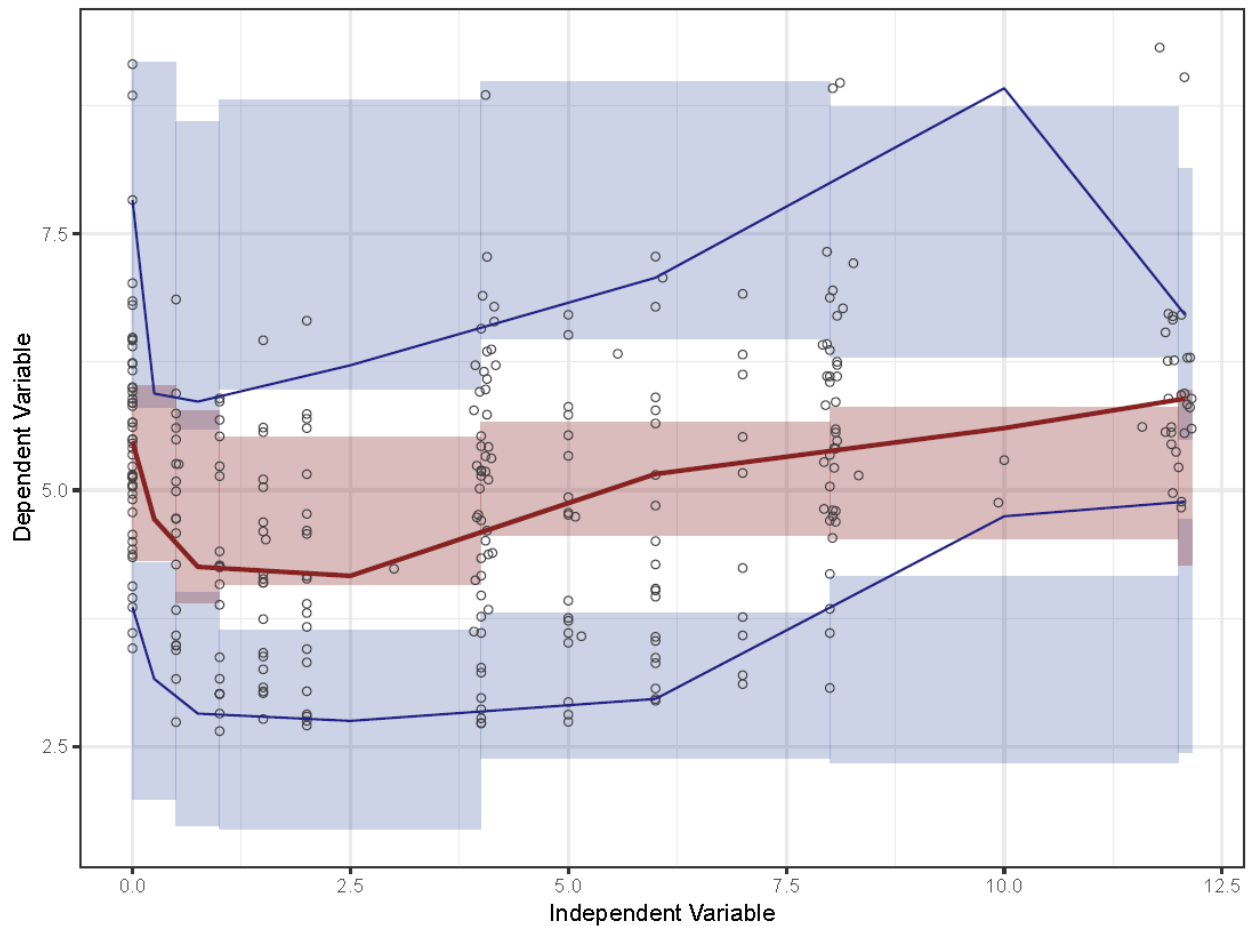


Figure 6-9. Predictive performance of the final model using prediction-corrected visual predictive check plots.

The model predicted pupil diameter were plotted against observed pupil diameter at each time point after a dose. Y-axis, Dependent variable represented pupil diameter; x-axis, Independent variable represented time after a dose. Open dots represented observed pupil diameters, solid blue lines represented the 5th, and 95th percentiles of observed pupil diameters; the solid red lines represented the 50th percentiles of the observed pupil diameter; shaded area represented the model predicted 95% confident intervals surrounding the 5th, 50th, and 95th percentiles from 1000 simulated datasets.

6.5 Discussion

In the present analysis, we evaluated the pharmacodynamics of buprenorphine in pregnant women. A linear mixed effect model analysis indicated that the AUCs of COWS scores in a dosing interval were significantly higher during pregnancy compared to the values during the postpartum period, which may be due to the significantly lower buprenorphine exposure in pregnant women that is observed in the clinical studies. A population PK /PD modeling analysis demonstrated that pupillary constriction was induced after administration of buprenorphine. The relationship between pupillary diameter and buprenorphine concentration was described by a sigmoidal E_{max} model with a hypothetical effect compartment. A time delay between buprenorphine plasma concentration and pupillary constriction indicates that there was a temporal dissociation of the distribution of buprenorphine between central and biophase compartment. The equilibrium half-life was 57 mins. The temporal dissociation between the time courses of buprenorphine plasma concentration and miotic effect may be due to the transfer of buprenorphine from blood to central nervous system. The IC_{50} of BUP was not significantly different during pregnancy and postpartum in the PK/PD model analysis of buprenorphine concentration and pupillary diameter, which suggested that there might be no significant changes in the sensitivity or number of μ -opioid receptors during pregnancy compared to non-pregnant women.

As the two BUP clinical studies were observational studies, the doses of BUP administered in study participants were prescribed for clinical purposes by caregivers of each individual patient. We used observed, rather than dose-normalized, AUC of BUP plasma concentration to evaluate the exposure of BUP in pregnant women. Using the observed AUC enables us to assess if the exposure of BUP is comparable in pregnant and non-pregnant women under the current clinic practice. The results revealed that the exposure of BUP as measured by the AUC in a dose interval

at steady state were significantly lower during pregnancy compared to the exposure during postpartum period.

The pharmacodynamic effect of buprenorphine inhibiting opioid withdrawal were assessed by COWS score in the two BUP clinical studies. The AUCs of COWS scores in a dosing interval of BUP were significantly higher during pregnancy than during postpartum. We also observed large interindividual variabilities in COWS scores. At prescribed doses, BUP is able to minimize opioid withdrawal symptoms and cravings in patients and eventually to help patients function normally. Lower the COWS score, better the patients feel; higher the COWS score, less satisfied the patients are. The observed significantly greater COWS scores during pregnancy compared to postpartum is likely the result of the lower buprenorphine exposure in pregnant women. A matrix plot suggested that that there was no relationship between COWS score and BUP plasma concentration. Further PK/PD analysis to study the correlation between BUP concentration and COWS score is needed.

As a substrate of μ -opioid receptor, buprenorphine binds to μ -opioid receptor in the central nervous system. The pharmacological effects associated with BUP binding to μ -opioid receptors include pain modulation, euphoria, pupillary constriction, etc. In the two BUP clinical studies, we observed that following administration of BUP miosis occurred and the sizes of pupillary diameter gradually returned back to the values of baseline at the end of a dose interval. Pupillary size is determined by the dilation or constriction of iris through sympathetic and parasympathetic nervous system. Opioids induced pupillary constriction has been observed in human, rabbits and dogs. Whereas, pupillary dilation has been seen in rats, mice, and cats. It has been shown that the opioid induced miosis or mydriasis are opioid receptor-mediated as these changes can be blocked by μ -opioid receptor antagonist, naloxone [25]. Currently, the exact site of action opioid mediated

pupillary diameter change is not clear; however, it is believed that the action site should be within the brain as no pupillary effect was observed by intraocular administration of morphine and the effective dose of morphine following an intracerebroventricular injection was hundredths of the intravenous administration [26, 27]. The possible mechanism of the pupillary constriction by opioids may be through the suppression of the inhibitory process to Edinger-Westphal nucleus, a place in the midbrain that regulates signal to iris muscle resulting in pupillary constriction [28, 29]. Several studies have observed that higher plasma concentration of morphine and methadone results in more pronounced effects on pupillary constriction or dilation in human and rats [30-35].

The population PK/PD modelling analysis of BUP concentration and pupillary diameter revealed that the miotic effect induced by administration of BUP can be described by an E_{max} relationship. The population PK/PD model estimated the concentration of BUP to induce half maximal constrictive effect of pupillary diameter to be 0.63 ng/mL. The small value of IC_{50} estimated by the model is consistent with high potency of buprenorphine for μ -opioid receptors as compared with other opioids. The IC_{50} of morphine and codeine for the miotic effects were 4.56 and 8.44 ng/mL [334]. The IC_{50} of BUP was not significantly different during pregnant and postpartum in the PK/PD model analysis, which suggested that there might be no significant changes in the sensitivity or number of μ -opioid receptors during pregnancy compared to postpartum. Lack of significant changes in the IC_{50} of BUP during pregnancy and postpartum might be a result of low power to identify statistically significant difference due to small patient sample sizes in the two BUP clinical studies. Clinical studies in larger patient population are needed to validate these findings from the present study.

The present population PK/PD modelling analysis of the relationship between pupillary diameters following administration of BUP only included BUP plasma concentration. Potential

miotic effects induced by the metabolites of BUP were not incorporated into the pharmacodynamic model. After administration, buprenorphine is extensively metabolized to norbuprenorphine, and norbuprenorphine is further metabolized to norbuprenorphine glucuronide. In addition, a portion of buprenorphine is directly conjugated to buprenorphine glucuronide. In vitro study showed that both norbuprenorphine and buprenorphine glucuronide also bind to mu-opioid receptors [95]. However, norbuprenorphine was found to be a substrate of P-glycoprotein, which may result in a limited exposure of norbuprenorphine in the brain [291]. The exposure of norbuprenorphine in the brain is limited based on the reported data from postmortem brain samples. In 6 overdose death cases, the concentrations of norbuprenorphine was 5.8 ng/g (BUP concentration was 151 ng/g) in one postmortem brain sample, and were not detectable in the other 5 postmortem brain samples (BUP concentration in these postmortem brain samples ranged 7.1 – 76.1 ng/g) [292]. Studies have found that morphine-6-glucuronide can induce pupillary constriction, but it was 22 times less potent than morphine [335]. Similar to morphine-6-glucuronide, as a substrate of mu-opioid agonist, the IC₅₀ of buprenorphine glucuronide was higher than buprenorphine (4.9 pM vs 2.7 pM) [95]. Considering that only a small portion of the administered dose of BUP is converted to BUP glucuronide and that buprenorphine glucuronide is more polar, the concentration of buprenorphine glucuronide might be limited in the brain. Taken together, it is anticipated that the contribution towards the pharmacological effects in the brain by the metabolites of BUP should be very limited.

In clinical study 1, pupil diameters were only collected at trough, 4, 8 and 12 hours after a dose of buprenorphine. In the second clinical study, the dose frequency of buprenorphine were three times a day or four times a day for most of the study participants. Only limited pupillary diameter sizes were collected at 10 and 12 hours after a BUP dose, which made the population PK /PD model inadequate to describe the time courses of pupil diameter after 10 hours following a

buprenorphine dose. In addition, we were unable to collect the true baseline of the pupil diameter when there was no buprenorphine exposure in the patients. The baseline pupil diameter was estimated by the model, which were predictions of the pupil diameter sizes when there was no buprenorphine in the patient.

Large interindividual variability was found in pupillary diameter in the clinical studies. The model estimated that the coefficient of variance of the shape of the sigmoidal E_{\max} model was 68.8%. Also, adding interoccasion variability to the baseline pupil diameter improved the model fit significantly. Although pupillary diameter is correlated with administration of BUP as shown in this modeling analysis, pupillary diameter may not be a meaningful biomarker to infer plasma concentration of buprenorphine in maintenance therapy as there is no direct link to the plasma concentration of BUP, and there is large interindividual and interoccasion variabilities. Further investigation of reliable and readily measurable biomarkers that are able to objectively assess opioid withdrawal to optimize dosing in pregnant women is warranted.

6.6 Conclusions

In the present study, we observed significantly lower plasma exposure of BUP and significantly higher AUC of COWS score in a dosing interval of BUP during pregnancy compared to the values during the postpartum period under the current dose regimen in pregnant women. There were no direct correlations between COWS score, pupillary diameter and the plasma concentration of BUP. The IC_{50} of BUP was not significantly different during pregnant and postpartum in the PK/PD model analysis of pupillary diameter. The results suggest an increase in

BUP doses may be needed during pregnancy in order to maintain a comparable BUP exposure and therapeutic effects of BUP in treating opioid use disorder.

7.0 SUMMARY AND FUTURE DIRECTIONS

7.1 Summary and Clinical Inference

Ideally, it is better to avoid medications during pregnancy because of the concerns for fetal safety. Pregnant women, however, may take medications to treat pregnancy related complications, such as nausea and vomiting, gestational diabetes, preeclampsia, hypertension, depression, and preterm delivery. Pregnant women may also take medications because of chronic preexisting illnesses, and substance abuse disorder. A survey showed that 96% of the pregnant women received at least one medication during their pregnancy and more than 62% of them used over the counter medications [336]. The average number of medication used during pregnancy increased from 2.5 in 1970's to 4.2 in 2000's [337]. However, limited data exists on changes in the PK/PD of drugs in pregnant women. Ironically, dosage regimens that are used in pregnancy are based on the recommendations for non-pregnant women and men, because pregnant women are normally excluded from clinical studies during drug development due to fetal safety issues. Use of medications during pregnancy which are not titrated for pregnancy induced alterations in physiological conditions may lead to therapeutic failure or drug related toxicities.

Pregnancy can alter drug disposition. Pregnancy induces many physiological changes including the development of placental-fetal compartment, increase in renal filtration, increase in fluid volume, increase in hepatic portal blood flow, as well as changes in the expression and activity of several drug metabolizing enzymes [125, 145, 147]. These pregnancy-induced physiological changes can impact drug absorption, distribution, metabolism, and elimination [148]. Specifically, pregnancy results in a decreased rate of absorption of certain drugs due to decreased gastric emptying and decreased intestinal motility. The exposure of certain drugs used during pregnancy may be decreased or increased depending on how the activity of drug metabolizing enzymes and transporters in the gut are altered during pregnancy. Pregnancy leads

to an increased volume of distribution because of the increased body fat, total body water, and blood volume. Pregnancy effect on metabolism of drug is drug specific. For example, the metabolism of drugs mediated by cytochrome P-450 (CYP) 2C9, CYP2D6, CYP3A4, uridine 5'-diphospho-glucuronosyltransferase (UGT) 1A4, and UGT2B7 are enhanced, whereas the metabolism of substrates of CYP1A2 and CYP2C19 are decreased [158]. Taken together, the physiologic and PK changes associated with pregnancy may result in an altered systemic exposure, and ultimately, lead to alterations in the efficacy and toxicity of drugs used in pregnant women. Several clinical studies have found significant changes in systemic exposure of certain drugs used during pregnancy [161-163]. Recent NICHD initiatives have focused on gathering more pharmacological data on drugs used in pregnancy. However, clinical studies in pregnant women are challenging and difficult to perform. Modeling and simulation has the potential to predict drug exposure in the presence of physiologic changes seen in pregnant women that can alter drug elimination and drug exposure and therefore drug response. This body of work is one of our first attempts to understand the pharmacokinetic and pharmacodynamic changes induced by pregnancy by combining small cohort clinical studies with different modeling approaches. We illustrated our approach using buprenorphine, a treatment option for substance abuse disorder in pregnant women.

In Chapter 2, we report the development and validation of a rapid, sensitive, and selective method for the determination of buprenorphine and its three metabolites, norbuprenorphine, buprenorphine glucuronide, and norbuprenorphine glucuronide, in human plasma using ultra performance liquid chromatography with tandem mass spectrometry (UPLC–MS/MS). A sample volume of 200 μ L of plasma was sufficient for quantification of BUP and its metabolites. Protein precipitation was applied to process plasma samples prior to chromatography. Deuterated

buprenorphine-D₄, norbuprenorphine-D₃, buprenorphine-D₄-3-β-D-glucuronide, norbuprenorphine glucuronide-D₃, were used as the internal standards (IS). Chromatographic separation was performed using Acquity UPLC Ethylene Bridged Hybrid (BEH) C₁₈ 1.7 μm column (2.1x100 mm) with a mobile phase consisting of [A] 5% Acetonitrile in water containing ammonium acetate (2 mM) and formic acid (0.1%), and [B] Acetonitrile containing ammonium acetate (2 mM) and formic acid (0.1%) delivered at a flow rate of 0.3 mL/min in a gradient elution. The total run-time was 7 min, with buprenorphine, norbuprenorphine, buprenorphine glucuronide and norbuprenorphine glucuronide eluting at 3.3, 1.64, 1.35, and 0.84 min, respectively. The analytes were detected by a XEVO TQS mass spectrometer in positive electron spray ionization (ESI) mode using multiple reaction monitoring (MRM). The assay was linear over the range of 0.05 – 100 ng/mL for buprenorphine, 0.2 – 100 ng/mL for norbuprenorphine, 0.2-200 ng/mL for buprenorphine glucuronide and norbuprenorphine glucuronide. The intra-day and inter-day accuracies expressed as percentage of the nominal concentrations were within 98.2-108.0 %. The intra-day and inter-day precision determined by the coefficient of variations were within 9 %. No significant matrix effects were observed for buprenorphine or the three metabolites in plasma samples. Buprenorphine and the three metabolites were stable under various storage and experimental conditions. This validated method was successfully applied to a clinical pharmacokinetic study after sublingual administration of buprenorphine to pregnant women at different trimesters and during postpartum. We observed a lower exposure of buprenorphine during pregnancy compared to postpartum. The AUC ratios of metabolites to parents demonstrated that CYP- and UGT- mediated buprenorphine metabolism were altered during pregnancy compared to postpartum, which may partially explain the lower exposure of buprenorphine during pregnancy.

In the next step we applied PBPK and PopPK approaches to evaluate the impact of pregnancy on BUP PK. In Chapter 3, we reported the process of building and validating a full-PBPK models of intravenous (IV) BUP in healthy non-opioid dependent and opioid dependent patient populations across a wide range of BUP doses. The full-PBPK models incorporate data on enzymatic metabolism of BUP and its distribution into 13 major tissues in the body following IV dosage. BUP PBPK IV models was able to predict BUP exposure in healthy population in the dose ranges of 4 to 32 mg. The predicted concentration-time profiles in the study-matched virtual patient population are consistent with the observed data across 5 independent studies in healthy non-opioid dependent and opioid dependent patient populations. The predicted IV BUP PK parameters fell within 85%-115% range of the corresponding PK parameters calculated from the IV BUP studies. BUP SL PBPK model was built by introducing SL absorption component to the validated IV BUP PBPK model, and validated through published clinical studies in healthy non-opioid dependent and opioid dependent patients. We performed inter-study and intra-study validations by comparing the mean area under plasma concentration-time curve (AUC, represent systemic exposure after a dose) of the predicted and observed data. Model performance was assessed by intra- and inter-study validations. For the intra-study validations, we used the clinical PK data from different dosing ranges from the same study that was used to build the PBPK profiles. For inter-study validations, we used data from several model naïve clinical PK studies that were not used in model building. For the validations, we performed visual plots of fitted and the predicted against the observed mean concentration-time profiles. The 5th to 95th intervals of the predicted concentrations were calculated to show the overall inter-patient variability. PBPK models of IV and SL BUP were developed and validated using 14 independent BUP PK studies in non-pregnant subjects (5

intravenous single dose, 5 SL single dose, and 4 SL multiple dose). We then adapted this validated SL BUP PBPK model to pregnancy-based model by incorporating physiological changes across trimesters that may impact BUP exposure, including increase in the expression CYPs 3A4, increase in cardiac output, plasma volume, and red blood cell volume, and decrease in hematocrit, and albumin. The BUP SL PBPK pregnancy model was validated with our two in-house prospective clinical trials in pregnant women in three trimesters and postpartum. The model predicted decreased BUP exposure in all three trimesters, compared to the postpartum period. The model predictions were consistent with the observations in the 1st, 2nd and 3rd trimester in a prospective pilot BUP PK study in pregnant women (Chapter 4).

We also applied nonlinear mixed effect model to explore population PK parameters including clearance, and volume of distribution of BUP, as well as between subject variability and between occasion variability (different trimesters) to study alteration of BUP metabolism during pregnancy. Specifically, we used first-order conditional estimation with interaction method to explore whether 1 or 2 compartment model fits the clinical data best. For the discrimination between different base models, we used AIC and certain diagnostic plots. As BUP was dosed via sublingual administration in the study, we also explored whether adding a lag time or additional absorption compartment through separate or combined sequential, parallel or linked zero and first absorption model would improve model fitting. After finalizing the base model, we used stepwise forward/backward method to explore categorical and continuous factors, including pregnancy, gestation weeks, and body weight, age that may influence BUP pharmacokinetics. Simulation based diagnostic methods, such as visual predictive check (VPC) and bootstrap were employed to evaluate the covariate models. A two-compartment model with 1st-order absorption containing

EHC and 1st-order elimination best described the absorption and disposition of buprenorphine following sublingual administration. Pregnancy was identified to be associated with significant differences in BUP PK with the apparent clearance of buprenorphine being increased 1.64-fold during pregnancy compared to the postpartum period. None of the other patient covariates explained interindividual variability in BUP PK in pregnant women (Chapter 5).

Lastly, we applied PK /PD analysis to evaluate the time course of the effect of buprenorphine on COWS score and pupillary diameters and to characterize the pharmacokinetic /pharmacodynamic properties of buprenorphine in order to optimize buprenorphine dosing in pregnant women. We observed significantly lower plasma exposure of BUP and significantly higher AUC of COWS score in a dosing interval of BUP during pregnancy compared to the values during the postpartum period under the current dosing regimen in the pregnant women. There were no direct correlation between COWS score, pupillary diameter and the plasma concentration of BUP. The relationship between pupillary diameter and buprenorphine concentration was described by a sigmoidal E_{max} model with a hypothetical effect compartment. The model estimated that buprenorphine was transferred from the central compartment to a theoretical biophase compartment with a 1st-order transfer kinetics at a rate constant at 0.723 hr^{-1} . The estimated maximal effect (E_{max}) and buprenorphine concentration at the theoretical effect site exerting a half-maximal effect (IC_{50}) were 82.9 % and 0.63 ng/mL, respectively. The model analysis revealed that buprenorphine was very potent in producing miotic effect. The population PK /PD modeling analysis demonstrated that pupillary constriction was induced after administration of buprenorphine. The pupillary diameter was associated with predicted buprenorphine concentration at a hypothetical effect compartment. The IC_{50} of BUP was not significantly different during pregnancy and postpartum in the PK/PD model analysis of pupillary diameter. The findings from

the modeling analysis were in accordance with the pharmacological mechanism of buprenorphine as a mu-opioid agonist (Chapter 7).

To conclude, an integration of small cohort of clinical studies, and model-based strategies such as PBPK and population PK/PD can facilitate clinical decision making in optimize doing of medications used in pregnant women.

Primary contribution of the current work

- A simple, selective, rapid and sensitive UPLC-MS/MS assay to simultaneously quantify plasma concentrations of buprenorphine, norbuprenorphine, buprenorphine glucuronide and norbuprenorphine glucuronide using a small volume of human plasma was developed and validated. This methodology was applied in a BUP pk study in pregnant women.
- Analysis of BUP metabolite to BUP parent molar concentration ratio demonstrated alterations in CYP- and UGT- mediated metabolic pathways during pregnancy.
- Physiologically-based pharmacokinetic models of IV and SL BUP were developed and validated using 14 independent BUP PK studies in non-pregnant subjects.
- A BUP SL PBPK pregnancy model was validated with our two in-house prospective clinical trials in pregnant women at three trimesters and postpartum.
- A population PK model was developed and the model –based analysis indicated the apparent clearance of buprenorphine to be increased 1.64-folds during pregnancy compared to the postpartum period.
- In the PK/PD analysis, we observed significantly lower plasma exposure of BUP and significantly higher AUC of COWS score during a dosing interval of BUP during

pregnancy compared to the values during the postpartum period under the current dose regimen.

- A population PK/PD model was developed to describe the time course of the changes in pupillary diameter with BUP concentrations. The IC_{50} of BUP was not significantly different during pregnant and postpartum in the PK/PD model analysis of pupillary diameter.

Clinical implications

- The clinical study, PBPK and PopPK modeling have identified that pregnancy is associated with increased BUP apparent clearance and decreased BUP exposure.
- To optimize BUP dosing in pregnant women higher doses or more frequent dosing are warranted (eg. double dose or TID, QID dosing).
- PBPK and PoPPK modeling and simulation can be used to predict drug exposure and response during pregnancy.

7.2 Limitations

- A relatively small number of patients (4) were enrolled during the 1st-trimester in the clinical studies. The time course of buprenorphine in the 1st trimester obtained from the 4 patients may not represent the general population in the 1st trimester. Additional patients are being enrolled in the 1st trimester in an ongoing clinical study and this will be used for further validation.
- Nausea is a common problem in pregnant women. Patients in the two clinical studies broke the SL tablet into smaller pieces to reduce the nausea and discomfort of holding the medication under the tongue. Breaking up a tablet decreases the disintegration and dissolution time, and can lead to a faster drug absorption. This may be a reason for the high variability observed in T_{max} in the clinical studies.
- In the analysis of the alterations of CYP- and UGT-mediated metabolism of buprenorphine, we observed greater mean ratios of AUC of metabolites to parent in both metabolic pathways. However, the ratios of AUC of metabolites to parent were decreased in some patients during pregnancy compared to the ratios at postpartum, especially in the CYP-mediated N-demethylation pathway. The decreases in the AUC ratios suggests that there is a decrease in the activity of that metabolizing pathway in these patients, which is not in agreement with observations in other studies. The changes in the directions of enzyme activities in these patients may be due to other factors such as altered compensatory effect of other metabolic pathways or potential drug interactions. In the clinical studies, we

did not analyze genotypes of all of the drug metabolizing enzymes that are responsible for the metabolism of buprenorphine and its impact is currently not clear. Genotypes of the drug metabolizing enzymes in the patients are being investigated in an ongoing study.

- The primary challenge in building a comprehensive fetal compartment is the limited information on the fetal physiological development and drug exposure in the fetus during pregnancy. In SimCyp®, the fetal-placental unit is considered as a combined compartment in pregnant women. The fetal-placental unit is simplified as a homogenous organ with the assumption that the components of the unit have similar characteristics of blood perfusion and drug partitioning. So we were not able to estimate BUP exposure in the fetus in this study.
- In the development of PBPK model, the brain was modelled as a perfusion-limited compartment due to the lack of information regarding active and passive transport of buprenorphine in the brain. In the PBPK model of BUP, the availability of μ -opioid receptor was assumed to have direct relationship with the plasma concentration of buprenorphine. The biological processes such as biophase distribution, drug-receptor interaction and signal transduction were not included in the simulation.
- In the clinical study 1, pupillary diameters were only measured at trough, 4, 8 and 12 hours after a dose of buprenorphine. In the second clinical study, the dosing frequencies of buprenorphine were three times a day or four times a day in most of the study participants. Only limited pupillary diameter sizes were collected at 10 and 12 hours after a BUP dose, resulted in inadequate description of the pupillary

diameter after 10 hours following a buprenorphine dose in the PK/PD model. In addition, due to patient safety concerns we were unable to collect the true baseline pupillary diameter when there was no buprenorphine in patients. The baseline pupillary diameters were estimated by the model, which were predictions of the pupil diameter sizes when there was no buprenorphine in the patient.

7.3 Future Directions

- Impact of plasma protein in binding changes: The unbound drug concentration is determined by the unbound fraction of drug and the total drug concentration in plasma. The decrease in the total concentration of buprenorphine and increase in the unbound fraction of buprenorphine may result in no changes in the unbound plasma concentration of buprenorphine during pregnancy. As only unbound drug is able to cross blood brain barrier, unbound buprenorphine concentration in the brain may not be different during pregnancy compared to the levels in non-pregnant women. We will measure the unbound fraction of buprenorphine in plasma to evaluate the changes of unbound concentration of BUP in pregnant women. Animals studied are being performed to evaluate the effect of pregnancy on brain distribution of BUP and its metabolites.
- Exposures at various trimesters: Currently, limited numbers of pregnant women have been studied. A clinical BUP PK/PD study in pregnant women is ongoing. More patients will be enrolled in the clinical study, especially patients in the 1st trimester. These data will be

added to the model to further validate and evaluate application of PBPK model at various trimesters in pregnancy.

- Fetal exposure: The present PBPK model has been developed to predict the plasma concentration of BUP in the mother. A PBPK model will be developed to predict BUP exposure in the fetus to understand the association between fetal BUP exposure and NAS.
- Metabolic pathways in pregnancy: The BUP metabolite to parent ratio appears to be altered perhaps due to the alteration of CYP- and UGT- mediated pathway of BUP during pregnancy. With more patient enrolled in the current clinical study, we will develop a simultaneous BUP parent/metabolite PBPK and PopPK model to quantify the changes of CYP3A4 and UGTs mediated metabolic pathways to better understand the modulations of the activities of these enzymes in pregnancy.
- There was a general trend for an increase in N-demethylation and glucuronidation pathway in pregnancy. However, in a few subjects the $\frac{AUC\ N\text{-demethylated}\ BUP}{AUC\ BUP}$ decreased in pregnancy. The reason for this should be further evaluated. We will further study the alterations of the activities of CYP3A4 during pregnancy and postpartum in study patients by analyzing the changes in the metabolism of endogenous compound, the ratio of 4 β -hydroxycholesterol/ cholesterol.
- The enzymes responsible for metabolism of BUP (CYPs and UGTs) are known to be polymorphic. Genotypes of CYPs and UGTs in these patients will be determined. The impact of genotype on the magnitude and direction of change in exposure during pregnancy will be evaluated in future studies.

- The exact contributions of CYPs and UGTs to the metabolism of BUP are unknown. An in vitro study will be performed to evaluate simultaneous biotransformation of BUP through the two pathways in hepatocytes.
- Additional work of BUP PBPK model: to further validate BUP PBPK model in liver disease population and drug-drug interaction studies using clinical data; to develop a 4-compartment BUP brain PBPK model in rats and validate predicted BUP concentration in the brain in rats with BUP PK study in rats; to extrapolate the 4-compartment BUP brain PBPK model in rats to human and predict BUP concentration in the brain in human.
- Additional PK /PD analysis: Currently, only the primary PD effects (COWS score and pupillary diameter) of BUP have been evaluated in pregnant women. We will also evaluate the time course of the effect of buprenorphine on other physiological measurements such as hear rate, respiratory rate, blood pressure and galvanic skin temperature in the ongoing clinical studies.

A better understanding of BUP PK /PD will facilitate better treatment protocols for pregnant women.

Appendix A

Table 7-1 Physicochemical and pharmacokinetic parameters used to develop buprenorphine profile in
Simcyp®

Parameter	Value	Reference/Source
Physicochemical		
MW (g/mol)	467.64	Pubchem/ DrugBank
Log P _{o:w}	4.98	[70]
Compound type	Diprotic Base	
pKa1, pKa2	9.62, 8.31	[70]
B/P	0.55	[89]
f _u	0.03	[338]/ Parameter optimization
Absorption		
Absorption model	1 st order absorption model	
f _a	0.80	Parameter estimation tool
K _a (1/h)	2.34	Parameter estimation tool
Lag time (h)	0.7	Parameter estimation tool
Q _{gut} (L/h)	8.12	Predicted
f _{uGut}	1	User input
Permeability predicted via	PSA	
	PSA (Å):62.16	Pubchem/ DrugBank
	HBD: 2	Pubchem/ DrugBank
Distribution		
Distribution model	Full PBPK model	
Prediction method of V _{ss}	Method 1 (Corrected Poulin-Theil)	
Predicted V _{ss} (L/kg)	2.48	
Elimination		

Clearance type	Enzyme kinetics
In vitro metabolic system	Recombinant
CYP3A4	[268]
V_{max} (pmol/min/pmol of	10.4
K_m (μ M)	13.6
CYP2C8	[268]
V_{max} (pmol/min/pmol of isoform)	1.4
K_m (μ M)	12.4
UGT1A1	[281]
Cl_{int} (μ L/min/pmol of	0.0162
UGT1A3	[281]
Cl_{int} (μ L/min/pmol of	0.0155
UGT2B7	[281]
Cl_{int} (μ L/min/pmol of	0.0116

Abbreviations to Appendix A.1: MW: molecular weight; $\log P_{o:w}$: logarithm of the octanol to water partition coefficient, pKa: negative logarithm of the acid dissociation constant, B/P: blood to plasma partition coefficient; f_u : Plasma fraction unbound; PSA: polar surface area; HBD: number of hydrogen bond donors; V_{ss} : apparent volume of distribution at steady state; Cl_{int} : intrinsic clearance.

A.2

Table 7-2Key pharmacokinetic parameters of buprenorphine in non-pregnant subjects (range, or mean \pm SD)

PK parameter	Value	Reference
CL (L/h)	50-62.5	[74, 78, 87, 88]
Bioavailability of SL dose	36 \pm 13%	[78]
T_{max} (h)	0.75-1.5	[66, 69, 283]
C_{max} (ng/mL, mean \pm SD) following 8 mg single SL dose	2.88 \pm 1.14	[339]
AUC _{0-inf} (ng*h/mL, mean \pm SD) following 8 mg single SL dose	28.39 \pm 10.22	[339]

Abbreviations: CL: Clearance, T_{max} : Time to reach maximum concentration, C_{max} : Maximum

concentration, $AUC_{0-\infty}$: Area under plasma concentration-time curve from time 0 to infinite.

Appendix B Clinical Opioid Withdrawal Scale

Clinical Opiate Withdrawal Scale (COWS)

Flow-sheet for measuring symptoms over a period of time during buprenorphine induction.
 For each item, write in the number that best describes the patient's signs or symptom. Rate on just the apparent relationship to opiate withdrawal. For example, if heart rate is increased because the patient was jogging just prior to assessment, the increase pulse rate would not add to the score.

Subject ID# _ _ _ _ _ _ _ _ _ _ Date: _____ Buprenorphine induction: Enter scores at time zero, 30min after first dose, 2 h after first dose, etc. <div style="text-align: right;">Times: _____</div>				
Resting Pulse Rate: (record beats per minute) <i>Measured after patient is sitting or lying for one minute</i> 0 pulse rate 80 or below 1 pulse rate 81-100 2 pulse rate 101-120 4 pulse rate greater than 120				
Sweating: <i>over past ½ hour not accounted for by room temperature or patient activity.</i> 0 no report of chills or flushing 1 subjective report of chills or flushing 2 flushed or observable moistness on face 3 beads of sweat on brow or face 4 sweat streaming off face				
Restlessness <i>Observation during assessment</i> 0 able to sit still 1 reports difficulty sitting still, but is able to do so 3 frequent shifting or extraneous movements of legs/arms 5 Unable to sit still for more than a few seconds				
Pupil size 0 pupils pinned or normal size for room light 1 pupils possibly larger than normal for room light 2 pupils moderately dilated 5 pupils so dilated that only the rim of the iris is visible				
Bone or Joint aches <i>If patient was having pain previously, only the additional component attributed to opiates withdrawal is scored</i> 0 not present				

1 mild diffuse discomfort 2 patient reports severe diffuse aching of joints/ muscles 4 patient is rubbing joints or muscles and is unable to sit still because of discomfort				
Runny nose or tearing <i>Not accounted for by cold symptoms or allergies</i> 0 not present 1 nasal stuffiness or unusually moist eyes 2 nose running or tearing 4 nose constantly running or tears streaming down cheeks				
GI Upset: <i>over last ½ hour</i> 0 no GI symptoms 1 stomach cramps 2 nausea or loose stool 3 vomiting or diarrhea 5 Multiple episodes of diarrhea or vomiting				
Tremor <i>observation of outstretched hands</i> 0 No tremor 1 tremor can be felt, but not observed 2 slight tremor observable 4 gross tremor or muscle twitching				
Yawning <i>Observation during assessment</i> 0 no yawning 1 yawning once or twice during assessment 2 yawning three or more times during assessment 4 yawning several times/minute				
Anxiety or Irritability 0 none 1 patient reports increasing irritability or anxiousness 2 patient obviously irritable anxious 4 patient so irritable or				
Gooseflesh skin 0 skin is smooth 3 piloerection of skin can be felt or hairs standing up on arms 5 prominent piloerection				
Total scores with observer's initials				

Score:

5-12 = mild;

13-24 = moderate;

25-36 = moderately severe;

More than 36 = severe withdrawal

BIBLIOGRAPHY

1. Nahin, R.L., Estimates of pain prevalence and severity in adults: United States, 2012. *J Pain*, 2015. **16**(8): p. 769-80.
2. Stites, M., Observational pain scales in critically ill adults. *Crit Care Nurse*, 2013. **33**(3): p. 68-78.
3. Pasero, C., Pathophysiology of neuropathic pain. *Pain Manag Nurs*, 2004. **5**(4 Suppl 1): p. 3-8.
4. Schaible, H.G. and F. Richter, Pathophysiology of pain. *Langenbecks Arch Surg*, 2004. **389**(4): p. 237-43.
5. Vallejo, R., R.L. Barkin, and V.C. Wang, Pharmacology of opioids in the treatment of chronic pain syndromes. *Pain Physician*, 2011. **14**(4): p. E343-60.
6. Akil, H., et al., Endogenous opioids: biology and function. *Annu Rev Neurosci*, 1984. **7**: p. 223-55.
7. Ashburn, M.A. and P.S. Staats, Management of chronic pain. *Lancet*, 1999. **353**(9167): p. 1865-9.
8. Devlin, J.W., et al., Clinical Practice Guidelines for the Prevention and Management of Pain, Agitation/Sedation, Delirium, Immobility, and Sleep Disruption in Adult Patients in the ICU. *Crit Care Med*, 2018. **46**(9): p. e825-e873.
9. Bovill, J.G., Mechanisms of actions of opioids and non-steroidal anti-inflammatory drugs. *Eur J Anaesthesiol Suppl*, 1997. **15**: p. 9-15.
10. Cherny, N.I., Opioid analgesics: comparative features and prescribing guidelines. *Drugs*, 1996. **51**(5): p. 713-37.
11. Pasternak, G.W., Pharmacological mechanisms of opioid analgesics. *Clin Neuropharmacol*, 1993. **16**(1): p. 1-18.
12. Pathan, H. and J. Williams, Basic opioid pharmacology: an update. *Br J Pain*, 2012. **6**(1): p. 11-6.
13. Benyamin, R., et al., Opioid complications and side effects. *Pain Physician*, 2008. **11**(2 Suppl): p. S105-20.
14. Di Chiara, G. and R.A. North, Neurobiology of opiate abuse. *Trends Pharmacol Sci*, 1992. **13**(5): p. 185-93.

15. Katz, N., et al., Tampering with prescription opioids: nature and extent of the problem, health consequences, and solutions. *Am J Drug Alcohol Abuse*, 2011. **37**(4): p. 205-17.
16. Koob, G.F., *Neurobiology of Addiction. Focus*, 2011. **IV**(1): p. 55-65.
17. Kosten, T.R. and T.P. George, The neurobiology of opioid dependence: implications for treatment. *Sci Pract Perspect*, 2002. **1**(1): p. 13-20.
18. Harduar Morano, L., A.L. Steege, and S.E. Luckhaupt, Occupational Patterns in Unintentional and Undetermined Drug-Involved and Opioid-Involved Overdose Deaths - United States, 2007-2012. *MMWR Morb Mortal Wkly Rep*, 2018. **67**(33): p. 925-930.
19. Rudd, R.A., et al., Increases in Drug and Opioid-Involved Overdose Deaths - United States, 2010-2015. *MMWR Morb Mortal Wkly Rep*, 2016. **65**(50-51): p. 1445-1452.
20. Centers for Disease, C. and Prevention, Vital signs: overdoses of prescription opioid pain relievers---United States, 1999--2008. *MMWR Morb Mortal Wkly Rep*, 2011. **60**(43): p. 1487-92.
21. and P.S. Lawrence Scholl, Mbabazi Kariisa, Nana Wilson, Grant Baldwin, Drug and Opioid-Involved Overdose Deaths — United States, 2013–2017. *MMWR Morb Mortal Wkly Rep*, 2018. **67**.
22. Bart, G., Maintenance medication for opiate addiction: the foundation of recovery. *J Addict Dis*, 2012. **31**(3): p. 207-25.
23. Dole, V.P. and M. Nyswander, A Medical Treatment for Diacetylmorphine (Heroin) Addiction. A Clinical Trial with Methadone Hydrochloride. *JAMA*, 1965. **193**: p. 646-50.
24. Barta, W.D., et al., Craving and self-efficacy in the first five weeks of methadone maintenance therapy: a daily process study. *J Stud Alcohol Drugs*, 2009. **70**(5): p. 735-40.
25. Johansson, B.A., M. Berglund, and A. Lindgren, Efficacy of maintenance treatment with methadone for opioid dependence: a meta-analytical study. *Nord J Psychiatry*, 2007. **61**(4): p. 288-95.
26. Marsch, L.A., The efficacy of methadone maintenance interventions in reducing illicit opiate use, HIV risk behavior and criminality: a meta-analysis. *Addiction*, 1998. **93**(4): p. 515-32.
27. Mattick, R.P., et al., Methadone maintenance therapy versus no opioid replacement therapy for opioid dependence. *Cochrane Database Syst Rev*, 2009(3): p. CD002209.
28. Sees, K.L., et al., Methadone maintenance vs 180-day psychosocially enriched detoxification for treatment of opioid dependence: a randomized controlled trial. *JAMA*, 2000. **283**(10): p. 1303-10.

29. Jasinski, D.R. and K.L. Preston, Comparison of intravenously administered methadone, morphine and heroin. *Drug Alcohol Depend*, 1986. **17**(4): p. 301-10.
30. Kristensen, K., C.B. Christensen, and L.L. Christrup, The mu1, mu2, delta, kappa opioid receptor binding profiles of methadone stereoisomers and morphine. *Life Sci*, 1995. **56**(2): p. PL45-50.
31. Stotts, A.L., C.L. Dodrill, and T.R. Kosten, Opioid dependence treatment: options in pharmacotherapy. *Expert Opin Pharmacother*, 2009. **10**(11): p. 1727-40.
32. Ward, J., W. Hall, and R.P. Mattick, Role of maintenance treatment in opioid dependence. *Lancet*, 1999. **353**(9148): p. 221-6.
33. Shi, J., et al., Long-term methadone maintenance reduces protracted symptoms of heroin abstinence and cue-induced craving in Chinese heroin abusers. *Pharmacol Biochem Behav*, 2007. **87**(1): p. 141-5.
34. Gourlay, G.K., D.A. Cherry, and M.J. Cousins, A comparative study of the efficacy and pharmacokinetics of oral methadone and morphine in the treatment of severe pain in patients with cancer. *Pain*, 1986. **25**(3): p. 297-312.
35. Kristensen, K., et al., Stereoselective pharmacokinetics of methadone in chronic pain patients. *Ther Drug Monit*, 1996. **18**(3): p. 221-7.
36. Meresaar, U., et al., Single dose pharmacokinetics and bioavailability of methadone in man studied with a stable isotope method. *Eur J Clin Pharmacol*, 1981. **20**(6): p. 473-8.
37. Oda, Y. and E.D. Kharasch, Metabolism of methadone and levo-alpha-acetylmethadol (LAAM) by human intestinal cytochrome P450 3A4 (CYP3A4): potential contribution of intestinal metabolism to presystemic clearance and bioactivation. *J Pharmacol Exp Ther*, 2001. **298**(3): p. 1021-32.
38. Bouer, R., et al., The roles of P-glycoprotein and intracellular metabolism in the intestinal absorption of methadone: in vitro studies using the rat everted intestinal sac. *Fundam Clin Pharmacol*, 1999. **13**(4): p. 494-500.
39. Kharasch, E.D., C. Hoffer, and D. Whittington, The effect of quinidine, used as a probe for the involvement of P-glycoprotein, on the intestinal absorption and pharmacodynamics of methadone. *Br J Clin Pharmacol*, 2004. **57**(5): p. 600-10.
40. Nilsson, M.I., U. Meresaar, and E. Anggard, Clinical pharmacokinetics of methadone. *Acta Anaesthesiol Scand Suppl*, 1982. **74**: p. 66-9.
41. Eap, C.B., T. Buclin, and P. Baumann, Interindividual variability of the clinical pharmacokinetics of methadone: implications for the treatment of opioid dependence. *Clin Pharmacokinet*, 2002. **41**(14): p. 1153-93.

42. Kharasch, E.D., et al., Methadone metabolism and clearance are induced by nelfinavir despite inhibition of cytochrome P4503A (CYP3A) activity. *Drug Alcohol Depend*, 2009. **101**(3): p. 158-68.
43. Eap, C.B., C. Cuendet, and P. Baumann, Binding of d-methadone, l-methadone, and dl-methadone to proteins in plasma of healthy volunteers: role of the variants of alpha 1-acid glycoprotein. *Clin Pharmacol Ther*, 1990. **47**(3): p. 338-46.
44. Garrido, M.J., et al., Alpha 1-acid glycoprotein (AAG) and serum protein binding of methadone in heroin addicts with abstinence syndrome. *Int J Clin Pharmacol Ther*, 2000. **38**(1): p. 35-40.
45. Kharasch, E.D., et al., Methadone pharmacokinetics are independent of cytochrome P4503A (CYP3A) activity and gastrointestinal drug transport: insights from methadone interactions with ritonavir/indinavir. *Anesthesiology*, 2009. **110**(3): p. 660-72.
46. Sullivan, H.R. and S.L. Due, Urinary metabolites of dl-methadone in maintenance subjects. *J Med Chem*, 1973. **16**(8): p. 909-13.
47. Totah, R.A., et al., Role of CYP2B6 in stereoselective human methadone metabolism. *Anesthesiology*, 2008. **108**(3): p. 363-74.
48. Bellward, G.D., et al., Methadone maintenance: effect of urinary pH on renal clearance in chronic high and low doses. *Clin Pharmacol Ther*, 1977. **22**(1): p. 92-9.
49. Inturrisi, C.E. and K. Verebely, Disposition of methadone in man after a single oral dose. *Clin Pharmacol Ther*, 1972. **13**(6): p. 923-30.
50. Billings, R.E., R.E. McMahon, and D.A. Blake, 1-Acetylmethadol (LAM) treatment of opiate dependence: plasma and urine levels of two pharmacologically active metabolites, 1974. *NIDA Res Monogr*, 1976(8): p. 54.
51. Henderson, G.L., B.K. Wilson, and D.H. Lau, Plasma l-alpha-Acetylmethadol (LAAM) after acute and chronic administration. *Clin Pharmacol Ther*, 1977. **21**(1): p. 16-25.
52. Walsh, S.L., et al., Intravenous and oral l-alpha-acetylmethadol: pharmacodynamics and pharmacokinetics in humans. *J Pharmacol Exp Ther*, 1998. **285**(1): p. 71-82.
53. Anglin, M.D., et al., Levo-alpha-acetylmethadol (LAAM) versus methadone maintenance: 1-year treatment retention, outcomes and status. *Addiction*, 2007. **102**(9): p. 1432-42.
54. Longshore, D., et al., Levo-alpha-acetylmethadol (LAAM) versus methadone: treatment retention and opiate use. *Addiction*, 2005. **100**(8): p. 1131-9.
55. Ritter, A.J., et al., A randomized trial comparing levo-alpha acetylmethadol with methadone maintenance for patients in primary care settings in Australia. *Addiction*, 2003. **98**(11): p. 1605-13.

56. Whysner, J.A. and G.L. Levine, Phase III clinical study of LAAM: report of current status and analysis of early terminations. *NIDA Res Monogr*, 1978(19): p. 277-90.
57. Wolstein, J., et al., A randomized, open-label trial comparing methadone and Levo-Alpha-Acetylmethadol (LAAM) in maintenance treatment of opioid addiction. *Pharmacopsychiatry*, 2009. **42**(1): p. 1-8.
58. Wieneke, H., et al., Levo-alpha-acetylmethadol (LAAM) induced QTc-prolongation - results from a controlled clinical trial. *Eur J Med Res*, 2009. **14**(1): p. 7-12.
59. Selley, D.E., et al., mu-Opioid receptor-stimulated guanosine-5'-O-(gamma-thio)-triphosphate binding in rat thalamus and cultured cell lines: signal transduction mechanisms underlying agonist efficacy. *Mol Pharmacol*, 1997. **51**(1): p. 87-96.
60. Selley, D.E., Q. Liu, and S.R. Childers, Signal transduction correlates of mu opioid agonist intrinsic efficacy: receptor-stimulated [35S]GTP gamma S binding in mMOR-CHO cells and rat thalamus. *J Pharmacol Exp Ther*, 1998. **285**(2): p. 496-505.
61. Dum, J.E. and A. Herz, In vivo receptor binding of the opiate partial agonist, buprenorphine, correlated with its agonistic and antagonistic actions. *Br J Pharmacol*, 1981. **74**(3): p. 627-33.
62. Walsh, S.L., et al., Clinical pharmacology of buprenorphine: ceiling effects at high doses. *Clin Pharmacol Ther*, 1994. **55**(5): p. 569-80.
63. Toll, L., et al., Standard binding and functional assays related to medications development division testing for potential cocaine and opiate narcotic treatment medications. *NIDA Res Monogr*, 1998. **178**: p. 440-66.
64. Huang, P., et al., Comparison of pharmacological activities of buprenorphine and norbuprenorphine: norbuprenorphine is a potent opioid agonist. *J Pharmacol Exp Ther*, 2001. **297**(2): p. 688-95.
65. Brewster, D., M.J. Humphrey, and M.A. McLeavy, The systemic bioavailability of buprenorphine by various routes of administration. *J Pharm Pharmacol*, 1981. **33**(8): p. 500-6.
66. Ciraulo, D.A., et al., Pharmacokinetics and pharmacodynamics of multiple sublingual buprenorphine tablets in dose-escalation trials. *J Clin Pharmacol*, 2006. **46**(2): p. 179-92.
67. Kuhlman, J.J., Jr., et al., Human pharmacokinetics of intravenous, sublingual, and buccal buprenorphine. *J Anal Toxicol*, 1996. **20**(6): p. 369-78.
68. Bullingham, R.E., et al., Sublingual buprenorphine used postoperatively: ten hour plasma drug concentration analysis. *Br J Clin Pharmacol*, 1982. **13**(5): p. 665-73.

69. Harris, D.S., et al., Pharmacokinetics and subjective effects of sublingual buprenorphine, alone or in combination with naloxone: lack of dose proportionality. *Clin Pharmacokinet*, 2004. **43**(5): p. 329-40.
70. Avdeef, A., et al., Octanol-, chloroform-, and propylene glycol dipelargonat-water partitioning of morphine-6-glucuronide and other related opiates. *J Med Chem*, 1996. **39**(22): p. 4377-81.
71. Weinberg, D.S., et al., Sublingual absorption of selected opioid analgesics. *Clin Pharmacol Ther*, 1988. **44**(3): p. 335-42.
72. Suboxone®, Monograph.
73. Belbuca®, Monograph.
74. Bai, S.A., Q. Xiang, and A. Finn, Evaluation of the Pharmacokinetics of Single- and Multiple-dose Buprenorphine Buccal Film in Healthy Volunteers. *Clin Ther*, 2016. **38**(2): p. 358-69.
75. Buprenex®, Monograph.
76. Butrans®, Monograph.
77. Bunavail®, Monograph.
78. Mendelson, J., et al., Bioavailability of sublingual buprenorphine. *J Clin Pharmacol*, 1997. **37**(1): p. 31-7.
79. Subtex®, Monograph.
80. Fischer, A., M. Jonsson, and P. Hjelmstrom, Pharmaceutical and pharmacokinetic characterization of a novel sublingual buprenorphine/naloxone tablet formulation in healthy volunteers. *Drug Dev Ind Pharm*, 2015. **41**(1): p. 79-84.
81. Jonsson, M., G. Mundin, and M. Sumner, Pharmacokinetic and pharmaceutical properties of a novel buprenorphine/naloxone sublingual tablet for opioid substitution therapy versus conventional buprenorphine/naloxone sublingual tablet in healthy volunteers. *Eur J Pharm Sci*, 2018. **122**: p. 125-133.
82. Zubsolv®, Monograph.
83. Cassipa®, Monograph.
84. White, J., et al., Open-label dose-finding trial of buprenorphine implants (Probuphine) for treatment of heroin dependence. *Drug Alcohol Depend*, 2009. **103**(1-2): p. 37-43.
85. Probuphine®, Monograph.
86. Sublocade®, Monograph.

87. Huestis, M.A., et al., Intravenous buprenorphine and norbuprenorphine pharmacokinetics in humans. *Drug Alcohol Depend*, 2013. **131**(3): p. 258-62.
88. Harris, D.S., et al., Buprenorphine and naloxone co-administration in opiate-dependent patients stabilized on sublingual buprenorphine. *Drug Alcohol Depend*, 2000. **61**(1): p. 85-94.
89. Mistry, M. and J.B. Houston, Glucuronidation in vitro and in vivo. Comparison of intestinal and hepatic conjugation of morphine, naloxone, and buprenorphine. *Drug Metab Dispos*, 1987. **15**(5): p. 710-7.
90. Iribarne, C., et al., Involvement of cytochrome P450 3A4 in N-dealkylation of buprenorphine in human liver microsomes. *Life Sci*, 1997. **60**(22): p. 1953-64.
91. Kobayashi, K., et al., Human buprenorphine N-dealkylation is catalyzed by cytochrome P450 3A4. *Drug Metab Dispos*, 1998. **26**(8): p. 818-21.
92. van Niel, J.C., J. Schneider, and T.M. Tzschentke, Efficacy of Full micro-Opioid Receptor Agonists is not Impaired by Concomitant Buprenorphine or Mixed Opioid Agonists/Antagonists - Preclinical and Clinical Evidence. *Drug Res (Stuttg)*, 2016. **66**(11): p. 562-570.
93. Brown, S.M., et al., P-glycoprotein is a major determinant of norbuprenorphine brain exposure and antinociception. *J Pharmacol Exp Ther*, 2012. **343**(1): p. 53-61.
94. Yassen, A., et al., Pharmacokinetic-pharmacodynamic modeling of the respiratory depressant effect of norbuprenorphine in rats. *J Pharmacol Exp Ther*, 2007. **321**(2): p. 598-607.
95. Brown, S.M., et al., Buprenorphine metabolites, buprenorphine-3-glucuronide and norbuprenorphine-3-glucuronide, are biologically active. *Anesthesiology*, 2011. **115**(6): p. 1251-60.
96. Everhart, E.T., et al., The mass balance of buprenorphine in humans. *Clinical Pharmacology & Therapeutics*, 1999. **65**(2): p. 152-152.
97. McLeod, R.L., et al., Nociceptin inhibits cough in the guinea-pig by activation of ORL(1) receptors. *Br J Pharmacol*, 2001. **132**(6): p. 1175-8.
98. Gonzalez, J.P. and R.N. Brogden, Naltrexone. A review of its pharmacodynamic and pharmacokinetic properties and therapeutic efficacy in the management of opioid dependence. *Drugs*, 1988. **35**(3): p. 192-213.
99. Resnick, R.B., et al., Naloxone-precipitated withdrawal: a method for rapid induction onto naltrexone. *Clin Pharmacol Ther*, 1977. **21**(4): p. 409-13.
100. Valentino, R.J., et al., Receptor binding, antagonist, and withdrawal precipitating properties of opiate antagonists. *Life Sci*, 1983. **32**(25): p. 2887-96.

101. Rothenberg, J.L., et al., Behavioral naltrexone therapy: an integrated treatment for opiate dependence. *J Subst Abuse Treat*, 2002. **23**(4): p. 351-60.
102. REVIA®, Monograph.
103. Vivtrol®, Monograph.
104. Li, J.X., L.R. McMahon, and C.P. France, Comparison of naltrexone, 6alpha-naltrexol, and 6beta-naltrexol in morphine-dependent and in nondependent rhesus monkeys. *Psychopharmacology (Berl)*, 2008. **195**(4): p. 479-86.
105. Sirohi, S., et al., The relative potency of inverse opioid agonists and a neutral opioid antagonist in precipitated withdrawal and antagonism of analgesia and toxicity. *J Pharmacol Exp Ther*, 2009. **330**(2): p. 513-9.
106. Ferrari, A., et al., Serum time course of naltrexone and 6 beta-naltrexol levels during long-term treatment in drug addicts. *Drug Alcohol Depend*, 1998. **52**(3): p. 211-20.
107. Wall, M.E., et al., Naltrexone disposition in man after subcutaneous administration. *Drug Metab Dispos*, 1984. **12**(6): p. 677-82.
108. Raynor, K., et al., Pharmacological characterization of the cloned kappa-, delta-, and mu-opioid receptors. *Mol Pharmacol*, 1994. **45**(2): p. 330-4.
109. Gan, T.J., et al., Opioid-sparing effects of a low-dose infusion of naloxone in patient-administered morphine sulfate. *Anesthesiology*, 1997. **87**(5): p. 1075-81.
110. Lewanowitsch, T., J.H. Miller, and R.J. Irvine, Reversal of morphine, methadone and heroin induced effects in mice by naloxone methiodide. *Life Sci*, 2006. **78**(7): p. 682-8.
111. Berkowitz, B.A., The relationship of pharmacokinetics to pharmacological activity: morphine, methadone and naloxone. *Clin Pharmacokinet*, 1976. **1**(3): p. 219-30.
112. Dowling, J., et al., Population pharmacokinetics of intravenous, intramuscular, and intranasal naloxone in human volunteers. *Ther Drug Monit*, 2008. **30**(4): p. 490-6.
113. Chiang, C.N. and R.L. Hawks, Pharmacokinetics of the combination tablet of buprenorphine and naloxone. *Drug Alcohol Depend*, 2003. **70**(2 Suppl): p. S39-47.
114. Gish, E.C., et al., Lofexidine, an α_2 -receptor agonist for opioid detoxification. *Ann Pharmacother*, 2010. **44**(2): p. 343-51.
115. Strang, J., J. Bearn, and M. Gossop, Lofexidine for opiate detoxification: review of recent randomised and open controlled trials. *Am J Addict*, 1999. **8**(4): p. 337-48.
116. Al Ghananeem, A.M., et al., Urine and plasma pharmacokinetics of lofexidine after oral delivery in opiate-dependent patients. *Am J Drug Alcohol Abuse*, 2009. **35**(5): p. 311-5.

117. Midgley, I., et al., Biotransformation of lofexidine in humans. *Xenobiotica*, 1983. **13**(2): p. 87-95.
118. Schuckit, M.A., Treatment of Opioid-Use Disorders. *N Engl J Med*, 2016. **375**(4): p. 357-68.
119. Cheung, K.L. and R.A. Lafayette, Renal physiology of pregnancy. *Adv Chronic Kidney Dis*, 2013. **20**(3): p. 209-14.
120. Desoye, G., et al., Correlation of hormones with lipid and lipoprotein levels during normal pregnancy and postpartum. *J Clin Endocrinol Metab*, 1987. **64**(4): p. 704-12.
121. Glinoe, D., The regulation of thyroid function in pregnancy: pathways of endocrine adaptation from physiology to pathology. *Endocr Rev*, 1997. **18**(3): p. 404-33.
122. Wang, Y. and S. Zhao, in *Vascular Biology of the Placenta*. 2010: San Rafael (CA).
123. Dickey, R.P. and J.F. Hower, Ultrasonographic features of uterine blood flow during the first 16 weeks of pregnancy. *Hum Reprod*, 1995. **10**(9): p. 2448-52.
124. Hunter, S. and S.C. Robson, Adaptation of the maternal heart in pregnancy. *Br Heart J*, 1992. **68**(6): p. 540-3.
125. Feghali, M., R. Venkataramanan, and S. Caritis, Pharmacokinetics of drugs in pregnancy. *Semin Perinatol*, 2015. **39**(7): p. 512-9.
126. Nakai, A., et al., Assessment of the hepatic arterial and portal venous blood flows during pregnancy with Doppler ultrasonography. *Arch Gynecol Obstet*, 2002. **266**(1): p. 25-9.
127. Dunlop, W., Serial changes in renal haemodynamics during normal human pregnancy. *Br J Obstet Gynaecol*, 1981. **88**(1): p. 1-9.
128. Griffiths, S.K. and J.P. Campbell, Placental structure, function and drug transfer. *Continuing Education in Anaesthesia Critical Care & Pain*, 2015. **15**(2): p. 84-89.
129. Tetro, N., et al., The Placental Barrier: the Gate and the Fate in Drug Distribution. *Pharm Res*, 2018. **35**(4): p. 71.
130. Staud, F., L. Cerveny, and M. Ceckova, Pharmacotherapy in pregnancy; effect of ABC and SLC transporters on drug transport across the placenta and fetal drug exposure. *J Drug Target*, 2012. **20**(9): p. 736-63.
131. Collier, A.C., et al., Metabolizing enzyme localization and activities in the first trimester human placenta: the effect of maternal and gestational age, smoking and alcohol consumption. *Hum Reprod*, 2002. **17**(10): p. 2564-72.

132. Pasanen, M., et al., Intrahepatic cholestasis of pregnancy impairs the activities of human placental xenobiotic and steroid metabolizing enzymes in vitro. *Placenta*, 1997. **18**(1): p. 37-41.
133. Nelson, D.R., et al., The P450 superfamily: update on new sequences, gene mapping, accession numbers, early trivial names of enzymes, and nomenclature. *DNA Cell Biol*, 1993. **12**(1): p. 1-51.
134. Syme, M.R., J.W. Paxton, and J.A. Keelan, Drug transfer and metabolism by the human placenta. *Clin Pharmacokinet*, 2004. **43**(8): p. 487-514.
135. Hakkola, J., et al., Xenobiotic-metabolizing cytochrome P450 enzymes in the human fetoplacental unit: role in intrauterine toxicity. *Crit Rev Toxicol*, 1998. **28**(1): p. 35-72.
136. Fokina, V.M., et al., Transplacental transfer and metabolism of buprenorphine in preterm human placenta. *Am J Perinatol*, 2011. **28**(1): p. 25-32.
137. Peck, T.M. and F. Arias, Hematologic changes associated with pregnancy. *Clin Obstet Gynecol*, 1979. **22**(4): p. 785-98.
138. Pitkin, R.M., Nutritional support in obstetrics and gynecology. *Clin Obstet Gynecol*, 1976. **19**(3): p. 489-513.
139. Abbassi-Ghanavati, M., L.G. Greer, and F.G. Cunningham, Pregnancy and laboratory studies: a reference table for clinicians. *Obstet Gynecol*, 2009. **114**(6): p. 1326-31.
140. Abduljalil, K., et al., Anatomical, physiological and metabolic changes with gestational age during normal pregnancy: a database for parameters required in physiologically based pharmacokinetic modelling. *Clin Pharmacokinet*, 2012. **51**(6): p. 365-96.
141. Bacq, Y. and O. Zarka, [Liver in normal pregnancy]. *Gastroenterol Clin Biol*, 1994. **18**(8-9): p. 767-74.
142. Vanthiel, D.H. and J.S. Gavalier, Pregnancy-Associated Sex Steroids and Their Effects on the Liver. *Seminars in Liver Disease*, 1987. **7**(1): p. 1-7.
143. Bacq, Y., et al., Liver function tests in normal pregnancy: a prospective study of 103 pregnant women and 103 matched controls. *Hepatology*, 1996. **23**(5): p. 1030-4.
144. Cietak, K.A. and J.R. Newton, Serial quantitative maternal nephrosonography in pregnancy. *Br J Radiol*, 1985. **58**(689): p. 405-13.
145. Carlin, A. and Z. Alfirevic, Physiological changes of pregnancy and monitoring. *Best Pract Res Clin Obstet Gynaecol*, 2008. **22**(5): p. 801-23.
146. Davison, J.M., Renal transplantation and pregnancy. *Am J Kidney Dis*, 1987. **9**(4): p. 374-80.

147. Isoherranen, N. and K.E. Thummel, Drug metabolism and transport during pregnancy: how does drug disposition change during pregnancy and what are the mechanisms that cause such changes? *Drug Metab Dispos*, 2013. **41**(2): p. 256-62.
148. Zhao, Y., M.F. Hebert, and R. Venkataramanan, Basic obstetric pharmacology. *Semin Perinatol*, 2014. **38**(8): p. 475-86.
149. Stillwell, W., An introduction to biological membranes Composition, Structure and Function. 2016: Elsevier.
150. Szachowicz-Petelska, B., Z. Figaszewski, and W. Lewandowski, Mechanisms of transport across cell membranes of complexes contained in antitumour drugs. *Int J Pharm*, 2001. **222**(2): p. 169-82.
151. Yan, Q., Membrane transporters and drug development: relevance to pharmacogenomics, nutrigenomics, epigenetics, and systems biology. *Methods Mol Biol*, 2010. **637**: p. 1-21.
152. Keogh, J.P., Membrane transporters in drug development. *Adv Pharmacol*, 2012. **63**: p. 1-42.
153. International Transporter, C., et al., Membrane transporters in drug development. *Nat Rev Drug Discov*, 2010. **9**(3): p. 215-36.
154. Yi, S.Y., et al., A variant 2677A allele of the MDR1 gene affects fexofenadine disposition. *Clin Pharmacol Ther*, 2004. **76**(5): p. 418-27.
155. Brinkmann, U., Functional polymorphisms of the human multidrug resistance (MDR1) gene: correlation with P glycoprotein expression and activity in vivo. *Novartis Found Symp*, 2002. **243**: p. 207-10; discussion 210-2, 231-5.
156. Marks, C., The Portal Venous System. 1973: Thomas.
157. Hebert, M.F., et al., Effects of pregnancy on CYP3A and P-glycoprotein activities as measured by disposition of midazolam and digoxin: a University of Washington specialized center of research study. *Clin Pharmacol Ther*, 2008. **84**(2): p. 248-53.
158. Jeong, H., Altered drug metabolism during pregnancy: hormonal regulation of drug-metabolizing enzymes. *Expert Opin Drug Metab Toxicol*, 2010. **6**(6): p. 689-99.
159. Conney, A.H., Pharmacological implications of microsomal enzyme induction. *Pharmacol Rev*, 1967. **19**(3): p. 317-66.
160. Eyal, S., et al., Pharmacokinetics of metformin during pregnancy. *Drug Metab Dispos*, 2010. **38**(5): p. 833-40.
161. Mazzucchelli, I., et al., Changes in the disposition of oxcarbazepine and its metabolites during pregnancy and the puerperium. *Epilepsia*, 2006. **47**(3): p. 504-9.

162. Pillai, V.C., et al., Population pharmacokinetics of oseltamivir in non-pregnant and pregnant women. *Br J Clin Pharmacol*, 2015. **80**(5): p. 1042-50.
163. Westin, A.A., et al., Serum concentration/dose ratio of levetiracetam before, during and after pregnancy. *Seizure*, 2008. **17**(2): p. 192-8.
164. Tsutsumi, K., et al., The effect of pregnancy on cytochrome P4501A2, xanthine oxidase, and N-acetyltransferase activities in humans. *Clin Pharmacol Ther*, 2001. **70**(2): p. 121-5.
165. Tracy, T.S., et al., Temporal changes in drug metabolism (CYP1A2, CYP2D6 and CYP3A Activity) during pregnancy. *Am J Obstet Gynecol*, 2005. **192**(2): p. 633-9.
166. McGready, R., et al., Pregnancy and use of oral contraceptives reduces the biotransformation of proguanil to cycloguanil. *Eur J Clin Pharmacol*, 2003. **59**(7): p. 553-7.
167. Hogstedt, S., et al., Pregnancy-induced increase in metoprolol metabolism. *Clin Pharmacol Ther*, 1985. **37**(6): p. 688-92.
168. Franco, V., et al., Changes in lamotrigine pharmacokinetics during pregnancy and the puerperium. *Ther Drug Monit*, 2008. **30**(4): p. 544-7.
169. Philipson, A., G. Stiernstedt, and M. Ehrnebo, Comparison of the pharmacokinetics of cephadrine and cefazolin in pregnant and non-pregnant women. *Clin Pharmacokinet*, 1987. **12**(2): p. 136-44.
170. Schou, M., A. Amdisen, and O.R. Steenstrup, Lithium and pregnancy. II. Hazards to women given lithium during pregnancy and delivery. *Br Med J*, 1973. **2**(5859): p. 137-8.
171. Hebert, M.F., et al., Effects of pregnancy on CYP3A and P-glycoprotein activities as measured by disposition of midazolam and digoxin: A University of Washington specialized center of research study. *Clinical Pharmacology & Therapeutics*, 2008. **84**(2): p. 248-253.
172. Amidon, G.L., et al., A theoretical basis for a biopharmaceutic drug classification: the correlation of in vitro drug product dissolution and in vivo bioavailability. *Pharm Res*, 1995. **12**(3): p. 413-20.
173. (CDER), U.S.D.o.H.a.H.S.F.a.D.A.C.f.D.E.a.R., Waiver of In Vivo Bioavailability and Bioequivalence Studies for Immediate-Release Solid Oral Dosage Forms Based on a Biopharmaceutics Classification System Guidance for Industry. 2017.
174. Benet, L.Z., The role of BCS (biopharmaceutics classification system) and BDDCS (biopharmaceutics drug disposition classification system) in drug development. *J Pharm Sci*, 2013. **102**(1): p. 34-42.

175. Wu, C.Y. and L.Z. Benet, Predicting drug disposition via application of BCS: transport/absorption/ elimination interplay and development of a biopharmaceutics drug disposition classification system. *Pharm Res*, 2005. **22**(1): p. 11-23.
176. Hassan, H.E., et al., Differential involvement of P-glycoprotein (ABCB1) in permeability, tissue distribution, and antinociceptive activity of methadone, buprenorphine, and diprenorphine: in vitro and in vivo evaluation. *J Pharm Sci*, 2009. **98**(12): p. 4928-40.
177. Wendell, A.D., Overview and epidemiology of substance abuse in pregnancy. *Clin Obstet Gynecol*, 2013. **56**(1): p. 91-6.
178. Jarlenski, M., et al., Trends in perception of risk of regular marijuana use among US pregnant and nonpregnant reproductive-aged women. *Am J Obstet Gynecol*, 2017. **217**(6): p. 705-707.
179. Patrick, S.W., et al., Increasing incidence and geographic distribution of neonatal abstinence syndrome: United States 2009 to 2012. *J Perinatol*, 2015. **35**(8): p. 650-5.
180. Maeda, A., et al., Opioid abuse and dependence during pregnancy: temporal trends and obstetrical outcomes. *Anesthesiology*, 2014. **121**(6): p. 1158-65.
181. Hudak, M.L., et al., Neonatal drug withdrawal. *Pediatrics*, 2012. **129**(2): p. e540-60.
182. Women, A.C.o.H.C.f.U. and M. American Society of Addiction, ACOG Committee Opinion No. 524: Opioid abuse, dependence, and addiction in pregnancy. *Obstet Gynecol*, 2012. **119**(5): p. 1070-6.
183. Dashe, J.S., et al., Opioid detoxification in pregnancy. *Obstet Gynecol*, 1998. **92**(5): p. 854-8.
184. Stewart, R.D., et al., The obstetrical and neonatal impact of maternal opioid detoxification in pregnancy. *Am J Obstet Gynecol*, 2013. **209**(3): p. 267 e1-5.
185. Terplan, M., The obstetric and neonatal impact of maternal opioid detoxification in pregnancy. *Am J Obstet Gynecol*, 2014. **210**(4): p. 375-376.
186. Terplan, M., et al., Opioid Detoxification During Pregnancy: A Systematic Review. *Obstet Gynecol*, 2018. **131**(5): p. 803-814.
187. Unger, A., V. Metz, and G. Fischer, Opioid dependent and pregnant: what are the best options for mothers and neonates? *Obstet Gynecol Int*, 2012. **2012**: p. 195954.
188. Jarvis, M.A., et al., Alterations in methadone metabolism during late pregnancy. *J Addict Dis*, 1999. **18**(4): p. 51-61.
189. Pond, S.M., et al., Altered methadone pharmacokinetics in methadone-maintained pregnant women. *J Pharmacol Exp Ther*, 1985. **233**(1): p. 1-6.

190. Wolff, K., et al., Changes to methadone clearance during pregnancy. *Eur J Clin Pharmacol*, 2005. **61**(10): p. 763-8.
191. Dryden, C., et al., Maternal methadone use in pregnancy: factors associated with the development of neonatal abstinence syndrome and implications for healthcare resources. *Bjog-an International Journal of Obstetrics and Gynaecology*, 2009. **116**(5): p. 665-671.
192. Albright, B., et al., Changes in methadone maintenance therapy during and after pregnancy. *J Subst Abuse Treat*, 2011. **41**(4): p. 347-53.
193. Fischer, G., Treatment of opioid dependence in pregnant women. *Addiction*, 2000. **95**(8): p. 1141-1144.
194. Jones, H.E., et al., Buprenorphine treatment of opioid-dependent pregnant women: a comprehensive review. *Addiction*, 2012. **107 Suppl 1**: p. 5-27.
195. Lacroix, I., et al., Buprenorphine versus methadone in pregnant opioid-dependent women: a prospective multicenter study. *Eur J Clin Pharmacol*, 2011. **67**(10): p. 1053-9.
196. Zedler, B.K., et al., Buprenorphine compared with methadone to treat pregnant women with opioid use disorder: a systematic review and meta-analysis of safety in the mother, fetus and child. *Addiction*, 2016. **111**(12): p. 2115-2128.
197. Nanovskaya, T., et al., Transplacental transfer and metabolism of buprenorphine. *J Pharmacol Exp Ther*, 2002. **300**(1): p. 26-33.
198. Sutter, M.B., L. Leeman, and A. Hsi, Neonatal opioid withdrawal syndrome. *Obstet Gynecol Clin North Am*, 2014. **41**(2): p. 317-34.
199. Mattick, R.P., et al., Buprenorphine maintenance versus placebo or methadone maintenance for opioid dependence. *Cochrane Database Syst Rev*, 2014(2): p. CD002207.
200. Lo-Ciganic, W.H., et al., Adherence trajectories of buprenorphine therapy among pregnant women in a large state Medicaid program in the United States. *Pharmacoepidemiol Drug Saf*, 2019. **28**(1): p. 80-89.
201. Bastian, J.R., et al., Dose-adjusted plasma concentrations of sublingual buprenorphine are lower during than after pregnancy. *Am J Obstet Gynecol*, 2017. **216**(1): p. 64 e1-64 e7.
202. Jones, H.E., et al., Neonatal abstinence syndrome after methadone or buprenorphine exposure. *N Engl J Med*, 2010. **363**(24): p. 2320-31.
203. Lejeune, C., et al., Prospective multicenter observational study of 260 infants born to 259 opiate-dependent mothers on methadone or high-dose buprenorphine substitution. *Drug Alcohol Depend*, 2006. **82**(3): p. 250-7.

204. Chandracharan NYaE. Anatomical and physiological changes in pregnancy and their implications in clinical practice. In: *Obstetric and Intrapartum Emergencies: A Practical Guide to Management*, e.E.C.U.P.
205. Horan C. *Obstetric Evidence based Guidelines*. 1st Editon. United Kingdom: Informa Healthcare.
206. Greenwald, M., et al., Buprenorphine duration of action: mu-opioid receptor availability and pharmacokinetic and behavioral indices. *Biol Psychiatry*, 2007. **61**(1): p. 101-10.
207. Tallarida, R.J., et al., Miosis and fluctuation in the rabbit pupil: effects of morphine and naloxone. *J Pharmacol Exp Ther*, 1977. **201**(3): p. 587-92.
208. Lee, H.K. and S.C. Wang, Mechanism of morphine-induced miosis in the dog. *J Pharmacol Exp Ther*, 1975. **192**(2): p. 415-31.
209. Murray, R.B., M.W. Adler, and A.D. Korczyn, The pupillary effects of opioids. *Life Sci*, 1983. **33**(6): p. 495-509.
210. Fliegert, F., B. Kurth, and K. Gohler, The effects of tramadol on static and dynamic pupillometry in healthy subjects--the relationship between pharmacodynamics, pharmacokinetics and CYP2D6 metaboliser status. *Eur J Clin Pharmacol*, 2005. **61**(4): p. 257-66.
211. Peacock, J.E., P.D. Henderson, and W.S. Nimmo, Changes in pupil diameter after oral administration of codeine. *Br J Anaesth*, 1988. **61**(5): p. 598-600.
212. Pickworth, W.B., et al., Intravenous buprenorphine reduces pupil size and the light reflex in humans. *Life Sci*, 1991. **49**(2): p. 129-38.
213. Pickworth, W.B., H. Lee, and P.J. Fudala, Buprenorphine-induced pupillary effects in human volunteers. *Life Sci*, 1990. **47**(14): p. 1269-77.
214. Pickworth, W.B., et al., Opiate-induced pupillary effects in humans. *Methods Find Exp Clin Pharmacol*, 1989. **11**(12): p. 759-63.
215. Weinhold, L.L. and G.E. Bigelow, Opioid miosis: effects of lighting intensity and monocular and binocular exposure. *Drug Alcohol Depend*, 1993. **31**(2): p. 177-81.
216. Barvais, L., et al., Effect site concentrations of remifentanil and pupil response to noxious stimulation. *Br J Anaesth*, 2003. **91**(3): p. 347-52.
217. Larson, M.D., et al., Alfentanil blocks reflex pupillary dilation in response to noxious stimulation but does not diminish the light reflex. *Anesthesiology*, 1997. **87**(4): p. 849-55.
218. Mathew, B.S., et al., A limited sampling strategy for tacrolimus in renal transplant patients. *Br J Clin Pharmacol*, 2008. **66**(4): p. 467-72.

219. Zhao, P., et al., Applications of physiologically based pharmacokinetic (PBPK) modeling and simulation during regulatory review. *Clinical Pharmacology & Therapeutics*, 2011. **89**(2): p. 259-267.
220. Ke, A.B., et al., Expansion of a PBPK model to predict disposition in pregnant women of drugs cleared via multiple CYP enzymes, including CYP2B6, CYP2C9 and CYP2C19. *Br J Clin Pharmacol*, 2014. **77**(3): p. 554-70.
221. Schaefer, N., et al., The feasibility of physiologically based pharmacokinetic modeling in forensic medicine illustrated by the example of morphine. *Int J Legal Med*, 2018. **132**(2): p. 415-424.
222. Willmann, S., et al., Risk to the breast-fed neonate from codeine treatment to the mother: a quantitative mechanistic modeling study. *Clin Pharmacol Ther*, 2009. **86**(6): p. 634-43.
223. Zhou, D., et al., Simulation and Prediction of the Drug-Drug Interaction Potential of Naloxegol by Physiologically Based Pharmacokinetic Modeling. *CPT Pharmacometrics Syst Pharmacol*, 2016. **5**(5): p. 250-7.
224. Fudala, P.J., et al., Office-based treatment of opiate addiction with a sublingual-tablet formulation of buprenorphine and naloxone. *N Engl J Med*, 2003. **349**(10): p. 949-58.
225. Concheiro, M., D.M. Shakleya, and M.A. Huestis, Simultaneous quantification of buprenorphine, norbuprenorphine, buprenorphine-glucuronide and norbuprenorphine-glucuronide in human umbilical cord by liquid chromatography tandem mass spectrometry. *Forensic Sci Int*, 2009. **188**(1-3): p. 144-51.
226. Kacinko, S.L., et al., Urinary excretion of buprenorphine, norbuprenorphine, buprenorphine-glucuronide, and norbuprenorphine-glucuronide in pregnant women receiving buprenorphine maintenance treatment. *Clin Chem*, 2009. **55**(6): p. 1177-87.
227. Kacinko, S.L., D.M. Shakleya, and M.A. Huestis, Validation and application of a method for the determination of buprenorphine, norbuprenorphine, and their glucuronide conjugates in human meconium. *Anal Chem*, 2008. **80**(1): p. 246-52.
228. Anand A. Joshi, N.V.M., Phillip M. Gerk, Simultaneous Quantitation of Buprenorphine and Its Metabolites Using LC-MS. spectroscopy, 2016. **14**(3): p. 15-19.
229. Poletini, A. and M.A. Huestis, Simultaneous determination of buprenorphine, norbuprenorphine, and buprenorphine-glucuronide in plasma by liquid chromatography-tandem mass spectrometry. *J Chromatogr B Biomed Sci Appl*, 2001. **754**(2): p. 447-59.
230. Luthi, G., et al., Buprenorphine and norbuprenorphine quantification in human plasma by simple protein precipitation and ultra-high performance liquid chromatography tandem mass spectrometry. *J Pharm Biomed Anal*, 2013. **77**: p. 1-8.

231. Joshi, A., et al., Quantitative determination of buprenorphine, naloxone and their metabolites in rat plasma using hydrophilic interaction liquid chromatography coupled with tandem mass spectrometry. *Biomed Chromatogr*, 2017. **31**(2).
232. Ceccato, A., et al., Sensitive determination of buprenorphine and its N-dealkylated metabolite norbuprenorphine in human plasma by liquid chromatography coupled to tandem mass spectrometry. *J Pharm Biomed Anal*, 2003. **32**(4-5): p. 619-31.
233. Murphy, C.M. and M.A. Huestis, Liquid chromatographic/electrospray ionization tandem mass spectrometric analysis for the quantification of buprenorphine, norbuprenorphine, buprenorphine-3-beta-D-glucuronide and norbuprenorphine-3-beta-D-glucuronide in human plasma. *J Mass Spectrom*, 2005. **40**(1): p. 70-4.
234. Regina, K.J. and E.D. Kharasch, High-sensitivity analysis of buprenorphine, norbuprenorphine, buprenorphine glucuronide, and norbuprenorphine glucuronide in plasma and urine by liquid chromatography-mass spectrometry. *J Chromatogr B Analyt Technol Biomed Life Sci*, 2013. **939**: p. 23-31.
235. Administration, U.F.a.D., Guidance for Industry – Bioanalytical Method Validation. US Department of Health and Human Services, Food and Drug Administration, Center for Drug Evaluation and Research and Center for Veterinary Medicine: Rockville, MD., 2013.
236. Compton, P., et al., Pharmacokinetics of buprenorphine: a comparison of sublingual tablet versus liquid after chronic dosing. *J Addict Med*, 2007. **1**(2): p. 88-95.
237. Greenwald, M.K., et al., Effects of buprenorphine maintenance dose on mu-opioid receptor availability, plasma concentrations, and antagonist blockade in heroin-dependent volunteers. *Neuropsychopharmacology*, 2003. **28**(11): p. 2000-9.
238. Concheiro, M., et al., Preliminary buprenorphine sublingual tablet pharmacokinetic data in plasma, oral fluid, and sweat during treatment of opioid-dependent pregnant women. *Ther Drug Monit*, 2011. **33**(5): p. 619-26.
239. Kuhlman, J.J., Jr., et al., Relationship of plasma buprenorphine and norbuprenorphine to withdrawal symptoms during dose induction, maintenance and withdrawal from sublingual buprenorphine. *Addiction*, 1998. **93**(4): p. 549-59.
240. Warner, M., et al., Drug poisoning deaths in the United States, 1980-2008. *NCHS data brief*, 2011(81): p. 1-8.
241. Control, C.f.D. and Prevention, Wide-ranging online data for epidemiologic research (WONDER). Atlanta, GA: CDC. National Center for Health Statistics, 2016.
242. Calcaterra, S., J. Glanz, and I.A. Binswanger, National trends in pharmaceutical opioid related overdose deaths compared to other substance related overdose deaths: 1999-2009. *Drug Alcohol Depend*, 2013. **131**(3): p. 263-70.

243. Control, C.f.D. and Prevention, CDC grand rounds: prescription drug overdoses-a US epidemic. *MMWR. Morbidity and mortality weekly report*, 2012. **61**(1): p. 10.
244. Akil, H., et al., Endogenous opioids: biology and function. *Annual review of neuroscience*, 1984. **7**(1): p. 223-255.
245. Barr, J., et al., Clinical practice guidelines for the management of pain, agitation, and delirium in adult patients in the intensive care unit: executive summary. *Am J Health Syst Pharm*, 2013. **70**(1): p. 53-58.
246. Ballantyne, J.C. and S.K. LaForge, Opioid dependence and addiction during opioid treatment of chronic pain. *Pain*, 2007. **129**(3): p. 235-255.
247. Chou, R., et al., Clinical guidelines for the use of chronic opioid therapy in chronic noncancer pain. *The Journal of Pain*, 2009. **10**(2): p. 113-130. e22.
248. Degenhardt, L. and W. Hall, Extent of illicit drug use and dependence, and their contribution to the global burden of disease. *The Lancet*, 2012. **379**(9810): p. 55-70.
249. Hulse, G., et al., The quantification of mortality resulting from the regular use of illicit opiates. *Addiction*, 1999. **94**(2): p. 221-229.
250. Volkow, N.D., et al., Medication-assisted therapies—tackling the opioid-overdose epidemic. *New England Journal of Medicine*, 2014. **370**(22): p. 2063-2066.
251. Fullerton, C.A., et al., Medication-assisted treatment with methadone: assessing the evidence. *Psychiatric Services*, 2014. **65**(2): p. 146-157.
252. Marsch, L.A., The efficacy of methadone maintenance interventions in reducing illicit opiate use, HIV risk behavior and criminality: a meta-analysis. *Addiction*, 1998. **93**(4): p. 515-532.
253. Barnett, P.G., J.H. Rodgers, and D.A. Bloch, A meta-analysis comparing buprenorphine to methadone for treatment of opiate dependence. *Addiction*, 2001. **96**(5): p. 683-690.
254. Volkow, N.D., et al., Medication-assisted therapies--tackling the opioid-overdose epidemic. *N Engl J Med*, 2014. **370**(22): p. 2063-6.
255. Johansson, B.A., M. Berglund, and A. Lindgren, Efficacy of maintenance treatment with naltrexone for opioid dependence: A meta-analytical review. *Addiction*, 2006. **101**(4): p. 491-503.
256. Walsh, S.L., et al., Acute administration of buprenorphine in humans: partial agonist and blockade effects. *Journal of Pharmacology and Experimental Therapeutics*, 1995. **274**(1): p. 361-372.
257. Martin, W., History and development of mixed opioid agonists, partial agonists and antagonists. *British journal of clinical pharmacology*, 1979. **7**(S3): p. 273S-279S.

258. Downing, J.W., W.P. Leary, and E.S. White, Buprenorphine: a new potent long-acting synthetic analgesic. Comparison with morphine. *Br J Anaesth*, 1977. **49**(3): p. 251-5.
259. Walsh, S.L., et al., Clinical pharmacology of buprenorphine: ceiling effects at high doses. *Clinical pharmacology and therapeutics*, 1994. **55**(5): p. 569-580.
260. Fudala, P.J., et al., Office-based treatment of opiate addiction with a sublingual-tablet formulation of buprenorphine and naloxone. *New England Journal of Medicine*, 2003. **349**(10): p. 949-958.
261. Barnett, P.G., J.H. Rodgers, and D.A. Bloch, A meta-analysis comparing buprenorphine to methadone for treatment of opiate dependence. *Addiction*, 2001. **96**(5): p. 683-90.
262. Teruya, C., et al., Patient perspectives on buprenorphine/naloxone: a qualitative study of retention during the starting treatment with agonist replacement therapies (START) study. *J Psychoactive Drugs*, 2014. **46**(5): p. 412-26.
263. Wesson, D.R. and W. Ling, The clinical opiate withdrawal scale (COWS). *Journal of psychoactive drugs*, 2003. **35**(2): p. 253-259.
264. De Boer, A., L. De Leede, and D. Breimer, Drug absorption by sublingual and rectal routes. *British journal of anaesthesia*, 1984. **56**(1): p. 69-82.
265. Zhao, P., et al., Applications of physiologically based pharmacokinetic (PBPK) modeling and simulation during regulatory review. *Clin Pharmacol Ther*, 2011. **89**(2): p. 259-67.
266. Fedorov, S., GetData graph digitizer. available at www.getdata-graph-digitizer.com, 2008.
267. Walter DS, I.C., Absorption, distribution, metabolism and excretion of buprenorphine in animals and humans. *Buprenorphine: combating drug abuse with a unique opioid*, ed. L.J. Cowan A. 1995, New York: Wiley-Liss.
268. Picard, N., et al., In vitro metabolism study of buprenorphine: evidence for new metabolic pathways. *Drug Metab Dispos*, 2005. **33**(5): p. 689-95.
269. Cubitt, H.E., J.B. Houston, and A. Galetin, Relative importance of intestinal and hepatic glucuronidation-impact on the prediction of drug clearance. *Pharm Res*, 2009. **26**(5): p. 1073-83.
270. Oechsler, S. and G. Skopp, An in vitro approach to estimate putative inhibition of buprenorphine and norbuprenorphine glucuronidation. *International journal of legal medicine*, 2010. **124**(3): p. 187-194.
271. Narang, N. and J. Sharma, Sublingual mucosa as a route for systemic drug delivery. *Int J Pharm Pharm Sci*, 2011. **3**(Suppl 2): p. 18-22.

272. Bullingham, R.E., et al., Buprenorphine kinetics. *Clin Pharmacol Ther*, 1980. **28**(5): p. 667-72.
273. Sawada, Y., et al., Prediction of the volumes of distribution of basic drugs in humans based on data from animals. *J Pharmacokinet Biopharm*, 1984. **12**(6): p. 587-96.
274. Berezhkovskiy, L.M., Volume of distribution at steady state for a linear pharmacokinetic system with peripheral elimination. *J Pharm Sci*, 2004. **93**(6): p. 1628-40.
275. Poulin, P., K. Schoenlein, and F.P. Theil, Prediction of adipose tissue: plasma partition coefficients for structurally unrelated drugs. *J Pharm Sci*, 2001. **90**(4): p. 436-47.
276. Poulin, P. and F.P. Theil, A priori prediction of tissue:plasma partition coefficients of drugs to facilitate the use of physiologically-based pharmacokinetic models in drug discovery. *J Pharm Sci*, 2000. **89**(1): p. 16-35.
277. Cone, E.J., et al., The metabolism and excretion of buprenorphine in humans. *Drug Metab Dispos*, 1984. **12**(5): p. 577-81.
278. Chang, Y. and D.E. Moody, Glucuronidation of buprenorphine and norbuprenorphine by human liver microsomes and UDP-glucuronosyltransferases. *Drug Metab Lett*, 2009. **3**(2): p. 101-7.
279. Chang, Y., D.E. Moody, and E.F. McCance-Katz, Novel metabolites of buprenorphine detected in human liver microsomes and human urine. *Drug Metab Dispos*, 2006. **34**(3): p. 440-8.
280. Proctor, N.J., G.T. Tucker, and A. Rostami-Hodjegan, Predicting drug clearance from recombinantly expressed CYPs: intersystem extrapolation factors. *Xenobiotica*, 2004. **34**(2): p. 151-78.
281. Oechsler, S. and G. Skopp, An in vitro approach to estimate putative inhibition of buprenorphine and norbuprenorphine glucuronidation. *Int J Legal Med*, 2010. **124**(3): p. 187-94.
282. Fihlman, M., et al., Voriconazole more likely than posaconazole increases plasma exposure to sublingual buprenorphine causing a risk of a clinically important interaction. *European Journal of Clinical Pharmacology*, 2016. **72**(11): p. 1363-1371.
283. McAleer, S.D., et al., Pharmacokinetics of high-dose buprenorphine following single administration of sublingual tablet formulations in opioid naive healthy male volunteers under a naltrexone block. *Drug Alcohol Depend*, 2003. **72**(1): p. 75-83.
284. Compton, P., et al., Pharmacokinetics, bioavailability and opioid effects of liquid versus tablet buprenorphine. *Drug Alcohol Depend*, 2006. **82**(1): p. 25-31.
285. Cone, E.J., et al., The metabolism and excretion of buprenorphine in humans. *Drug Metabolism and Disposition*, 1984. **12**(5): p. 577-581.

286. Lewis, J.W. and D. Walter, Buprenorphine-background to its development as a treatment for opiate dependence. NIDA research Monograph, 1993. **121**: p. 5-5.
287. Everhart, E.T., Polly Cheung, John Mendelson, Robert Upton, Reese T. Jones. "The mass balance of buprenorphine in humans." *Clinical Pharmacology & Therapeutics* 65.2 (1999): 152-152.
288. Welsh, C. and A. Valadez-Meltzer, Buprenorphine: a (relatively) new treatment for opioid dependence. *Psychiatry (Edgmont)*, 2005. **2**(12): p. 29.
289. Abbo, L.A., et al., Pharmacokinetics of buprenorphine following intravenous and oral transmucosal administration in dogs. *Veterinary therapeutics: research in applied veterinary medicine*, 2008.
290. Brown, S.M., et al., Buprenorphine metabolites, buprenorphine-3-glucuronide and norbuprenorphine-3-glucuronide, are biologically active. *The Journal of the American Society of Anesthesiologists*, 2011. **115**(6): p. 1251-1260.
291. Brown, S.M., et al., P-glycoprotein is a major determinant of norbuprenorphine brain exposure and antinociception. *Journal of Pharmacology and Experimental Therapeutics*, 2012. **343**(1): p. 53-61.
292. Tracqui, A., P. Kintz, and B. Ludes, Buprenorphine-related deaths among drug addicts in France: a report on 20 fatalities. *J Anal Toxicol*, 1998. **22**(6): p. 430-4.
293. Centers for Disease, C. and Prevention, CDC grand rounds: prescription drug overdoses - a U.S. epidemic. *MMWR Morb Mortal Wkly Rep*, 2012. **61**(1): p. 10-3.
294. Davis, C.S., J.E. Johnston, and M.W. Pierce, Overdose Epidemic, Prescription Monitoring Programs, and Public Health: A Review of State Laws. *Am J Public Health*, 2015. **105**(11): p. e9-e11.
295. McCarthy, M., Containing the opioid overdose epidemic. *BMJ*, 2012. **345**: p. e8340.
296. Rudd, R.A., et al., Increases in Drug and Opioid Overdose Deaths--United States, 2000-2014. *MMWR Morb Mortal Wkly Rep*, 2016. **64**(50-51): p. 1378-82.
297. Patrick, S.W., et al., Neonatal abstinence syndrome and associated health care expenditures: United States, 2000-2009. *JAMA*, 2012. **307**(18): p. 1934-40.
298. Women, A.C.o.H.C.f.U., ACOG Committee Opinion No. 524: opioid abuse, dependence, and addiction in pregnancy. *Obstetric Anesthesia Digest*, 2013. **33**(2): p. 79-80.
299. Hudak, M.L., et al., Neonatal drug withdrawal. *Pediatrics*, 2012. **129**(2): p. e540-e560.
300. Zedler, B.K., et al., Buprenorphine compared with methadone to treat pregnant women with opioid use disorder: a systematic review and meta-analysis of safety in the mother, fetus and child. *Addiction*, 2016.

301. in Clinical Guidelines for the Use of Buprenorphine in the Treatment of Opioid Addiction. 2004: Rockville (MD).
302. Nanovskaya, T., et al., Transplacental transfer and metabolism of buprenorphine. *Journal of Pharmacology and Experimental Therapeutics*, 2002. **300**(1): p. 26-33.
303. Caritis, S.N., et al., An evidence-based recommendation to increase the dosing frequency of buprenorphine during pregnancy. *Am J Obstet Gynecol*, 2017.
304. Dallmann, A., et al., A Physiologically Based Pharmacokinetic Model for Pregnant Women to Predict the Pharmacokinetics of Drugs Metabolized Via Several Enzymatic Pathways. *Clin Pharmacokinet*, 2017.
305. Dallmann, A., et al., Gestation-Specific Changes in the Anatomy and Physiology of Healthy Pregnant Women: An Extended Repository of Model Parameters for Physiologically Based Pharmacokinetic Modeling in Pregnancy. *Clin Pharmacokinet*, 2017. **56**(11): p. 1303-1330.
306. Dallmann, A., et al., Physiologically Based Pharmacokinetic Modeling of Renally Cleared Drugs in Pregnant Women. *Clin Pharmacokinet*, 2017. **56**(12): p. 1525-1541.
307. De Sousa Mendes, M., et al., A Physiologically-Based Pharmacokinetic Model to Predict Human Fetal Exposure for a Drug Metabolized by Several CYP450 Pathways. *Clin Pharmacokinet*, 2017. **56**(5): p. 537-550.
308. Jogiraju, V.K., et al., Application of physiologically based pharmacokinetic modeling to predict drug disposition in pregnant populations. *Biopharm Drug Dispos*, 2017. **38**(7): p. 426-438.
309. Zhang, Z. and J.D. Unadkat, Development of a Novel Maternal-Fetal Physiologically Based Pharmacokinetic Model II: Verification of the model for passive placental permeability drugs. *Drug Metab Dispos*, 2017. **45**(8): p. 939-946.
310. Kalluri, H.V., et al., A Physiologically Based Pharmacokinetic Modeling Approach to Predict Buprenorphine Pharmacokinetics following Intravenous & Sublingual Administration. *Br J Clin Pharmacol*, 2017.
311. Yanamandra, N. and E. Chandrachan, Anatomical and physiological changes in pregnancy and their implications in clinical practice. *Obstetric and Intrapartum Emergencies: A Practical Guide to Management*, ed. E.C.a.S.S. Arulkumaran. 2012:1-8, Cambridge University Press. 1-8.
312. Yanamandra N, C.E., Anatomical and physiological changes in pregnancy and their implications in clinical practice. Cambridge University Press, 2012: p. 8.
313. Horan, C., *Obstetric Evidence based Guidelines*. 1st ed. 2007, United Kingdom: Informa Healthcare.

314. Harding, S.D., et al., The IUPHAR/BPS Guide to PHARMACOLOGY in 2018: updates and expansion to encompass the new guide to IMMUNOPHARMACOLOGY. *Nucleic Acids Res*, 2018. **46**(D1): p. D1091-D1106.
315. Alexander, S.P., et al., THE CONCISE GUIDE TO PHARMACOLOGY 2017/18: G protein-coupled receptors. *Br J Pharmacol*, 2017. **174 Suppl 1**: p. S17-S129.
316. Alexander, S.P., et al., THE CONCISE GUIDE TO PHARMACOLOGY 2017/18: Enzymes. *Br J Pharmacol*, 2017. **174 Suppl 1**: p. S272-S359.
317. Nylen, H., et al., Cytochrome P450 3A activity in mothers and their neonates as determined by plasma 4 beta-hydroxycholesterol. *European Journal of Clinical Pharmacology*, 2011. **67**(7): p. 715-722.
318. Rodgers, T. and M. Rowland, Mechanistic approaches to volume of distribution predictions: understanding the processes. *Pharm Res*, 2007. **24**(5): p. 918-33.
319. Product Information: buprenorphine HCl sublingual tablets, b.H.s.t.R.L., Inc. (per manufacturer), Columbus, OH, 2012.
320. Jiao, Z., et al., Population pharmacokinetic modelling for enterohepatic circulation of mycophenolic acid in healthy Chinese and the influence of polymorphisms in UGT1A9. *Br J Clin Pharmacol*, 2008. **65**(6): p. 893-907.
321. Honda, M., et al., Quantitative analysis of serum alpha 1-acid glycoprotein levels in normal and diabetic pregnancy. *Diabetes Res Clin Pract*, 1990. **10**(2): p. 147-52.
322. Laffont, C.M., et al., Population Pharmacokinetic Modeling After Repeated Administrations of RBP-6000, a New, Subcutaneously Injectable, Long-Acting, Sustained-Release Formulation of Buprenorphine, for the Treatment of Opioid Use Disorder. *J Clin Pharmacol*, 2016. **56**(7): p. 806-15.
323. Ng, C.M., et al., Population Pharmacokinetic Model of Sublingual Buprenorphine in Neonatal Abstinence Syndrome. *Pharmacotherapy*, 2015. **35**(7): p. 670-80.
324. Ohtani, M., et al., Pharmacokinetic analysis of enterohepatic circulation of buprenorphine and its active metabolite, norbuprenorphine, in rats. *Drug Metab Dispos*, 1994. **22**(1): p. 2-7.
325. de Winter, B.C., et al., Pharmacokinetic role of protein binding of mycophenolic acid and its glucuronide metabolite in renal transplant recipients. *J Pharmacokinetic Pharmacodyn*, 2009. **36**(6): p. 541-64.
326. Drug Overdose Deaths in the United States, -. NCHS Data Brief No. 329, November 2018.
327. Drug and Opioid-involved Overdose Deaths - United States, -. Morbidity and Mortality Weekly Report, Weekly / January 4, 2019 / 67 (5152); 1419 - 1427.

328. Bateman, B.T., et al., Patterns of opioid utilization in pregnancy in a large cohort of commercial insurance beneficiaries in the United States. *Anesthesiology*, 2014. **120**(5): p. 1216-24.
329. Vucinovic, M., et al., Maternal and neonatal effects of substance abuse during pregnancy: our ten-year experience. *Yonsei Med J*, 2008. **49**(5): p. 705-13.
330. Winkelman, T.N.A., et al., Incidence and Costs of Neonatal Abstinence Syndrome Among Infants With Medicaid: 2004
2014. *Pediatrics*, 2018. **141**(4).
331. Jansson, L.M., M. Velez, and C. Harrow, The opioid-exposed newborn: assessment and pharmacologic management. *J Opioid Manag*, 2009. **5**(1): p. 47-55.
332. Milliren, C.E., et al., Hospital Variation in Neonatal Abstinence Syndrome Incidence, Treatment Modalities, Resource Use, and Costs Across Pediatric Hospitals in the United States, 2013 to 2016. *Hosp Pediatr*, 2018. **8**(1): p. 15-20.
333. Sullivan, L.E. and D.A. Fiellin, Buprenorphine: its role in preventing HIV transmission and improving the care of HIV-infected patients with opioid dependence. *Clin Infect Dis*, 2005. **41**(6): p. 891-6.
334. Lotsch, J., et al., Evidence for morphine-independent central nervous opioid effects after administration of codeine: contribution of other codeine metabolites. *Clin Pharmacol Ther*, 2006. **79**(1): p. 35-48.
335. Lotsch, J., et al., The transfer half-life of morphine-6-glucuronide from plasma to effect site assessed by pupil size measurement in healthy volunteers. *Anesthesiology*, 2001. **95**(6): p. 1329-38.
336. Refuerzo, J.S., et al., Use of over-the-counter medications and herbal remedies in pregnancy. *Am J Perinatol*, 2005. **22**(6): p. 321-4.
337. Mitchell, A.A., et al., Medication use during pregnancy, with particular focus on prescription drugs: 1976-2008. *Am J Obstet Gynecol*, 2011. **205**(1): p. 51 e1-8.
338. Walter, D., and Inturrisi, C., Absorption, Distribution, Metabolism, and Excretion of Buprenorphine in Animals and Humans. *Buprenorphine: Combatting Drug Abuse With a Unique Opioid.*, ed. A. Cowan, and Lewis, J.W. 1995, New York: Wiley-Liss.
339. Subutex®, Drug Monograph